The explosive volcanism of Teide-Pico Viejo volcanic complex, Canary Island

Olaya García Pérez

THE EXPLOSIVE VOLCANISM OF TEIDE-PICO VIEJO VOLCANIC COMPLEX, CANARY ISLAND.

Olaya García Pérez

Departament of Geodinamic and Geophysisc

Universidad de Barcelona

Barcelona 2013

A mi abuelo Miguel

que me enseñó a pintar las piedras.

Acknowledgements

I would first like to thank my thesis supervisor Joan Marti who has guided and advised me during these years of thesis research and who has taught me that with hard work and patience anything can be achieved.

My deepest gratitude goes to Costanza Bonadona and Laura Pioli for their invaluable help, support and guidance without which this project would not have succeeded and also for their warmth and hospitality which made me feel so welcome during my stay in Geneva.

Thanks to Gerardo Aguirre for all his help in teaching me in the field and for helping me with all my doubts with such good humour.

Of course thanks must go to Silvina Guzman for all her time and energy helping me to bring this project to fruition, her personal and professional support and valuable contributions.

Thanks must also go to IGN, especially the whole team from the Canary Geophysical Centre of Tenerife, who guided me and helped me in every way possible during my stay with them. Special thanks go to Pedro Torres and David Moure for their company and persistence on my many field trips.

Thanks very much to the staff of the Central Geophysical Observatory, especially to Natividad Luengo, who accompanied me on long field trips and who always made tedious work easier and not forgetting Alicia Felpeto - many thanks for the comments and showing me all the relevant my work collected during the years.

I would also like to thank Fidel Costa, Andrea Dimuro, Rosa Sobradelo for all their comments and clarifications that have helped me to improve this work .

A big thank you must go to my friend and colleague Stephanie Barde-Cabusson for joining me on all those days in the field and for her constant encouragement to continue doing what I love. Thank you so much for your advice and support.

Big thanks must got to my friends and family for being by my side and a very special thanks to my mother and father who have helped me to get here and who always supported me in all of my decisions. Last but not least, a special thanks to my colleague and partner James who has shown me his full and unconditional support. Thank you for believing in my projects and for being there for me at all times.

Contents

Anexo 3. Pyroclastic density currents from Teide-Pico Viejo (Tenerife, Canary Islands): implications on hazard assessment

Anexo 4. The 5,660 yBP Boquerón explosive eruption, Teide–Pico Viejo complex, Tenerife

Anexo 5. Eruptive scenarios of phonolitic volcanism at Teide-Pico Viejo volcanic complex (Tenerife, Canary Islands)

Abstract:

The explosive events in Teide Pico Viejo (TPV) complex in Tenerife Island (Spain) have traditionally been restricted to the subplinian eruption of Montaña Blanca, which occurred about 2000 years ago. A recent revision of the stratigraphy of TPV shows that phonolitic explosive activity has been significant during the Holocene, with several distinct episodes related to eruptions ranging from Strombolian to sub-plinian. Using field, mineralogical and geochemical stratigraphic correlations, we have identified 11 phonolitic explosive eruptions related to the satellite domes present all around TPV complex**.** One of the most representative eruptions is that of El Boqueron (5,660 yBP), a dome that generated an explosive event of VEI 3 with a minimum volume of 4-6x10^7 m^3 and produced a plume with a height of up to 9km above sea level (MER 6.9-8.2x10^5 kg/s, during 9-15 h). The occurrence of these explosive events in the recent eruptive record of TPV is of major importance in evaluating the risk imposed by the volcanic complex on Tenerife. These eruptions have generated a wide range of direct hazards, such as fallout, emplacement of pyroclastic density currents, debris flows, lahars, and rock avalanches, which could occur again in case of a renewal of volcanic activity. The results obtained in our study are relevant to define realistic and precise eruptive scenarios for TPV and to assess its associated hazard, a necessary step in the evaluation and mitigations of volcanic risk in Tenerife.

Resumen:

El complejo volcánico Teide Pico Viejo (TPV) es un stratovolcano situado en la isla de Tenerife, Islas Canarias, y ha sido considerado por la UNESCO el sistema volcánico activo más peligroso en Europa. Los eventos explosivos en el complejo TPV se han limitado tradicionalmente a la erupción subplinian de Montaña Blanca, que ocurrió hace unos 2000 años. Una reciente revisión de la estratigrafía muestra que la actividad explosiva fonolítica asociada a TPV ha sido significativa durante el Holoceno, presentado distintos episodios relacionados con erupciones que varían en tamaño de estromboliano a sub-pliniano. A través de las correlaciones estratigráficas obtenidas mediante observaciones de campo y datos de mineralógicos y geoquímicos, se han identificado 11 erupciones explosivas fonolítica relacionados con los domos satélite presentes en todo complejo TPV.

Una de las erupciones más representativa es El Boquerón (5660 YBP), un domo que generó un evento explosivo de VEI 3 con un volumen mínimo de 4-6x107 m3 y produjo una columna con una altura de hasta 9 kilometros sobre el nivel del mar (MER 6.9-8.2x105 kg / s, durante 9-15 h). La ocurrencia de estos eventos explosivos en el reciente registro eruptivo del complejo TPV es de gran importancia para evaluar el riesgo impuesto por el complejo volcánico en Tenerife. Estas erupciones han generado una amplia gama de amenazas directas, como los depósitos de caida, emplazamiento de las corrientes piroclásticas densidad, flujo de derrubios, lahares y avalanchas de roca, lo que podría ocurrir de nuevo en caso de renovación de la actividad volcánica. Los resultados obtenidos en nuestro estudio son relevantes para definir escenarios eruptivos realista y precisos para el complejo TPV y para evaluar su riesgo asociado, un paso necesario en la evaluación y mitigación del riesgo volcánico en Tenerife.

Part I:

1. Introduction

The Canarian archipelago comprises seven volcanic islands situated in the Atlantic Ocean in front of the African cost, between 27º37' and 29º24'N and 18º10' and 13º37' W, on the Atlantic Mesozoic tholeitic oceanic crust, on a seafloor fracture zone extending off the continental slope of Northwest Africa.

Tenerife is the most populated (>900000 inhabitants) and largest of the Canary Islands (~2500Km^2) and one of the largest volcanic islands on Earth. It shows a large variety of well exposed volcanic features. The central part of Tenerife is occupied by the impressive Las Cañadas Caldera where stands the late-Quaternary central edifice Teide –Pico Viejo Complex (TPV) (Fig1). Its summit is Pico Teide that rises to 3718m a.s.l. This central complex is formed by two active basanite to phonolite twin stratovolcanoes, Teide and Pico Viejo, and several satellite vents systems. TPV complex has been considered one of the most potentially dangerous active volcanic systems in Europe and was included in the past Decade of Natural Hazards by UNESCO. In 1992, it was also selected as one of the Laboratory Volcanoes by the European Commission.

Spatial and temporal distribution of recent volcanism on Tenerife demonstrates that the island is a highly active volcanic zone and that more eruptions have a high probability to occur in the future. Recent signs of activity have been observed with an unrest episode in 2004 (Perez et al. 2005; Garcia et al. 2006; Gottsmann et al. 2006; Martí et al. 2009; Domínguez Cerdeña et al. 2011). Even, if the highest probability of new eruptions on Tenerife corresponds to basaltic eruptions from the currently active

rift zones, sub-plinian and plinian eruptions from the TPV Complex are not impossible, as indicated by the abundance of Holocene eruptions (Carracedo et al. 2007; Martí et al., 2008)

Unfortunately, volcanic hazard from volcanoes with a long-term recurrence tends to be underestimated, especially when little or no historical observation exists. TPV has traditionally been considered as an effusive volcano (Carracedo et al 2007), where most of the eruptions have been of phonolitic compositions and triggered by intrusion of deep basaltic magma into a shallow felsic magma chamber (Marti et al. 2008). This produced phonolitic lava flows and exogenous domes with very few explosive activity represented only by the subplinian eruption of Montaña Blanca (2020 b.p). However, a detailed revision of the stratigraphy and physical volcanology of TPV Complex showed that the explosive activity is much more significant than previously thought (Martí et al. 2008) A considerable number of explosive deposits as clastogenic lava flows, pyroclastic flows and pumice fall deposits can be recognized in the stratigraphic record of TPV Complex. Therefore, a characterization of all these deposits is necessary to determine the potential of TPV to produce explosive eruptions in the past and in the future, so as to provide a better knowledge of its eruptive behavior to improve hazard assessment.

The related studies that compose this PhD Thesis are aimed at documenting the recent explosive volcanic history of TPC complex, in order to characterize, correlate and quantify them, and to improve hazard assessment at Teide-Pico Viejo. .

1.2 State of the art and geological setting

Tenerife is the largest of the Canary Islands and its subareal evolution started in the late Miocene with the construction of overlapping mafic shield volcanoes, which developed mainly between 12.0 and 4.5 Ma and presently form about the 90% of the island. Nowadays, they are preserved as eroded massifs in the NE and NW extremes of the island (Abdel-Monem at al., 1972; Ancochea et al., 1990). These overlying shields were growing through two main rift zones (Dorsal rift zone and Santiago rift zone) and occupying also the central part of the island. The middle part of the island developed to an extensive post-shield volcanic complex, around 4 to 0,2 Ma which comprises the Las Cañadas edifice a NE-SW elliptical structure of around 16 km wide, a composite basaltic to phonolitic volcanoes (Fuster et al., 1968; Araña, 1971; Ancochea et al., 1990; Martí et al.,1994). This volcanic edifice was affected by several vertical collapses (Ucanca in the west, Guajara and Diego Hernández in the centre-east) forming the Las Cañadas caldera. These collapses were associated to explosive activity by emptying low depth magma chambers. Occasional lateral collapse of the volcano flanks also occurred modifying the morphology of the resulting caldera depression (Martí et al. 1994; 1997; Martí and Gudmundsson 2000) Las Cañadas caldera has a controversial origin, on account of there is different hypothesis to explain it. Some authors was cope with a lateral landslide origin (Bravo, 1962; Coello, 1973; Navarro and Coello, 1989; Carracedo, 1994; Watts and Mason, 1995; Teide Group, 1997; Ancochea et al., 1999; Masson et al., 2002), although some of the valley associated to the central complex have been recognized as landslide origin in the case of Caldera edifice there is not existing data do not allow to determinate its headwall location. (Watts and Mason,

1995; Ablay and Hürlimann, 2000; Masson et al., 2002; Hürlimann et al., 2004).
Other authors explain the Las Cañadas caldera origin by a vertical collapse hypothesis related the voluminous ignimbrite deposits in the southern part of Tenerife (Bandas del Sur Formation) to the explosive products of different major caldera-forming events in Las Cañadas edifice (Martí et al., 1994; Bryan et al., 1998; Bryan et al., 2000; Edgar et al., 2002, 2007). Also as Marti et al. (1997) and Hürliman advocate that vertical and lateral collapses have interaction in the origin of the actual Cañadas structure, relation several calderas in Las Cañadas edifice (Guajara and Diego Hernández caldera) with the main Valley in the North side of Tenerife (La Orotava and Icod Valley).

The TPV volcanic complex started to build up inside of the Las Cañadas caldera about 180 Ka ago. Its two twin stratovolcanoes evolved simultaneously from the interaction of two different shallow magma systems and that produced numerous satellite vents. (Hausen 1956; Araña 1971; Ablay 1997; Ablay et al. 1998; Ablay and Matí 2000; Carracedo et al. 2003; Carracedo et al. 2007; García et al. 2012)

The eruptions of the active TPV central complex have been mainly characterized by a complete series from basalt to phonolite products (Ridley, 1970; 1971; Ablay et al., 1997; Ablay et Marti, 2000), which have been covering the Las Cañadas caldera and the adjacent Icod and La Orotava valleys (Fig1). The mafic to intermediate lavas that partially fill Las Cañadas caldera are interpreted to be the first products of Teide-Pico Viejo (Ablay and Martí, 2000). Although the first phonolites appeared at about 35 Ka, they became predominant in the recent eruptions of the TPV complex with an overall increase of the volume of the eruptions.

In order to understand the evolution of the TPV complex it is important to

explain the relation between the different eruption centers and their composition. Eruptions at Teide and Pico Viejo volcanoes have occurred from their central vents but also from a multitude of vents distributed radially around their flanks, along several eruptive fissures, and have produced mafic and felsic eruptions. The Santiago and Dorsal rift axes, which are well expressed outside the Las Cañadas caldera, are supposed to join beneath the Las Cañadas calderas and TPV complex and seem to have controlled mafic volcanism along the flanks of these volcanoes (Ablay and Marti 2000). The Santiago del Teide rift explains the orientation of eruptive fissures of some flank vents at the western side of Pico Viejo. On the eastern side of Teide some vents are also associated with eruptive fissures oriented in the direction of the Dorsal Ridge (Carracedo et al. 1994; Ablay and Marti, 2000). However, flank volcanism has also produced felsic eruptions which are not oriented parallel to the rift systems. On the contrary, they seem to follow a structural pattern that is controlled by the influence of the shallow phonolitic magma chambers that have existed below Teide and Pico Viejo (Ablay and Martí, 2000; Martí et al., 2008; Martí and Geyer, 2009). As occurs with central phonolitic eruptions, flank eruptions also show evidence of magma mixing, thus suggesting that two plumbing systems affect the TPV complex (Araña et al., 1994; Ablay and Marti, 2000; Martí et al., 2008; Wiesmaier et al., 2012) Phonolitic magmatism is associated with the development of shallow magma chambers at the interior of the Tenerife central volcanic edifice. The position and the shape of the phonolitic shallow magma chambers have changed significantly during the whole evolution of the central volcanic complex, as it is suggested by experimental petrology data (Andujar 2007). These changes in location and in shape have probably been induced by changes in the local stress field after each chambers forming episode (Marti

and Gudmunsson 2000; Martí and Geyer, 2009). The sub-radial pattern of eruptive fissures associated with Teide and Pico Viejo felsic flank vents suggests the influence of the shallow, felsic magma chamber below the volcanoes (Ablay and Martí, 2000; Martí and Geyer, 2009).

The available petrological data support that Teide-Pico Viejo phonolites were stored in different magma chambers at a shallow depth beneath these stratovolcanoes (<2 km below sea level), feeding central and flank eruptions (Ablay, 1997; Ablay et al., 1998; Triebold et al., 2006; Andujar, 2007). Petrologically most of the phonolitic eruptions from Teide-Pico Viejo and Las Cañadas show signs of magma mixing, indicating that eruptions were triggered by intrusion of deep basaltic magmas into shallow phonolitic reservoirs (Wolff, 1995; Araña et al., 1994; Thiebolt et al., 2006; Martí et al 2008). Basaltic activity has acted in some cases as a precursor to phonolitic activity, controlling the dynamics and frequency of eruptions at TPV. Nevertheless, the basaltic volcanism shows different source regions, with a wide range of compositions registering different processes of crystal fractionation, assimilation and mixing with the magma stored at different depths. So the basaltic system drives primitive and evolved mafic magma to the surface through the rifts, feeds the central zone, mix with the evolved magma stored at shallow depth and sometimes can pass directly to the central system and reach the surface as flank eruptions. This explains why we find different compositions in the recent volcanic history of the TPV (Martí et al., 2008).

Phonolitic eruptions from Teide and Pico Viejo range in volume from 0.01 to 1 km^3 and have mostly generated thick lava flows and domes, some of them associated with minor to major explosive phases. Some produced subplinian eruptions, such as the Montaña Blanca at the eastern flank of Teide, 2000 years ago (Ablay et al., 1995) and

Boquerón, 5660 yBP (García et al, 2012). Several significant basaltic eruptions have also occurred from the flanks and the central vents of the Teide–Pico Viejo complex. Although the volume of phonolitic eruptions is globally larger than mafic eruptions (0,01 to 1km^3) they are less studied.

1.3 Aims of dissertation:

Tenerife island is considered a highly active volcanic zone and since the last eruption that occurred about 100 years ago the island has experienced important demographic (population) expansion and development due to the economic progress derived from the massive arrival of tourism during the last decades. The potential impact of volcano eruptions on populated areas has raised the attention of scientists and administrators in the last years as a consequence of the significant socio-economic impact that some recent eruptions have caused even at a global scale. Unfortunately the last eruption on Tenerife occurred more than one century ago, so the volcanic threat is today mostly ignored by the population and its governing. This is still more relevant when we consider Teide and Pico Viejo volcanoes, as their last eruptive activity is goes back to one thousand year ago and, consequently, they are considered as extinct volcanoes. However, the unrest episode occurred in 2004 (García et al.2006; Pérez et al. 2005; Gottsmann et al. 2006; Martí et al.2009; Domínguez Cerdeña et al. 2011) reminded us that these volcanoes are still active and that they may erupt in the future, so that it is necessary to estimate their associated hazards and their potential impact on the Tenerife population.

The recent volcanism on Tenerife demonstrates that future eruptions may occur from many different vent sties on the island focus in the NW dorsal rift and TPV

Complex. Historical eruptions correspond to low energy basaltic eruptions that produced cinder cones, made of scoria lapilli and ash and lavas flows of several kilometers of extension, which caused relatively low damage. The same type of eruptions today would cause a significantly higher impact, as the increase in population and infrastructure has made Tenerife much more vulnerable. Hence it is necessary to have a good knowledge of the recent volcanism to quantify the possible risk scenarios.

The TPC complex is still not well known and represents part of the last volcanic formation of the island. Its recent eruptions involve relatively violent explosive episodes, as ~~is~~ revealed by its geological record (Ablay et al. 1995; Martí et al. 2008). In such a densely populated area with the evacuation difficulties caused by being an island, even a minor eruption could be catastrophic if it is not well forecasted and managed by the scientists and the corresponding authorities. This is essential in all volcanic areas and Tenerife is not an exception, although, in recent times a greater research effort was made to understand Tenerife recent volcanism (see e.g. Martí and Wolf , 2000; Carracedo et., 2003, 2007, Marti et al 2008; Martí et al 2012)

The aim of this PhD thesis is to provide a first approach to the characterization of Teide- Pico Viejo phonolite explosive eruptions. The recent volcanic activity of these twin stratovolcanoes has been analyzed and carefully studied, assuming that similar explosive eruptions have a high probability of occurrence in the near future. Therefore it is essential to better characterize these explosive episodes to evaluate the possible hazards of the island.

The PhD Thesis is divided into several parts, each one corresponding to a separate scientific paper, with the objective to describe the stratigraphy and main characteristics of Teide-Pico Viejo explosive phonolitic deposits, to interpret them in

terms of eruption dynamics, and to assess their potential hazards. In this sense, we provide relevant information on the stratigraphy and extend of these deposits, number of explosive events, chronological data, chemical mineralogy of the deposits, etc. The results obtained will contribute to a better understanding of the volcanological evolution of the central magmatism of Tenerife.

Each of the scientific papers reflect the main objectives of this PhD.

- Firstly, to identify and characterize the type and number of deposits derived from explosive phonolitic eruptions in the TPV complex. As in Garcia et al, 2011.
- A second objective is to map and conduct a facies analysis and stratigraphic correlations of these explosive deposits in order to find their volcanic sources, volumes, and their position in the stratigraphic record of TPV. In this case we present and discuss this objective in García et al 2012 and García et al 2013.
- Finally the third main objective is to use the data obtained from these explosive deposits to recreate their eruptive scenarios conduct hazard assessment, and evaluate potential impacts of this type of volcanism on Tenerife today. This is explained in the article Martí et al. 2012.

1.4 Thesis structure:

This PhD Thesis has been divided into three parts in order to facilitate explanation and compression (comprehension). The first part focuses on the research project introduction, which describes the area of study and the general objective that have been taking in consideration to develop this PhD Thesis. We will make a statement of facts that demonstrate the importance of this research project, the contribution involved to the knowledge of the area and their direct usefulness to society.

The second part presents all the published papers and submits papers that have grouped together to form this thesis. Also this part shows the evolution of my research, and the main results obtained so far. The core of the thesis corresponds to 4 research papers already published or still under review in relevant international journals. The order in which these chapters are presented does not correspond chronologically to their publication or submission but are arranged to present in a logical sequence the data obtained and its interpretation. Its editorial format is presented in an appendix at the end of the thesis.

The third part consists of a general overview of all the articles with all the results obtained in the research project , the discussion of these results and the final conclusions.

Part II:

1. Stratigraphic, mineralogical and geochemical correlation of phonolitic explosive episodes of Teide- Pico Viejo Complex, Tenerife

This paper has been submitted to Journal of the Geological Society. The authors of the papers are:

Olaya García, Instituto de Ciencias de la Tierra Jaume Almera, CSIC, Lluis Solé Sabarís s/n, 08028 Barcelona, Spain.

Joan Martí, Instituto de Ciencias de la Tierra Jaume Almera, CSIC, Lluis Solé Sabarís s/n, 08028 Barcelona, Spain.

Silvina Guzman IBIGEO (CONICET-UNSa), Museo de Ciencias Naturales, Universidad Nacional de Salta, Mendoza 2, 4400, Salta, Argentina

The reference of this paper is: Stratigraphic correlation of Holocene phonolitic explosive episodes of the Teide-Pico Viejo Complex, Tenerife) (García O., Martí J., Guzmán S. (Submit) The Geological Society.

1. 1 Introduction

Teide and Pico Viejo are twin stratovolcanoes situated on the island of Tenerife (Canary Islands) that constitute one of the most important active oceanic island volcanic complexes in the world. They started to grow inside the caldera of Las Cañadas less than 200 ka ago and have continued to be active up to the present day, with the last central eruption (Lavas Negras) having occurred about 1000 years ago (Carracedo *et al*. 2007).

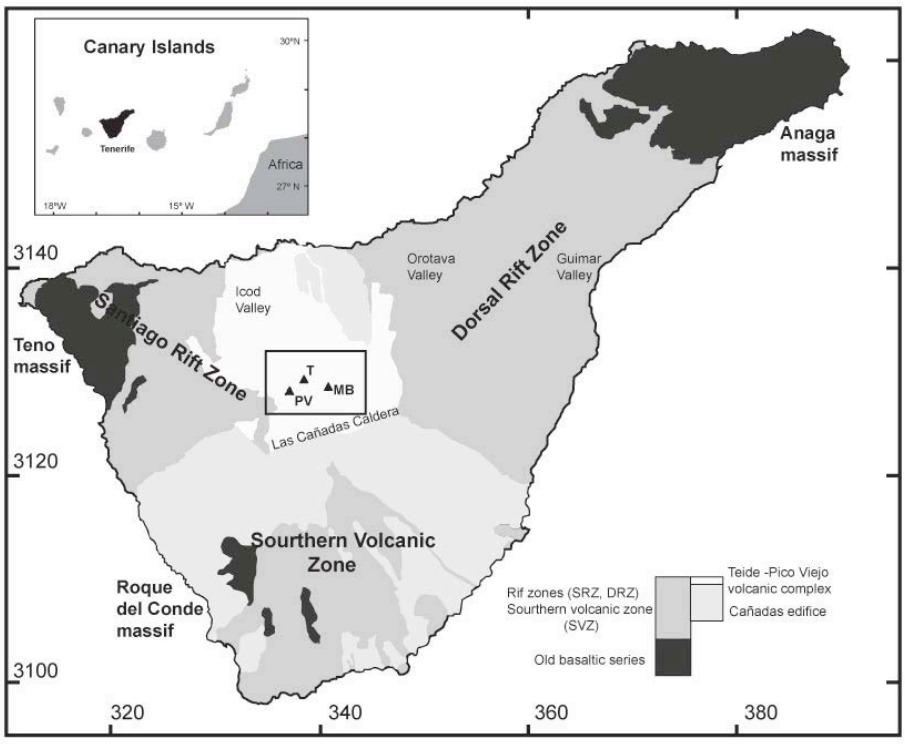

Fig. 1. a) Location of the Canary Islands and Tenerife. b) Simplified geology and stratigraphy of Tenerife. Main vents are shown as black triangles, *T* Teide, *PV* Pico Viejo and *MB* Montaña Blanca.

The activity of this volcanic complex has generated magmas that have evolved from basaltic to phonolitic in the period dating from 35 000 years ago to the present (Martí *et al*. 2008). Most of the products that have been preserved in TPV correspond to thick lava flows of phonolitic composition that outcrop on the surface (Ablay & Martí 2000; Carracedo *et al.* 2007), basaltic-to-intermediate lava flows forming most of the inside of the volcanic edifices (Ablay & Martí 2000; Thiebolt *et al.* 2006; Martí *et al.* 2008), minor phreatomagmatic deposits of mafic composition (Pérez Torrado *et al.* 2004; Martí *et al.* 2008; García *et al*. 2011) and phonolitic pumice deposits mostly originating from the 2020 YBP eruption of the satellite cone of Montaña Blanca (Ablay *et al.* 1997). This has traditionally led to the assumption that TPV is essentially effusive and so its associated hazard is relatively minor. However, field revisions carried out in recent years (Martí *et al.* 2008; García *et al*. 2011, García *et al.* 2012) have revealed that the amount of explosive volcanism associated with TPV is much greater than was once thought. This has led Martí *et al.* (2011) to reconsider the threat that this active volcanic complex represents for the island of Tenerife and to analyze the potential explosive scenarios that could presumably develop in the near future.

We studied the most recent explosive episodes that have been preserved in the geological record of TPV in order to advance the analysis of the past eruptive activity in TPV and to characterize its explosive events with more accuracy, thereby improving the evaluation of its potential for future explosive episodes. The lack of continuous outcrops – due to the erosion of the deposits – and the apparent similarity of most of these deposits mean that stratigraphic correlation and the determination of the relative ages of these outcrops is not a straightforward task. Therefore, in addition to field and physical volcanology work, we also undertook a detailed petrological and geochemical

study including mineral chemistry to identify possible fingerprints that would establish a precise correlation between these deposits and determine their relative stratigraphy. In this paper we 1) describe the relative stratigraphy of the deposits, 2) describe their petrological and geochemical characteristics, 3) establish the correlations between these deposits and their potential vents and, finally, 4) discuss the relevance of explosive volcanism in the Teide-Pico Viejo complex.

1. 2 Geological Background

The TPV complex consists of two stratovolcanoes and several flank vents, which started to grow simultaneously within the caldera of Las Cañadas around 180–190 ka ago (Fig.1) (Hausen *et al.* 1956; Araña *et al.* 1971; Ablay 1997; Ablay *et al.* 1998; Ancochea *et al.* 1999; Ablay & Martí 2000; Carracedo *et al.* 2007). This volcanic depression originated as a result of several vertical collapses of the edifice of Las Cañadas, the former central volcanic edifice on Tenerife (Martí *et al.* 1997; Martí & Gudmundsson 2000). The TPV complex has a maximum elevation of 3718 m a.s.l (the summit of Teide) and steeply sloping flanks.

The volcanic stratigraphy of TPV was characterized by Ablay & Martí (2000) on the basis of a detailed field and petrological study. Subsequently, Carracedo *et al.* (2003, 2007) provided the first group of isotopic ages from TPV products. The eruptive history of the TPV complex consists of a main eruption period characterized by mafic-to-intermediate lavas that form the core of these stratovolcanoes and filled in most of the depression of Las Cañadas and the adjacent La Orotava and Icod valleys. Phonolitic eruptions predominated from 35 ka ago onwards and their products today

cover the volcanoes' flanks and the infill sequence of the Icod Valley and part of La Orotava Valley (Ablay *et al.* 1998; Ablay & Martí 2000; Martí *et al.* 2008).

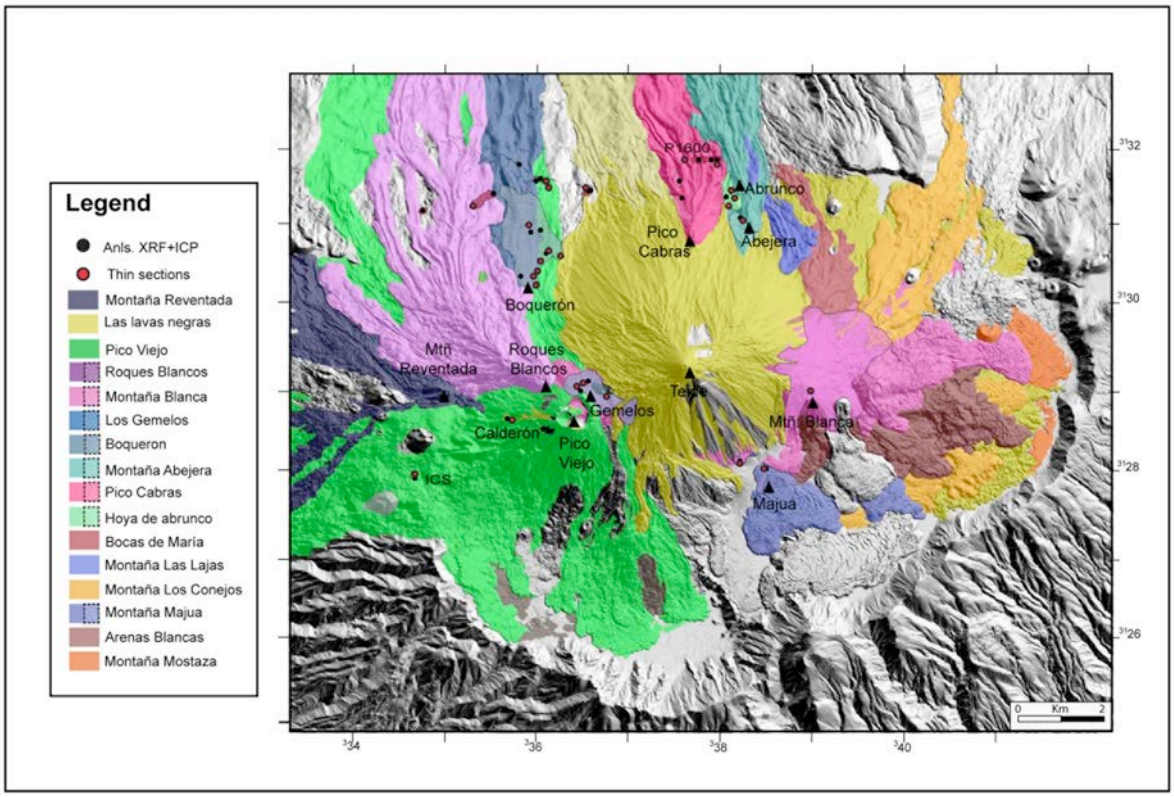

Fig. 2. Simplified geological map of the Teide-Pico Viejo complex (modified from Ablay & Martí 2000) showing the central and flank Holocene eruptions of felsic and hybrid compositions. Geochronological data from Carracedo *et al.* (2007). Main vents are shown as black triangles. The studied deposits and the corresponding samples are indicated by red circles (XRF+ICP analysed samples are indicated with blue circles). The pumice deposits associated with the main flanks of the volcanoes of TPV are shown with white dots. (projection: UTM 28N)

Phonolitic eruptions from TPV occurred both from the central vents and from a number of satellite vents distributed on the flanks. These flank vents have generated both effusive (i.e. lava flows and domes) and explosive eruptions, ranging in

size from 0.01 to > 1 km^3 Dense Rock Equivalent (DRE). Effusive eruptions occurred during the whole period of phonolitic volcanism and generated thick lava flows and domes. Explosive eruptions were mostly concentrated in the Holocene and caused extensive pumice fall deposits and pyroclastic density currents (PDCs), some of which have been associated with dome and lava-flow gravitational collapses during sub-Plinian to Plinian eruptions (Martí *et al.* 2008, 2011, García *et al.* 2011). Each of these eruptive centres is associated with a single eruption in which several phases can be distinguished (Ablay & Martí 2000).

1. 3 Methodology

We conducted a detailed field study whose aim was to identify and characterize the different pyroclastic deposits present in TPV and to locate their possible vents and establish their relative stratigraphy. Fieldwork included the study of these outcrops (Fig.2) in an attempt to locate their potential vents on the basis of their stratigraphic positions, the macroscopic textural and mineralogical characteristics of their deposits, variations in grain-size and thickness, and macroscopic componentry analysis. Fieldwork also included sample collection for subsequent geochemical and mineralogical analysis whose aim was to identify fingerprints that would confirm stratigraphic correlations.

The mineralogical and geochemical analyses of the studied samples were only performed for correlative purposes given that a more detailed petrological and petrogenetic study was beyond the scope of this work. Our working hypothesis – based

on previous petrological studies of TPV rocks (Ablay *et al.* 1997; Wiesmayer *et al.* 2011; Andújar *et al.* 2013) – was that products from the same eruption would have relatively homogenous mineralogical and geochemical compositions, while products from different eruptions would not. Whole rock analyses of 67 samples from different outcrops were performed by the GeoAnalytical Laboratory at Washington State University using its X-Ray Fluorescence (XRF) and Inductively Coupled Plasma Mass Spectrometry (ICP-MS) facilities (Table 1). The relative error of the measurement was less than 1% for the major and trace elements using the XRF method, less than 5% for the REEs and less than 10% for the remaining trace elements with ICP-MS.

Mineral compositions were determined using an electron microprobe (Camara SX-50, Serveis Científic-Tècnics, University of Barcelona) with an acceleration voltage of 20 kV. The sample current was 6 nA for glasses and 15 nA for minerals, while the beam size was 1 mm for minerals and 10 mm for glasses. Although Na was analysed initially for only 20 s to minimize loss, the peak counting times for the other elements were 10 s.

The charcoal that was found in association with three different pumice units was analysed using accelerator mass spectroscopy (AMS) techniques by Beta Analytic Inc. (Laboratory of Miami, USA) to study its carbon isotopic composition. These samples were taken from different parts of the study area. Charcoal sample P1600 was located on the main track that crosses the whole north face of the Teide-Pico Viejo Complex at the bottom of the pumice deposit that overlies a paleosoil; 4 gr of the sample (laboratory number Beta-301363) was taken and its age of 1790±30 yBP was determined using the IntCal04 calibration curve (Reimer *et al.* 2004). Sample RB1 was from the Boquerón deposit yielded an age of 5630±60 yBP (García *et al*. 2012). The final ICS charcoal sample (laboratory number Beta-293009), found at the top of the pumice deposit below an altered scoria unit in an outcrop in the south of the study area, was aged at 3520±30 yBP.

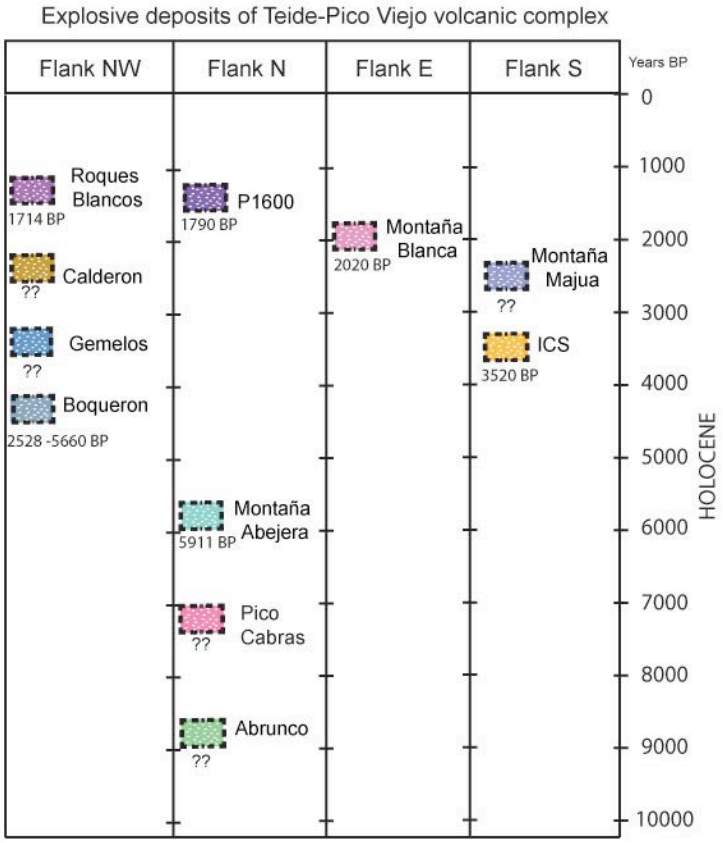

Fig. 3: Age of the Holocene pumice fall out deposit of the Northwest (NW), North (N), East (E) and South (S) of the Teide - Pico Viejo volcanic complex. Geochronological data from García et al. (2011) and Carracedo et al. (2007). The legend colours fit with the map Fig. 2.

1. 4 Stratigraphy

Stratigraphic reconstruction, along with the variations in thickness and grain size established during the fieldwork, enabled us to identify several pyroclastic deposits at different sites and stratigraphic positions (Fig. 2 and 3; Table1) of these deposits, while some were clearly associated with vents located on the flanks of TPV, the source vent

of others remains unknown. The flank vents on TPV represent an episode of felsic activity that produced about 1.7 ± 0.5 km^3 of phonolitic products from at least 10 satellite vents, located mostly on the NW, N, E and SE flanks of TPV between 2200 and 2600 m a.s.l. and include (in clockwise order) Roques Blancos, El Boquerón, Pico Cabras, Hoya del Abrunco, Montaña Las Lajas, Bocas de Marie, Montaña Blanca, Los Roquillos, Montaña Majua and Montaña de la Cruz (Fig. 1). The flank vents situated in the caldera of Las Cañadas that only emitted mafic magmas were not considered to be part of the TPV complex (Ablay & Martí 2000) given that they are associated with the activity of the rift systems.

Eruption Name	**Years BP**	**Total Erupted volume (DRE)[(b)] in m^3**	**Total Erupted Mass, (kg)**	**Magnitude Scale**
Montaña Reventada	895	138,194,471.1	3,45486E+11	4,54
Roques Blancos	1714-1790	833,890,093.4	2,08473E+12	5,32
Montaña Blanca	2020	107382578,7	2,68456E+11	4,43
ICS [(a)]	***3520***	Unknown	Unknown	Unknown
El Boqueron	2528-5660	44,283,790.64	1,10709E+11	4,04
Abejera Baja	5486	285,594,326	7,13986E+11	4,85
Abejera Alta	5911	361,123,567.2	9.02809E+11	4,96
Pico Cabras	5911-7900	285594326	7,13986E+11	4,85
Abrunco	<10000	2,086,022.525	5,215,056,313	2,72

Table 1. Geochronological data from Carracedo *et al.* (2003, 2007) and García *et al.* (2012). The deposits studied in this paper are shown in grey. [(a)] Dating from the outcrop inside the caldera of unknown origin. [(b)] Dense Rock Equivalent.

For practical purposes, we separated the TPV pumice outcrops into two main groups on the basis of their known or unknown potential vent sources: the pumice deposits that in the field could be traced to known vents were Abejera, Abrunco, Pico Cabras, El Boquerón, Montaña Majua, Montaña Blanca, Roques Blancos and Los Gemelos, while the samples with unknown vents were named as 1600, ICS and Calderón.

The largest fallout deposit is associated with the products of a substantial explosive eruption that occurred on Montaña Blanca on the eastern side of Teide (Fig.2). This deposit corresponds to an intermediate phase of the Montaña Blanca eruption that occurred about 2 ka ago and generated phonolitic domes and lava flows (Ablay *et al.* 1997). This fallout deposit contains well-sorted, pale and angular pumice with a high concentration of lithic fragments of obsidian and lavas. In proximal areas on Montaña Blanca the top of this deposit corresponds to a welded facies consisting of flow-banded, poorly vesiculated obsidian with a relict clastic texture, supporting poorly inflated angular pumice. This pumice fall deposit was interpreted as deriving from a sub-Plinian phase from the main vent at Montaña Blanca that formed a 9-km high eruption column (Ablay 1997; Folch & Felpeto 2005).

A second pumice fallout deposit is to be found inside the caldera of Las Cañadas at the bottom of the Teide volcano and is associated with Montaña Majua, a denuded pumice cone of ca. 700 m in diameter breached to the southeast by the emplacement of a thick lobate phonolite lava flow (~0.03±0.01 km^3). This pumice fallout deposit is a single, well-sorted, reversely graded deposit formed by non-welded angular pumice lapilli with a low content of juvenile obsidian and oxidised lithic fragments of lava. Proximal exposures reveal crude, centimetre-scale stratification and the development of

crystal-rich layers in the basal portions. Distal localities are unstratified. This deposit was classified as Strombolian on the basis of dispersal criteria (Ablay 1997; Ablay & Martí 2000). Part of the Montaña Majua pumice deposits cover part of the slopes of El Teide, 0.6–1.2 km to the northwest.

An extensive pumice fallout field lies on the shoulder between the edifices of El Teide and Pico Viejo and has been associated with the phonolitic domes of Los Gemelos (Ablay *et al.* 1997). This field corresponds to well sorted, bedded, angular, pale-green pumice lapilli fallout deposits, grading upwards locally into densely welded spatter, with a high content of juvenile lithic clasts of obsidian and lavas.

The dome of Roques Blancos on the north-western flank of Pico Viejo (Fig.2) consists of two vents (Balcells & Hernández Pacheco 1989), both of phonolitic composition. Roques Blancos is the most voluminous (0.83±0.1 km^3) of all the compound phonolite lava flows that erupted from the parasitic fissure vents on TPV. It covers an area of 18±2 km^2, extending down the north flank of Pico Viejo and filling in the Icod Valley (Ablay & Martí 2000, Martí *et al*. 2011). There is a pyroclastic succession associated with Roques Blancos that consists of an up-to-65-cm thick lapilli-size pumice fall deposit characterized by poor exposure, with proximal outcrops with a stratified, inversely graded pumice deposit formed by non-welded, micro-vesiculated, angular-to-sub-angular lapilli pumice, with a low (>2 wt%) content of lithic clasts (obsidian and lava fragments). This deposit is discontinuously distributed along the north-western flank of TPV (Fig. 2).

El Boquerón is a dome complex located on the north-western flank of the Pico Viejo stratovolcano close to the Roques Blancos dome complex (Fig. 2). The final eruption of El Boquerón occurred 5600 yBP (García *et al.* 2012) and generated a widely

dispersed pumice fall deposit and 0.04 km^3 of lava flows, which flowed down into the Icod Valley. As in the case of the Montaña Blanca pumice, El Boquerón has been interpreted as being the result of a sub-Plinian eruption with a MER of 6.9–8.2 x 10^5 kg/s, DRE volume of 4–6 x 10^7 m^3 and a 9-km high eruption column (García *et al.* 2012). The pumice deposit is poorly preserved and has poor exposure. It corresponds to a well-sorted deposit composed of non-welded, micro-vesicular, angular-to-subangular, yellow-to-grey lapilli pumice with subordinate lithic clasts of obsidian and phonolitic lavas.

On the north flank of Teide between Abrunco and Pico Cabras (Fig. 2) there is a phonolitic pumice cone, approximately 900 m in diameter, that is breached by the emplacement of a phonolitic lava flow around 200 m to the west. This flow covers part of the pumice cone corresponding to Abrunco, the oldest of the vents on the north flank of TPV (García *et al*. 2011). Associated with this eruption there is a PDC deposit covered by fallout deposit originating from the same eruption (García *et al.* 2011). This pumice fall deposit is composed of well-sorted, yellow-to-grey angular lapilli pumice, with a few obsidian lithic fragments. The distal deposits have mostly been eroded out but in proximal areas may reach up to 2 m in thickness. The PDC deposit is fairly heterogeneous and poorly exposed and has different lithofacies throughout the outcrop (see García *et al*. 2011). This deposits overlies a clastogenic lava flow that was locally eroded by the pyroclastic current during its emplacement.

Other pumice deposits found on the north flank of El Teide are associated to the Pico Cabras and Abejera domes (Fig. 2), two volumetrically significant vent complexes whose lava-flow products extend into the Icod Valley and almost reach the northern cost of Tenerife. Abejera is the youngest of these two domes and consists of two vents

that produced three blocky lava flows of evolved phonolite with a DRE volume of ~0.36 km^3 (Ablay & Martí 2000). Abejera also includes a partially reworked fallout deposit, a few centimetres thick in proximal areas, formed of sub-rounded-to-rounded, poorly vesiculated lapilli pumice, and a few obsidian lithic fragments (4% vol.). On the other hand, Pico Cabras emitted an important lava flow (0.28 km^3 DRE volume) and a few well-preserved, locally reworked outcrops of well-stratified, well-sorted, green-to-grey subangular lapilli pumice, with well-defined stratification. Proximal deposits reach up to 2 m in thickness. However, we found no stratigraphic indicators that could be used to correlate individual layers in the different outcrops and so we describe the Pico Cabras pumice deposits as a single unit.

The ICS deposit is found within the calderas of Las Cañadas, inside the Ucanca depression (Fig. 2). This deposit overlies an older lava flow and consists of a 1.7-m thick yellow, angular, highly vesicular fine lapilli pumice, unconformably overlain by a 40-cm thick red scoria deposit. Between the red scoria deposit and the pumice deposit we found charcoal fragments that give a C^{14} age of 3450 +/- 30 yBP.

Another pumice deposit that is widely distributed on the northern flank of the TPV complex – in particular along the road that runs E-W at an altitude of 1600 m a.s.l (Fig. 2) – consists of a series of disperse outcrops of pumice fall deposits of unknown provenance. All these outcrops have similar lithological, textural and compositional characteristics and so we grouped them in the same deposit (P1600 deposit). Some of these outcrops situated on the eastern side of TPV (Fig. 2) overlie the Pico Cabras lava flow, while towards the west they are located between the Roques Blancos lava flows, as have been describe before. This pyroclastic deposit consists of well-stratified, inversely graded, sub-angular, grey-to-yellow, highly vesicular fine lapilli pumice, with

a few lithic obsidian clasts (>2 wt%), reaching a maximum thickness of 65 cm. Charcoal fragments found in a dark brown soil at the base of this deposit give an age of 1770+/- 80 yBP, the same age as Carracedo *et al.* (2003, 2007) attributed to the Roques Blancos dome. However, field stratigraphic relationships did not provide any convincing evidence that could correlate this pumice deposit with the Roques Blancos vent.

The final pumice deposit of unknown provenance identified in this field survey was found inside El Calderón subsidence structure (Fig. 2) and consists of an asymmetric, circular collapse structure of unknown origin, 30 m in diameter and with a depth of 4 m in its shallowest part and around 15 m in the deepest part (e.g. Araña *et al*. 1989; Ablay & Martí 2000). On the walls of this depression a succession of three pyroclastic units is exposed with a maximum thickness of 77 cm and a 3-m covering of clastogenic lava from Cuevas Negras (Carracedo *et al.* 2007). From top to bottom we distinguished: Unit III, formed of 40 cm of unsorted grey pumice clasts, with variable grain size from lapilli to bomb; Unit II, formed of a 20-cm thick, well-sorted dark grey mafic scoria clasts with lava fragments (6 % volume); and Unit I, formed of a 17-cm thick layer of non-sorted lapilli-to-bomb pumice, yellow-to-grey in colour with highly elongated vesicles, lithic clasts of lavas and obsidian (10 % volume) with its upper 5–8 cm consisting of a red, welded pumice layer. The absence of stratigraphic discontinuities suggests that these three units were deposited continuously, although their origin is unknown. The differences between Unit II (mafic) and the other units (phonolitic) and the absence of any evidence of mixing in the felsic units suggest that the intermediate layer has a different provenance. It is possible that the two eruptions took place at the same time, with Unit II originating from the rift zone and Units I and

III from the TPV complex. This is not unusual in either the TPV record or the pre-TPV Las Cañadas edifice (Ablay & Martí 2000; Edgar *et al.* 2007).

1. 5 Petrology and geochemistry

1. 5.1 Petrographic characteristics:

Representative randomly collected pumice samples from all recognized pyroclastic units from each deposit were examined. All the studied juvenile lapilli pumice samples were microvesicular, glassy and phenocryst poor and in some cases had a total lack of phenocrysts (i.e. Roques Blancos).

The overall phenocryst phases (Table 2) are represented by feldspar (Kfsp, Plg), clinopyroxene (Cpx), biotite (Bt), titanomagnetite (Ttn-Mag), and ilmenite (Ilm); the phenocryst content in the deposits varies between < 0.5 (vol. %) in Pico Cabras and P1600 and 3 (vol. %) in El Boquerón. Feldspar was the most common type of phenocryst found and were euhedral-to-subhedral, with a maximum size of 2 mm and

an average size of 0.5 mm. A certain number of microlites (<100μm) were found in all deposits except in Pico Cabras, El Calderón Unit III and Abrunco, where the microlite content was very low. Clinopyroxene was less abundant, with an average size of 0.65 mm and a maximum size of 2 mm. Biotite was present in the pumice samples (elongate and rectangular shapes) as phenocrysts of around 1 mm and as microlites in the groundmass (<100 μm). Fe-Ti oxides were the least abundant minerals and were always relatively small (around 500–200 μm).

Pumice clasts were moderately-to-poorly vesicular and had heterogeneous textures that varied in terms of their degree of vesicularity and crystallinity. Vesicles ranged in size from a few millimeters to few micrometers and in shape from spherical to elongate or flat. The thickness of the vesicle walls ranged from just a few to tens of micrometres, suggesting the occurrence of high nucleation rates and an expansion-dominated coalescence (Szramek *et al.* 2006). Vesicles were usually preserved, although a few amygdales replenished by secondary mineralization by calcite and, more rarely, by barite were also identified.

In deposits such as those at El Boquerón, El Abrunco and Los Gemelos groundmass crystallinity varies at specimen scale and is correlated with the degree of vesicularity: microlite-poor areas (5 % vol. of microlites) are also vesicle-poor, with only small round vesicles; microlite-rich areas (50 vol. % of microlites) have vesicularity up to 45 % vol. This relationship between vesicles and groundmass crystallinity is probably due to the effects of post-fragmentation expansion or even to clast recycling during less explosive phases (see Wright *et al*. 2006). Microlites consist of acicular sanidine with major axes ranging between 200 and 10 μm, as well as elongated biotite with major axis size of around 200 and 20 μm. Clinopyroxenes were less frequent than microlites and of different shapes (elongate and rectangular), and ranged in size from 200 to 10 μm. Occasionally, microlites were gathered in small groups in the crystal-rich glass, but more commonly were found as individual crystals. Clasts from incipiently welded facies had highly heterogeneous textures with abrupt variations in vesicle size and spherulitic aggregates.

1 5.2 Mineral Chemistry:

Microprobe analysis (phenocrysts and vitric groundmass) was performed on pumice samples from all the different deposits. Clinopyroxene was present in all the pumice samples except in those from P1600, Roques Blancos, ICS and Pico Cabras. Following the classification of Morimoto (1988), most of the phenocrysts analysed correspond to diopside ($Wo_{51-46}En_{40-36}$ Fs_{15-10}), although El Calderón Units I and III correspond to augite (Wo_{45-31} En_{44-40} Fs_{25-15}) (Fig.4a). Most of the diopside crystals show slight normal and inverse zoning in Mg and Fe portions. In Fig.4b the variation diagrams of Mg vs. Fe^{2+} and Fe_2O_3 and SiO_2 vs. MgO for clinopyroxenes are shown and enable the different deposits to be differentiated.

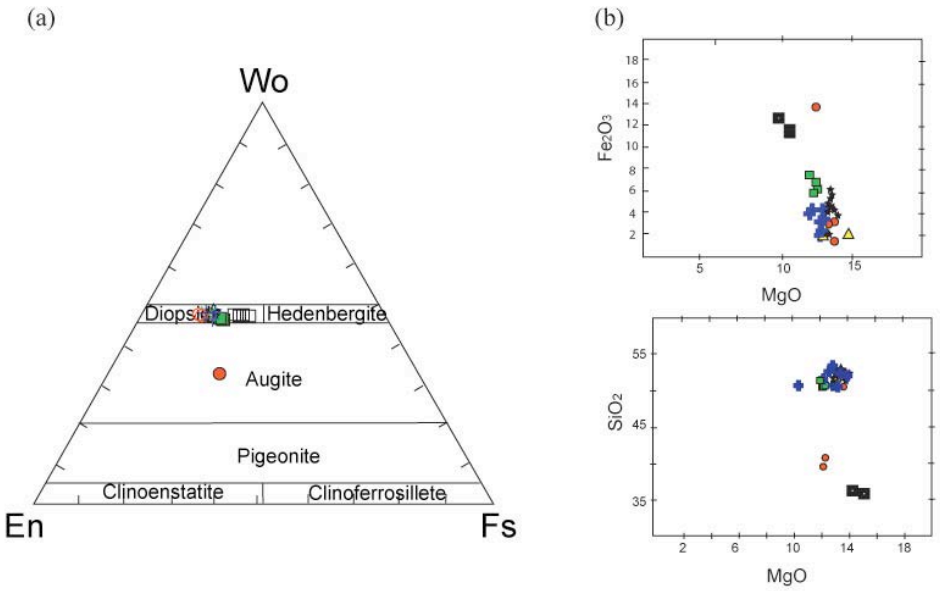

Fig. 4. a) Classification diagram of clinopyroxenes (Morimoto 1988) from the TPV pumice deposits. Clinopyroxene are classified using the total number of cations on a 6-oxygen basis; the Fe_2O_3 was estimated according to the method used by Droop (1987). Red full circles, Calderon Unit I; red empty circles, Calderon Unit III; black squares, Mtn. Blanca; yellow triangles, Mtn. Majua; blue cross, El Boquerón; green squares, Los Gemelos; black stars, Abrunco PDC; white starts, Abrunco (fall out). b) Selected correlation diagrams of core analysis from the clinopyroxenes of the TPV pumice deposits SiO_2 vs. MgO, and Fe_2O_3 vs. MgO.

Feldspar phenocrysts occur in all pumice deposits except those of El Calderón Unit III and Pico Cabras; their composition ranges from anorthoclase to sanidine and, exceptionally, oligoclase (El Calderón Unit I) (Fig. 5). Alkali feldspar of sanidine composition was found in the deposits from Montaña Blanca, P1600 and Abrunco but was not as common as anorthoclase, which were found in most of the studied deposits (Los Gemelos, Montaña Majua, Abrunco, ICS, Montaña Blanca and El Boquerón). Microprobe profile analyses performed on different feldspar phenocrysts showed zonation patterns in both the sanidine and the anorthoclase crystals. Analyses of feldspar crystal cores are shown in Fig. 5.

All the biotite crystals correspond to Mg and Ti-rich biotite and were present in the Los Gemelos, El Boquerón, Pico Cabras, ICS, Montaña Majua and El Calderón Unit I deposits (Fig.6a). The highest Mg and Ti content was found at ICS and Montaña Majua. (Fig.6b).

Fe-Ti oxides correspond to spinels (magnetite and ilmenite). Titano-magnetite compositions range from $Ups_{41.95}$ to $Ups_{56.71}$ and vary from one deposit to another: El Boquerón $Usp_{54.58}$; Majua $Ups_{47.39}$; Los Gemelos $Ups_{52.18}$; Pico Cabras $Ups_{46.75}$, Abrunco PDC $Ups_{42.98}$, Abrunco CMP $Ups_{41.95}$, El Calderón unit I $Ups_{56.71}$ and Montaña Blanca Ups $_{52.80,}$ (Fig.7). Ilmenite compositions range from $Ilm_{88.58}$ to $Ilm_{93.28}$: El Boquerón $Ilm_{93.21}$, Majua $Ilm_{91.63}$; Gemelos $Ilm_{93.28}$; Abrunco $Ilm_{89.07}$.

1. 5.3 Whole rock Geochemistry:

Representative whole rock analyses of the studied pumice deposits are given in Table 3 and Fig. 8. All the pumice samples studied from the TPV succession had a peraluminous (A/CNK >1) phonolitic-to-trachy-phonolitic composition, with a SiO_2 content ranging from 51.21 to 60.56 wt %, and a total alkali content (Na_2O+K_2O) between 10.46 and 15.12 wt %.

These pumice deposits show the typical geochemical features of evolution by fractional crystallisation, as indicated by the corresponding positive and negative correlations between major and trace elements (Figs. 11 and 12) that occurs in the TPV phonolitic lavas (Ridley 1970; Araña *et al*. 1989; Andújar *et al*. 2010; Wiesmaier *et al*. 2011).

Trace elements including REE show a similar pattern in all samples (Figs. 11 and 12) albeit with some differences in the concentration of Ba, Sr, Ti and P, which are more evident for the samples from El Calderón Unit I, ICS, Montaña Majua, and Abrunco PDC. There is also a slight departure from the general REE pattern in these samples (Fig. 12), showing subtle to absent Eu anomalies.

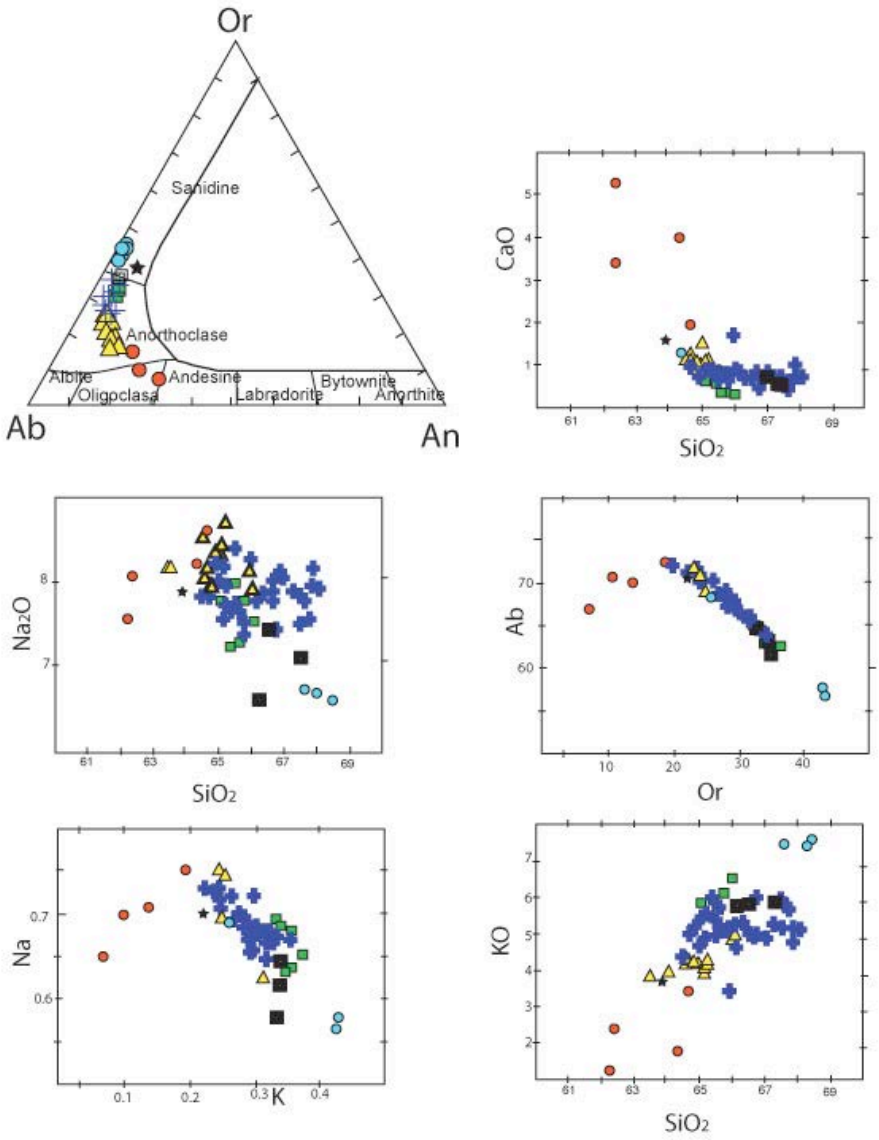

Fig. 5. Classification diagram of the feldspar (Ab-An-Or) TPV pumice deposit. The formula composition was calculated on an 8-oxygen basis following the method described by Deer *et al.* (1992). Major elements diagram of the feldspar core analysis: SiO_2 vs. K_2O, Na_2O, CaO_2. Red circles, Calderon Unit I; black squares, Mtn. Blanca; blue circles, P1600 deposit; blue cross, El Boquerón; green squares, Los Gemelos; black stars, Abrunco PDC; white starts, Abrunco (fall out).

Table 3: Selected whole-rock analyses fro representantive pumice deposits.

Unit	Boqueron					Pico Cabras			Calderon	
Sample	P.U.L	B.H11	B.RT	B.RTJ1	B.RTJ2	PC.H4	P.CABRAS.C	PC-1	CALD.N.1	CALD.N.3
Locate (Lat/long)	335411E 3132795N	335636E 3131111N	335487E 3131660N	335290E 3131613N	335290E 3131613N	338793E 3132399N	339622E 3133287N	338715E 3132788N	334745E 3127300N	334745E 3127300N
SiO2	57,44	57,31	58,44	56,84	57,01	57,92	58,91	58,63	56,25	58,89
TiO2	0,687	0,679	0,628	0,696	0,694	0,662	0,633	0,628	1,129	0,760
Al2O3	19,43	19,44	18,90	19,43	19,28	19,10	18,89	18,90	19,63	19,06
FeO*	3,40	3,35	3,51	3,41	3,41	3,58	3,50	3,49	4,52	3,68
MnO	0,196	0,189	0,195	0,185	0,181	0,199	0,197	0,198	0,177	0,189
MgO	0,37	0,38	0,34	0,38	0,40	0,38	0,32	0,35	0,89	0,49
CaO	0,80	0,78	0,75	0,83	0,84	0,77	0,74	0,74	2,05	1,03
Na2O	8,53	8,76	9,07	8,34	8,53	8,83	9,18	9,26	8,66	9,34
K2O	5,14	5,23	5,42	5,02	5,08	5,30	5,45	5,46	4,76	5,36
P2O5	0,097	0,083	0,081	0,100	0,093	0,094	0,084	0,083	0,267	0,125
Sum	96,09	96,20	97,33	95,23	95,52	96,82	97,92	97,74	98,31	98,92
LOI (%)	3,79	2,92	2,35	4,11	3,64	2,21	1,94	1,63	0,99	1,24
Ni	3	2	3	3	2	3	3	3	5	3
Cr	1	2	2	3	3	4	2	4	0	1
Sc	1	0	1	1	2	1	2	2	1	2
V	15	14	8	14	17	13	7	9	18	16
Ba	113	94	24	135	129	47	26	29	1393	134
Rb	170	173	170	165	169	166	171	168	134	163
Sr	16	15	7	19	26	12	7	5	426	77
Zr	1047	1024	989	1031	1025	985	992	991	759	934
Y	37	37	38	37	37	37	38	38	35	36
Nb	236	231	225	234	232	225	226	226	199	217
Ga	28	30	29	28	29	29	29	28	27	28
Cu	2	1	1	2	1	1	2	2	3	3
Zn	118	121	125	114	114	127	126	126	114	123
Pb	21	21	20	20	20	20	20	20	20	18
La	112	106	112	108	108	110	108	110	105	108
Ce	191	193	186	192	191	188	187	189	181	186
Th	31	30	28	31	31	28	28	29	25	26
Nd	58	55	56	56	56	55	54	57	58	54
U	8	8	8	8	7	6	8	6	6	8

Table 3. Whole rock analyses of pumice deposits in Teide - Pico Viejo volcanic complex.

Table 3: continued

Unit	Abejera	P.1600								
Sample	M.A.P	P1600.ANL1	P.1600ANL2	P.1600ANL3	P.1600ANL4	P.1600ANL5	ROQ.BLAN.6	ROQ.BLAN.7	ROQ.BLAN.8	P1600.32
Locate (Lat/long)	340144E 3131919N	339467E 3133283N	339619E 3133302N	339181E 3133290N	336669E 3132612N	335519E 3132838N	334423E 3132503N	332773E 3132085N	335025E 3133164N	336600E 3132532N
SiO2	56,72	58,37	58,51	58,31	57,79	58,35	58,11	57,97	57,99	58,64
TiO2	0,776	0,635	0,634	0,635	0,647	0,625	0,632	0,627	0,638	0,628
Al2O3	19,67	18,86	18,84	18,95	19,01	18,73	19,00	18,72	19,02	18,81
FeO*	3,92	3,53	3,48	3,52	3,53	3,37	3,48	3,55	3,57	3,45
MnO	0,193	0,197	0,197	0,197	0,198	0,196	0,193	0,195	0,197	0,197
MgO	0,45	0,35	0,34	0,34	0,35	0,34	0,34	0,33	0,34	0,33
CaO	0,94	0,75	0,76	0,74	0,77	0,74	0,78	0,76	0,74	0,74
Na2O	8,23	9,12	9,15	9,12	8,90	8,97	8,94	8,97	8,80	9,09
K2O	4,93	5,42	5,44	5,42	5,31	5,40	5,30	5,35	5,33	5,47
P2O5	0,142	0,087	0,082	0,084	0,100	0,083	0,079	0,085	0,092	0,083
Sum	95,96	97,31	97,43	97,33	96,61	96,82	96,87	96,55	96,72	97,44
LOI (%)	3,97	1,94	1,88	1,88	2,63	2,45	2,40	2,29	2,93	2,14
Ni	3	3	3	3	3	3	2	4	3	3
Cr	4	3	2	2	2	1	2	1	2	2
Sc	2	1	1	1	1	1	0	1	1	1
V	18	11	9	9	9	12	9	10	11	9
Ba	134	24	24	24	37	28	26	24	40	26
Rb	155	169	171	169	165	168	167	169	169	171
Sr	61	6	8	6	13	7	7	7	8	4
Zr	991	990	986	989	991	979	991	984	1001	991
Y	35	38	37	37	38	37	38	37	36	37
Nb	226	226	225	225	225	223	226	225	226	226
Ga	28	28	29	30	29	29	30	29	30	30
Cu	3	2	1	1	2	1	5	1	2	2
Zn	122	125	124	122	125	124	123	123	124	129
Pb	20	20	19	20	21	20	19	21	20	20
La	105	110	105	110	111	105	111	105	106	111
Ce	184	191	190	187	191	191	190	188	186	190
Th	29	28	28	29	29	28	28	28	29	28
Nd	55	58	55	54	57	56	58	57	55	56
U	7	6	10	7	8	7	6	7	9	7

Table 3. Whole rock analyses of pumice deposits in Teide - Pico Viejo volcanic complex.

Table 3: continued

Unit	Montaña Blanca	ICS	Gemelos		Majua		Abrunco	
Sample	MTNBLANCA	ICS	Gemelos2	GEMELOS3	M.M.1	M.M.2	PDC	FALL OUT
Locate (Lat/long)	341702E 3128019N	332586E 3125928N	336413E 3127941N	336595E 3128168N	340736E 3126130N	340144E 3126170N	339798E 3132411N	334002E 3132228N
SiO2	58,35	57,36	58,95	58,82	55,69	58,45	59,68	58,80
TiO2	0,623	0,780	0,660	0,644	0,883	0,692	0,767	0,764
Al2O3	19,19	19,39	19,17	19,42	20,01	19,13	18,95	18,82
FeO*	3,53	3,07	3,63	3,58	3,84	3,28	3,06	2,98
MnO	0,200	0,166	0,190	0,201	0,191	0,191	0,167	0,167
MgO	0,31	0,43	0,38	0,32	0,58	0,38	0,44	0,44
CaO	0,71	0,91	0,76	0,72	0,96	0,79	0,86	0,86
Na2O	9,41	7,42	9,30	9,49	7,54	8,81	9,05	8,55
K2O	5,41	4,84	5,40	5,42	4,65	5,41	5,32	5,26
P2O5	0,072	0,128	0,081	0,076	0,168	0,105	0,108	0,104
Sum	97,79	94,48	98,54	98,67	94,52	97,22	98,39	96,74
LOI (%)	1,85	4,77	1,47	1,37	4,27	2,81	1,55	2,37
Ni	3	3	3	2	6	3	2	2
Cr	2	3	5	1	6	1	2	1
Sc	0	1	1	0	0	1	0	2
V	7	18	12	12	25	12	18	20
Ba	16	559	52	26	416	102	570	563
Rb	179	150	174	174	145	175	154	153
Sr	3	36	14	6	72	10	17	17
Zr	1065	858	1023	1059	922	1007	837	828
Y	39	30	39	40	36	37	30	29
Nb	242	190	234	242	207	228	185	184
Ga	31	26	29	30	27	29	27	26
Cu	1	0	3	2	5	2	1	0
Zn	131	99	127	130	119	122	107	106
Pb	22	17	21	23	19	20	16	17
La	112	97	110	118	106	107	94	94
Ce	198	162	193	199	189	188	163	163
Th	32	25	30	32	28	29	25	25
Nd	60	46	57	60	57	57	48	49
U	8	7	8	10	8	8	7	7

Table 3. Whole rock analyses of pumice deposits in Teide - Pico Viejo volcanic complex.

1 6 Discusion

Our detailed field study enabled us to identify a number of new phonolitic pyroclastic deposits associated with the recent (Holocene) eruptive history of the TPV complex. The presence of these deposits and the previously studied deposits generated by the Montaña Blanca (Ablay *et al.* 1995) and El Boquerón (García *et al.* 2012) eruptions thus confirm the significance of explosive volcanism in TPV. Although some of the pyroclastic deposits identified in this study can be clearly correlated in the field with their corresponding vents located on the flanks of the Teide and Pico Viejo stratovolcanoes, others are of unknown origin.

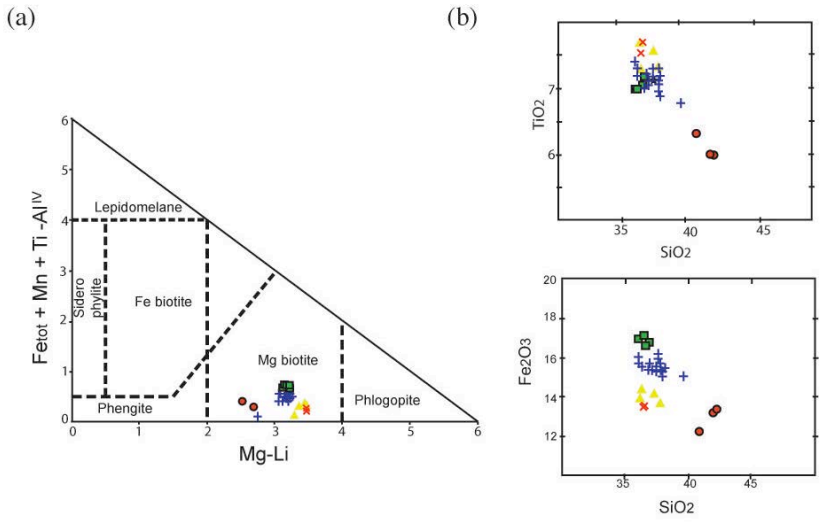

Fig. 6. a) Plot of the studied samples in the classification diagram for micas (Tieschendorf 1995). The micas were calculated on a 24-oxygen basis and 4 OH group following the method described in Deer *et al.* (1992). All the samples from TPV are classified as Mg- Biotite using Tieschendorf's (1995) classification. The estimate for Li_2O is based on Yavurt *et al.* (2001) and the equation Li_2O wt.%=155*$(MgO)^{-3.1,}$ for SiO_2>34 wt%; and MgO>6wt%. b) Haker diagrams of biotite analysis, SiO_2 vs. Fe_2O_3 and SiO_2 vs. TiO_2. Yellow triangles, Montaña Majua; red cross, ICS deposit; blue circles, El Boquerón; green squares, Los Gemelos; red circles, Calderón Unit I.

The use of existing stratigraphic (Ablay & Marti 2000; Carracedo *et al*. 2007) and geochronologic (Carracedo *et al*. 2007) data from the TPV complex and comparisons with the new field data enabled us to establish the stratigraphy of these pyroclastic deposits, which all date from the Holocene.

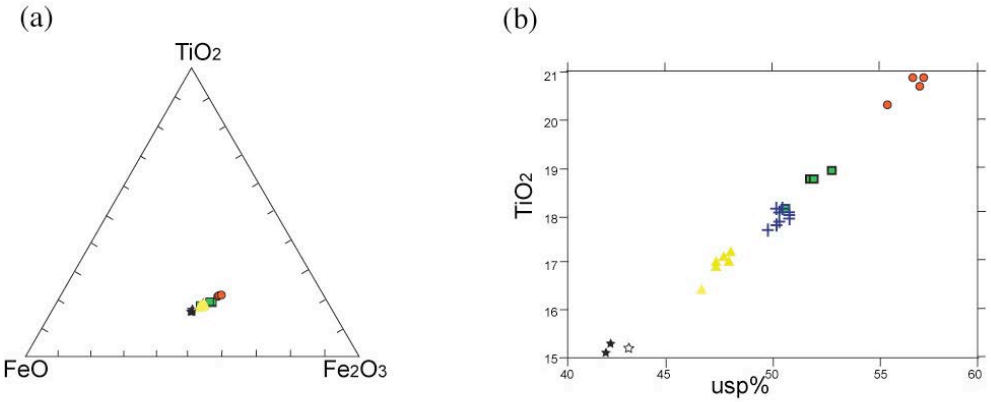

Fig. 7. Plots of Fe and Ti oxide compositions: a) FeO-TiO_2-Fe_2O_3 diagram. b) Usp% vs. TiO_2 diagram. Magnetite and ilmenite formulas were calculated on a 4-oxygen basis; the total FeO was recalculated following Carmichael's (1967) method. Red circles, Calderon Unit I; yellow squares, Mtn. Majua; blue cross, El Boquerón; green squares, Los Gemelos; black stars, Abrunco PDC; white starts, Abrunco (fall out).

According to the stratigraphic relationships, the P1600 pumice deposit could be related to either Pico Cabras or Roques Blancos. This deposit overlies the lavas from these two eruptions but is closest to the pumices from Roques Blancos in terms of its geochemical and petrological characteristics. Pico Cabras dates from more than 5911 yBP (see Fig. 3; Table 1) and so cannot be related to Roques Blancos. In fact, this latter eruption dates from 1714 yBP (Carracedo *et al.* 2007), which is similar to the age we

obtained for the P1600 deposits (1770+/- 80 yBP) (see Fig.3; Table 1). Therefore, we propose that the P1600 pumice deposit is a distal facies of the Roques Blancos eruption.

The other two deposits of unknown origin, ICS and El Calderón, could not be correlated to any known vent area using either field stratigraphic criteria or a mineralogical or geochemical basis. In the case of the deposits in El Calderón, we mention above that the interbedding of mafic and felsic units could indicate the occurrence of two simultaneous eruptions, one from the north-western rift zone and the other from the central complex, respectively. However, we failed to find any evidence that could correlate the units in El Calderón with any specific eruption or vent site. Another possibility would be to associate the sequence at El Calderón with a single eruption generating both mafic and felsic magmas. A more recent example of this type of eruption is the Montaña Reventada, a young flank eruption developed from a fissure vent system on the western flank of Pico Viejo. It generated a composite lava flow consisting of lower basanite and upper trachy-phonolite units. Previous studies have suggested that the Montaña Reventada erupted from the transition zone between two separate plumbing systems, that is, the phonolitic system of the TPV complex and the basanite north-western rift zone, which would explain the evolution of the exposed lavas but not the associated explosive deposits (Araña *et al*. 1994; Wiesmaier *et al*. 2011).

The ICS deposits found in the interior of the Ucanca depression in the caldera of Las Cañadas cannot be clearly correlated to any known vent. The similar biotite composition in the ICS and Montaña Majua deposits (Fig. 7) suggest that these deposits have a common origin. This genetic relationship is also suggested by the similar patterns in the trace and REE elements present in both deposits (Figs. 13 and 14).

However, the Montaña Majua deposits disperse southeast from the vent (Ablay *et al*. 1997; Ablay & Martí 2000), thus making any correlation with the ICS deposit located to the west unlikely (Fig. 2). Although the deposits at Montaña Blanca, Los Gemelos and Montaña Majua have been related by Ablay *et al.* (1997) to the same eruptive event (albeit to different vents), our data do not support this assumption. The mineralogical and geochemical composition of these deposits (Figs 5, 6, 8 and 9) is sufficiently different to attribute them to different eruptive events originating from different magma pockets. In addition, Carracedo *et al*. (2007) propose different ages for these three deposits and so they should be considered as corresponding to different eruptions.

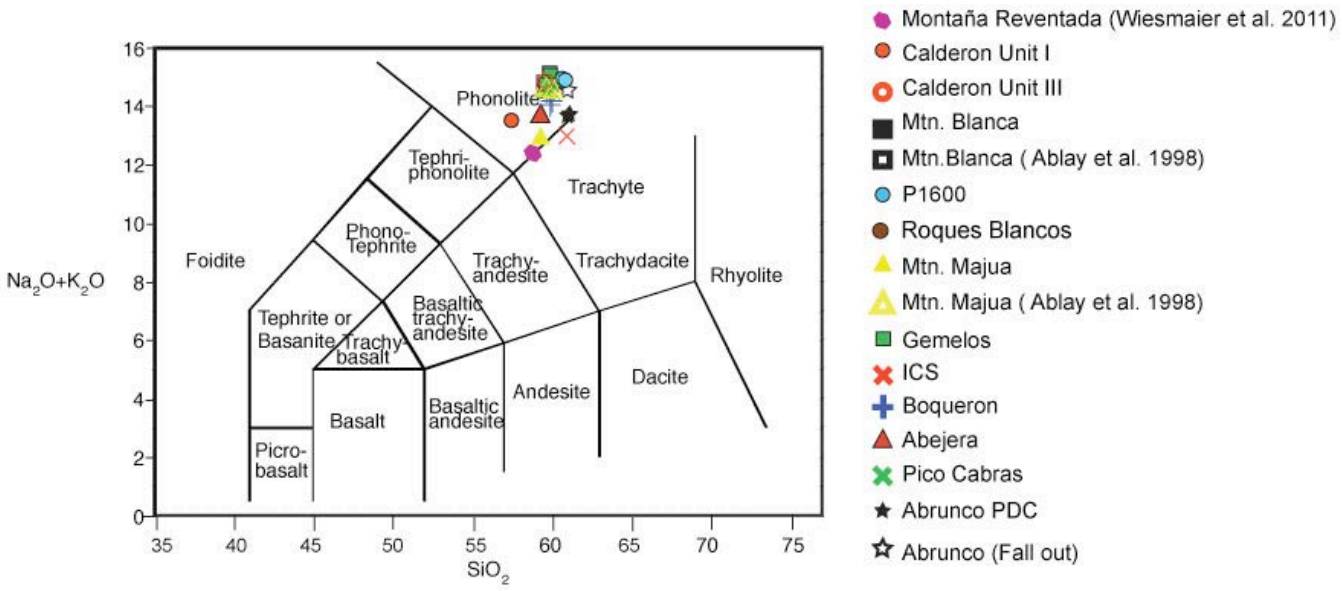

Fig. 8: Total alkalis-silica classification diagram (le Bas *et al.* 1986). Diagrams include some data from Ablay *et al.* (1998) for comparison.

Therefore, despite their apparent compositional homogeneity, whole rock geochemistry and mineral chemistry allow us to distinguish different deposits and to

identify them as originating from different eruptions. Thermodynamic constraints show how sensitive the TPV phonolitic magmas are to changes in their constitutive parameters (Andújar *et al*. 2013). As well, stress studies on TPV systems have shown that each eruption is fed by a different batch of phonolitic magma that accumulated in a different position inside the edifice. This implies that different eruptions may produce deposits that are slightly different in composition. In a general sense the studied rocks can be divided roughly into two groups, a relatively more evolved group (Pico Cabras, El Boquerón, Los Gemelos, Montaña Blanca, P1600) and a less evolved group (El Calderón, Abrunco PDC and CMP, ICS, Abejera, Montaña Majua), a classification that coincides with mineralogical compositions. Major and trace element compositions suggest that all studied deposits derive from cogenetic magmas and that the existing differences correspond to different evolutionary histories of the final pre-eruptive stages, which may include differences in the position of each phonolitic reservoir, in the oxygen fugacity or in the existence or otherwise of pre-eruptive mixing with deeper magmas (see Ablay *et al*. 1997; Martí *et al.* 2008, Martí & Geyer 2009; Wiesmaier *et al.* 2012; Andujar *et al.* 2013). The REE contents do not define these groups quite so clearly but do nevertheless indicate that the deposits at ICS, El Calderón Unit I and Abrunco depart slightly from the general trend. (Figs. 11 and 12) Consequently, mineralogical and geochemical correlations as well as field relationships can be useful tools for determining the stratigraphic constraints of the studied deposits.

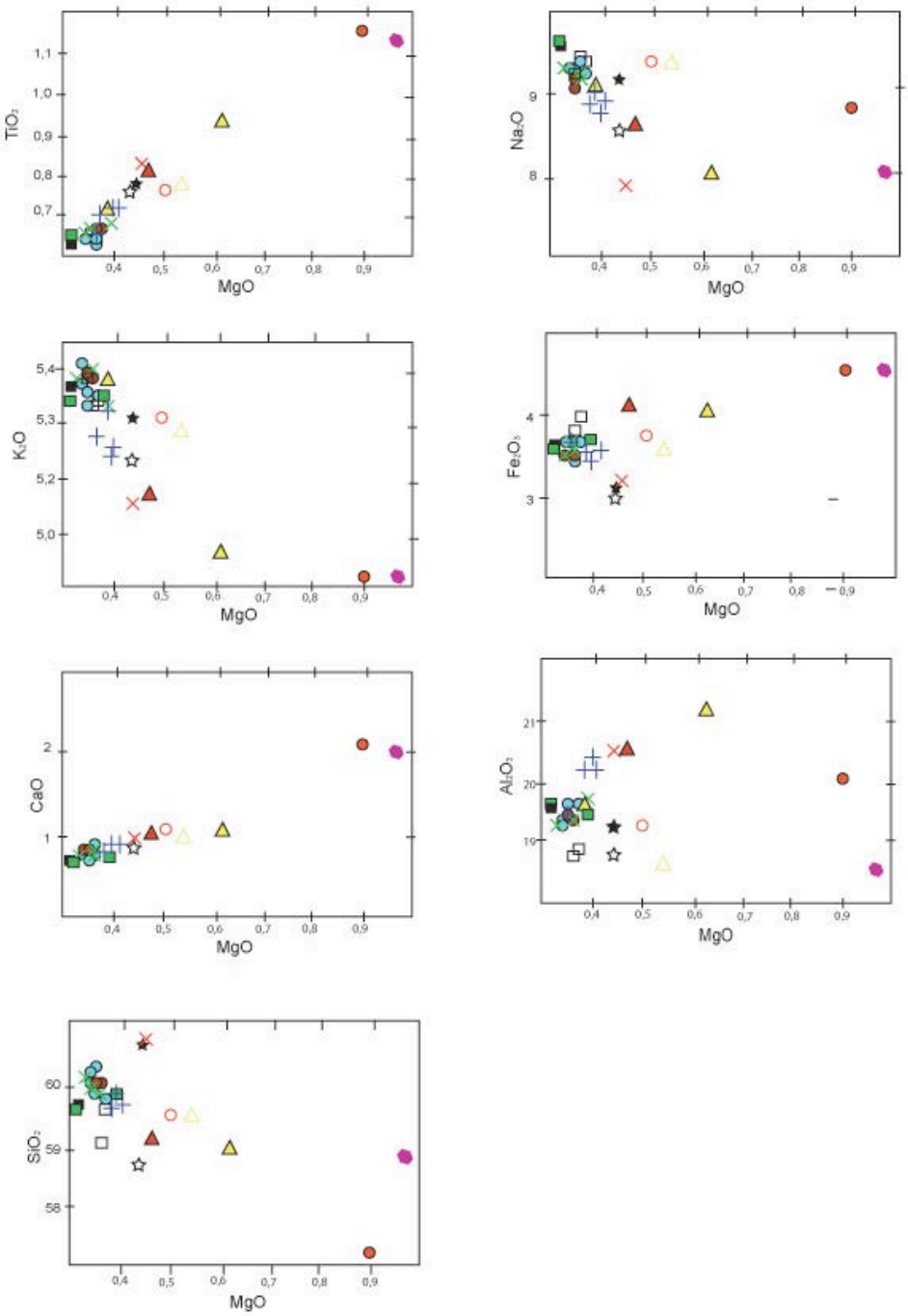

Fig. 9: Variation of selected major oxides vs. MgO (wt%) for TPV pumice deposits. Three analyses from Montaña Blanca and Montaña Majua by Ablay *et al.* (1998) have been included.

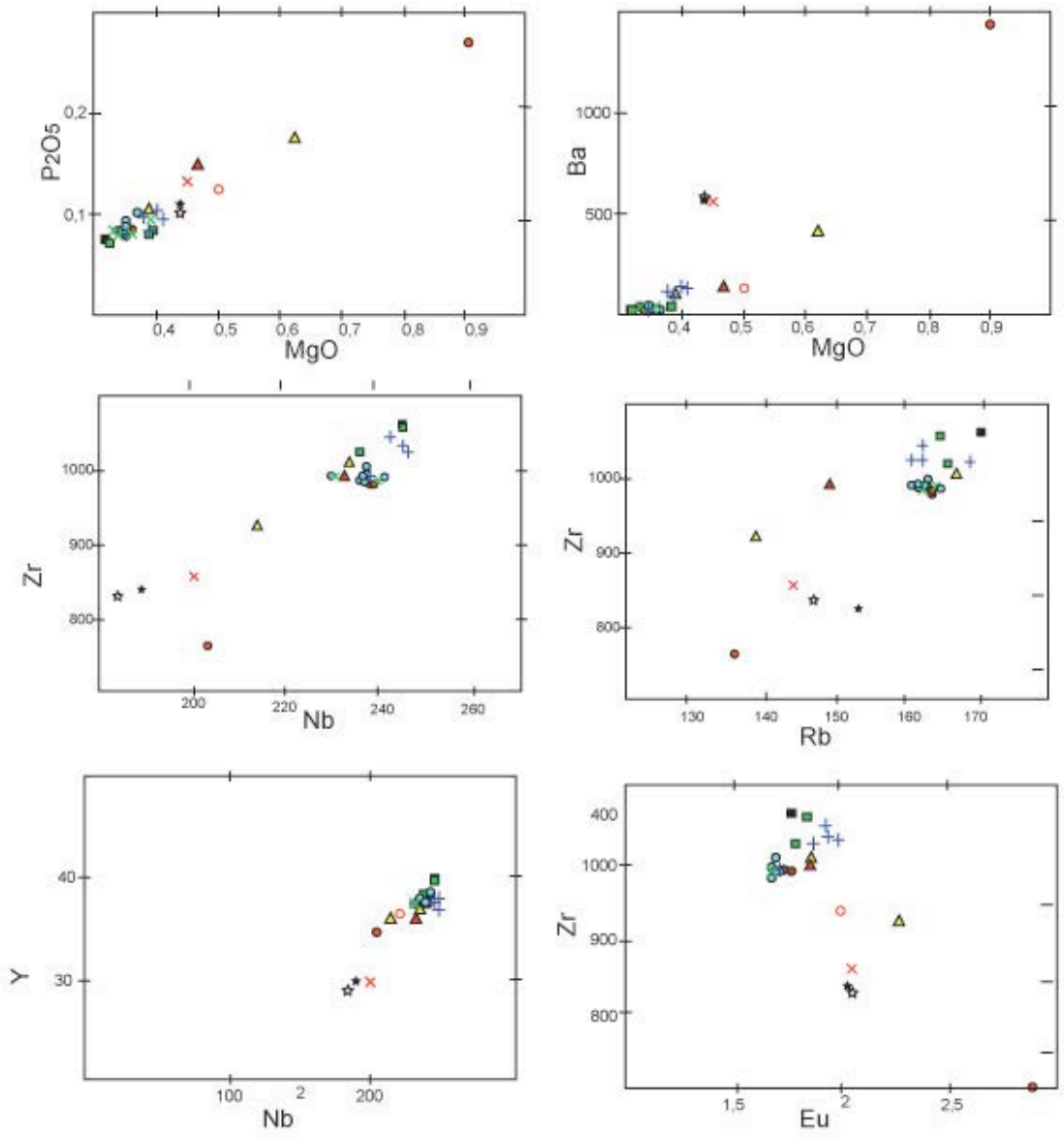

Fig. 10: Variation diagrams of selected trace elements vs. MgO and Zr (wt%) for TPV pumice deposits. Red full circles, Calderon Unit I; red empty circles, Calderon Unit III; black square, Montaña Blanca; blue circle, P1600 deposit; brown circle, Roques Blancos; yellow triangles, Montaña Majua; green squares, Los Gemelos; red cross, ICS deposit; blue cross, El Boquerón; red triangles, Abejera deposit; green cross, Pico Cabras; black stars, Abrunco PDC; white starts, Abrunco (fall out).

All the deposits that can be correlated with their respective vents (Montaña Blanca, El Boquerón, Roques Blancos, Los Gemelos, Montaña Majua, Abrunco, Pico Cabras and Abejera) are also associated with the extrusion of lavas and/or domes of, in some cases, significant volume and extension. This indicates that in all these cases the explosive volcanism corresponded to complex eruptions that also included effusive episodes. In some cases the explosive phase occurred at the beginning of the eruption (Montaña Majua, El Boquerón, Abrunco and Los Gemelos), while in others it took place at the end (Pico Cabras and Abejera) or even during an intermediate stage (Montaña Blanca and Roques Blancos). This implies that, despite the relatively similar composition of their magmas, these eruptions had different dynamics, possibly as a consequence of local variations in the gas content of the erupting magma in pre-eruptive and eruptive degassing conditions and/or in the pre-eruptive conditions. It is also worth mentioning that none of the eruptions with identified vents occurred from the central vents. This also suggests that different eruption behaviours may have governed both flank and central eruptions. Despite using different approaches, both Martí & Geyer (2009) and Andújar *et al.* (2013) were able to demonstrate that flank eruptions are fed by reservoirs located at different depths and are subject to different stress conditions from those feeding central eruptions.

The fact that all the studied deposits date from the Holocene raises the question as to whether the TPV complex is entering a more explosive stage, as has been suggested by Martí *et al.* (2008). Even though the erosion on the northern side of TPV is quite severe and has affected the pyroclastic deposits in this sector, it seems unlikely that older deposits – if they exist – would have been completed removed. It seems more

plausible to suggest that no pyroclastic deposits were produced in previous phonologic eruptions from TPV.

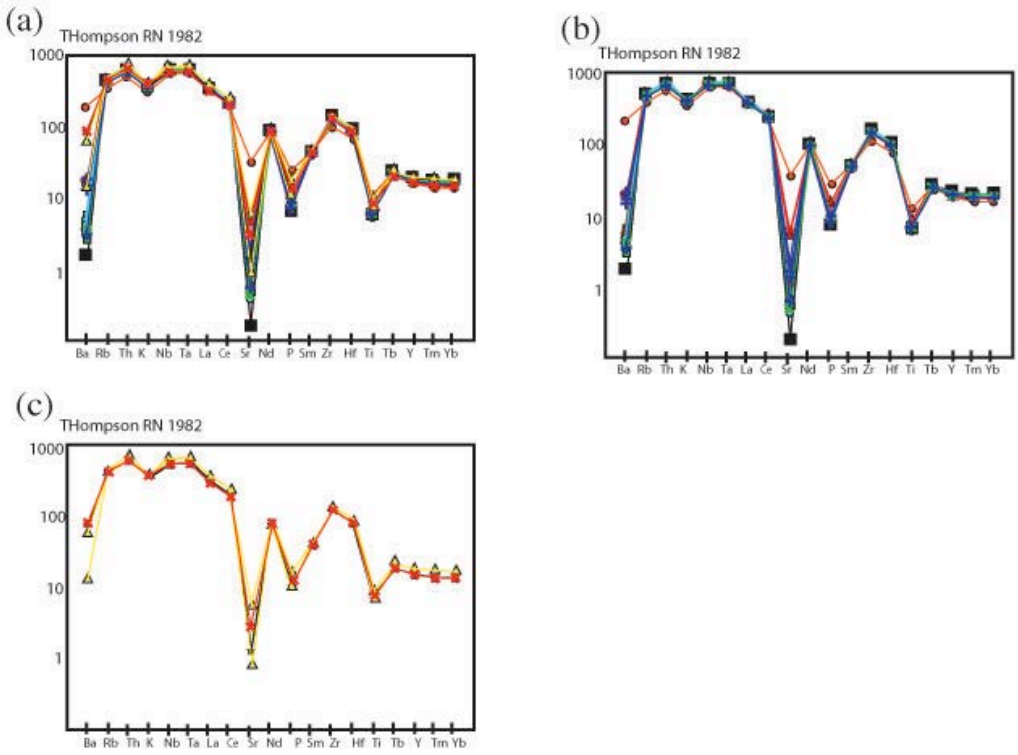

Fig. 11: Multi-element variation diagram for the pumice deposits in the TPV complex, normalized to chondrite values as per Thompson *et al.* 1982. a) Analysis of all the pumice deposits; b) Abrunco (black-and-white star), ICS (red cross), Majua (yellow triangles); c) Montaña Blanca (black square), El Boquerón (blue cross), Pico Cabras (green cross), Los Gemelos (green square), P1600 (blue sphere), Roques Blancos (brown sphere), Abejera (red triangles) and Calderón Unit I (orange sphere).

Furthermore, we were unable to find any TPV pyroclastic deposits older than those identified in this study inside the calderas of Las Cañadas. Likewise, previous studies that used information from water boreholes drilled inside the caldera reported no such type of deposits (Ablay & Martí 2000). All these findings tend to support the idea that the explosive character of TPV has increased during the Holocene. This agrees with

the petrological evolution from basanites to phonolites shown by TPV magmas (Ablay *et al.* 1997; Wiesmaier *et al.* 2012) and the tendency over time to move towards more evolved phonolitic terms that are richer in volatiles (Ablay *et al.* 1997).

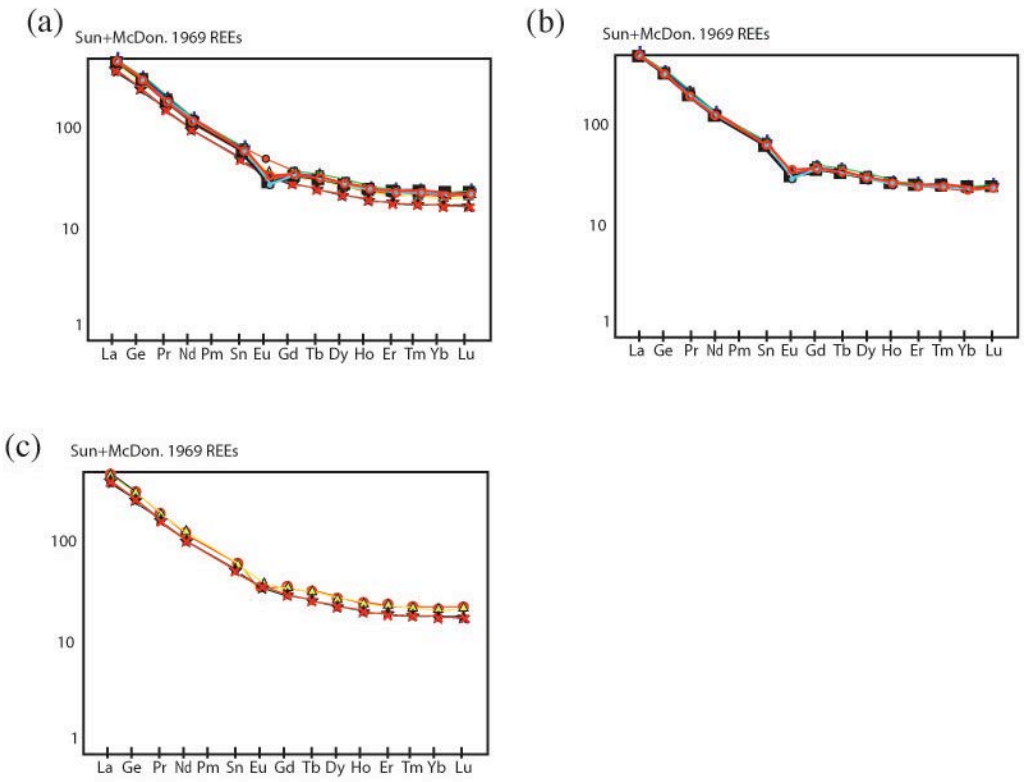

Figure 12: Multi-element variation diagram for the pumice deposits of the TPV complex, normalized to primitive mantle values as per McDonough and Sun (1969). a) Analysis of all the pumice deposits; b) Abrunco (black-and-white star), ICS (red cross), Majua (yellow triangles); c) Montaña Blanca (black square), El Boquerón (blue cross), Pico Cabras (green cross), Los Gemelos (green square), P1600 (blue sphere), Roques Blancos (brown sphere), Abejera (red triangles) and Calderón Unit I (red sphere).

1. 7 Conclusion

We have demonstrated the existence of at least eleven Holocene phonolitic explosive episodes, ranging from Strombolian to sub-Plinian, associated with the TPV complex. Field and petrological data have permitted us to establish the relative stratigraphy of these deposits and to place them within the general stratigraphy of the TPV that has been proposed in previous studies. The presence of these phonolitic pyroclastic deposits in the recent stratigraphy of Teide demonstrates that phonolitic explosive activity is more significant than previously thought and represents an important hazard for the island of Tenerife. Moreover, the fact that all the studied deposits date from the Holocene and that no older deposits of similar characteristics have been identified in this study suggest that the TPV complex is entering into a more explosive stage, which coincides with the evolution shown by the different phonolitic cycles identified in the pre-TPV Las Cañadas edifice.

2. Pyroclastic density currents from Teide-Pico Viejo (Tenerife, Canary Islands): implications for hazard assessment.

This paper has been published in Terra Nova. The authors of the papers are:

Olaya García, Centro Geofísico de Canarias del I.G.N. C/La Marina 20, 2º, 38001 S/C de Tenerife, Spain

Joan Martí, Instituto de Ciencias de la Tierra Jaume Almera, CSIC, Lluis Solé Sabarís s/n, 08028 Barcelona, Spain.

Gerardo Aguirre-Diaz, Centro de Geociencias, Campus UNAM-Juriquilla, Querétaro, Querétaro CP 76230, México

Adelina Geyer, Instituto de Ciencias de la Tierra Jaume Almera, CSIC, Lluis Solé Sabarís s/n, 08028 Barcelona, Spain.

Ilazkiñe Irribaren, Centro Geofísico de Canarias del I.G.N. C/La Marina 20, 2º, 38001 S/C de Tenerife, Spain

The reference of this paper is: García O, Martí J, Aguirre-Díaz G, Geyer A, Iribarren I (2011) Pyroclastic density currents from Teide-Pico Viejo (Tenerife, Canary Islands): implications on hazard assessment. TerraNova 23:220-224. doi: 10.1111/j.1365-3121.2011.01002.x

2. 1 Introduction

Teide-Pico Viejo twin stratovolcanoes, on the island of Tenerife, form one of the largest active volcanic complexes in Europe. Their eruptive activity has traditionally been considered as effusive (Ablay and Martí, 2000, Carracedo et al., 2007), with the only exception of the subplinian eruption of Montaña Blanca, that occurred about 2000 years ago (Ablay et al., 1995), and minor pyroclastic deposits of unknown origin. This belief has led to assume that volcanic hazard at Teide-Pico Viejo is mostly related to the emplacement of lava flows (Carracedo et al., 2007), which according to their field and physical characteristics correspond to relatively cold, slow-motion flows, with fronts of several tens of metres thick, and run-out distances up to 15 km. However, a recent revision of the past history of Teide-Pico Viejo (Martí et al 2008), reveals the explosive activity related to phonolitic magmas has been more significant than initially thought, so that their potential for generating explosive eruptions in the near future should not be neglected.

We have conducted a detailed field revision of Teide-Pico Viejo products, focussing in particular on those derived from explosive eruptions of phonolitic magmas. We have concentrated our study mostly on the northern side of Teide-Pico Viejo, an inaccessible and relatively unexplored area, which is poorly known, compared to other sectors of these volcanoes.

We have able to identify and document for the first time the presence of several pyroclastic density current (PDC) deposits associated with different explosive episodes of Teide-Pico Viejo. The PDC deposits observed include ignimbrites and block and ash deposits, which derive from markedly different eruption and emplacement mechanisms.

We describe the field characteristics and discuss their origin and significance in the volcanological evolution of Teide-Pico Viejo. Finally, we evaluate the importance of the presence of these deposits in terms of hazard assessment at Teide- Pico Viejo.

2.2 Volcanic evolution of Teide-Pico Viejo

Teide–Pico Viejo stratovolcanoes started to grow c. 180–190 ka ago within the Las Can˜ adas caldera (Fig. 1) (Ablay and Martı, 2000). This central volcanic complex originated from the interaction of two di*ff*erent magmatic systems that evolved simultaneously, giving rise to a complete series from basalt to phonolite (Ablay et al., 1998; Martıí et al., 2008). The structure and volcanic stratigraphy of the Teide– Pico Viejo stratovolcanoes were characterized by Ablay and Martıí (2000), based on a detailed field and petrological study. More recently, Carracedo et al. (2007) have provided the first group of isotopic ages from Teide–Pico Viejo products.

The eruptive history of the Teide– Pico Viejo comprises a main stage of eruption of mafic to intermediate lavas that form the core of the volcanoes and also infill most of the Las Cañadas depression and the adjacent La Orotava and Icod valleys (Fig. 1). About 35 ka ago phonolites became predominant at Teide–Pico Viejo. These felsic eruptions occurred from central and flank vents, range in volume from 0.01 to 1 km^3 (DRE), and have mostly generated thick lava flows and domes. Most of the phonolitic eruptions from Teide–Pico Viejo show signs of magma mixing, suggesting that they were triggered by intrusion of basaltic magmas into shallow phonolitic reservoirs (Martıí et al., 2008). In addition, basaltic eruptions have also occurred from the flanks or the central vents of the Teide-Pico Viejo stratovolcanoes alternating with phonolitic

volcanism.

2.3 Pyroclastic density current deposits

Phonolitic pyroclastic deposits are present along the Icod Valley (Fig.1) from the highest slopes to the coast, while at the southern side of Teide these outcrops are less abundant. The stratigraphy of these eruptive products is not well established yet, and further work combining petrology, mineral chemistry, geochronology and stratigraphy is required to determine the exact position and distribution of each unit in the stratigraphic record and its significance in the evolution of these volcanoes. However, we have identified several di*ff*erent types of PDC deposits and of discontinuous coarse to fine grained, pumice fall deposits, which suggest the existence of explosive eruptions from Teide–Pico Viejo and di*ff*erent from the Montan˜ a Blanca eruption. Phonolitic fallout deposits have been deeply eroded and show a variable degree of preservation depending on topography and burial by younger products. This makes it di*ffi*cult to establish reliable stratigraphic correlations at present. In contrast, PDC deposits, despite having been deeply eroded too, have been partially preserved within gullies on the northern flank of Teide–Pico Viejo and show features that allow them to be identified and interpreted in terms of eruption dynamics and emplacement mechanisms. We have observed the presence of pumice-rich, ignimbrites and block and ash deposits which show very distinctlothological and sedimentological characteristisc.

2.3.1 Pumice rich, pyroclastic flow deposits (ignimbrites)

Comparisons between the relative stratigraphy and composition of the different deposits reveal that they represent the products of several explosive episodes that occurred during the recent (Holocene) history of Teide–Pico Viejo. The poor degree of preservation of most of these deposits, as well as the discontinuity of their outcrops makes it difficult to determine their exact stratigraphic position and extent. However, in some cases the preserved outcrops allow to identify the main characteristics of the deposits and to infer their eruption and emplacement mechanisms.

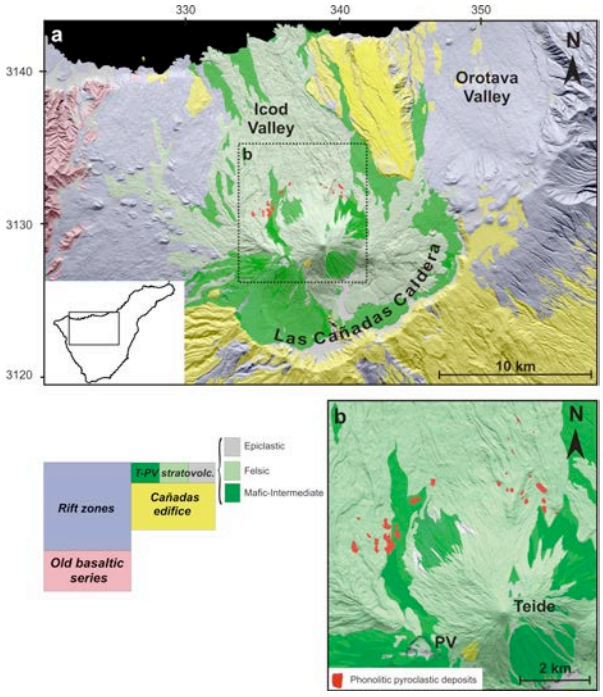

Figure 1: Simplified geological map of Teide–Pico Viejo stratovolcanoes, based on IGME (2009) and Ablay and MartıÅL (2000), and location of the main outcrops (in red) of phonolitic pyroclastic deposits identified in this study. Upper inset: Tenerife contour and studied area. Lower inset: general stratigraphy of Tenerife (see Martí et al. (2008) for more details).

This is the case, for instance, of the Abrunco ignimbrite, a non-welded, pumice-rich, pyroclastic flow deposit that outcrops, between the Pico Cabras and Abejera lava domes (Fig. 1), which is the best preserved example and representative of other pumice flow deposits observed. The Abrunco ignimbrite can be recognized in at least three separated outcrops where it overlies previous lava flows and reworked deposits and shows an irregular and discontinuous upper contact with clastogenic lava of the same mineralogical composition. The ignimbrite is not homogeneous and shows different lithofacies irregularly distributed along the deposit (Fig. 2). A *fine-grained laminated lithofacies* appears at the base of the ignimbrite irregularly. Distributed along the three outcrops. It is ostly composed of coare to fine juvenile ash together with surbordinate ash size lithic clasts. It does not contain pumice fragments of lapilli size or larger. This facies is thinly laminated and occasionally shows cross-bedding. The characteristics of this facies suggest that it could correspond to a pyroclastic surge deposit immediately preceding the emplacement of the ignimbrite. A *pumice-rich lithofacies*, forming a non-welded, poorly sorted, massive deposit, is normally found at the central part of the ignimbrite. It contains abundant angular pumice lapilli of both dense and vesicular (i.e. spherical and tube), which are supported by a fine ash matrix. Sometimes this facies forms lenses surrounded by the matrix-rich facies towards the lower part of the ignimbrite.

A *matrix rich lithofacies* is composed of scarce dense and expanded, including tube and spherical, pumice clasts surrounded by an abundant lapilli and ash matrix of the same composition. The size of pumice lapilli ranges from a few centimetres to 30 cm. Rare vent-derived, angular lithic clasts also appear in this lithofacies and are similar in size to the pumices. The matrix-rich lithofacies is commonly found in the upper parts

of the ignimbrite and defines an irregular contact with the overlying clastogenic lavas. This finding, together with the fact that fragments of the clastogenic lavas are engulfed by the ignimbrite while some pumice blocks have been eroded and incorporated into the lava, suggest that the emplacement of the clastogenic lava occurred when the ignimbrite was still unconsolidated. This indicates that the emplacement of the ignimbrite and the clastogenic lava were not separated by a significant time break, probably corresponding to two consecutive phases of the same eruption.

The contacts between the different ignimbrite facies are always irregular, sometimes discontinuous and even gradual in some occasions, but we have not observed erosional contacts among them. The absence of fragments from the clastogenic lavas and the presence of vent-derived lithic clasts in the ignimbrites suggest that they formed from an explosive eruption rather than by gravitational collapse of lava domes or advancing lava flows. The variety of lithofacies observed in the Abrunco ignimbrite may have resulted either from changes at source or by flow changes during emplacement. The presence of the thinly laminated unit at the base of the deposits could be interpreted as a ground surge deposit generated by the turbulent ash cloud flow front, which could be caused by high flow front velocity and considerable topographical irregularity (ground roughness). The abrupt and irregular topography of the northern side of Teide, characterized by frequent slope breaks, may have also favoured changes in the flow regime during the emplacement of the main ignimbrite bodies. This may have created localized highly turbulent conditions which lead to the elutriation of fines and the deposition of isolated pumice lenses and the pumice-rich facies in a similar way to the lee side pumice lenses in the Taupo Ignimbrite described by (Wilson, 1985) or in other ignimbrites from Tenerife (Pittari et al., 2005). The

continuation of the flow on a topographically modified ground may have led to the deposition of the massive part of the ignimbrite body thus forming the matrix-rich facies. We have not been able to correlate these ignimbritic deposits with the pumice fallout deposits that crop out at the north of Teide, so we cannot confirm if these ignimbrites formed by collapse of sustained column during plinian or subplinian eruptions or from transient vulcanian explosions associated with lava domes and flows, such as those observed in Montserrat (Calder et al., 1999; Loughlin et al., 2002). Anyway, the intimate association of the studied ignimbrites with clastogenic lavas at the top suggests that ignimbrites and lavas derive from the same eruption, which would have initiated with an explosive event progressively decreasing in intensity till a fire fountaining episode which would have generated the clastogenic lavas. The presence of pumice fall deposits, ignimbrites and clastogenic lavas at several stratigraphic horizons suggests that repeated phonolitic explosive eruptions have occurred during the Holocene at Teide–Pico Viejo.

Another characteristic of these ignimbrite deposits is the presence of lenses of reworked material irregularly interbedded with the pyroclastic facies. This reworked material is composed of abundant sub-rounded to rounded lithic and pumice fragments supported by a scarce reworked matrix. Pumices and lithics of these epiclastic lenses are of the same nature as those from the associated ignimbrite. These characteristics suggest a syn-depositional reworking of the ignimbrite by aqueous flows probably generated by a heavy rainfall triggered by the eruption (see e.g. Woods, 1993), and ⁄or latter by seasonal rain that usually causes torrential effects on such steep topography. This would also explain the lack of preservation of most of the ignimbrite deposit(s).

2.3.2 Block and ash deposits

The second type of PDC deposit that we have recognized around the north side of Teide–Pico Viejo are block and ash deposits. These deposits are always of relatively small volume compared to some lavas, and can be followed for several kilometres downslope. Thickness varies from less than one metre to several metres depending on the palaeotopography on which they were emplaced. In some cases they grade downslope into debris flow deposits, some of them arriving at the northern coast of Tenerife. The block and ash deposits are nearly monolithological and are mostly composed of fragments of clastogenic lavas, and minor non-welded dense and expanded pumices of the same composition as the clastogenic lava fragments (Fig. 3).

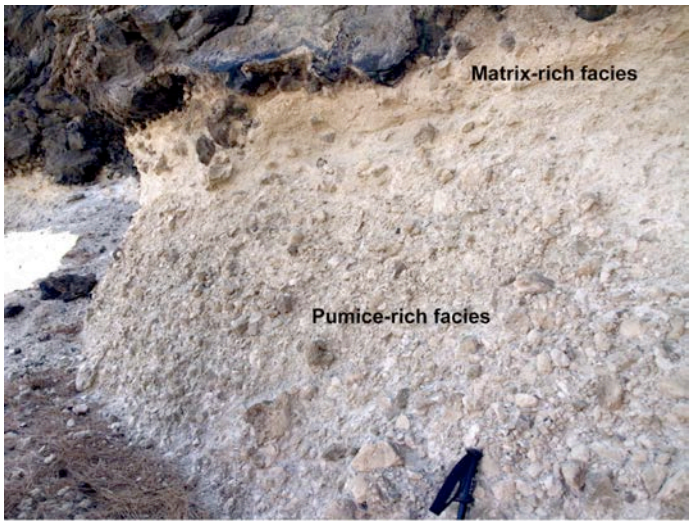

Fig. 2 Detail of the ignimbrite showing the matrix-rich and pumice-rich facies. Note the irregular contact of the ignimbrite with the clastogenic lava above and how fragments of the clastogenic lava are engulfed by the ignimbrite while some pumice blocks have been eroded and incorporated into the lava.

All these fragments are surrounded by an ash to fine lapilli size matrix mostly composed of juvenile clasts and some lithic fragments derived from the fragmentation and attrition of the previous components. These lithological and sedimentological characteristics make a clear distinction between block and ash and debris flow deposits also present on the northern slopes of Teide, as these last incorporate clasts from other lithologies, reduce significantly the amount of pumice and ash matrix, and show a better rounding of clasts and internal organization of the deposits compared to the block and ash deposits.

Field relationships and comparison of chemical and mineral compositions and textures show that the observed block and ash deposit derive from clastogenic lavas flows or lava domes. Most of the recent phonolitic lava domes and lava flows from Teide and Pico Viejo have a clastogenic nature and formed by agglutination and stretching of large juvenile fragments parallel to the flow direction. In some places these clastogenic lavas and domes include abundant non-welded pumices, suggesting that they derive from explosive episodes rather than from purely effusive eruptions. We propose that some of these clastogenic lavas, which were still very rich in gases, became block and ash flows when they collapsed gravitationally at an abrupt slope change, a common morphological features at the northern side of Teide-Pico Viejo.

Fig. 3 Example os a block and ash deposit found at the northern side of Teide-Pico Viejo in the Icod Valley. Fragments of sub-rounded clastogenic lavas are supported by an ash-lapilli size matrix of the same composition.

2.4 Discussion and conclusion.

A detailed field study has allowed us to identify for the first time the presence of ignimbrites and block and ash deposits associated with the recent (Holocene) eruptive history of Teide– Pico Viejo. The presence of these deposits, together with fall products means that we should reconsider notions that Teide–Pico Viejo are predominantly effusive volcanoes that do not represent a significant threat to their surroundings.

The fact that the volume of pyroclastic deposits visible today is small compared to that of lavas does not necessarily imply that explosive activity has been insignificant in the recent evolution of Teide–Pico Viejo. On the contrary, we claim that phonolitic explosive activity has been more significant than previously thought in Teide–Pico Viejo during the Holocene. The evidence we have presented for the syn-depositional erosion of ignimbrites suggests that heavy rainfalls may have occurred in the area

during these eruptions, which could already explain the rapid disappearance of a significant part of these deposits. Moreover, we must take into account the existence of important seasonal rainfall that would have also contributed to the erosion of the unconsolidated pyroclastic material. In fact, the Icod valley is characterized by the presence of prominent S-N narrow gullies that deeply erode the Teide–Pico Viejo products, and of abundant lahar and debris flow deposits that infill their lower parts.

Other evidence of the relevance of explosive volcanism in Teide–Pico Viejo is the presence of several discontinuous outcrops of thick (occasionally up to 4 m), primary (non-reworked) pumice fall deposits in some sectors of the north of Teide (Fig. 1). At least three of these outcrops have different stratigraphic positions and are older than the 2000 bp Montan˜ a Blanca pumice. However, some other pumice fall deposits from the northern side of Teide may correlate with the Montan˜ a Blanca pumice. Radiometric ages of some of these pumice fall deposits (Carracedo et al., 2007) are similar to the Montan˜ a Blanca, which implies that the Montan˜ a Blanca eruption was larger than previously thought (Ablay et al., 1995; Folch and Felpeto, 2005) and may well have been Plinian in dimension. A first comparison of the mineralogy and geochemistry of all these pumice deposits does not provide definitive clues to discriminate them, so a more detailed petrological work will be required to interpret the sequence of explosive eruptions in the recent geological record of Teide–Pico Viejo.

Hazard assessment at Teide–Pico Viejo, one of the largest volcanic complexes in Europe, is necessary to reduce risk in Tenerife, an island extensively populated and one of the main tourist destinations in Europe. It is widely accepted that pyroclastic density currents are one of the main volcanic hazards. Therefore, the presence of pyroclastic deposits in the recent volcanic history of Teide–Pico Viejo has implications for future

hazard and in particular for the Icod valley, an area with a permanent population of more than 30 000 inhabitants which has received the direct impact of explosive volcanism from Teide–Pico Viejo in the past. In contrast with considerations that Teide–Pico Viejo represents only a modest hazard level for Tenerife (Carracedo et al., 2007), we suggest that phonolitic explosive volcanism during the Holocene at Teide–Pico Viejo volcanoes and the existence of unquestionable signs of activity in historical times (fumaroles, seismicity) and even a clear unrest episode in 2004 (Martıí et al., 2009), implies that hazard at Teide–Pico Viejo is not negligible. Although a detailed reconstruction of the original extent of the phonolitic pyroclastic deposits of Teide–Pico Viejo is not possible due to the lack of preservation, their characteristics and comparison with similar deposits from recent eruptions (e.g.: Calder et al., 1999; Loughlin et al., 2002).

3. The 5660 yBP Boquerón explosive eruption, Teide-Pico Viejo Complex, Tenerife.

This paper has been published in Bulletin of Volcanology. The authors of the papers are:

Olaya García, Centro Geofísico de Canarias del I.G.N. C/La Marina 20, 2º, 38001 S/C de Tenerife, Spain

Costanza Bonadonna, Département de Minéralogie, Section des sciences de la Terre et de l'environnement, Université de Genève. Rues des Maraichers 13, 1205 Genève, Switzerland.

Joan Martí, Instituto de Ciencias de la Tierra Jaume Almera, CSIC, Lluis Solé Sabarís s/n, 08028 Barcelona, Spain.

Laura Piolli, Département de Minéralogie, Section des sciences de la Terre et de l'environnement, Université de Genève. Rues des Maraichers 13, 1205 Genève, Switzerland.

The reference of this paper is: García O., Bonadonna C., Martí J., Pioli L. (2012) The 5,660 yBP Boquerón explosive eruption, Teide–Pico Viejo complex, Tenerife. Bulletin of Volcanology 74: 2037-2050 doi:10.1007/s00445-012-0646-5

3. 1 Introduction

The Holocene explosive volcanic activity in Tenerife Island is concentrated mainly in the central volcanic complex (Ablay et al. 1998; Ablay and Martí 2000; Martí et al. 2008).

This central complex started to grow at about 4.5 Ma or earlier, and remains active. Its evolution Included several constructive and destructive episodes that gradually formed Las Cañadas caldera at the centre of the island (Martí et al 1994; Ancochea et al 1999). The last episode in the construction of the Tenerife central volcanic complex formed the Teide and Pico Viejo stratovolcanoes (TPV complex) within Las Cañadas caldera (Ablay and Martí 2000; Carracedo et al. 2007). Traditionally considered as mainly effusive volcanoes, current knowledge of TPV remains poor given that they form one of the main active volcanic complexes in Europe and are a significant threat to Tenerife (Martí et al 2011; Marrero et al 2012). Recent studies have revealed that explosive activity has been underestimated in the reconstructed TPV eruptive history (Martí et al. 2008, 2011; García et al. 2011; Boulesteix et al. 2011). This implies that hazards at Tenerife might be underestimated if explosive volcanism from TPV is not considered. No precise data on the products of TPV explosive volcanism exist, however, and one of the most urgent needs is to characterise and quantify these eruptions.

The knowledge we have of explosive volcanism at TPV is restricted to a detailed study of the 2000 BP Montaña Blanca sub-plinian eruption (Ablay et al. 1995; Folch and Felpeto 2005) and the identification of new fallout and PDC deposits on the northern flank of TPV (Perez Torrado et al. 2004; Martí et al. 2008; García et al. 2011).

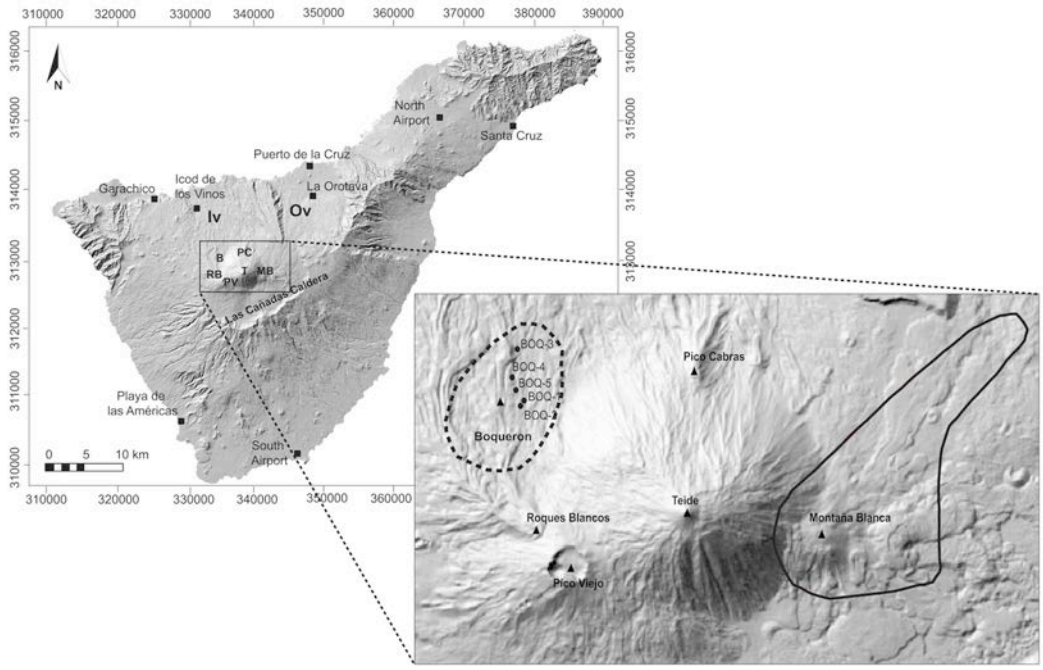

Fig. 1 Location map of study area and topographic map of Tenerife. Main vents and main drainage cuts of Boqueron lava flow are shown as black triangles and black solid lines respectively. Black circles indicate our main outcrops (Fig.2), the dashed line represents the 50 cm isopach contour of isopach A (Fig. 3) and the thick line represents the 30 cm isopach contour. *B* Boqueron, *MB* Montaña Blanca, *RB* Roques Blancos, *T* Teide, *PC* Pico Cabras, *PV* Pico Viejo, *Iv* Icod Valley, *Ov* Orotava Valley. (projection: UTM 28N)

Even this limited e information suggests that an explosive eruption from TPV would today have a serious impact on critical infrastructures and the economy of the island as it would affect the air traffic, and some of the main energy and water lifelines (Martí et al 2011; Marrero et al 2012). In this paper we present a detailed study of the pumice fall deposits associated with El Boqueron dome complex, one of the Holocene flank vents located on the north of the Pico Viejo stratovolcano (Fig. 1). These deposits form the main unit produced by the El Boqueron explosive eruption and have not been described before. We infer the eruption characteristics (i.e., plume height, erupted

volume, mass eruption rate and duration) based on a stratigraphic and textural analysis and discuss implications for associated hazards.

3.2 Geological Background

The TPV complex consists of two stratovolcanoes which started to grow simultaneously within Las Cañadas caldera at around 180-190 ka (Hausen 1956; Araña 1971; Ablay 1997; Ablay et al. 1998; Ablay and Martí 2000; Carracedo et al. 2007) (Fig.2). This volcanic depression originated as a result of several vertical collapses of the former Tenerife central volcanic edifice, Las Cañadas edifice (Martí et al. 1997; Marti and Gudmundsson 2000). The TPV complex has a maximum elevation of 3718 m a.s.l at the top of Teide and shows a very sharp morphology characterised by steep flanks. The eruptive activity of TPV produced about 150 km^3 of mafic, intermediate and felsic material (Ablay et al. 1998; Ablay and Martí 2000; Martí et al. 2008).

TPV stratovolcanoes have been very active during the Holocene, with more than 16 known eruptions (Carracedo et al. 2007; Marti et al. 2011), the last (Lavas Negras) having occurred at 1,150 yr BP (Fig.2).

The volcano stratigraphy of the TPV was characterized by Ablay and Marti (2000) based on a detailed field and petrological study (Fig.2). In addition, Carracedo et al. (2003, 2007) provided the first group of isotopic ages from TPV products. The eruptive history of TPV consists of a main stage of eruption of mafic to intermediate lavas that form the core of the stratovolcanoes and filled most of the Las Cañadas depression and the adjacent La Orotava and Icod valleys. Phonolitic eruptions have

become predominant since 35 ka and their products cover the volcanoes' flanks and the infill sequence of the Icod Valley and part of La Orotava valley (Fig. 1).

Phonolitic eruptions from TPV were generated both from the central vents and from a multitude of vents distributed around their flanks. The flank vents define several radial eruptive fissures on the slopes of the twin volcanoes, and have generated both effusive (i.e. lava flows and domes) and explosive eruptions, ranging in size from 0.01 to > 1km^3 Dense Rock Equivalent (DRE). Effusive eruptions have produced thick lava flows and domes. Explosive eruptions have generated extensive pumice fall deposits and pyroclastic density currents (PDCs) associated with both subplinian and plinian eruptions and also with dome- and lava-flow gravitational collapses in the cases of PDCs (Martí et al. 2008; 2011; García et al. 2011). All these eruptive centres are associated with a single eruption in which several phases may be distinguished (Ablay and Martí 2000). The Boquerón is a dome complex located on the northwestern flank of TPV volcano. The last Boqueron eruption is of Holocene age (Carracedo et al. 2003) and produced both a large pumice fall deposit and 0.04 km^3 of lava flows, which reached the coastline along the Icod valley (i.e., 7.2 km run out) (Fig.1) (Martí et al. 2011). In this paper we present a detailed study of the fall deposit.

3.3 Methods

Given the poor exposure of the Boqueron deposit, the relevant outcrops were first identified based on aerial photographs and then thoroughly analysed and correlated through field investigations. Most of the studied outcrops are located on the northwest flank of TPV, at the base of Roques Blancos dome complex, and are concentrated in a

15 km^2 area around Boqueron (Fig. 1). The stratigraphy of the whole sequence of deposits was characterised based on detailed fieldwork. Correlations among the different units from different outcrops were made mainly based on textural features and crystal content and composition. Deposit thickness and maximum lithic sizes were determined at most outcrops. Forty samples were also collected in order to investigate grainsize, chemistry, density and vesicularity of the juvenile pumices. The fraction coarser than -3 f (i.e., > 8 mm) was sieved manually in the field, whereas finer fractions > -3 f (< 8mm) were dried and sieved in the laboratory. Componentry analysis was made for particles coarser than 0 f.

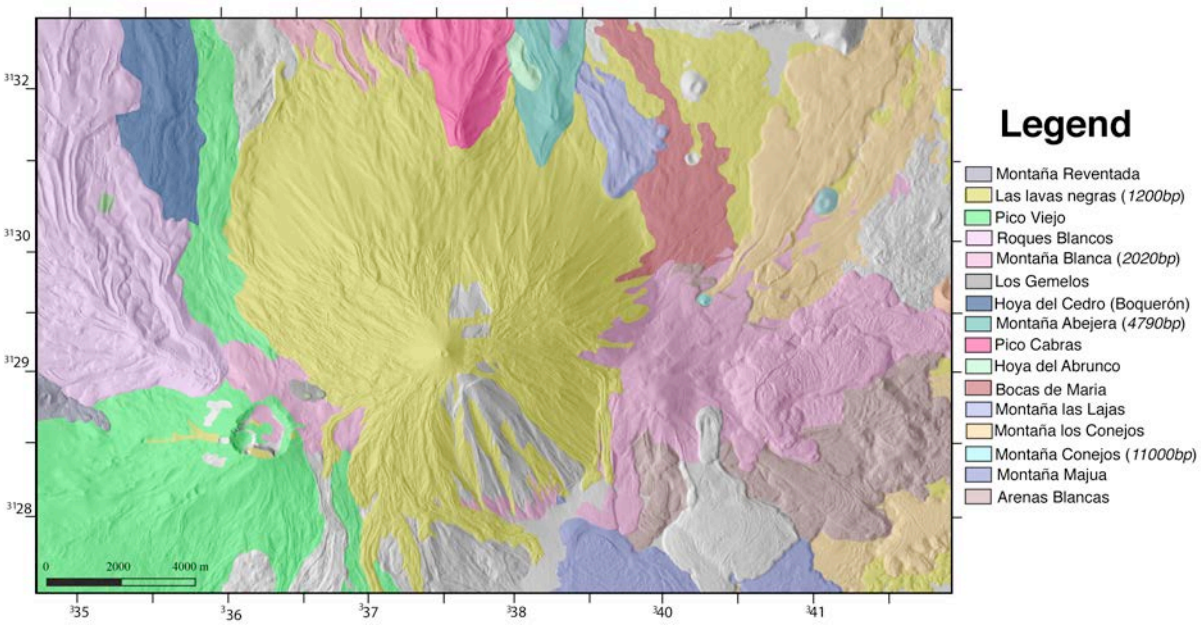

Fig. 2 Geological map of the Teide-Pico Viejo complex. Adapted from Ablay and Martí, (2000). The figure does not include all the volcanic events related to Pico Viejo-Teide stratovolcanoes, only those

central and flank Holocene eruptions with felsic and hybrid composition. Geochronological data from Carracedo et al (2003,2007)

Density was measured on 100 juvenile clasts from the entire unit, collected at the outcrop BOQ-4 and with diameters ranging between 16 and 32 mm (Fig. 3). Pumice clasts were dried at 60ºC for 24 hours and then cleaned with a brush, numbered and weighed. Finally, all clasts were coated with cellulose acetate, dried and weighed again. Relative density was obtained comparing water and the dry weights. The results were converted into absolute density and bulk vesicularity using the Dense Rock Equivalent (DRE) density measured on finely crushed pumice specimens using a water pycnometer at the University of Geneva. The deposit density in the field was obtained by weighing a known *in situ* volume of pumice clasts, plus intergranular porosity and matrix from BOQ-3 outcrop. To investigate variations in morphology and vesicularity of juvenile clasts of the main unit, we used the Scanning Electron Microscope (SEM) JEOLJSM 6400 at the University of Geneva.

Whole Rock analyses were performed by the GeoAnalytical Laboratory at the Washington State University using X-ray fluorescence (XRF) and Inductively coupled plasma mass spectrometry (ICP-MS) facilities. The relative error of the measurement is lower than 1% for the major and trace elements for XRF method, less than 5% for the REEs and less than 10% for the remaining trace elements. Charcoal was also found in the soil below the bottom unit of Boquerón deposit, which overlies the paleosol, and 2.2 gr of sample was analyzed by Beta Analytic Inc. laboratory of Miami (USA) for carbon isotopic composition with Accelerator Mass Spectroscopy (AMS) techniques. The specimen (i.e. laboratory number Beta-298872) age was determined after the IntCal04 calibration curve (Reimet et al. 2004)

Physical parameters of the main unit were also derived. The erupted volume was calculated applying the methods of exponential, power-law and Weibull integration (Pyle 1989; Bonadonna and Houghton 2005; Bonadonna and Costa 2012). Given the poor exposure of the deposits, two potential isopach maps were compiled based on the same dataset in order to investigate the uncertainty in the volume calculation. The thickness dataset was constructed based on 61 trenches excavated down to the underlying lava flow (in medial areas) or down to a maximum of 2 meters when the lava flow was not present (in proximal areas).

The plume height was determined applying the method of Carey and Sparks (1986) to the isopleth map of lithic clasts. The maximum lithic sizes were measured based on the geometric mean average of the three axes of the five largest clasts sampled based on a horizontal sampling area of 0. 5 m^2. We also compiled an isopleth map using the 50^{th} percentile of the 20 largest clasts following the recommendations of the IAVCEI Commission on Tephra Hazard Modelling (Bonadonna et al. 2011; Bonadonna et al. 2012).

3.4 Composition, stratigraphy and characteristics of deposits

The Boqueron eruption is associated with an old dome in the northwest flank of Pico Viejo stratovolcano. Charcoal fragments found in the dark red soil at the base of Boqueron deposit had a 13C/12C ratio of -22.9 ‰, corresponding to a conventional age of 5630 ±60 yBP, corresponding to a calibrated radiocarbon age of 5660± 60 BP. The

composition (shown in Table 1) of both the Boqueron juvenile fragments and lava flow is phonolitic, similar to other Holocene products of TPV (see Ablay et al. 1995).

Fig. 3 Pumice fall deposit from the Boqueron eruption. a) distal area: outcrop BOQ-3A, b) proximal area of pumice deposit with a large lithics : outcrop BOQ-2.TOP.

The pyroclastic succession of the Boqueron deposit consists of a main pumice fall deposit characterised by a poor exposure, with proximal outcrops showing some evident stratification and some welding phenomena (Fig. 3). Individual layers are difficult to correlate and tend to merge in distal areas. As a result, we have characterised the Boqueron deposit as a single unit. Five representative outcrops were selected for detailed stratigraphic, grainsize, componentry and textural studies and are shown in Fig.4.

The Boqueron tephra deposit is dispersed over an area of about 15 km^2 NW of Teide. In distal areas (Fig. 2; BOQ-3) it consists of a several cm- thick, well-sorted, non-welded, massive bed of pumice lapilli. Grain size distribution of the studied samples is characterised by Md phi and sorting varying between -1.4 and -3.2 phi and 1.4 and 1.0 respectively.

Unit	Boqueron	Boqueron	Boqueron
Sample	Boq.r23	Boq.r1	Boq.pr
	Major and minor elements (oxides wt%)		
SiO_2	59.46	58.44	59.14
TiO_2	0.727	0.63	0.70
Al_2O_3	19.34	18.9	19.44
FeO^*	3.45	3.51	3.41
MnO	0.19	0.19	0.19
MgO	0.43	0.34	0.38
CaO	0.87	0.75	0.76
Na_2O	8.92	9.07	9.08
K_2O	5.50	5.42	5.59
P_2O_5	0.114	0.081	0.070
Total	99.0	97.33	98.77
LOI(%)	0.89	2.35	0.87
	Trace Elements (ppm)		
,Ni	4	3	4
Cr	2	2	2
Sc	0	1	1
V	14	8	13
Ba	192	24	87
Rb	169	170	186
Sr	13	7	10
Zr	964	989	1041
Y	36	38	38
Nb	219	225	235
Ga	28	29	29
Cu	1	1	2
Zn	119	125	125
Pb	19	20	20
La	110	112	112
Ce	186	186	192
Th	28	28	30
Nd	55	56	57
U	7	8	7

Table 1 Whole rock analyses of representative Boqueron samples. Boq.r23 is a lava from a Boqueron lava flow, it was taking in one point close to point 6 (Table 2) and Boq.r1 and Boq.pr are juvenile lapilli clasts were taking from no-welded bed at point 4 (Table 2)

Lithic content is mostly constant for all deposits, increasing slightly from the bottom (7 vol.%) to the top (10 vol.%) (Fig. 4); lithic clasts predominantly consist of obsidian and phonolitic lava fragments. Juvenile clasts consist of microvesicular, crystal-poor, angular to subangular yellow to grey pumice lapilli. At medial locations (Fig. 4; BOQ-2) the unit has a thickness of a few decimetres and displays internal stratification with symmetric, coarse-fine-coarse graded bedding. The contact between beds is gradational. At proximal locations (Fig. 4; BOQ-5 and BOQ-2) the deposit consists of an alternation of moderately to incipiently welded lapilli and bomb beds and

non-welded lapilli beds with exposed thickness up to 6.37 m (outcrop BOQ-5). These layers are moderately to poorly sorted with average size from lapilli to bombs. In the welded beds, the degree of welding increases from bottom to top with gradual transition to the lower non-welded beds. The welded beds are typically lithic-poor. At some locations, the welded beds display rheomorphic features suggesting remobilization on steep slopes. The welding of the proximal deposits suggests higher deposition rates and high depositional temperatures associated with low magma viscosity, favouring clast agglutination and deformation (Carey et al., 2008). This appears to be a common process in the phonolitic eruptions of the TPV complex, and also affected the older plinian fall deposits cropping out in the Las Cañadas walls (Ablay et al., 1995; Soriano et al., 2002).

In contrast, the contact between non-welded layers is sharp (Fig. 4; BOQ-4). The bottom of the whole unit lies over a paleosol or, in distal areas, directly above lava flows. Carracedo et al. (2003) located the vent of this eruption at the S margin of the lava flow. This hypothesis is confirmed by the distribution of thickness and grain size of the tephra layer (Fig. 5 and Table 2).

3.5. Results

3.5.1 Volume

In order to estimate the error associated with the volume calculation of a poorly exposed tephra deposit, we decided to hand draw two possible isopach maps based on the same dataset (isopach maps A and B in Fig. 5 with associated thickness shown in

Table 2). Map A is compiled based on a conservative interpretation of field data, while Map B can be considered as just an example of possible contouring that can be drawn to consider a larger dispersal than Map A but still compatible with the same dataset. In fact, Map B is compiled based on the assumption of a more gradual thinning where the

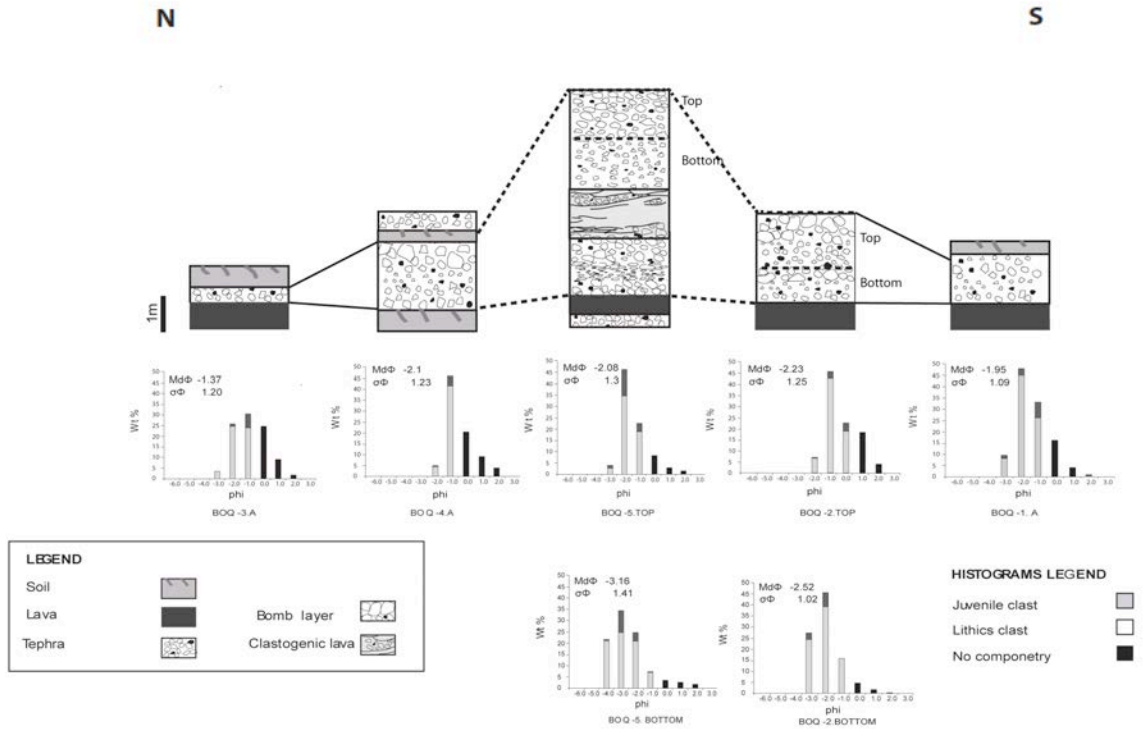

Fig. 4 Stratigraphic columns of five representative sections from Boqueron deposits with the associated grain-size and componentry. Location of the outcrops is shown in Fig. 1. and thickness in Table 2.

deposit is not accessible (i.e. mainly to the SW and NE of the vent) and can be then considered as an upward boundary for the volume calculation (with a relative difference of 30% in the square root of area value of the 50 cm contour). The thinning trends resulting from each map can be described by one exponential segment and both a

Weibull and a power-law curve on a semi-log plot of thickness versus square root of isopach area.

Volume calculations were then made from the two different maps applying the methods of exponential, power-law and Weibull integrations (Pyle 1989; Bonadonna and Houghton 2005; Bonadonna and Costa 2012) (Table 3). The calculated volumes are 1.0 and 1.7 x 10^7 m^3 for the two exponential integrations, 3.7±0.4x10^7 and 7.3±1.2x10^7 m^3 for the two power-law integrations and 4.2x10^7 and 6.3x10^7 m^3 for the two Weibull integrations (for isopach A and B respectively; Fig. 5). The erupted mass varies between 0.6 and 4.4x10^{10} kg based on a deposit density of 600 kg m^{-3}. The distal limits of integration for the power-law calculation (50 to 100 km square root of area values; Table 3) were chosen based on both the thinning trend of Boqueron and Montaña Blanca (Ablay et al. 1995). In fact, these two deposits show very similar features with a thickness of about 10-50 cm around 3-5 km from the vent (square root of area values). We assume that the most distal sedimentation would then occur around 50 to 100 km from the vent (square root of area values). The error of the power-law integration was calculated based on the variation of these distal integration limits. The uncertainty associated with the compilation of the isopach map is 40% for exponential method, 50% for the Power Law Method and 32% for the Weibull method. As a result, we base our discussion below on the most stable values given by the Weibull integration. The associated DRE volume, based on a deposit density of 600 kg/m^3 and a magma density of 2570 kg/m^3, ranges from 9.9x10^6 to 1.5x10^7 m^3.

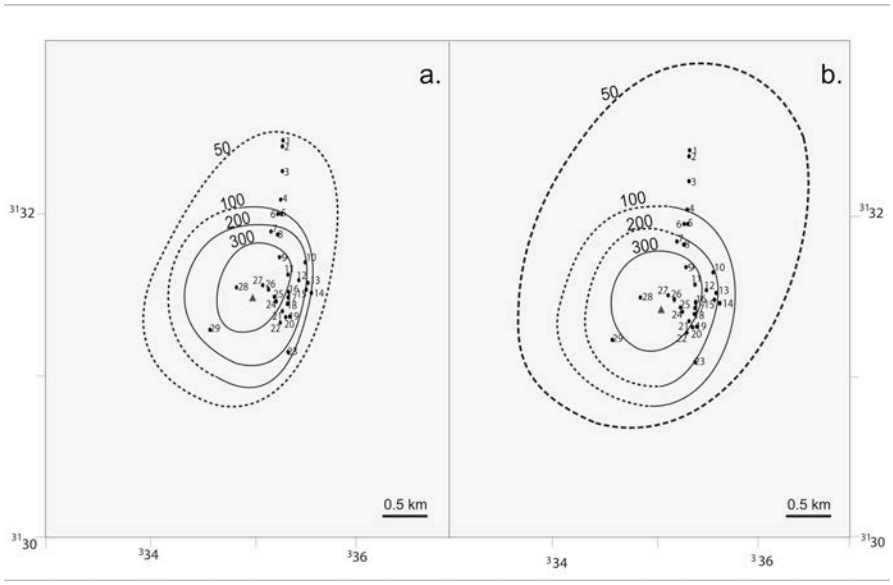

Fig. 5 Isopach maps of the Boqueron deposit with thickness expressed in cm: a) isopach map A; b) isopach map B. Sample numbers are indicated on the map and thickness values are reported in table 1. Dashed lines are extrapolated contours. Given the poor exposure of the deposit, two isopach maps have been compiled that are compatible with our dataset in order to estimate the error in the volume calculation.

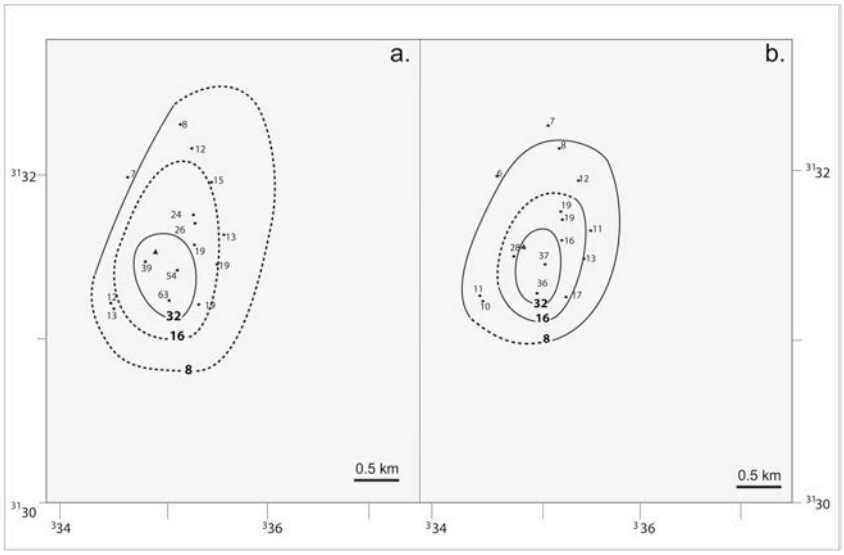

Fig. 6 Isopleth maps of Boqueron deposit for the largest lithics using two different methods: a) the average of the 3 axes of the 5 largest clasts; b) 50th percentile of a 20-clast population. Dashed lines are extrapolated contours

3.5.2 Plume height, wind speed, mass eruption rate and eruption duration

As mentioned above, two isopleth maps were compiled based on the 5 largest lithics (Fig. 6a) and on the 50th percentile of a population of 20 lithics (Fig. 6b). Plume height and wind velocity at the time of the eruption were derived by applying the method of Carey and Sparks (1986) to both isopleth maps. Only the 0.8 cm isopleth contour gave consistent estimates for both maps, and resulted in a plume height of about 7 km above the vent (i.e., about 9 km a.s.l.) for both the 5 largest clasts and the 50th percentile method and wind velocities up to 10 m/s. The Boqueron tephra deposit was mainly dispersed northeastward, in agreement with the dominant wind direction in the area. In fact, the average wind direction in TPV complex, as calculated based on NOAA local wind data collected in the last 10 years, shows a dominant eastward wind direction from 5 to 20 km a.s.l. with uniform seasonal distribution and standard deviation decreasing from ±90 to ±45 degrees with altitude (fig. 7).

The mass eruption rate (MER) was calculated applying both the method of Wilson and Walker (1987) and Sparks (1986) (Table 4). The method of Wilson and Walker (1987) resulted in a MER of 6.9x10^5 kg/s, while the method of Sparks (1986) resulted in a MER of 8.2 x10^5 kg/s (for a tropical atmosphere and a plume temperature of 600ºC appropriate for phonolitic magmas). The eruption duration was estimated between about 9-10 hours for isopach A and about 13-15 hours for isopach B based on the ratio between erupted mass (Weibull integration) and the two MER values described above (Table 4).

Point	Thickness (cm)	UTM X	UTM Y
1	60	335356	3132377
2	62	335356	3132337
3	**40**	**335328**	**3132052**
4	37	335314	3131765
5	58	335312	3131620
6	50	335285	3131609
7	**164**	**335288**	**3130977**
8	>120	335225	3131436
9	**637**	**335311**	**3131145**
10	>79	335636	3131111
11	>120	335416	3130977
12	>165	335546	3130946
13	>79	335655	3130878
14	110	335698	3130773
15	>140	335636	3130811
16	**271**	**335437**	**3130789**
17	>180	335416	3130722
18	>188	335402	3130645
19	>112	335426	3130531
20	>197	335390	3130520
21	>140	335340	3130583
22	>99	335315	3130456
23	>180	335412	3130163
24	>160	335266	3130698
25	>185	335254	3130733
26	>180	335172	3130816
27	**>160**	**335092**	**3130857**
28	>165	334801	3130818
29	>200	334463	3130400

Table 2 Thickness values of samples points in isopach maps A and B of Fig.3.Numbers in bold show the thickness of the main outcrops; *Point 3* is BOQ-3.

3.5.3 Classification

Based on the volume range described above, the Boqueron explosive phase classifies as having a Volcanic Explosivity Index (VEI) of 3. The associated magnitude is between 2.8 to 3.6 and the intensity is 9 on the scales of Pyle (2000) (Table 3). The bt vs bc/bt plot of Pyle (1989) suggests an eruptive style between strombolian and subplinian, with the subplinian field being characterised by minimum plume heights of 14 km (Fig. 8). The thinning trend, however, follows the typical pattern of subplinian

eruptions and, in particular, shows similar characteristics to that of the Montaña Blanca deposit (Fig. 9).

		Volume ($\times 10^7$ m^3)	Mass ($\times 10^{10}$ kg)	Magnitude		
					bt (km)	bc/bt
Exponential	Isopach A	1.0	0.6	2.8	2.0	0.3
	Isopach B	1.7	1.0	3.0	1.3	0.4
					m	
Power Law	Isopach A	3.7 ±0.4	2.2 ±0.3	3.3	1.8	-
	Isopach B	7.3 ±1.2	4.4 ±0.7	3.6	1.6	-
					θ	λ
Weibull	Isopach A	4.2	2.5	3.4	4.7	13.8
	Isopach B	6.3	3.8	3.6	5.5	18.1

Table 3 Summary of volume calculations associated with the exponential (Pyle 1989), power-law (Bonadonna and Houghton 2005) and Weibull (Bonadonna and Costa 2012) integrations. Mass is calculated based on a deposit density of 600 kg/m^3; Magnitude is calculated according to Pyle (2000); bt and bc are the thickness half-distance and the half-distance ratio respectively calculated according to Pyle (1989); m is the absolute value of the coefficient of the power-law best fit; θ and λ are two characteristic scales of the Weibull best fit. The error of the power-law integration is calculated based on variable distal limits of integrations (i.e., 50, 75 and 100 km).

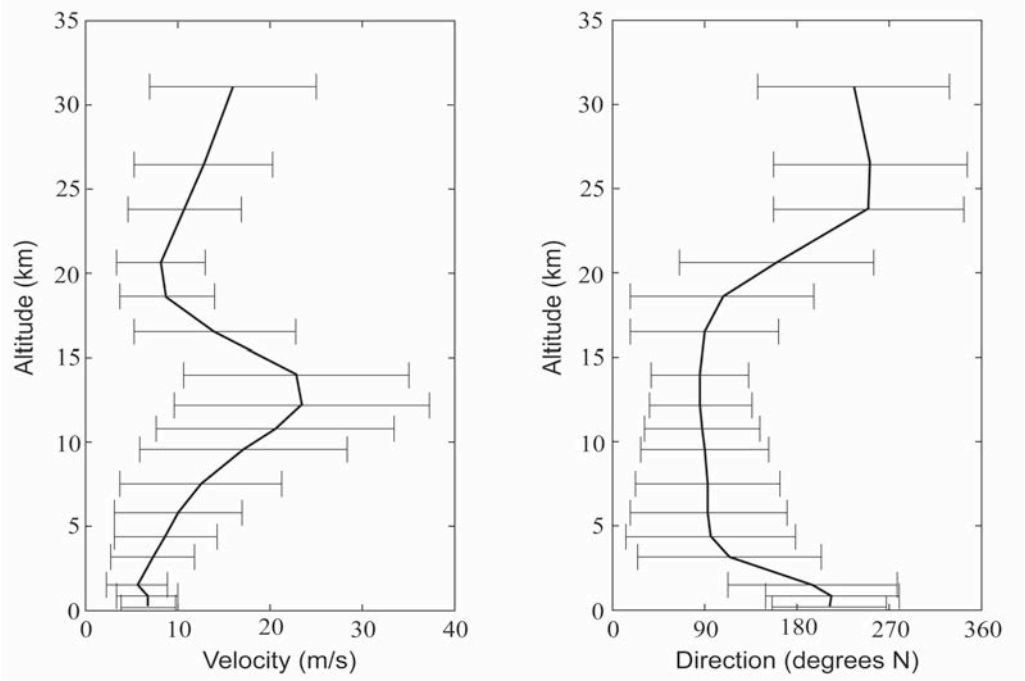

Fig. 7 Wind profiles calculated for Teide –Pico Viejo Volcano for the last ten years (2000-2010) (wind data from NOAA, U.S. National Oceanic and Atmospheric Administration, www.cdc.noaa.gov); a) variation of wind velocity profile with altitude; b) variation of wind direction, which is expressed as degrees from north where the wind blows. Data are presented as a median value with associated error bars.

Values of thickness half distance (bt) for Boqueron maps A and B are between 0.3-0.5 km in agreement with bt values of Montaña Blanca deposit (i.e., 0.4-0.8 km), of the 26 September 1997 Vulcanian explosion of Montserrat (i.e., 0.7 km), of Chaiten layer a (i.e. 0.7 km) and with the proximal bt values of Ruapehu (i.e. 0.2 km) and Chaiten layer b (i.e., 0.8 km). These values are lower than values of Plinian eruptions that typically range from 1 to 60 km (Pyle 1989).

3.5.4 Clast vesicularity and textural characterization

The phenocryst content of the Boqueron pumices account for 3 to 7 vol%. Phenocrysts consist of mm sized, euhedral biotite, alkaline feldspar, clinopyroxene and minor apatite, magnetite and ilmenite.

Juvenile lapilli are usually microvesicular, glassy and phenocryst poor. The differences between juvenile clasts can be substantial, both in density and texture (Figs 10 and 11). Their density ranges from 360 to 1150 kg/m^3 with average of 744 kg/m^3 and standard deviation of 190 kg/m^3 (Fig.10). The density distribution is unimodal with a dense tail. Considering a measured DRE density of 2540 ±133 kg/m^3 the vesicularity ranges from 86 to 33 vol.% and the clasts could be classified as from poorly to highly vesicular (Houghton and Wilson, 1989).

Vesicles range from a few mm to few μm in size and display different shapes, from spherical to elongate or flat (Fig. 10a). The largest vesicles have complex and irregular shapes (Fig. 10a). The majority of clasts display homogenous textures with high vesicularity, small vesicles with complex shapes and glassy groundmass (Fig. 10b) and vesicle walls thickness ranges from few μm to a few tens of μm. suggesting high nucleation rates, and an expansion dominated coalescence (Szramek et al., 2006).

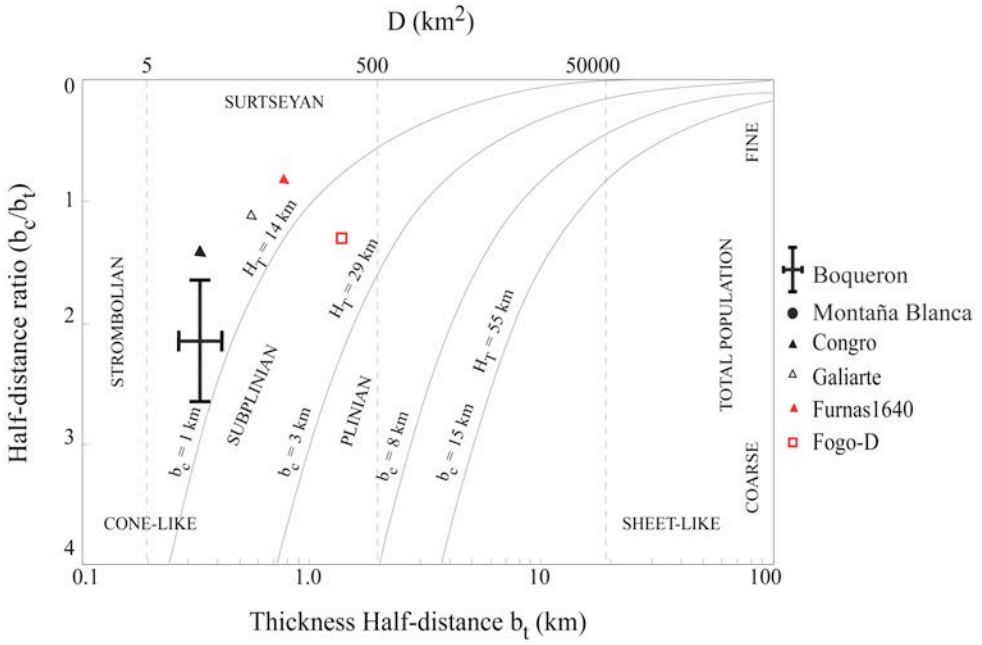

Fig. 8 Classification plot of Pyle (1989). Boqueron data are indicated as median value with associated error bar. Error bar is calculated based on the two isopach maps of Fig. 3. Data of Congro, 3800 yBP, Sao Miguel, Azores (Booth et al. 1978), Furnas 1640, Sao Miguel, Azores (Thorarinsson and Sigvaldson 1972), Fogo D, Cape Verde (Rose et al. 1983) and Montaña Blanca, 2 Ka Tenerife (Ablay et al. 1995) eruptions are also shown for comparison.

Moderately to poorly vesicular clasts have heterogeneous textures, with vesicularity and crystallinity varying at the mm scale. Vesicles are separated by thicker (a few tens to few hundreds of μm) walls (Fig. 11d) and cluster in groups. Larger

vesicles are usually confined to the central portion of the clasts. In addition, groundmass crystallinity varies at the specimen scale and is correlated with the vesicularity: microlite-poor areas (5 vol. % of microlites) are also vesicle-poor, with only small round vesicles; microlite-rich areas (50 vol. % of microlites) have vesicularity up to 45 vol. %. This relationship between vesicles and groundmass crystallinity is possibly due to the effects of postfragmentation expansion or even by clast recycling during lower explosivity phases (Wright et al., 2006). The boundaries between microlite-poor areas and microlite-rich areas are generally sharp (Fig. 11b).

Microlites consist of acicular sanidine with major axes ranging between 200 and 10 μm. Occasionally microlites are gathered in small groups in the crystal-rich glass, but it is more common to see individual crystals. Clasts from incipiently welded facies show highly heterogeneous textures with abrupt variations in vesicles size and spherulitic aggregates.

3.6 Discussion

The Boqueron subplinian eruption produced a vigorous plume reaching up to 9 km a.s.l.. The wind dispersion was to the Northeast in agreement with the main wind pattern of the area and with the dispersion of the Montaña Blanca eruption (Ablay et al, 1995; Folch and Felpeto, 2005). Despite the low column height, the Boqueron eruption is also comparable to other subplinian events in terms of deposit dispersal, erupted volume and thinning trend (Fig. 9). As an example, the Boqueron volume and thinning trends are very similar to those for the eruptions of Montaña Blanca (i.e., 1.4×10^8 m^3 based on isopach map from Ablay et al., 1995) and Fuego 1974 (Rose et al. 2008). The

complex stratigraphy, which is evident at proximal locations, could be indicative of complex eruption dynamics, coupling a main climactic phase to minor explosive phases that formed the welded horizons in the deposit, or to fluctuations in the eruptive intensity. Finally, we note that our new radiometric data suggest a maximum age for the Boqueron eruption of 5660 yBP. This age is much older, but compatible with the value (2528 yBP +/- 185) obtained by Carracedo et al. (2007) from a charcoal in the paleosol. Both ages are consistent with the regional stratigraphy (Ablay and Marti, 2000).

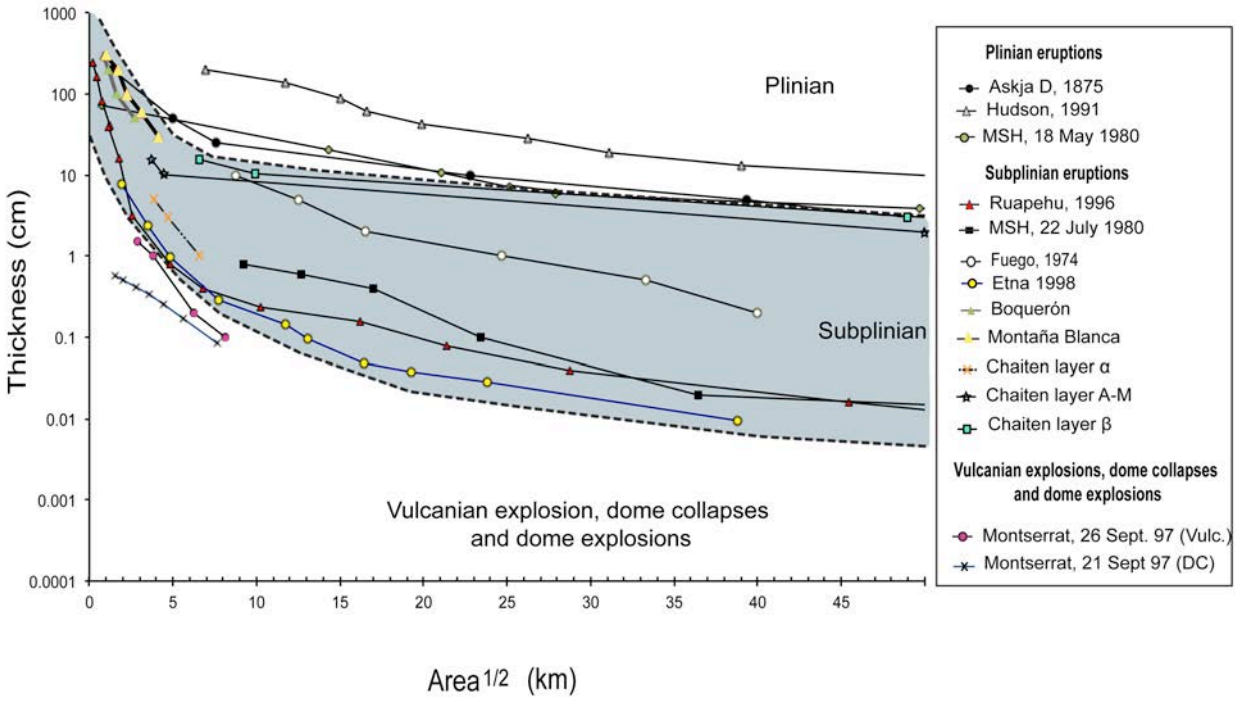

Fig. 9 Semi-log plot of thickness versus the square root of the area of the Boqueron deposit compared with the thinning trend of other deposits produced by explosive eruptions. Data are from: Askja D, 1875 (Sparks et al. 1981); Hudson 1991 (Scasso et al. 1994); Mount St. Helens 18 May, 1980 (Sarna-Wojciki et al. 1981); Ruapehu, 17 June 1996 (Bonadonna and Houghton 2005); Montserrat 26 September, 1997 (Bonadonna et al. 2002); Montserrat 21 September, 1997 (Bonadonna et al. 2002); Fuego, 1974 (Rose et al. 2008); Etna 1998 (Bonadonna and Costa 2012); Montaña Blanca, 2 Ka (Ablay et al. 1995); Chaiten May, 2008 (Alfano et al. 2010).

3.6.1 Deposit dispersal, eruption column and duration.

In order to estimate the uncertainty involved in calculating the volumes of deposits characterised by poor exposure, we constructed two possible isopach maps based on the same set of data. The error associated with the two compilations of the isopach map is about 30%, 40% and 50% for Weibull, the exponential and the power-law method respectively. These values are of the same order of magnitude of other estimations of volume-calculation uncertainties made on better exposed deposits (e.g., 30% estimated uncertainty for the exponential method by Cioni et al. (2011) on the 512 AD Vesuvius eruptions). In addition, Bonadonna and Costa (2012) have already shown how the stability of the Weibull method is better than that of the other two empirical methods because it dependends on only three free parameters (i.e., l, q, n). As a result, the volume can be constrained more easily (when ≥ 3 points are available) and without the need of arbitrary and subjective choices, such as the number of exponential segments and the integration limits.

	MER ($\times 10^5$ kg/s)	Duration (Isopach A) (hours)	Duration (Isopach B) (hours)
Wilson and Walker (1987)	6.9	10.2	15.1
Sparks (1986)	8.2	8.6	12.7

Table 4 Summary of the MER and eruption duration calculation based on a plume height of 6.8 km (calculated with the method of Carey and Sparks 1986) and for the methods of Wilson and Walker (1987) and Sparks (1986). The eruptions duration is calculated based on the ratio between the erupted mass (calculated based on the Weibull integration applied to isopach A and B of Fig. 3) and the two values of MER.

The plume height was derived using the method of Carey and Sparks (1986). In particular, the height derived based on the average of geometric mean of the 5 largest clasts was compared to the height derived based on the 50th percentile of a 20-clast population suggested by the IAVCEI Commission on Tephra Hazard Modelling (Bonadonna et al. 2011; Bonadonna et al., submitted). In fact, the method of the 50th percentile is considered more stable even though it still needs to be calibrated with the original plots of Carey and Sparks (1986). As a result, we confidently conclude that the plume reached a maximum height of 7 km above the vent (i.e. 9 km a.s.l) The uncertainty in the calculation of the MER based on two different methods is around 16% (Wilson and Walker 1987; Sparks 1986), which results in an uncertainty in the inferred eruption duration of up to 43% based on the two MER values and the Weibull-derived volume associated with isopach maps A and B (Table 4).

3.6.2 Textures

Boqueron juvenile pumice fragments have been characterised on the basis of vesicularity and groundmass texture. The differences between juvenile clasts can be substantial, both in density and texture (Figs 10 and 11). The majority of clasts display homogenous textures with high vesicularity, small vesicles with complex shapes and glassy groundmass, suggesting high nucleation rates, and an expansion-dominated coalescence (Szramek et al., 2006). In contrast, the lower vesicularity clasts display heterogeneous textures with smaller, rounded vesicles and higher groundmass crystallinity, possibly due to the effects of postfragmentation expansion and clasts

recycling during lower explosivity phases (Wright et al., 2006). In addition, the welding of the proximal deposits suggests higher deposition rates and high depositional temperatures associated with low viscosity, favouring clast agglutination and deformation (Carey et al., 2008). This appears to be a common process for phonolitic eruptions of the TPV complex, and for older plinian fall deposits cropping out in the Las Cañadas walls (Ablay et al., 1995; Soriano et al., 2002).

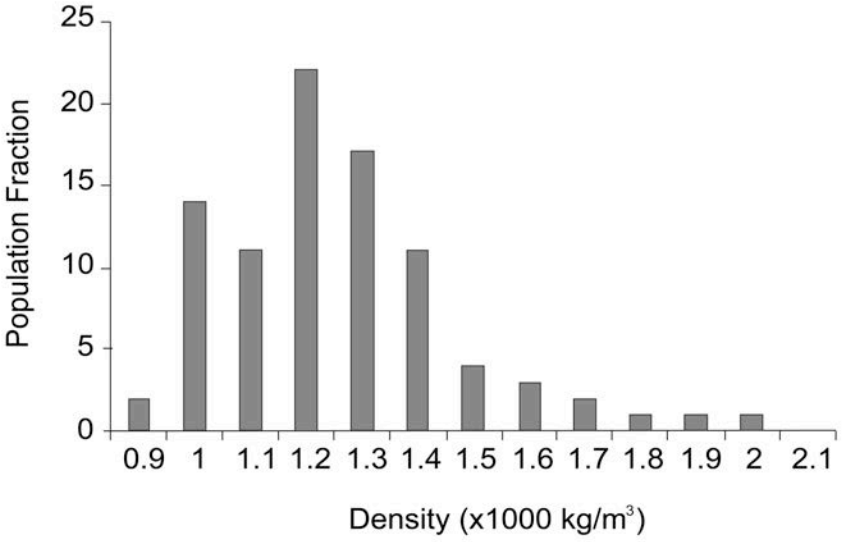

Fig. 10 Density distribution histogram of juvenile clasts from Boquerón Unit.

3.6.3 Volcanic hazard and risk

TPV is one of the largest volcanic complexes in Europe, and is located at the top of a densely populated island that is also a very popular destination for tourism. The main known volcanic hazard is associated with basaltic fissural eruptions which mainly

take place along the two active rift zones. However, there is also clear evidence of effusive and explosive phonolitic volcanism during the Holocene, with significant hazard implications, not only for the Las Cañadas area, but also for the Icod valley, which connects the TPV complex to the N coast of the island. In fact, among the known lateral eruptions of the TPV complex, at least 16 have produced phonolitic magmas, which can also be associated with highly-mobile low-viscosity lava flows (Dingwell et al. 1998; Giordano et al. 2000; Gottsmann and Dingwell 2011).

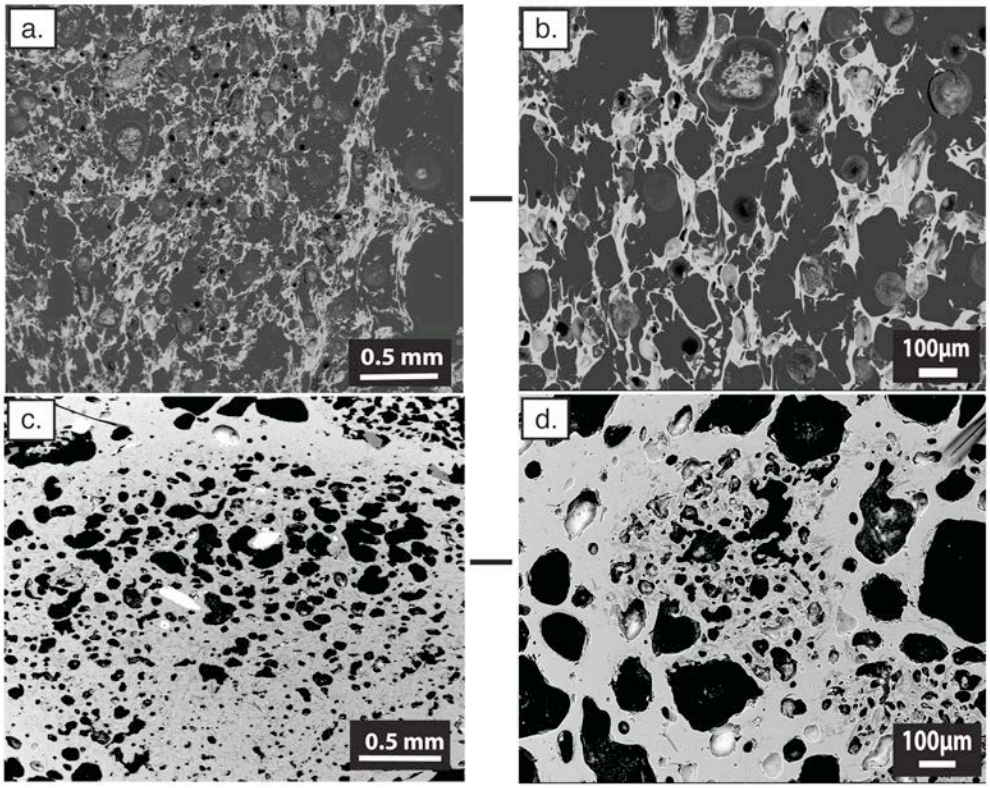

Fig. 11 Selected backscattered SEM images (25x and 200x magnification-) of juvenile clasts of different vesicularity. Vesicles are in black, while the glass and microlites groundmass are in grey. a) sample with high vesiculation; b) detail of vesicles in the sample with high vesiculation; c) sample with low vesiculation; d) Detail with vesicles in the sample of low vesiculation.

Like the Boqueron, most of these eruptions were also dome forming with vents located at the flanks of the TPV (2300 m a.s.l), and they also had associated PDCs (Martí et al 2008; 2011). Among them, the Montaña Blanca (2020 BP) is the best known and most recent eruption (Ablay et al. 1995). It produced a 10 km high eruption column and a tephra deposit with a volume of $1.4x10^8$ m^3 dispersed over an area of 30 km^2 (based on maps of Ablay et al. 1995). The last eruption in Tenerife was the basaltic strombolian eruption of Chinyero, 1909, on the NW rift, which did not cause major disruption to population (Solana and Aparicio, 1998). The only known eruption that has caused fatalities and major disruption in Tenerife occurred in 1706, when a basaltic lava flow, originated from a vent on the Santiago rift (outside the TPV), almost destroyed Garachico, the former capital of the island, inducing a massive spontaneous evacuation (Solana and Aparicio, 1998). Since then Tenerife has experienced population growth significantly higher than the national average, and it is now the most populated island of Spain with more than 900,000 inhabitants. In addition, Tenerife is one of the main tourist destinations in Europe with more than five million visitors per year, and the main populated municipalities in Tenerife (Santa Cruz, San Cristobal de la Laguna and Puerto de la Cruz) are less than 30 km away from the TPV. Aviation could also be significantly affected by a new explosive eruption of the TPV. In fact, all Canarias airports fall in a circle of 300 km radius centred on the TPV complex, with the Canary Islands lying along one of the main civil aviation corridors for flights from Europe to Central and South America and vice versa. Marti et al. (2011) have already shown that a subplinian eruption from the Boqueron vent (i.e., calculations based on a plume height of 9 km above sea level and volume of 0.05 km^3) would significantly affect the Northern coast of Tenerife, including the towns of Icod de los Vinos, Santa Cruz, La Orotava, Puerto de

la Cruz, and the North airport. All the roads in the northern part of the island and the main road that connects the North to the South would be covered by 1mm to 5cm of ash. Given that our detailed study of the Boqueron eruption results in a similar plume height and volume as modeled by Marti et al. (2011) (i.e., 7 km and 0.04-0.06 km^3 respectively), we would expect that another eruption of this type would be associated to disruption equivalent to that described by Marti et al. (2011).

3.7 Conclusions

Despite poor levels of exposure, we have provided an accurate study of the deposits associated with the last Boqueron eruption based on a detailed description of stratigraphy and sedimentological features, including the morphology, textural features and composition of the juvenile fraction. This has allowed for a reconstruction of the eruption dynamics and the main physical parameters. As a result, we can conclude that:

1) Empirical calculations resulted in a tephra volume between 1-8x10^7 m^3 with the best estimate between 4-6x10^7 m^3 (based on the Weibull integration of two possible maps). The uncertainty associated with the volume calculation of tephra deposits is about 30%, 40% and 50% for the Weibull, exponential and the power-law integrations respectively.

2) The plume reached a maximum height of 9 km above sea level (i.e. 7 km above the vent) with a corresponding MER and duration of 6.9-8.2x10^5 kg/s and 9-15 hours, respectively.

3) The explosive phase could be classified as a VEI=3 subplinian eruption based on dispersal and thinning characteristics. Magnitude and intensity are 3.4-3.6 and

9, respectively.

4) The proximal welding and stratification of the deposit, together with th typical pumiceous textures of the majority of the lapilli, suggest complex dynamics, shifts from highly explosive phases to minor phases, and dispersal high temperature bombs in proximal locations.

5) If a Boqueron-style eruption were to happen again, it would have a large impact on the now densely populated island of Tenerife, particularly towards the north, and on various economic sectors, such as the aviation business.

4. Eruptive scenarios of phonolite volcanism at Teide-Pico Viejo volcanic complex (Tenerife, Canary Islands)

This paper has been published in the Bulletin of Volcanology. The authors of the papers are:

Joan Martí, Institute of Earth Sciences "Jaume Almera", CSIC, Lluis Solé Sabarís s/n, 08028 Barcelona, Spain

Rosa Sobradelo, Institute of Earth Sciences "Jaume Almera", CSIC, Lluis Solé Sabarís s/n, 08028 Barcelona, Spain.

Alicia Felpeto, Observatorio Geofísico Central, Instituto Geográfico Nacional (IGN), c/Alfonso XII, 3, 28014 Madrid, Spain .

Olaya García, Centro Geofísico de Canarias, Instituto Geográfico Nacional (IGN), c/La Marina 20, 2º, 38001 S/C de Tenerife, Spain

.The reference of this paper is: Martí J, Sobradelo R, Felpeto A, García O (2012) Eruptive scenarios of phonolitic volcanism at Teide-Pico Viejo volcanic complex (Tenerife, Canary Islands) Bulletin of Volcanology 74: 767-782 doi: 10.1007/s00445-011-0569

4.1 Introduction

Tenerife is the largest (2.050 km$^{2)}$ and most populated (>900.000 inhabitants) of the Canary Islands. As for the rest of this volcanic archipelago, its mild climate and impressive volcanic landscapes, including the dormant Teide and Pico Viejo complex (TPV), have contributed to make it one of the main tourist destinations in Europe with more than five million visitors per year. The presence of recurrent historical volcanism on this island is a convincing reason to undertake volcanic hazard assessment for risk-based decision-making in land-use planning and emergency management and, consequently, to improve the security of its inhabitants and its numerous visitors.

The main concern about potential future volcanic activity on Tenerife has traditionally been addressed towards basaltic eruptions taking place along the two active rift zones, as they have occurred in historical times (Carracedo et al. 2007, 2010). However, despite the occurrence of numerous eruptions during the Holocene (Carracedo et al. 2007) and of unequivocal signs of activity in historical times (fumaroles, seismicity) (IGN seismic catalogue) and even an unrest episode in 2004 (García et al. 2006; Pérez et al. 2005; Gottsmann et al. 2006; Martí et al. 2009; Domínguez Cerdeña et al. 2011), TPV has not been considered as a major threat.

Although the highest probability of having a new eruption on Tenerife corresponds to a basaltic eruption along the rift zones, which today would also represent a significant trouble for the island, the probability of having a new eruption from the TPV central complex is not negligible. This is indicated by the number of eruptions that it has produced during the Holocene (see Carracedo et al. 2007), most of them of

phonolitic composition and triggered by intrusion of deep basaltic magma into shallow felsic magma chambers (Marti et al. 2008).

The complexity of any volcanic system and its associated eruptive processes, together with the lack of data that characterises many active volcanoes, particularly those with long periods between eruptions, makes volcanic hazard quantification very challenging, as there is often not enough observational data to build a robust statistical model. This is the case for TPV, about which information on their past eruptive history and its present state of activity is still incomplete. This restricts the existing techniques for forecasting its future behaviour to within a minimum margin of confidence. However, different efforts have been made to assess volcanic hazard at TPV in the form of event tree structures representing possible eruptive scenarios and using the available geological and geophysical information (Martí et al. 2008b; Sobradelo and Martí 2010). Bayesian inference and expert judgement elicitation techniques have been applied to these event trees to estimate the long-term probability for each scenario within a given time window. This has allowed us to rationalise our current knowledge of TPV and provides a tool for understanding and anticipating the future behaviour of these volcanoes. These previous studies have not yet, however, been able to quantify the recurrence and extent for each possible scenario.

In order to move one step forward in the hazard assessment at TPV, it is important to estimate the temporal and spatial probability of an eruption for various time windows in the near future and study in detail-specific eruptive scenarios for each of the main associated hazards. This study focusses on phonolitic volcanism, as it has been clearly dominant at TPV through the Holocene and also because it would produce the

most hazardous scenarios. In this paper, we first do a threat analysis of the TPV complex using the Ewert et al. (2005) template in order to compare them with other volcanoes of similar characteristics. Then we calculate the temporal and spatial probability of a phonolitic eruption from TPV using available data. After that, we computed several significant scenarios using the GIS-based VORIS 2 software (Felpeto et al. 2007) in order to evaluate the potential extent of the main eruption hazards expected from TPV. Finally, we discuss the results obtained and compare them with the Bayesian technique previously applied to estimate the long-term hazard. The elaboration of a quantitative hazard map for the whole island of Tenerife, including a probabilistic estimate for each point of the map of being impacted by the different hazards considered, is beyond the purpose of this study and will constitute the specific.

4.2 Geological background

TPV complex is composed by the twin Teide and Pico Viejo stratovolcanoes that started to grow simultaneously at about 180–190 ka within the Las Cañadas caldera (Fig. 1), which is a volcanic depression formed by several vertical collapses of the former Tenerife central volcanic edifice (Las Cañadas edifice) following explosive emptying of a high-level magma chamber. Occasional lateral collapses of the volcano flanks also occurred and modified the resulting caldera depression (Martí et al. 1994, 1997; Martí and Gudmundsson 2000). The construction of the present central volcanic complex on Tenerife encompasses the formation of these twin stratovolcanoes, which derive from the interaction of two different shallow magma systems that evolved

simultaneously, giving rise to a complete series from basalt to phonolite (Ablay et al. 1998; Martí et al. 2008a).

The structure and volcanic stratigraphy of the TPV was characterised by Ablay and Martí (2000), based on a detailed field and petrological study. Later, Carracedo et al. (2003, 2007) provided the first group of isotopic ages from TPV products, and Martí et al. (2008a)analysedthe potential for future TPV activity. More recently, García et al. (2011) identified the products of several explosive eruptions of phonolitic composition from these volcanoes. The reader will find in these works more complete descriptions of the stratigraphic and volcanological evolution of TPV.

TPV mostly consists of mafic to intermediate products, with felsic materials volumetrically subordinate overall (see Martí et al. 2008a). Felsic products, however, dominate the recent output of the TPV system. Eruptions at TPV have occurred from their central vents but also from a multitude of vents distributed on their flanks (Fig. 1). Mafic and phonolitic magmas have been erupted from these vents. The Santiago del Teide and Dorsal rift axes (Fig. 1), the two main tectonic lineations currently active on Tenerife, probably join beneath TPV complex (Carracedo 1994; Ablay and Martí 2000). Some flank vents at the western side of Pico Viejo are located on eruption fissures that are sub-parallel to fissures down the Santiago del Teide rift and define the main rift axis. On the eastern side of Teide, some flank vents define eruption fissures orientated parallel to the Dorsal rift.

The eruptive history of the TPV comprises a main stage of eruption of mafic to intermediate lavas that form the core of the volcanoes and also infill most of the Las Cañadas depression and the adjacent La Orotava and Icod valleys. At about 35 ka, the first phonolites appeared, and since then, they have become the predominant

composition in the TPV eruptions. Basaltic eruptions have also continued mostly associated with the two main rift zones. The available petrological data suggest that the interaction of a deep basaltic magmatic system with a shallow phonolitic magmatic one beneath central Tenerife controls the eruption dynamics of TPV (Martí et al. 2008a). Most of the phonolitic eruptions from TPV show signs of magma mixing, suggesting that eruptions were triggered by intrusion of deep basaltic magmas into shallow phonolitic reservoirs.

Phonolitic activity from TPV shows repose intervals around 250–1,000 years, according to the isotopic ages published by Carracedo et al. (2003, 2007).

Phonolitic eruptions from TPV range volumen from 0.01 to >1 km^3 and mostly produce thick clastogenic lava flows and domes, occasionally associated with explosive episodes ranging from subplinian to plinian, which have generated extensive pumice fall deposits and PDCs (Ablay et al. 1995; Martí et al. 2008a; García et al. 2011). The emplacement of clastogenic lava flows and domes have also generated explosive episodes when block and ash flows were generated by gravitational collapses (García et al. 2011).

Some significant basaltic eruptions have occurred as well from the flanks or the central vents of TPV. All basaltic eruptions have developed explosive strombolian to violent strombolian phases leading to the construction of scoria cones and occasionally producing intense lava fountaining and violent explosions with the formation of ash-rich eruption columns. Violent basaltic phreatomagmatic eruptions have also occurred from the central craters of the TPV, generating high-energy, pyroclastic density currents. Table 1 summarises 16 phonolitic eruptions documented geologically for TPV during Holocene.

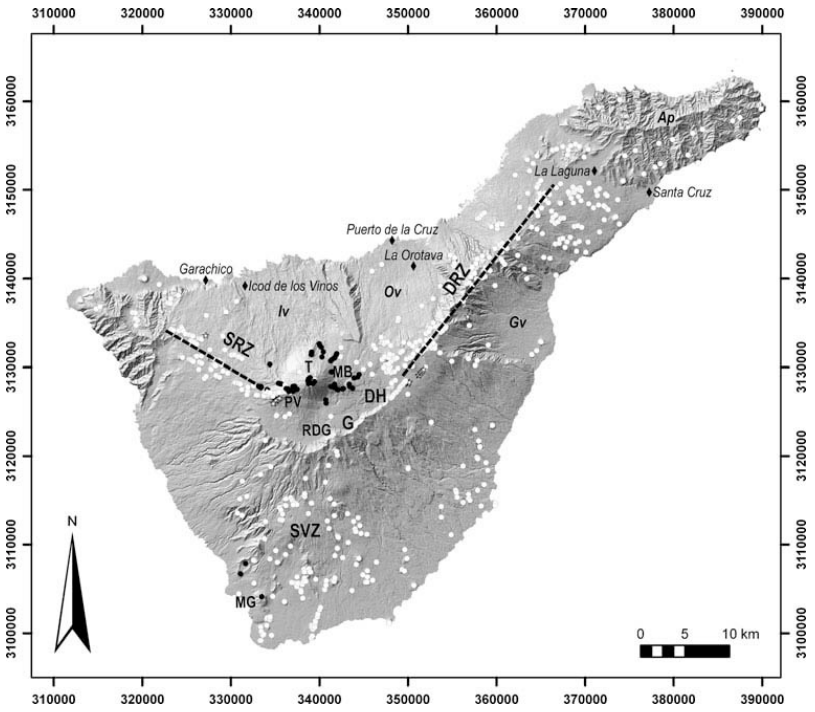

Fig.1 Simplified geological and topographic map pf Tenerife illustrating the genral distribution of visible vents. *Black symbols* mafic and intermedie vents; *white symbols* felsic vents; *stars* historic and subhistoric vents; *circles* other vents. *Grey squares* some main population centres. *DH* Diego Hernández, *DRZ* Dorsal rift zone, *G* Guajara, *MB* Montaña Blanca, *MG* Montaña Guaza, *RDG* Roques de García, *T* Teide volcano, *PV* Pico Viejo volcano, *SRZ* Santiago rift zone, *SVZ* sourth volcanic zone, *Iv* Icod valley, *Ov* Orotava valley, *Gv* Güimar valley, *Ap* Anaga peninsula (projection: UTM 28N)

4.3 Threat analysis

Quantification of the threat posed by volcanoes is an important issue when trying to define the monitoring level required by each volcano, especially in comparison with others. Ewert et al. (2005) developed the National Volcano Early Warning System (NVEWS) intending to assess the threat posed by US volcanoes, proposing an analysis scheme based on several factors. These factors can be divided into two main groups:

those associated with hazard and those associated with exposure of human, social and economical elements potentially affected by the hazard, i.e. with risk. The product of the sums of all the factors of each type gives a threat score that allows the classification of the US volcano in four categories, grouped by the required monitoring level.

Event ID	Eruption Name	Years BP	Total Erupted DRE in m^3	Total Erupted Mass, in kg	Magnitude Scale
1	Montaña Reventada	895	138194471,1	3,45486E+11	4,5384
2	Lavas Negras	1,150	474,452,978	1.18613E+12	5.0741
3	Roques Blancos	1714-1790	833890093,4	2,08473E+12	5,3190
4	Montaña Blanca	2020	107382578,7	2,68456E+11	4,4289
5	Montaña Majua	3520?	69744811,59	1,74362E+11	4,2415
6	El Boqueron	2528-5660	44283790,64	1,10709E+11	4,0442
7	Cañada Blanca	2,528-5,911	70,115,211.27	1.75288E+11	4.2438
8	Abejera Baja	5486	285594326	7,13986E+11	4,8537
9	Abejera Alta	5911	361,123,567.2	9.02809E+11	4,96
10	Pico Cabras	5911-7900	285594326	7,13986E+11	4,8537
11	Abrunco	<10000	2,086,022.525	5,215,056,313	2.7173
12	Montaña de la Cruz	<10000	131,444,541.8	3.28611E+11	4.5167
13	Arenas Blancas	<10000	101,381,078.6	2.53453E+11	4.4039
14	Montaña de los Conejos	≥10000	70,723,423.92	1.76809E+11	4.2475
15	Bocas de María	≥10000	23,265,710.9	58,164,277,258	3.7647
16	Montaña Las Lajas	≥10000	10,769,291.55	26,923,228,872	3.4301

Tabla 1 TPV Holocene phonolitic eruptions. Ages from Carracedo et al. (2007) and García et al. (2012)

Other authors have applied NVEWS analysis to other volcanoes, such as Kinvig et al. (2010), who recently applied this analysis to Nysiros volcano (Greece). In this paper, we applied the NVEWS scheme in order to quantify the threat posed by TPV

and to facilitate the comparison with other volcanoes. Scores given to each factor (labelled from (a) to (y)) and the total result are shown in Table 2. Brief explanations of the factors we took into account are given in the next sections, while Table 2 caption indicates how the corresponding scores were assigned and lists the bibliographic/web sources used.

4.3.1 Hazard factors

TPV includes two stratovolcanoes (a), with major explosive activity during the last 10,000 years (see Table 1) with calculated magnitudes up to 5. In a few cases where associated pyroclastic fall deposits have been preserved, it has been also possible to estimate a Volcanic Explosivity Index (VEI) value, which combines magnitude, intensity (eruption rate) and explosivity (eruption column high) of the eruption (Newhall and Self 1982), for these particular cases, which ranges from 3 to 4 (b) (d) (see below). The historical period of Tenerife is relatively short as it starts with the conquering of the island by the Spanish crown in 1496. Since then, four eruptions (all of them basaltic) have occurred on the island, only one on TPV (1798, Chahorra eruption). During the Holocene, at least 16 phonolitic eruptions occurred in TPV as shown in Table 1 (e), including most of the volcanic hazards: pyroclastic flows, lava flows, lahars… (f)(g)(h), although there is no evidence for a volcanic tsunami (j). TPV hydrothermal systems are large enough to justify its potential for hydrothermal explosions (i). This fact plus the steep slopes of their flanks and their history of sector collapses (Ablay and Martí 2000) show its potential for new sector collapses (k). In 2004– 2005, an episode of volcanic unrest took place in the island of Tenerife, characterised by a great increase on the seismic activity around the TPV system and changes in the fumarolic system (m)(o).

4.3.2 Exposure factors

The first exposure factors measures the population in a circle of 30 km centred on the volcano. This circle centred on TPV comprises most of Tenerife Island, leaving out only the Anaga peninsula, which includes the two most populated municipalities of the island (Santa Cruz and San Cristóbal de la Laguna), so almost the same population lives inside and outside the circle. Based on public data published by the National Institute of Statistics for 2009, the population included in the circle is about 442,000. However, Tenerife is one of the main tourist destinations of Europe, so the touristic population should also be taken into account. During 2009, the mean daily hotel occupancy in the island was about 52,000 tourists, so the value of (p) factor can reach 5 (see Table 2). There is almost no difference in the population downstream of the volcano that lies beyond, versus within, the abovemention circle.

No fatalities have been recorded during eruptions at Tenerife. A massive evacuation occurred during 1706, when basaltic lava flows almost destroyed Garachico, the former capital of the island, but that basaltic eruption had its vent on Santiago rift, not on TPV (s).

TPV poses a significant threat to aviation, as all the eight Canarian airposrts fall in a circle of 300 km radius centred between the two stratovolcanoes. The mean number of daily passengers in this circle was around 82,200 during 2009 (t)(u). The Canary Islands constitute one of the main civil aviation corridors for flights from Europe to Central and South America and vice versa.

Table 2 TPV NVEWS socring factor.

		Scoring Range
Teide-Pico Viejo	hazard Factors	
(a)	Volcano type	1
(b)	Maximum Volcanic Explosivity Index	2
(c)	Explosive activity in past 500 years?	0
(d)	Major explosive activity in past 5000 years?	1
(e)	Eruption recurrence	1
(f)	Holocene pyroclastic flows?	1
(g)	Holocene lahars?	1
(h)	Holocene lava flow?	1
(i)	Hydrothermal explosion potential?	1
(j)	Holocene tsunami?	0
(k)	Sector collapse potential?	1
(l)	Primary lahar source?	0
(m)	Observed seismic unrest?	1
(n)	Observed ground deformation?	0
(o)	Observed fumarolic or magmatic degassing?	1
	Total of Hazard Factors	11
Teide-Pico Viejo exposure factors		
(p)	Log10 of Volcano Population Index (VPI) at 30 km	4
(q)	Log10 of approximate population downstream or downslope	0
(r)	Historical fatalities?	0
(s)	Historical evacuations?	0
(t)	Local aviation exposure	2
(u)	Regional aviation exposure	5
(v)	Power infrastructure	1
(w)	Transportation infrastructure	1
(x)	Major development or sensitive areas	1
(y)	Volcano is a significant part of a populated island	1
	Total of Exposure Factors	15
	Sum of all hazard factors X Sum of all exposure factors	

We tried to use conservative values for the scores of each factor in order to minimize the uncertainty caused by the lack of data in some cases, so that the threat score obtained is a minimum. (a) Volcano type tries to quantify how dangerous a volcano is and has two categories: type 0 volcanoes, including cinder cones, basaltic volcanic fields, shields, tuff rings and fissure vents, and type 1 volcanoes which are generally more explosive, including stratovolcanoes, lava domes, complex volcanoes, maars and calderas. (b) The VEI is an indicator of the explosive character and size of an eruption (Newhall and Self 1982). In the NVEWS scheme, the scores are 1 for VEI of 3–4, 2 for a VEI of 5–6 and 3 for a VEI of 7–

8. (c) Explosive activity and (d) major explosive activity refer to the presence of repeated explosive episodes in the past eruptions record, as scores as 1 for VEI≥3 within the last 500 years and VEI≥4 within

the last 5,000 years, respectively. (e) Eruption recurrence: It scores 4 if the eruption interval is 1–99 years, 3 if it is 100–1,000, 2 if it 1,000 to several thousands, 1 if eruption interval is 5,000–10,000 years and 0 if there are not Holocene eruptions. For factors (f) to (o), possible scores are 1 or 0 if the answer is yes or not, respectively (see Ewert et al. 2005 for more details). For exposure factors and their possible scores, see text and Ewert et al. (2005, p. 47). Information sources: (a) Ablay and Martí (2000); (b) García et al. (2011); (c)–(e) Carracedo et al. (2007); (f)–(h) Martí et al. (2008b) and García et al. (2011); (i) Del Potro and Hurlimann (2008) and Rodriguez Losada et al. (2009); (k) Ablay and Martí (2000) and Ablay and Hürlimann (2000); (m) Spanish Geographical Institute (http:// www.ign.es), García et al. (2006) and Martí et al. (2009); (o) Hernández et al. (1998), Pérez et al. (2005) and Martí et al. (2009); (p) Spanish National Institute of Statistics (http:\\www.ine.es); (t)–(u) Association of Spanish Airports (http://www.aena.es)

4.4 Evaluation of temporal and spatial probability of a phonolitic eruption in TPV

4.4.1 Temporal probability

Mid/long-term assessment of the temporal probability of occurrence of a volcanic eruption of certain (or exceeding a) magnitude or size is usually computed by analyzing the sequence of past eruptions in a volcano and characterizing them by a measure of their size or magnitude (Pyle 2000). This may be indicated as magnitude, understanding it as a measure of the total volume of magma erupted, or as VEI. Unfortunately, only a small proportion of eruptions have been witnessed, so for most cases the data required to estimate the size of an eruption have to be collected in the field from physical volcanology studies of the eruption products. An additional

complexity comes from the fact that it is very common that the record of volcanic eruptions is incomplete, especially for the pre-historical section of the record and the low-magnitude eruptions, and this may significantly affect the accuracy and completeness of the reconstruction of the volcano's eruption record.

In the case of TPV, at least 16 phonolitic eruptions can be identified on stratigraphic and geochronological bases in the Holocene (Carracedo et al. 2007; Martí et al. 2008a; García et al. unpublished data, 2011). At least 15 of these eruptions were of magnitude M greater than 3, based on minimum volumes exposed (Table 1) and applying the equation proposed by Pyle (2000) to calculate the magnitud scale as follows:

$$Magnitude\ (M) = \log 10\,(total\ erupted\ mass, kg) - 7 \qquad (1)$$

For example the magnitude for the first eruption in Table "Montaña Reventada" is $Magnitude\ (M) = \log 10\,(3.45486E + 11) - 7 = 4.5384$. Some of these eruptions also included explosive phases that generated fall deposits of different extents and thicknesses. Despite the poor preservation of these deposits, their characterization in terms of grain size and thickness variations has allowed us to assign a minimum VEI value to each of them. It was not possible to determine with precision the total volume corresponding to the fall deposits, so the total volume of erupted magma (magnitude) for the eruptions including effusive and explosive phases was probably underestimated compared to those volumes for eruptions without associated fall deposits. The absence of pyroclastic deposits does not necessarily mean that these other eruptions were not explosive at all, as it is also possible that the corresponding pyroclastic deposits could

have been completely eroded. For this reason, we used *M,* principally based on the volume of lavas exposed, instead of VEI, as it offers a better estimate of the minimum size of the TPV eruptions and allows comparisons among them.

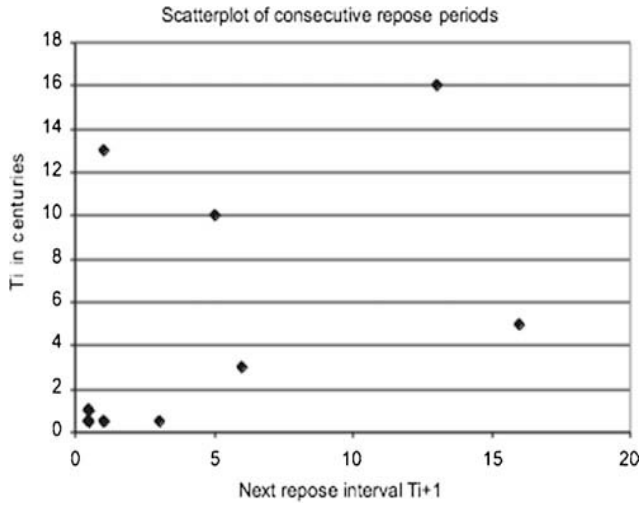

Fig.2 Scatterplot of consecutive repose intervals for TPV time series.

In this paper, we used a non-homogeneous Poisson process with a generalized Pareto distribution (GPD) as an intensity function (NHGPPP) to model the TPV time series and compute the temporal probabilities of at least one eruption in a given time interval (Coles 2001; Mendoza-Rosas and De la Cruz-Reyna 2008; Sobradelo et al. 2011). NHGPPP is an extreme value theory statistical method, very robust for modelling small time series of incomplete geological records and useful for obtaining estimates of the probability of intermediate-to high-magnitude eruption events (Coles 2001). We used this method because the incomplete geological record of the eruption products from TPV requires an estimation technique that is not very sensitive to the fact that we have a small dataset. This method is also appropriate when we have a time series of extreme values like this which is a dataset containing very few, probably incomplete,

data. The GPD is a robust tool which allows modelling extreme values, such as the "rare" high-magnitude eruptions.

The fact that there is one eruption documented with $M< 3$ and that the number of eruptions with $M =3$ is significantly lower than those of $M=4$ makes us believe that the catalogue may be incomplete. To account for the possible missing data or inaccuracies in the catalogue, the occurrence rates for Ms 4 and 5 were used to extrapolate unobserved records using the best fit to the class VEI values of eruptions. In order to estimate these values, we used the power law described by Newhall and Self (1982), which was originally defined for VEIs but that in our case is applied to magnitudes, as higher magnitudes also imply potentially higher VEI. We therefore redefine this power law by saying that the eruption occurrence rate λM (number of eruptions per unit time) of each class M is related to the eruption size as:

$$log\lambda_M = a - b\ x\ M \tag{2}$$

where a and b are constants that describe the power law decay of occurrences with increasing size *M* over a given time interval.

In order to apply the NHGPPP, we used the exceedance over a threshold (EOT) to sample the original data; this is Xi>u for some value of i. The reader will find a complete explanation of this methodology in Coles (2001) and Mendoza-Rosas and De la Cruz-Reyna (2008). Sobradelo et al. (2011) have applied the same method to the Canary Islands historical records.

The EOT method includes all the values of the variable that exceed an a priori established threshold, u, fixed according to the model needs, providing a physically

based definition of what must be considered an extreme event. The choice of the threshold value has a strong subjective component. This random variable is defined by the transformed random variable $Y=u$, for all $Xi>u$ where Y is the excess over the threshold u, the M value in our case. The parameter that was used as random variable to estimate the probability of occurrence of a future eruption and thus the volcanic hazard was the time interval T between eruptions, also called repose period, together with the M size.

Figure 2 shows a scatterplot of the repose periods, where the duration of the interval Ti+1 between two successive eruptions is plotted against the duration of the previous repose interval Ti. The diagram in Fig. 2 shows a large dispersion of points. The correlation coefficient between consecutive repose times is 0.5457, indicating a low serial correlation. We do not have enough evidence to say that consecutive repose intervals are time-dependent based on these data, so we assume independence of repose times for the purpose of this study.

For the particular case of volcanic eruptions, the size of the eruptions and the time of their occurrence are viewed as points in a two-dimensional space, which formally is the realisation of a point process. The intensity measure 321 $\Lambda_B>u$ of this two-dimensional Poisson process on the space $B = [t_1, t_2]\times(u, \infty)$ with $[t_1, t_2] \subset [0,1]$ is given by

$$\Lambda_B = (t_2, t_1)\left(1 - \frac{\beta(1-u)}{\theta}\right)^{1/\beta} \qquad (3)$$

where β and θ are the parameters of the GPD, computed using a diagnostic method introduced by Davison and Smith (1990) which also serves to decide how well

the model fits the data. This method is based on the property that the mean excess over a threshold u, for any $u>0$, is a linear function of u. The mean excess is defined as

$$E(X-u|X>u)=\frac{\theta-\beta u}{1+\beta} \qquad (4)$$

for $\beta>1$, $u>0$and $(\theta-\beta u)>0$. The expected value was estimated using the sample mean excess computed from the data. In Fig. 3, we plot the sample mean of the excesses versus their thresholds. The x-axis is the threshold and the y-axis is the sample mean of all excesses over that threshold. As we can see, the mean excess follow as an early straight line, with an R^2 of 0.9996, suggesting a good fit. A regression line for the mean of excedances over the threshold has been added to confirm the series follows the GPD.

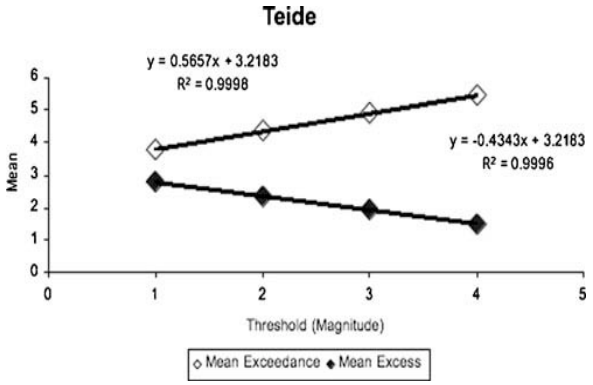

Fig. 3 Plot of excedance and excess mean vs. Threshold for TPV.

Hence, according to Davison and Smith (1990), the preceding results indicate that the NHGPPP was satisfactory and appropriate to model our data. The Pareto generalized parameters for the process, derived from the regression parameters in Fig. 3 and Eq. 4, are 0.768 for shape and 5.689 for the scale. Using Eq. 2, we estimated the intensity λ of the NHGPPP and obtained the probability estimations of at least one eruption of a certain M size in a given time interval. Table 3 shows the probability of

having at least one eruption Pr ($X \geq 1$) computed as 1 minus the probability of having no eruption $1-\Pr(X=0)$ of a certain M size in a given time window, estimated using the NHGPPP with intensity rate λ. To measure the volatility of the estimated probabilities, we computed the standard deviation σ the estimator using the delta method to determine its asymptotic distribution.

Years	Pr(X=0) (%)	bl	Pr(X=>1) (%)	bs
M>2				
1	99.8	0.002	0.2	0.0002
20	95.4	0.047	4.6	0.003
50	88.9	0.118	11.1	0.007
100	79.0	0.236	21.0	0.011
500	30.7	1.180	69.3	0.009
	1,000	09.4	2.360	90.6
	0.002			
M>3				
1	99.8	0.002	0.2	0.0001
20	96.3	0.038	3.7	0.003
50	90.9	0.095	9.1	0.006
100	82.7	0.190	17.3	0.010
500	38.6	0.951	61.4	0.011
	1,000	14.9	1.901	85.1
	0.003			
M>4				
1	99.9	0.001	0.1	0.0001
20	97.1	0.029	2.9	0.002
50	92.9	0.073	7.1	0.005
100	86.4	0.146	13.6	0.008
500	48.1	0.732	51.9	0.013
	1,000	23.1	1.464	76.9
	0.006			
M>5				
1	99.9	0.001	0.1	0.0001
20	97.9	0.021	2.1	0.002
50	94.9	0.052	5.1	0.004
100	90.0	0.105	10.0	0.007
500	59.2	0.525	40.8	0.014
	1,000	35.0	1.050	65.0
	0.010			
M>6				
1	99.9	0.001	0.1	0.0001
20	98.7	0.013	1.3	0.001
50	96.7	0.033	3.3	0.002
100	93.6	0.066	6.4	0.004
500	71.8	0.332	28.2	0.013
1,000	51.5	0.663	48.5	0.014

Table 3 Probability of at least one event of size $M>x$ in the next t years in the TPV complex estimated with a NHGPPP ($\Pr(X=0)$ and $\Pr(X\geq 1)$ are the probability of having no eruption and the probability of

having at least one eruption, respectively, of a certain size in a particular time interval; is the estimated parameter rate for the NHGPPP, and is the estimated standard deviation for the Pr($X \geq 1$) computed with the NHGPPP, bases on the delta method)

4.4.2 Spatial probability

Felpeto et al. (2007) and Martí and Felpeto (2010) have proposed the term volcanic susceptibility for the spatial probability of vent opening. Martí and Felpeto (2010) compute this probability for long-term analysis based on a multicriteria analysis. Similarly, Marzocchi et al. (2010)in their system BET-VH compute the spatial probability based on a Bayesian approach.

The evaluation of susceptibility of phonolitic eruptions in the island of Tenerife made by Martí and Felpeto (2010) assumed tha tthe main stress field in the island has remained constant for the last 35 ky. The input data used were the location of felsic centers and felsic alignments younger than 35 ka, all of them belonging to TPV complex. Intensity functions for each dataset were computed separately applying the kernel technique (Connor and Hill 1995; Martin et al. 2004), and finally, the susceptibility map (Fig. 4) was computed assuming a non-homogeneous Poisson process whose intensity function is a combination of the previously calculated functions (see Martí and Felpeto 2010 for details).

4.4.3 Spatiotemporal probability

Once both the temporal and the spatial probability of occurrence of a phonolitic eruption in TPV were calculated, the next step consisted in the computation of a map that, for a specific time interval t and a specific magnitude M, showed the probability

for each cell of hosting a future vent. We assumed to have N possible cells that could host a future vent and that we had computed the spatial probability of each cell using the spatial probability method explained above. Let si be the spatial probability of a vent opening in cell i, for i ranging from 1 to N. Let Pt,M be the temporal probability of having an eruption (and consequently a vent opening) of magnitude M within the next t years, computed using the NHGPPP explained earlier. The group of N cells used to compute the spatial probability are mutually exclusive and exhaustive; that is, the same vent cannot be in more than one cell at the same time, and the sum of all s_i is 1.

As this paper is a first step to assess the spatiotemporal probability for TPV, for simplicity in the methodology, we assumed the two probabilities were independent. This means that the probability of having an eruption of size *M* in *t* years does not depend on the location. In other words, both the temporal and spatial probabilities were calculated separately using methods previously developed independently of one another. In this respect, we may be underestimating the total probabilities. Further work is needed to develop a more complete model which takes into account the three variables together: time, size and location.

The spatiotemporal probability of having an eruption of magnitude *M* within the next *t* years in cell *i* is:

$$qi_{t,M} = s_i \times p_{t,M} \tag{5}$$

For *i*=1, …; *N; M*=2,3,4,5,6; *t*=1,20,50,100,500,1000 where

$$\sum_{i=1}^{N} s_i \times p_{t,M} \tag{6}$$

the cells are exhaustive and

$$\sum_{i=1}^{N} s_i \times p_{i,M} \tag{7}$$

With the aim of obtaining the group of N cells that are mutually exclusive and exhaustive that represent TPV system, we selected from Fig. 4 the area of susceptibility values higher than $3*10^{-5}$ that enclose the 98.7% of the total probability of the susceptibility map. The values of this area were normalized by dividing by the integral across the whole area, obtaining an exhaustive group of cells. Figure 5 shows an example of how the spatiotemporal probability is computed using Eq. 5, for the probability of having an eruption of magnitude >2 in the next 20 years.

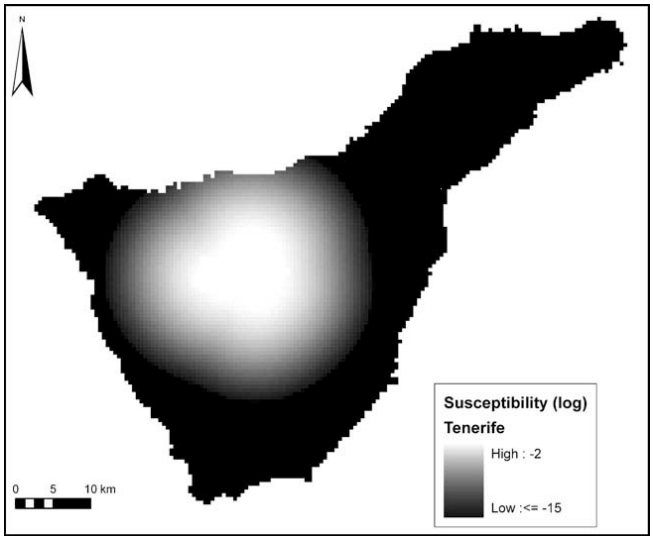

Fig. 4 Susceptibility map of phonolitic eruption in Tenerife with cell size of 500-500 (from Martí and Felpeto 2010)

4.5 Eruptive scenarios

In order to illustrate potential future phonolitic eruptions on TPV, we have computed several representative scenarios. We chose lava flows, ash fall and pyroclastic density currents (PDC) as the three main hazards that can be expected in a phonolitic eruption from TPV, based on what can be seen in the geological record (Martí et al. 2008b; García et al. 2011.

Simulations were performed considering different vents, including central vents located at both craters of Teide and Pico Viejo and flank vents located around TPV edifice at approximately 2,300 m a.s.l. Both kinds of eruptions can be expected in TPV, as shown in the Holocene eruptive record and in numerical studies simulating magma emplacement inside TPV (Martí and Geyer 2009). All the scenarios have been computed with the GIS-based system VORIS (Felpeto et al. 2007, www.gvb-csic.es).

5.5.1 Lava flows

The numerical simulation of phonolitic lava flows were computed with a maximum slope model (Felpeto et al. 2001). Parameters required by the model are maximum flow length and height correction, whose values were chosen based on recent phonolitic lava flows (lmax= 30 km, hc=10 m). Simulations were performed over a digital elevation model (DEM) with 50 m of cell size. Due to the morphology of both central peaks and the characteristics of the model selected, Teide central vent was considered to be an area of 0.17 km2 centered in the peak, and Pico Viejo central vent was considered to be an area of 0.17 km2 around the crater rim. The result of each simulation is a probability map showing the probability of each cell to be invaded by

phonolitic lava flows. Examples of the simulations for the central vents are shown in Fig. 6.

4. 5.2 PDCs

Numerical simulations of PDCs were computed with the energy cone model (Malin and Sheridan 1982; Sheridan and Malin 1983), over a DEM with a 50-m cell size. The values chosen for the input parameters are 200 m for equivalent collapse height and 0.21 for Heim coefficient. The result of each simulation is the area potentially reachable by the PDC and the expected flow velocity value in each cell, computed following Toyos et al. (2007). Figure 7 shows the simulations for both central eruptions, where the potentially reachable area is very wide, and a simulation for a flank vent at the north, whose reachable area is considerably smaller.

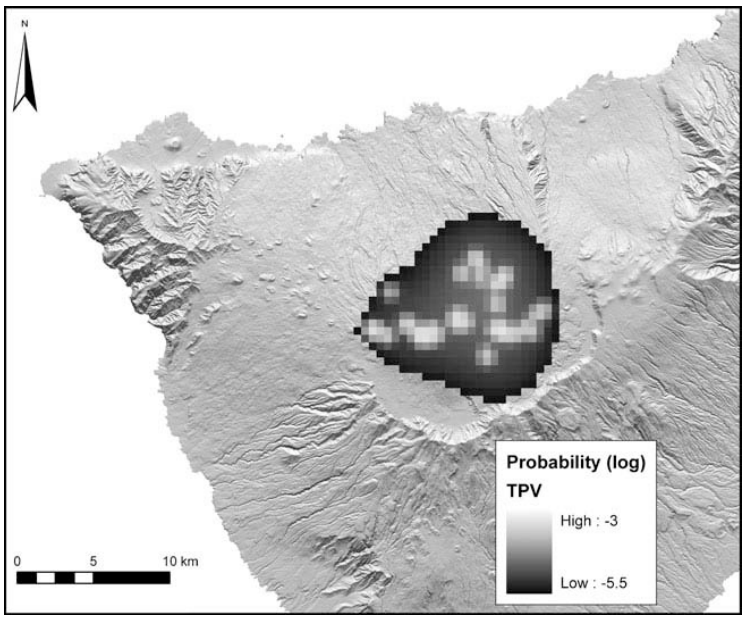

Fig. 5 Probability map of phonolitic eruption $M \geq 3$ in the next 20 years (cells size 500x500 m). The are outside the central *black-grey* zone is assumed to have a zero probability for hosting phonolitic eruption

with $M \geq 3$ in the next 20 years.

4.5.3 Ash fall

Ash fall from phonolitic eruptions in TPV could be expected from different eruptive styles. Those considered in this paper are violent strombolian, subplinian and plinian, which are the most significant ones in terms of probability of occurrence according to the long-term event trees published for TPV (Martí et al. 2008a; Sobradelo and Martí 2010). All the simulations were done considering a vent located in the northern flank of TPV at the same distance from the two craters. The wind data used were obtained from a deep atmospheric sounding of an arbitrarily selected day (1 April 2010).

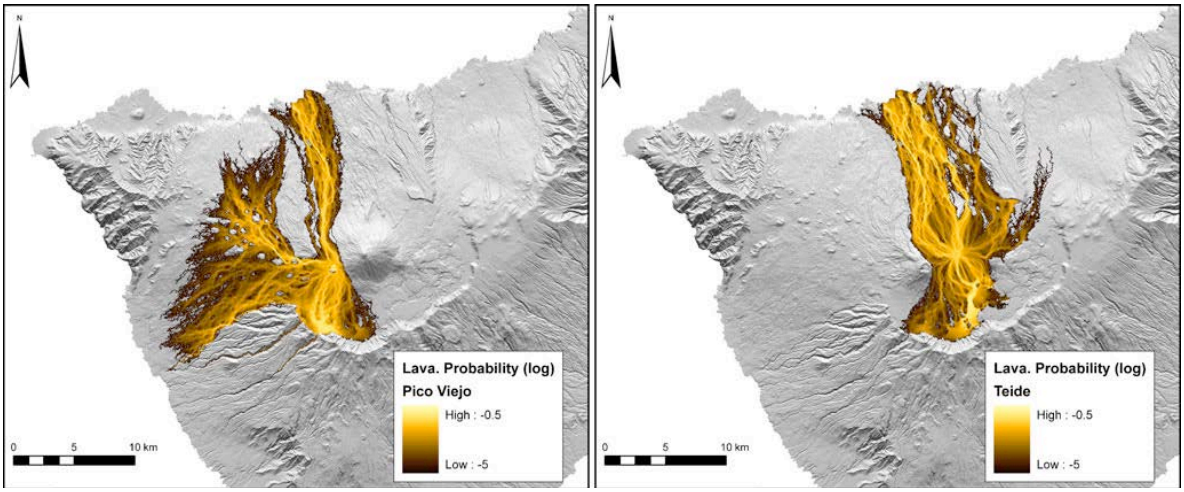

Fig. 6 Phonolitic lava flow scenarios for Pico Viejo (left) and Teide (right) central vents (see text for details)

Plinian and subplinian events were simulated with the advection–diffusion model described in Folch and Felpeto (2005) considering the source term described by the Suzuki (1983) expression. Simulation of violent strombolian eruption was computed with FALL3D 6.1 model (Costa et al. 2006). The input parameters for the subplinian

eruption reproduce the best known explosive event of TPV, the Montaña Blanca eruption (Ablay et al. 1995; Folch and Felpeto 2005). Due to the lack of detailed data of deposits from the other two eruption types, the input parameters were chosen based on bibliographic data from other volcanoes. A summary of the input parameters is shown in Table 4. Figure 8 shows the results of the simulations.

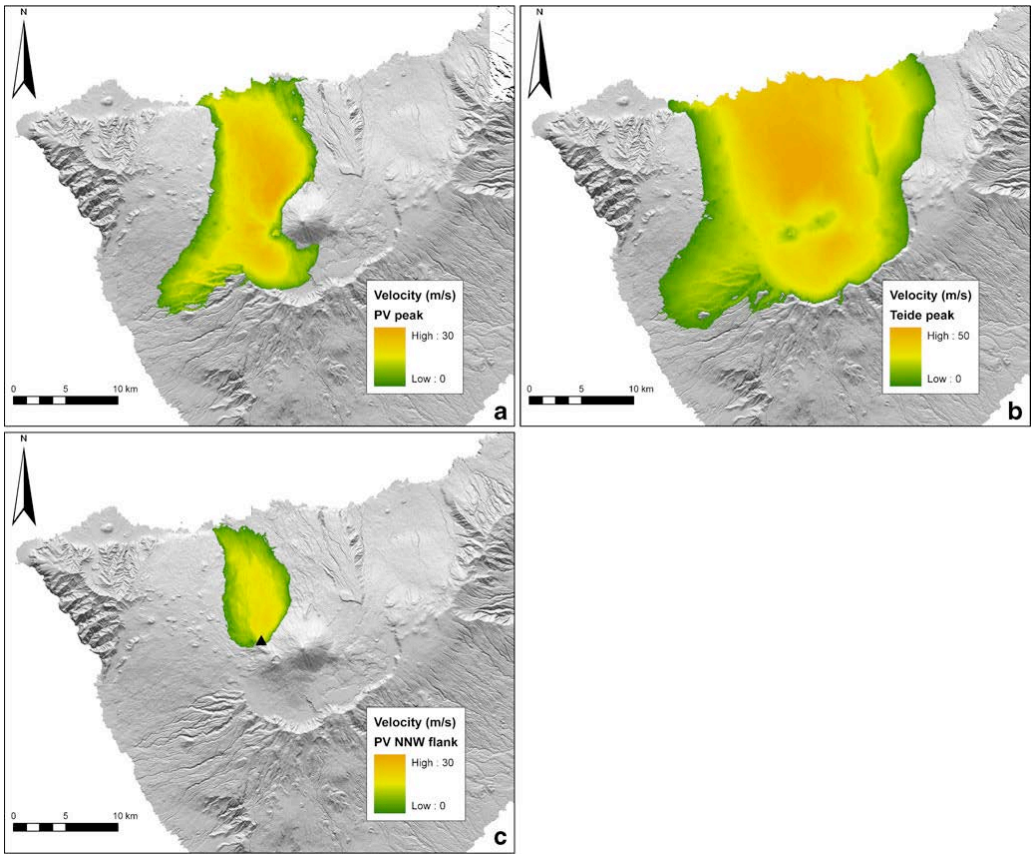

Fig. 7 PDC scenarios. a Pico Viejo central vent, b Teide central vent and c vent located on black triangle (see text for details

MODEL	Violent strombolian FALL3D	Subplinian Folch and Felpeto (2005)	Plinian Folch and Felpeto (2005)
Column height	1.4 km	8 km	25 km

Volume emmitted		0.05 km^3	0.8 km^3
Mass flow rate	5 x 10^4 kg/s		
Duration	3 h		
Mean φ/ φ standard deviation	1 / 1	-2 / 1.5	0 / 1.5

Table 4 Summary of the input parameters used in the simulations of ash fallout scenarios.

4.6 Validation of results

Based on existing geological data, we assessed the volcanic hazard for Teide–Pico Viejo as probabilities of occurrence of at least one eruption exceeding a certain magnitude over different time periods. Like this, for example, given the data and assuming a future behavior of the volcano similar to the past 10,000 years, we can say that in the next 50 years, there will be at least one eruption on TPV of magnitude $M > 2$ with a probability of 11.1%. This probability jumps to 21.0% for the next 100 years, and a probability of 90.6% is obtained for the next 1,000 years (Table 3). The escalation rate is more significant in the first 500 years (Fig. 9).

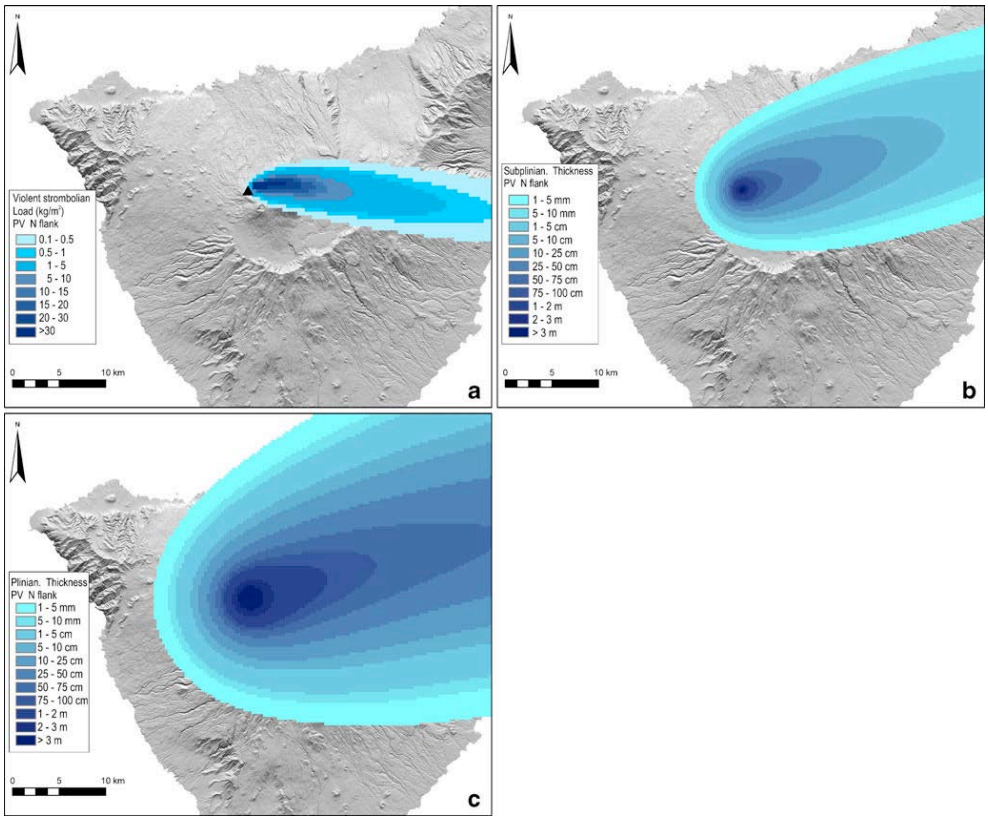

Fig. 8 Ash fall scenarios. **a** Violent strombolian, **b** subplinian and **c** plinian (see test for details).

To validate the model, we compared the probability results in Table 3 with the probability obtained from the Bayesian event tree model of Sobradelo and Martí (2010). The event tree was built to outline all possible eruptive scenarios at TPV and to assign a long-term probability of occurrence to each scenario. The Bayesian probabilities were computed only for the time window of 100 years. Therefore, when comparing with the results from the extreme value theory method in Table 3, we can only compare the probabilities of an eruption of different sizes within one time window of 100 years. Table 5 shows on the second row the probabilities of having a magmatic unrest episode with magmatic eruption of phonolitic composition anywhere in the TPV during the next 100 years, computed using the Bayesian event tree model.

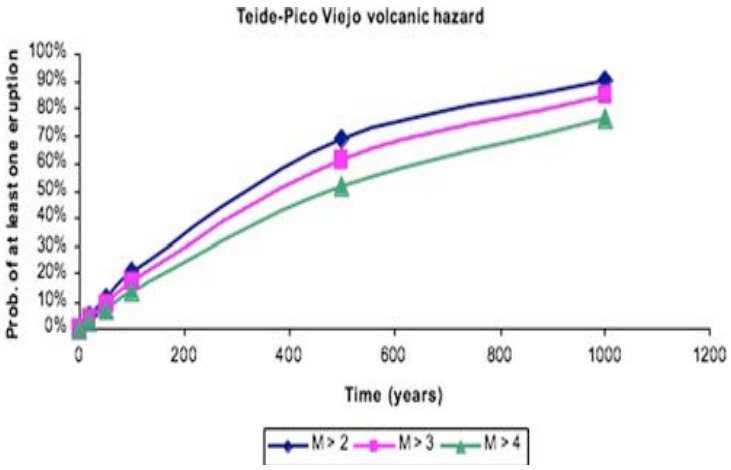

Fig. 9 Probabilities calculated with NHGPPP of at least one eruption, with a size M greater than a given size for the TPV eruptive series.

The extreme value method was built using the number of eruptions occurring over time intervals, expressed in terms of the eruption occurrence rate for each class magnitude *M*, and extrapolated using the more complete records in the catalogue (Mendoza-Rosas and De la Cruz-Reyna 2008). The extreme value method takes into account the possible incompleteness of the data by extrapolating from the most reliable data points. The Bayesian model, on the other hand, is a subjective approach which starts with the state of total uncertainty and computes the final probabilities based on an incomplete data catalogue, without further adjustment. This explains why the Bayesian probability in Table 5 second row for magnitude >4 (3.0%) falls abruptly relative to that for magnitude >3 (11.2%). The NHGPPP gives more weight to the more extreme events, such as events of magnitude >4 (13.6% versus 3.0%). For events of magnitude >2, the Bayesian probability (14.2%) is lower than the NHGPPP probability (21.1%) since the latter uses a larger number of extrapolated occurrences for events of magnitude 3, while the Bayesian method computes the results based on the single event registered

in the catalogue. This comparison allows us to validate the consistency of the probability results obtained here, but also reassures us in the choice of using the extreme value method to overcome the limitations in the data.

Time (years)	*M*>2(%)	*M*>3(%)	*M*>4(%)	
100	21.1	17.3	13.6	Extreme value theroy
100	14.2	11.2	3.0	Bayesian event tree

Table 5. Comparison of probability results from Bayesian tree (Sobradelo and Martí 2010) and NHGPPP presented in this paper.

4.7 Discussion

The TPV constitutes one of the main potentially active volcanic complexes in Europe but traditionally has not been considered to be explosive and to represent a significant threat to the island of Tenerife. However, the results obtained in this work suggest that hazard associated with TPV is not negligible and should be carefully considered in order to quantify volcanic risk in Tenerife. Although NVEWS (Ewert et al. 2005) was specially designed to identify the level of monitoring required by US volcanoes in order to define an effective early warning system, it offers a simple approach for classifying active volcanoes according to their level of threat. In this sense, we consider NVEWS perfectly applicable to TPV, and the resulting value representative of the real level of threat TPV represents for Tenerife. The NVEWS analysis of volcanic threat, even assuming very conservative values for some of the evaluated factors, gives a value of 165, which classifies TPV as a very high threat volcano, comparable to

Redoubt, Crater Lake or Augustine in the USA. It is worth mentioning that the level of volcano monitoring in Tenerife has improved significantly since 2004, when the Spanish Geographic Institute (IGN) implemented its multiparametric surveillance network (see www.ign.es), so that it can be said that TPV now has the required monitoring level that is appropriate to a very high threat volcano according to the NVEWS (Ewert et al. 2005).

Eruptions of volcanoes considered "dormant" or "inactive" have produced major disasters in the past. The volcanic hazard from volcanoes with a long recurrence interval tends to be ignored, especially when little or no historical data exist. This is the case for TPV. The probability results obtained here using extreme value theory, consistent with the results obtained in previous work using Bayesian inference, confirm once again the existence of significant volcanic hazard from TPV. This together with others signs of activity mentioned earlier should constitute sufficiently convincing reasons to accept that TPV is an active volcanic complex that may erupt again in the near future. Unfortunately, we have increasing evidence of the sudden awakening of long dormant volcanoes (e.g. Chichón 1982, Unzen 1991, Pinatubo 1991, Montserrat 1995–, Chaitén 2008). Conducting hazard assessment of volcanoes where knowledge of the past volcanological history is poor, geochronological data are scarce and there is not historical eruptive activity and is not an easy task. In these cases, the lack of knowledge of previous unrest episodes and of the precursors to previous eruptive events precludes using repetitive patterns of precursors to anticipate new eruptions (see Sandri et al. 2004). This is the case at TPV, meaning that we do not know how a future reawakening would manifest and which could be the precursory patterns for new eruptions. Comparison with better known volcanoes, in particular with those that have erupted in

recent times and from which we have good monitoring records, could help in predicting the future behavior of TPV. However, experience demonstrates that each volcano has its own behavior and that the definition and application of common patterns to interpret eruption precursors, particularly if we are dealing with composite volcanoes, should be done with care.

In the case of TPV, Martí et al. (2008a) indicated that its eruptive behavior is controlled by the close relationship between deep basaltic and shallow phonolitic magma systems, to the extent that most of the TPV phonolitic products show evidence of magma mingling and/or mixing. From the existing radiometric ages and the stratigraphic relationships between the erupted products, it is clear that most of phonolitic eruptions are preceded by several basaltic eruptions and in some cases both occur simultaneously (e.g. Montaña Reventada, Araña et al. 1994; Wiesmaier et al. 2011). A similar pattern has also been observed in the pre-TPV central complex (Las Cañadas Edifice) (Martí et al. 2008a). Therefore, it is logical to infer that similar mechanisms have controlled the accumulation, evolution and eruption of magma at shallow levels during the past history of the Tenerife central complex, despite a progressive decrease in the magma available with time. In other words, the eruption of phonolitic magma at TPV is directly dependent on the amount of basaltic magma delivered at shallow depths into the central system. We then suggest that the eruption frequency at TPV is related to the eruption frequency of basaltic volcanism on Tenerife, which in historical times has produced eruptions in 1492, 1705, 1706, 1798 and 1909, with the last eruption from Teide dated at 1,150 years B.P. (Carracedo et al. 2007).

The main phonolitic erupted products of TPV correspond to lava flows that were emplaced towards the south into Las Cañadas depression and to the north in the Icod

and La Orotava valleys. Most of the phonolitic lavas from TPV are clastogenic lavas formed by agglutination of large pyroclastic fragments generated in fire fountaining episodes. The rheological properties and flow behavior of these lavas (Dingwell et al. 1998; Giordano et al. 2000; Gottsmann and Dingwell 2001) are characterized by a low viscosity at relatively low temperatures, which allow them to flow for long distances preserving an average thickness of tens of meters. In some cases, these lavas have flowed down into the Icod valley for more than 16 km reaching the coast, an area that today is highly populated. These lavas typically preserve a considerable amount of magmatic gas. This is consistent with the relative large amount of volatiles found in the TPV phonolites (Ablay et al. 1995). An effect of this high content of gas in the TPV lavas is that they may transform into block and ash flows when they collapse gravitationally in slope breaks. Deposits of such pyroclastic density currents have been found in stratigraphic continuity with some lavas inside the gullies of the Icod valley, sometimes reaching the coast or being transformed into debris flow deposits at distal facies (García et al. 2011). In addition to the fragmental origin of most of the TPV lavas and their occasional explosive transformation into pyroclastic density currents, there is evidence of larger explosive eruptions at TPV (García et al. 2011). This evidence is provided by the presence of discontinuous outcrops of pumice fall deposits, but their precise stratigraphic location in the TPV eruptive record is still not known. However, we can confirm that at least three phonolitic explosive eruptions of subplinian dimension, or perhaps even plinian, different from that of the already known Montaña Blanca eruption (Ablay et al. 1995; Folch and Felpeto 2005), have occurred from TPV during the Holocene. Moreover, the presence of ignimbrites is also confirmed in the eruption record of TPV, some of them with minimum run-out distances of several

kilometers as it is indicated by the remnants of these deposits found in the Icod Valley, but which could have reached the coasts and entered the sea if we compare them with other ignimbrites of similar characteristics and volume (e.g. Calder et al. 1999; Loughlin et al. 2002). The ignimbrites may have derived either from collapse of eruption columns or from gravitational collapse of domes and clastogenic lava flows. This second option is certainly at least the origin for the block and ash deposits found in the Icod Valley, where the steep topography has facilitated such processes (García et al. 2011). Therefore, we have considered in our analysis fall deposition and PDC hazards, in addition to lava flows, as representative of the potential hazards that might occur in a future eruption of TPV. The scenarios we have generated allow us to assess their potential extent. All these primary hazards would today easily reach the main populated áreas to the north of TPV but could even reach other important locations on the other flanks in the case of plinian and subplinian fallout depending on wind direction.

In addition to the direct hazards that we have assumed in this paper, it is also important to take into account those hazards that could indirectly derive from a renewal of the eruptive activity at TPV. These mainly include debris flows and sector collapses, for which there is also evidence in the recent geological record. Some of the ignimbrites from TPV show evidence of syn-depositional erosion which suggest that heavy rainfalls may have occurred in the area during these eruptions (García et al. 2011). It is also significant that at the north of Tenerife, important seasonal rainfalls contribute to the erosion and remobilisation of the unconsolidated volcanic material, forming important debris flows. The existence of small-scale sector collapses at the north flank of TPV has also been pointed out by previous authors (Ablay and Martí 2000; Ablay and Hürlimann 2000) In this study, we have only considered the phonolitic eruptions, as they have the

potential to generate the most important hazards at TPV, but it is worth noting that basaltic eruptions have also occurred at this volcanic complex. Most of these eruptions have been strombolian to violent strombolian and have generated lava flows with a variable extent and restricted scoria lapilli deposits. Some significant phreatomagmatic episodes have also occurred related at the former craters of Teide and the present one in the case of Pico Viejo (Ablay and Martí 2000; Perez-Torrado et al. 2004). These phreatomagmatic eruptions produced high-energy pyroclastic surges that flowed to the north for several kilometers into the Icod valley. The extent of these deposits is similar to some of the phonolitic PDCs from TPV, so the hazard scenarios we have developed for phonolitic PDCs also apply to potential basaltic surges emplaced towards the north of TPV.

4.8 Conclusions

In this study, we have presented the temporal and spatial probabilities for a phonolitic eruption at TPV and have discussed their implications in terms of hazard assessment. The computation of both temporal and spatial probabilities of a phonolitic eruption at TPV and the characterization of the main expected scenarios constitute the fundamental basis for building up the phonolitic hazard maps for TPV. An important conclusion we can draw from these results is that TPV has to be identified as a volcanic complex that may pose serious hazard on the island of Tenerife and in particular to its northern side. The hazard scenarios we have simulated show that the southern flank of Tenerife is protected by the Cañadas caldera wall against lava flows and pyroclastic density currents, but not against ash fallout. The Icod Valley, and in a minor extent also

the La Orotava valley, is directly exposed to most of TPV hazards, in particular to the gravity driven flows, due to the steep topography of that side of the island and the lack of topographic barriers. According to these results and to the fact that Tenerife is a densely populated island, it is strongly recommended that preparedness plans, emergency and disaster management procedures be put into place to quickly react and minimize loss during a volcanic crisis.

Part III

1. Summary and results.

This PhD Thesis includes three research papers already published and one under review, in relevant international journals that show the evolution of my research, and the main results obtained so far. The order in which these chapters ar presented does not correspond chronologically to their publication or submission but are arranged to present in a logical sequence of the data obtained and their interpretation.

This study about explosive deposits of Teide Pico Viejo volcanic complex presents an identification of several pumice deposits derived from explosive phonolitic eruptions associated to the TPV complex. Teide and Pico Viejo are twin stratovolcanoes (TPV) that form one of the largest alkaline volcanic complexes in the world. They began forming inside the caldera of Las Cañadas about 200 ka ago and are largely made up of an accumulation of mafic, intermediate and more recent felsic products that form lava flows. However, a number of significant pyroclastic deposits dating from the Holocene are also present. In order to quantify the explosive contribution to the construction of TPV we re-examined its stratigraphy and identified several Holocene phonolitic explosive episodes ranging from Strombolian to sub-Plinian that are represented by fallout and pyroclastic density current deposits (PDCs). Although some of the pumice deposits have been related to known vent sites, a few are still of unknown origin. The use of field criteria as well as geochemical and mineralogical analysis helps provide reliable criteria for robust correlations and for establishing the relative stratigraphy of

the deposits. The presence of these pyroclastic deposits in the recent history of the TPV complex suggests that these stratovolcanoes are entering into a more explosive stage that represents a non-avoidable hazard for the island of Tenerife.

An important part of the fieldwork has been the reconstruction of the TPC complex explosive eruptive record, which was poorly studied until now. It improves our knowledge of the volcano-stratigraphy and physical volcanology aspects in the study area which contributes to a comprehensive hazard assessment of these volcanoes. A detailed field investigation of the northern side of Teide–Pico Viejo, a poorly known area, permitted to identify eleven deposits of explosive phonolitic eruptions. For the first time, the presence of PDCs, including ignimbrites and block and ash deposits is reported in the Holocene eruptive history of the Teide–Pico Viejo stratovolcanoes. The characteristics of these deposits, their eruption mechanisms and their implications for hazard assessment at Teide– Pico Viejo, are described in the paper García et al. 2010.

The field data allow us to present the characterization the previously unknown subplinian eruption of El Boquerón (5,660 yBP), a satellite dome located on the northern slope of the Pico Viejo stratovolcano. Stratigraphic data suggest complex shifting from effusive phases with lava flows, to a highly explosive phase that generated a relatively thick and widespread pumice fallout deposit. This explosive phase is classified as a subplinian eruption of VEI 3 that lasted for about 9–15 h and produced a plume with a height of up to 9 km above sea level (i.e. 7 km above the vent; MER of 6.9–8.2°—105 kg/s). The tephra deposit (minimum bulk volume of 4–6°—107 m^3) was dispersed to the NE by up to 10 m/s winds. A similar eruption today would significantly

impact the economy of Tenerife (e.g. tourism and aviation), with major consequences mainly for the communities around the Icod Valley, and to a minor extent, the Orotava Valley. This vulnerability implies that a better knowledge of the past explosive history of TPV and an accurate estimate of future potential to generate violent eruptions are required in order to quantify and mitigate the associated volcanic risk.

Finally the data obtain from the Boqueron eruption have been used for the assessment of the volcanic hazard through the paper Martí et al. 2012. It includes a statistical analysis of the time series of past eruptions and the spatial extent of their erupted products, including lava flows, fallout and PDCs. An extreme value theory statistical method is used to calculate eruption recurrence. The analysis of past activity and extent of some well-identified deposits (described in the previous chapters of this PhD Thesis) is used to calculate the eruption recurrence probabilities and for different time periods to evaluate their potential hazard. This study represents a step forward in the evaluation of volcanic hazard at TPV with regard to previous studies, and the results obtained should be useful for intermediate and long-term land-use and emergency planning.

2. Discussion of the results

The results obtained in this work prove that explosive activity associated to phonolitic magmas have been more frequent in the construction of the twin stratovolcanoes Teide and Pico Viejo (TPV) during the last 10000 years than previously thought. This suggests that explosive hazard associated with TPV is not negligible and should be carefully considered in order to quantify volcanic risk in Tenerife. The detailed field work carried out in this study based on a precise description of the stratigraphy and sedimentology of explosive deposits, including petrological and geochemical analysis of their juvenile components, has allowed us to characterize several pyroclastic deposits situated mainly at the northern side of the volcanic complex, which are associated to different flank vents. Despite the poor exposure of these pyroclastic deposits, which have been extensively eroded and remobilized by the seasonal rainfalls and partially covered by younger lava flows from TPV, we have detected 11 explosive eruptions from at least 16 phonolitic eruptions occurred in the recent volcanic history (Holocene) of TPV. The presence of these phonolitic pyroclastic deposits in the recent stratigraphy of Teide have changed the idea that we had about TPV in the sense that it was mostly an effusive volcanic complex.

The established relative stratigraphic correlation of these deposits and to placing them within the general stratigraphy of the TPV, was based on field work, petrological and geochemical data (García et al, submitted), have allowed most of the studied deposits to be assigned to their corresponding vents, although this correlation has not been possible in a few cases because they have been

considerate as unknown origina. However, we have been able to determine the relative stratigraphy for the whole succession, using in some cases a precise radiometric dating (C^{14}) identifying eleven explosive eruptions between strombolian and subplian.

This methodology is a combination of fieldwork data supported by petrological and geochemical data, which has been used by other authors to support similar studies of the relative stratigraphy (Guzman et al. 2011; Giordano et al. 2013)

Some of the deposits have been difficult to relate with known vents such as ICS deposit and El Caderon deposit but others such as P1600 deposit we can establish a known origin. According to the stratigraphic relationships, the P1600 pumice deposit could be related to either Pico Cabras and Roques Blancos deposits by stratigraphic relation and petrological and geochemical characteristic. Although the presence of some carbon data has established a similar age for the P1600 deposits and Roques Blancos, so we deduce that both deposit have the same origin.

The ICS deposits found in the interior of the Ucanca depression in the caldera of Las Cañadas cannot be clearly correlated to any known vent. The similar petrological and geochemical composition with Montaña Majua deposits suggests that these deposits have a common origin. . However, the Montaña Majua deposits disperse southeast from the vent (Ablay *et al*. 1997; Ablay & Martí 2000), thus making any correlation with the ICS deposit located to the west unlikely.

The other deposit of unknown origin El Calderón, could not be correlated to any known vent area using either field stratigraphic criteria or a mineralogical or geochemical basis. In the case of the deposits in El Calderón, we mention above that the interbedding of mafic and felsic units could indicate the occurrence of two simultaneous

eruptions, one from the north-western rift zone and the other from the central complex, respectively. However, we failed to find any evidence that could correlate the units in El Calderón with any specific eruption or vent site. Another possibility would be to associate the sequence at El Calderón with a single eruption generating both mafic and felsic magmas. As the Montaña Reventada, a young flank eruption developed from a fissure vent system on the western flank of Pico Viejo which generated a composite lava flow consisting of lower basanite and upper trachy-phonolite units.

For the first time in the volcanological literature of TPV, the presence of pyroclastic density current (ignimbrites and block and ash) deposits associated with its recent eruptive history have been described (García et al. 2011). The pyroclastic density current deposit associated with Abrunco vent is an ignimbrite formed by the collapse of sub-plinian eruption column, which was covered by latter fallout deposits. The original extent of these pyroclastic flow deposits, as well as their high emplacement velocity and the wide dispersion of the smaller particles in the air, have to be taken into consideration in hazard scenarios for potential future eruptions (Martí et al. 2012).

In addition to these ignimbrite deposits, the presence of a number of block and ash deposits possibly associated with the gravitational collapse of phonolitic domes and clastogenic lava flows, in the recent eruptive record of TPV, is also relevant. They then constitute a significant hazard for this sector of Tenerife.

Similar deposits have been described in the south of Tenerife (Bandas del Sur groups) which consist of a complex successions of plinian fall, surge and flow deposits associated in origin with Las Cañadas caldera collapse episodes (Martí et al. 1994; Bryan et al.,1998, 2000; Wolff et al., 2000; Brown et al. 2003; Pittari et al. 2006; Edgar

et al. 2007). Those PDC deposits have been associated just with the TPV complex, other authors as Edgar et al. 2006, describe similar deposits (Tarasca Member) in the Orotava Valley and have been produced by a gravitational collapse of the lava dome. Also Perrez Torrado et al. describe similar deposits as succession of thick, block-supported and thin, fine, matrix-supported facies Las Calvas deposits in the north part of TPV complex.

Part of the block and ash that have been described in this Thesis are mostly composed of fragments of clastogenic lavas, and minor non-welded dense and expanded pumices of the same composition as the clastogenic lava fragments. These clastogenic lavas formed by agglutination of large pumice fragments generated in fire fountaining episodes. They present characteristic rheological proprieties, such as relative low viscosity and temperature and high gas content (Ably et al. 1995, Dingwell et al. 1998; Giordano et al. 2000; Gottsmann and Dingwell 2001). They could favour the formation of pyroclastic density currents when they collapse gravitationally in the slope breaks, flowing down at high velocity in the Icod Valley.

These lithological and sedimentological characteristics make a clear distinction between block and ash and debris flow deposits also present on the northern slopes of Teide, as these last incorporate clasts from other lithologies, reduce significantly the amount of pumice and ash matrix, and show a better rounding of clasts and internal organization of the deposits compared to the block and ash deposits.

The poor preservation of the pyroclastic deposits in the northern side of TPV, is a fact but we were able to provide an accurate study of the deposits associated with the last Boqueron eruption, dated at 5660 B.p (García et al. 2012). This explosive event generated an eruption column 9 km high a.s.l with a northeastern wind dispersion as

occurred with the previously described Montaña Blanca eruptions (2020 BP) (Ablay et al, 1995; Folch and Felpeto, 2005). The Boqueron eruption is also comparable to other subplinian events in terms of deposit dispersal, erupted volume and thinning trend . As an example, the Boqueron volume and thinning trends are very similar to those for the eruptions of Montaña Blanca (i.e., 10 km high eruption column and a tephra deposit with a volume 1.4 x 10^8 m^3 based on isopach map from Ablay et al., 1995) and Fuego 1974 (Rose et al. 2008). In spite of the Boqueron eruption classifies as a VEI=3 sub-plinian type eruption, which reached a MER (eruption rate) of 6.9-8.2x10^5 kg/s during 9-15 hours producing a total volume of the order of 4-6x10^7 m^3.

In order to estimate the uncertainty involved in calculating the volumes of deposits characterized by poor exposure, we constructed two possible isopach maps based on the same set of data. The error associated with the two compilations of the isopach map is about 30%, 40% and 50% for Weibull, the exponential and the power-law method respectively. These values are of the same order of magnitude of other estimations of volume-calculation uncertainties made on better-exposed deposits.

Therefore, we have considered in our analysis fall deposition and PDC hazards, in addition to lava flows, as representative of the potential hazards that might occur in a future eruption of TPV. Given that our detailed study of the Boqueron eruption results in a similar plume height and volume as modeled by Marti et al. (2011) (i.e., 7 km and 0.04-0.06 km^3 respectively) The scenarios we have generated allow us to assess their potential extent. we would expect that another eruption of this type would be associated to disruption equivalent to that described by Marti et al. (2011).

All these primary hazards would today easily reach the main populated areas to the

north of TPV but could even reach other important locations on the other flanks in the case of plinian and subplinian fallout depending on wind direction. Also important to take into account those hazards that could indirectly derive from a renewal of the eruptive activity at TPV. These mainly include debris flows and sector collapses, for which there is also evidence in the recent geological record. Some of the ignimbrites from TPV show evidence of syn-depositional erosion which suggest that heavy rainfalls may have occurred in the area during these eruptions It is also significant that at the north of Tenerife, important seasonal rainfalls contribute to the erosion and remobilization of the unconsolidated volcanic material, forming important debris flows.

3. Final conclusions

The results obtained in this PhD Thesis will be useful to improve our geological and volcanological knowledge of TPV. Also, it will provide a tool for understanding and anticipating the future eruptive behavior of TPV, facilitating the construction of realistic hazard models. These simulation models are necessary to conduct realistic volcanic hazard assessment, a first step in the quantification of volcanic risk in Tenerife (Martí et al., 2012). For example, the results obtained in this thesis show how an eruption similar to the one of the Boqueron would significantly affect the northern coast of Tenerife, including the towns of Icod de los Vinos, Santa Cruz, La Orotava, Puerto de la Cruz, and the North airport.

The results obtained also show the impact that indirect hazards derived explosive activity have had in the past eruptive history of TPV and could have in it immediate future. This is, for example, the case of debris flows and sector collapses (Ablay and Martí 2000; Ablay and Hürlimann 2000; Martí et al 2008; 2012; García et al., 2011), for which there is also evidence in the recent geological record. As shown here (García et al., 2011) there are some pyroclastic density current deposits with evidence of syn-depositional erosion which suggest that heavy rainfalls may have occurred in the area during these eruptions, transforming these primary pyroclastic deposits into secondary ones with a much longer run out distance, thus increasing their potential hazard.

This PhD Thesis contributes to complete our knowledge on the TPV characterizing by the first time its recent explosive activity. We have been able to

identify several magmatic explosive deposits not characterized before, as well as to identify among them the presence of the pyroclastic density current (ignimbrites and block and ash) deposits. The existence of highly explosive episodes, as Boqueron eruption, in the recent eruptive history of Teide-Pico Viejo implies that this kind of activity may repeat in the future, increasing significantly the potential risk for the island of Tenerife and in particular for the Icod Valley. For this reason, it is important to take into consideration in future studies the computation of both the temporal and spatial probabilities for a phonolitic explosive eruption at TPV, presenting and characterizing he main expected scenarios. This should constitute one of the fundamental goals for building up precise hazard maps for TPV, which is an essential target to reduce risk in Tenerife, the most populated island of Spain with more than 900,000 inhabitants, an one of the main tourist destinations in Europe with more than five million visitors per year.

Futures research work includes: location of the vents for several block and ash located in the north side of the Teide-Pico Viejo Complex, modeling the dispersion of these explosive eruptions with the actual topography, update data of the relative chemistry of the different pumice deposits

References

Ablay GJ, Ernst GGJ, Martí J, Sparks RSJ (1995) The 2ka subplinian eruption of Montaña Blanca, Tenerife. Bull Volcanol 57:337-355

Ablay GJ (1997) Evolution of the Teide-Pico Viejo complex and magma system, Tenerife, Canary Islands. Dissertation. University of Bristol

Ablay GJ, Carroll MR, Palmer MR, Martí J, Sparks RSJ (1998) Basanite- phonolite lineages of the Teide-Pico Viejo volcanic complex, Tenerife, Canary Islands. J Petrol 39:905-936

Ablay GJ, Hürlimann M (2000) Evolution of the north flank of Tenerife by recurrent giant landslides. J Volcanol Geotherm Res 103:135–159

Araña V, Martí J, Aparicio A, García-Cacho L, García-García R (1994) Magma mixing in alkaline magmas: an example from Tenerife (Canary Islands). Lithos 32:1–19

Alfano F., Bonadonna C, Volentik ACM., Connor CB, Watt SFL, Pyle DM, Connor LJ (2010) Tephra stratigraphy and eruptive volume of the May, 2008, Chaitén eruption, Chile. Bull Volcanol 73:613-630. doi:10.1007/s00445-010-0428-x

Ancochea E, Huertas MJ, Fuster JM, Cantagrel JM, Coello J, Ibarrola E (1999) Evolution of the Cañadas edifice and its implications for the origin of the Cañadas caldera (Tenerife, Canary Islands). J Volcanol Geotherm Res 88:177-199

Andújar J., Costa F., Martí J., 2010. Magma storage conditions of the last eruption of Teide volcano (Canary Islands, Spain). Bulletin of Volcanology **72**, 381-395.

Andújar J., Costa F., Scaillet B. 2013. Storage conditions and eruptive dynamics of central versus flank eruptions in volcanic islands: the case of Tenerife (Canary

Islands, Spain) Journal of Volcanol Geothermal Researcher, doi: 10.1016/j.jvolgeores.2013.05.004

Araña V, Martí J., Apricio A., Garcia-Cacho L., García-García R., 1994. Magma mixing in alkaline magmas: An example from Tenerife (Canary Islands). Lithos 32, 1-19

Araña V., Barberi F., Ferrara G. 1989. El complejo volcanico del Teide-Pico Viejo. In: Los volcanes y la caldera del Parque Nacional del Teide (Tenerife, Islas Canarias). Editors V. Araña and J. Coello.

Araña V (1971) Litología y estructura del edificio Cañadas, Tenerife (Islas Canarias). Est Geol 27:95-135

Balcells R., Hernandez-Pacheco A., 1989. El domo colada de Roques Blancos. In: Coello, J., Araña, V. (Eds.), Los Volcanes y La Caldera del Parque Nacional del Teide (Tenerife, Islas Canarias). ICONA, Madrid, 227-234.

Bonadonna C, Cioni R, Pistolesi M, Connor CB, Scollo S, Pioli L (2012) Determination of the largest clasts of tephra deposits for the characterization of explosive eruptions: recommendations from the IAVCEI Commission on Tephra Hazard Modelling, Bull Volcanol, submitted

Bonadonna C, Costa A (2012) Estimating the volume of tephra deposits: a new simple strategy, Geology 40:415-418. doi: 10.1130/G32769.1

Bonadonna C, Scollo S, Cioni R, Pioli L, Pistolesi M (2011) Determination of the largest clasts of tephra deposits for the characterization of explosive volcanic eruptions. Report of the IAVCEI Commission on Tephra Hazard Modelling.

Bonadonna C, Houghton BF (2005) Total grain size distribution and volume of tephra–fall deposits. Bull Volcanol 67:441–456. doi:10.1007/s00445-004-0386-2

Bonadonna C, Macedonio G, Sparks RSJ (2002) Numerical modelling of tephra fallout associated with dome collapses and Vulcanian explosions: application to hazard assessment on Montserrat. In: Druitt TH, Kokelaar BP (eds) The eruption of Soufrière Hills Volcano, Montserrat, from 1995 to 1999. Geol Soc Lond pp.517–537

Booth B, Croasdale R, Walker GPL (1978) A quantitative study of five thousand years of volcanism on Sao Miguel, Azores. Phil Trans R Soc London A288:271-319

Boulesteix T, Hildenbrand A, Soler V, Gillot PY (2012) Eruptive response of oceanic islands to giant landslides: new insights from the geomorphologic evolution of the Teide-Pico Viejo volcanic complex (Tenerife, Canary). Geomorphology 138:61-73. doi: 10.1016/j.geomorph.2011.08.025

Calder, E.S., Cole, P.D., Dade, W.B., Druitt, T.H., Hoblitt, R.P., Huppert, H.E., Ritchie, L., Sparks, R.S.J. and Young, S.R., 1999. Mobility of pyroclastic flows and surges at the Soufriere Hills Volcano, Montserrat. Geophys. Res. Lett., 26(5), 537–540.

Carmichael I.S E. 1967. The iron-titanium oxides of salic volcanic rocks and their associated ferromagnesian silicates. Contributions to Mineralogy and Petrology, **14,**36-64.

Carey S, Sparks RSJ (1986) Quantitative models of the fallout and dispersal of tephra from volcanic eruption columns. Bull Volcanol 48:109-125

Carey R, Houghton B, Thordarson T (2008) Contrasting styles of welding observed in the proximal Askja 1875 eruption deposits I: Regional welding. J Volcanol Geotherm Res 171:1–19. doi:10.1016/j.jvolgeores.2007.11.020

Carracedo JC (1994) The Canary Islands: an example of structural control on the growth of large oceanic-island volcanoes. J Volcanol Geotherm Res 60:225–241

Carracedo JC, Paterne M, Guillou H, Pérez-Torrado FJ, Paris R, Rodríguez-Badiola E, Hansen A (2003) Dataciones radiométricas (14C y K/Ar) del Teide y el rift noroeste, Tenerife, Islas Canarias. Est Geol 59:15–29

Carracedo, J.C., Rodrıguez-Badiola, E., Guillou, H., Paterne, M., Scaillet, S., Peí rez-Torrado, F.J., Paris, R., Fra-Paleo, U. and Hansen, A., 2007. Eruptive and structural history of Teide volcano and rift zones of Tenerife, Canary Islands. Geol. Soc. Am. Bull., 119, 1027–1051.

Carracedo JC, Guillou H, Nomade S, Rodríguez-Badiola E, Pérez-Torrado FJ, Rodríguez-González A, Paris R, Troll VR, Wiesmaier S, Delcamp A, Fernández-Turiel JL (2010) Evolution of ocean-island rifts: The northeast rift zone of Tenerife, Canary Islands. Geol Soc Am Bull. doi:10.1130/B30119.1

Cioni R, Bertagnini A, Andronico D, Cole PD, Mundula F (2011) The 512 AD eruption of Vesuvius: complex dynamics of a small scale subplinian event. Bull Volcanol 73:789-810. doi:10.1007/s00445-011-0454-3

Coles S (ed) (2001) An introduction to statistical modeling of extreme values. Springer, London, p 228

Connor CB, Hill BE (1995) Three nonhomogeneous Poisson models for the probability of basaltic volcanism: application to the Yucca Mountain region. J Geophys Res 100:10,107–10,125

Costa F., Chakraborty S., Dohmen R., 2003. Diffusion coupling between trace and major elements and a model for calculation of magma residence times using plagioclase. Geochimica et Cosmochimica Acta, **67**, 2189–2200.

Costa A, Macedonio G, Folch A (2006) A three-dimensional Eulerian model for transport and deposition of volcanic ashes. Earth Planet Sci Lett 241:634–664

Deer W.A., Howie R.A., Zussman, J., 1992. An Introduction to the Rock-Forming Minerals, 2nd ed. AddisonWesley Longman China Limited, Hong Kong.

Dingwell DB, Hess KU, Romano C (1998) Extremely fluid behavior of hydrous peralkaline rhyolites. Earth Planet Sci Lett 158:31–38

Domínguez Cerdeña I, Del Fresno C, Rivera L (2011) New insight on the increasing seismicity during Tenerife's 2004 volcanic reactivation. J Volcanol Geotherm Res 206:15–29

Davison A, Smith R (1990) Models for exceedances over high thresholds. J Roy Statis Soc 52:393–442

Del Potro R, Hurlimann M (2008) Geotechnical classification and characterisation of materials for stability analyses of large volcanic slope. Engi Geol 98:1–17

Edgar C.J., Wolf J.A., Olin P.H., Nichols H.J., Pittari A., Cas R.A.F., Reiners P.W., Spell T.L., Martí J., 2007. The late Quaternary Diego Hernandez Formation, Tenerife: a cycle of voluminous explosive phonolitic eruptions. Journal of Volcanology and Geothermal Research **160,** 59–85.

Ewert J, Guffanti M, Murray T (2005) An assessment of volcanic threat and monitoring capabilities in the United States—framework for a National Volcanic Early Warning System, NVEWS. US Geoll Sur Open-File Rep 1164:1-6

Felpeto A, Araña V, Ortiz R, Astiz M, García A (2001) Assessment and modeling of lava flow hazard on Lanzarote (Canary Islands) Nat Haz, 23:247-257. doi: 10.1023/A:1011112330766

Felpeto A, Martí J, Ortiz R (2007) Automatic GIS-based system for volcanic hazard assessment. J Volcanol Geotherm Res 166:106–116

Folch A, Felpeto A (2005) A coupled model for dispersal of tephra during sustained explosive eruptions. J Volcanol Geotherm Res 145:337-349. doi: 10.1016/j.jvolgeores.2005.01.010

García O, Martí J, Aguirre-Díaz G, Geyer A, Iribarren I (2011) Pyroclastic density currents from Teide-Pico Viejo (Tenerife, Canary Islands): implications on hazard assessment. TerraNova 23:220-224. doi: 10.1111/j.1365-3121.2011.01002.x

García A, Vila J, Ortiz R, Macià R, Sleeman R, Marrero JM, Sánchez N, Tárraga M, Correig AM (2006) Monitoring the reawakening of Canary Island's Teide volcano. EOS Trans 87(61):65

Geyer A., Martí J. 2009. Stress fields controlling the formation of nested and overlapping calderas: Implications for the understanding of caldera unrest. Journal of Volcanology and Geothermal Research , **181**, 185-195.

Giordano D, Dingwelll DB, Romano C (2000) Viscosity of a Teide phonolite in the welding interval. J. Volcanol Geotherm Res 103:239–245

Giordano D, Dingwelll DB, Romano C (2000) Viscosity of a Teide phonolite in the welding interval. J Volcanol Geotherm Res 103:239–245

Gottsmann J, Dingwell DB (2001) Cooling dynamics of spatter-fed phonolite obsidian flows on Tenerife, Canary Islands. J Volcanol Geotherm Res 105:323–342

Gottsmann J, Wooller L, Marti, Fernandez J, Camacho A, González P, García A, Rymer H (2006) New evidence for the reawakening of Teide volcano. Geophys Res Lett 33(L20311). doi:10.1029/ 2006GL027523

Guzman S., Petrinovic 1.A., Bord J.A., Hongn F.D., Seggiaro R.E., Montero C., Carniel R., Dantas E.L., Sudo M. (2011) Petrology of the Luingo caldera (SE margin of the Puna plateau): A middle Miocene window of the arc–back arc configuration.. J Volcanol Geotherm Res 200:171–191. doi:10.1016/j.jvolgeores.2010.12.008

Hausen H (1956) Contributions to the geology of Tenerife (Canary Islands) Soc. Sci. Fennicae, Comm. Phys-Mat, 18:254

Hernández PA, Pérez N, Salazar JML, Nakai S, Notsu K, Wakita H (1998) Diffuse emission of carbon dioxide, methane and helium3 from Teide volcano, Tenerife, Canary Islands. Geophys Res Lett 25:3311–3314

Houghton B, Wilson CJN (1989) A vesicularity index for pyroclastic deposits. Bull Volcanol 51:451–462.

IGME, 2009. Digital Continuos Geological Map of Spain at 1:50000 (Plan MAGNA). Tenerife. http://www.igme. es/internet/default.asp. Accessed 08 September 2009.

Kinvig HS, Winson A, Gottsmann J (2010) Analysis of volcanic threat from Nisyros Island, Greece, with implications for aviation and population exposure. Nat Haz Earth Syst Sci 10:1101–1113

Le Bas M.J., Le Maitre, R.W., Streckeisen A., Zanetti B., 1986. A chemical classification of volcanic Rocks based on the total alkali – silica diagram. Journal of Petrology, **27**, 745-754.

Loughlin SC, Calder ES, Clarke A, Cole PD, Luckett R, Mangan MT, Pyle DM, Sparks RSJ, Voight B, Watts RB (2002) Pyroclastic flows and surges generated by the 25 June 1997 dome collapse, Soufriere Hills Volcano, Montserrat. In: Druitt TH, Kokelaar BP (eds) The eruption of Soufriere Hills Volcano, Montserrat, from 1995

to 1999. Mem Geol Soc London 21. Geological Society of London, London, pp 191–209

Malin MC, Sheridan MF (1982) Computer-assisted mapping of pyroclastic surges. Science 217:637–639

Marrero JM, García A, Llinares A et al (2012) A direct approach to estimating the number of potencial fatalities from an eruption: Application to the Central Volcanic Complex of Tenerife Island. J Volcanol Geotherm Res 219-220:33-40. doi: 10.1016/j.jvolgeores.2012.01.008

Martí J, Gudmundsson A (2000) The Las Cañadas caldera (Tenerife, Canary Islands): an overlapping collapse caldera generated by magma-chamber migration. J Volcanol Geotherm Res 103:161-173

Martí J, Mitjavila J, Araña V (1994) Stratigraphy, structure and geochronology of the Las Cañadas caldera (Tenerife, Canary Islands). Geol Mag 131:715–727

Martí J, Hurlimann M, Ablay GJ, Gudmundson A (1997) Vertical and lateral collapses in Tenerife and other ocean volcanic islands. Geology 25:879–882

Martí J, Gudmundsson A (2000) The Las Cañadas caldera (Tenerife, Canary Islands): an overlapping collapse caldera generated by magma-chamber migration. J Volcanol Geotherm Res 103:161– 173

Martí J, Aspinall WP, Sobradelo R, Felpeto A, Geyer A, Ortiz R, Baxter P, Cole P, Pacheco JM, Blanco MJ, Lopez C (2008) A long-term volcanic hazard event tree for Teide-Pico Viejo stratovolcanoes (Tenerife, Canary Islands). J Volcanol Geotherm Res 178:543–552

Martı, J., Geyer, A., Andujar, J., Teixidoí , F. and Costa, F., 2008. Assessing the potential for future explosive activity from Teide-Pico Viejo stratovolcanoes

(Tenerife, Canary Islands). J. Volc. Geoth. Res., 178, 529–542. doi:10.1016/j.jvolgeores.2008.07.011

Martı, J., Ortiz, R., Gottsmann, J., Garcia, A. and De La Cruz-Reyna, S., 2009. Characterising unrest during the reawakening of the central volcanic complex on Tenerife, Canary Islands, 2004–2005, and implications for assessing hazards and risk mitigation. J. Volc. Geoth. Res., 182, 23–33.

Martí J, Geyer A (2009) Central vs flank eruptions at Teide–Pico Viejo twin stratovolcanoes (Tenerife, Canary Islands). J Volcanol Geotherm Res 181:47–60

Martí J, Felpeto A (2010) Methodology for the computation of volcanic susceptibility. An example for mafic and felsic eruptions on Tenerife (Canary Islands). J Volcanol Geotherm Res 195:69– 77

Martí J, Sobradelo R, Felpeto A, García O (2011) Eruptive scenarios of Phonolitic volcanism at Teide-Pico Viejo volcanic complex (Tenerife, Canary Islands). Bull Volcanol 74:767-782. doi:10.1007/s00445-011-0569-6

Martin AJ, Umeda K, Connor CB, Weller JN, Zhao D, Takahashi M (2004) Modeling long-term volcanic hazards through Bayesian inference: an example from the Tohoku volcanic arc, Japan. J Geophys Res 109:B10208

Marzocchi W, Sandri L, Selva J (2010) BET_VH: a probabilistic tool for long-term volcanic hazard assessment. Bull Volcanol 72:705– 716 doi:10.1007/s00445-010-03578

Mendoza-Rosas AT, De la Cruz-Reyna S (2008) A statistical method linking geological and historical eruption time series for volcanic hazard estimations: applications to active polygenetic volcanoes. J Volcanol Geotherm Res 176:277–290

Newhall CG, Self S (1982) The volcanic explosivity index (VEI): an estimate of the explosive magnitude for historical eruptions. J Geophys Res 87:1231–1238

Pérez NM, Coello C, Marrero R, González Y, Brrancos PJ (2005) Premonitory geochemical and geophysical signatures of volcanic unrest at Tenerife, Canary Islands. Geophys Res Abst 7:09993, SRef-ID: 1607-7962/gra/EGU05-A-09993

Perez-Torrado FJ, Carracedo JC, Paris R, Hansen A (2004) Descubrimiento de depósitos freatomagmáticos en la laderas septentrionales del estratovolcán Teide (Tenerife, Islas Canarias): relaciones estratigráficas e implicaciones volcánicas. Geotemas 6:163–166

Pittari,A.,Cas,R.A.F., andMartı,J.,2005. The occurrence and origin of prominent massive, pumice-rich ignimbrite lobes within the Late Pleistocene Abrigo Ignimbrite, Tenerife, Canary Islands. J. Volc. Geoth. Res., 139, 271–293.

Pyle DM (1989) The thickness, volume and grain size of tephra fall deposits. Bull Volcanol 51:1–15.

Pyle DM (2000) Size of Volcanic Eruptions. In: Sigurdsson H (ed) Encyclopedia of Volcanoes. Academic Press, London, pp 263-269.

Reimar P.J., Baillie M.G.L., Bard E., Bayliss A. 2004. Radiocarbon **46**, 1029–1058

Ridley W. 1970. The abundance of rock types on Tenerife, Canary Islands, and its petrogenetic significance. Bulletin of Volcanology, **34,**196-204.

Rodríguez-Losada J, Hernández-Gutiérrez LE, Olalla C, Perucho A, Serrano A, Eff-Darwich A (2009) Geomechanical parameters of intact rocks and rock masses from the Canary Islands: implications on their flank stability. J Volcanol Geotherm Res 182:67–75

Rose WI, Wunderman RL, Hoffman MF, Gale L (1983) A volcanologist's review of atmospheric hazards of volcanic activity: Fuego and Mt St Helens. J Volcanol Geotherm Res 17:133-157

Rose WI, Self S, Murrow PJ, Bonadonna C, Durant AJ, Ernst GGJ (2008) Nature and significance of small volume fall deposits at composite volcanoes: Insights from the October 14, 1974 Fuego eruption, Guatemala. Bull Volcanol 70:1043-1067

Sandri L, Marzocchi W, Zaccarelli L (2004) A new perspective in identifying the precursory patterns of eruptions. Bull Volcanol 66:263–275

Sarna-Wojcicki AM, Shipley S, Waitt JR, Dzurisin D, Wood SH (1981) Areal distribution thickness, mass, volume, and grain- size of airfall ash from the six major eruptions of 1980. US Geol Surv Prof Pap 1250:577–600

Scasso R, Corbella H, Tiberi P (1994) Sedimentological analysis of the tephra from 12–15 August 1991 eruption of Hudson Volcano. Bull Volcanol 56:121–132

Self S (1976) The recent volcanology of Terceira, Azores. J Geol Soc London 132:645-666

Sheridan MF, Malin MC (1983) Application of computer-assisted mapping to volcanic hazard evaluation of surge eruption: Vulcano, Lipari, Vesuvius. Explosive volcanism. J Volcanol Geotherm Res 17:187–202

Sobradelo R, Martí J (2010) Bayesian event tree for long-term volcanic hazard assessment: application to Teide-Pico Viejo stratovolcanoes, Tenerife, Canary Islands. J Geophys Res 115: B05206. doi:10.1029/2009JB006566

Sobradelo R, Martí J, Mendoza-Rosas AT, Gómez G (2011) Volcanic hazard assessment for the Canary Islands (Spain) using extremeevent statistics. Nat Hazards Earth Syst Sci 11:2741–2753. doi:10.5194/nhess-11-2741-2011

Solana MC, Aparicio A (1998) Reconstruction of the 1706 Montaña Negra eruption. Emergency procedures for Garachico and El Tanque, Tenerife, Canary Islands. In: Firth CR, McGuire WJ (ed) Geol Soc London Spec Pub 161, pp 209-216

Soriano C, Zafrilla S, Martí J, Bryan S, Cas R, Ablay G (2002). Welding and rheomorphism of phonolitic fallout deposits from the Las Canadas caldera, Tenerife, Canary Islands. Geol Soc Am Bull 114: 883–895

Sparks RSJ, Wilson L, Sigurdsson H (1981). The pyroclastic deposits of the 1875 eruption of Askja, Iceland. Philos. Trans R Soc Lond 299, 241–273

Sparks RSJ (1986). The dimensions and dynamics of volcanic eruption columns. Bull Volcanol 48, 3-15

Suzuki T (1983) A theoretical model for dispersion of tephra. In: Shimozuru D, Yokoyama I (eds) Arc volcanism: physics and tectonics. Terra Scientific, Tokyo, pp 95–113

Sun S., McDonough W.F. 1989. Chemical and isotopic systematics of oceanic basalts: implications fro mantle composition and processes. Geological Society, London, Special Publications, **42**, 313-345. doi:10.1144/GSL.SP.1989.042.01.19

Szramek L, Gardner J, Larsen J (2006). Degassing and microlite crystallization of basaltic andesite magma erupting at Arenal Volcano, Costa Rica. J Volcanol Geother Res 157:182–201. doi:10.1016/j.volgeores.2006.03.039

Talma AS, Vogel JC (1993) A simplified approach to the calibration of radiocarbon dates. Radiocarbon 35:317-322

Thorinsson S, Sigvaldson GE (1972) The Hekla eruption of 1970. Bull Volcanol 36:269-288

Thompson R.N. 1982. Magmatism of the British Tertiary province Scottish. Journal of Geology, **18**, 49-107.

Tierbold S., Kronz A., Gerhard W. 2006. Anorthite-calibrated backscattered electron profiles, trace elements and growth textures in feldspars from Teide-Pico Viejo volcanic complex (Tenerife). Journal of Volcanol Geothermal Researcher, **154**, 117-130. doi:10.1016/j.jvolgeores.2005.09.023

Tischendorf G., Gottesmann B., Föster H.J., Trumbull R.B. 1997. On Li-bearing micas: estimating Li from electron microprobe analyses and improved diagram for graphical representation. Mineralogy Magazine, **61**, 809–834.

Toyos G, Cole P, Felpeto A, Martí J (2007) A GIS-based methodology for hazard mapping of small volume pyroclastic density currents. Nat Haz 41:99–112

Zellmer G.F., Blake S., Vance D., Hawkesworth C., Tuner S., 1999. Plagioclase residence times at two island arc volcanoes (Kameni Islands, Santorini, and Soufriere, St. Vincent) determined by Sr diffusion systematics. Contribution of Mineral Petrology, **136**, 345–357.

Zellmer G.F., Sparks R.S.J., Hawkesworth C., Wiedenbeck M., 2003. Magma emplacement and remobilization timescales beneath Montserrat: insights from Sr and Ba zonation in Plagioclase phenocrysts. Journal of Petrology, **44**, 1413-1431.

Wiesmaier S, Deegan FM, Troll VR, Carracedo JC, Chadwick JP, Chew DM (2011) Magma mixing in the 1100 AD Montaña Reventada composite lava flow, Tenerife, Canary Islands: interaction between rift zone and central volcano plumbing system. Contrib Mineral Petrol. Doi: 10.1007/s00410-010-0596-x

Wiesmaier S, Troll VR., Carracedo JC , Ellam MRM, Bindeman I., Wolf J. (2012) Bimodality of Lavas in the Teide-Pico Viejo succession in Tenerife, the role of

crustal melting in the Origin of Recent Phonolites. Journal of Petrology, **53**, 2465-2495.

Wilson, C.J.N., 1985. The Taupo eruption, New Zealand: II. The Taupo ignimbrite. Phil. Trans. Roy. Soc. London, A 314, 229–310

Wilson L, Walker GPL (1987) Explosive volcanic eruptions –VI. Ejecta dispersal in plinian eruptions: the control of eruption conditions and atmospheric properties. Geophys J R Astr Soc. 89:657-679

Wright HMN, Cashman KV, Rosi M, Cioni R (2006) Breadcrust bombs as indicators of vulcanian eruptions at Guagua Pichincha volcano, Ecuador. Bull Volcanol 69:281–300. doi:10.1007/s00445-006-0073-6

Woods, A.W., 1993. Moist convection and the injection of volcanic ash into the atmosphere. J. Geophys. Res., 98, 17627– 17636.

Appendix 1 Contribution to the papers.

Inform from the director of the thesis on the impact factor or the categorization of the publications to be found in the doctoral thesis and report of the director of the thesis explaining my participation in the papers that have been presented and where I am coauthor.

MINISTERIO
DE ECONOMIA Y
COMPETITIVIDAD

CONSEJO SUPERIOR
DE INVESTIGACIONES
CIENTÍFICAS
CSIC

JOAN MARTI I MOLIST, Professor d'Investigació del CSIC adscrit a l'Institut de Ciències de la Terra "Jaume Almera" de Barcelona i Director de al Tesi Doctoral realitzada per Na Olaya García titulada "

CERTIFICA:

1) que, d'acord amb la normativa vigent de la Universitat de Barcelona referent a la presentació de Tesis Doctorals, aquest Tesi Doctoral es presenta com a compendi de les següents publicacions científiques de les que s'indica el seu factor d'impacte a l'any de la publicació:

- GARCÍA, O., MARTÍ, J., AGUIRRE-DIAZ, G., GEYER, A. and IRIBARREN, I. Pyroclastic density currents from Teide (Tenerife, Canary Islands): implications on hazard assessment. TerraNova (2011) 23, 220–224. Factor d'impacte: 2,339

- GARCIA, O., BONADONNA, C., MARTI, J., PIOLI, L. The Boquerón (edad) explosive eruption, Teide- Pico Viejo Complex, Tenerife. Bulletin of Volcanology (2012) 74 (9), 2037-2050, DOI 10.1007/s00445-012-0646-5. Factor d'impacte: 2,205

- GARCÍA, O., MARTÍ, J., GUZMAN, S., Stratigraphic, mineralogical and geochemical correlation of phonolitic explosive episodes of Teide- Pico Viejo Complex, Tenerife, Journal of the Geological Society (sbmitted). Factor d'impacte: 3,196

- MARTI., J., SOBRADELO, R., FELPETO, A., GARCIA, O. Hazard assessment at Teide-Pico Viejo volcanic complex (Tenerife, Canary Islands). Bulletin of Volcanology (2012), 74, 767-782 DOI 10.1007/s00445-011-0569-6. Factor d'impacte: 2,205

2) que tots els treballs han estat realitzats en col·laboració amb altres investigadors, havent estat la doctoranda la persona encarregada de realitzar la major part de treball, la seva redacció i revisió, en les tres primeres publicacions, mentre que en la quarta la seva aportació ha esta fonamental per poder establir els escenaris eruptius i els models de perillositat espacial, havent també participat activament en la seva redacció.

I perquè així consti i a tots el efectes oportuns signo el present certificat en Barcelona a vint de maig de dos mil tretze.

ICTJA
INSTITUTO DE CIENCIAS DE LA TIERRA JAUME ALMERA

C/ SOLÉ I SABARÍS, S/N
08028 BARCELONA ESPAÑA
TELF. +34 93 409 54 10
FAX.: +34 93 411 00 12

Appendix 2. Stratigraphic correlation of Holocene phonolitic explosive episodes of the Teide-Pico Viejo Complex, Tenerife)

Stratigraphic correlation of Holocene phonolitic explosive episodes of the Teide-Pico Viejo Complex, Tenerife.

Olaya García[1], Silvina Guzmán[2], Joan Martí[1]

1. Instituto de Ciencias de la Tierra Jaume Almera, CSIC, Lluis Solé Sabarís s/n, 08028 Barcelona, Spain.

2. IBIGEO (CONICET-UNSa), Museo de Ciencias Naturales, Universidad Nacional de Salta, Mendoza 2, 4400, Salta, Argentina

Corresponding author: Olaya García (email: garciaperez.olaya@gmail.com)

Running title: Explosive episodes of Teide-Pico Viejo.

Submitted to the Journal of the Geological Society

Abstract: Teide and Pico Viejo are twin stratovolcanoes (TPV) that form one of the largest alkaline volcanic complexes in the world. They began forming inside the caldera of Las Cañadas about 200 ka ago and are largely made up of an accumulation of mafic, intermediate and more recent felsic products that form lava flows. However, a number of significant pyroclastic deposits dating from the Holocene are also present. In order to quantify the explosive contribution to the construction of TPV we re-examined its stratigraphy and identified several Holocene phonolitic explosive episodes ranging from Strombolian to sub-Plinian that are represented by fallout and pyroclastic density current deposits. Although some of the pumice deposits have been related to known vent sites, a few are still of unknown origin. The use of field criteria as well as geochemical and mineralogical analysis help provide reliable criteria for robust correlations and for establishing the relative stratigraphy of the deposits. The presence of these pyroclastic deposits in the recent history of the TPV complex suggests that these stratovolcanoes are entering into a more explosive stage that represents a non-avoidable hazard for the island of Tenerife.

Keywords: Teide-Pico Viejo Complex; explosive volcanism, pumice deposit, Tenerife

Teide and Pico Viejo are twin stratovolcanoes situated on the island of Tenerife (Canary Islands) that constitute one of the most important active oceanic island volcanic complexes in the world. They started to grow inside the caldera of Las Cañadas less than 200 ka ago and have continued to be active up to the present day, with the last central eruption (Lavas Negras) having occurred about 1000 years ago (Carracedo *et al*. 2007).

The activity of this volcanic complex has generated magmas that have evolved from basaltic to phonolitic in the period dating from 35 000 years ago to the present (Martí *et al*. 2008). Most of the products that have been preserved in TPV correspond to thick lava flows of phonolitic composition that outcrop on the surface (Ablay & Martí 2000; Carracedo *et al.* 2007), basaltic-to-intermediate lava flows forming most of the inside of the volcanic edifices

(Ablay & Martí 2000; Thiebolt *et al.* 2006; Martí *et al.* 2008), minor phreatomagmatic deposits of mafic composition (Pérez Torrado *et al.* 2004; Martí *et al.* 2008; García *et al.* 2011) and phonolitic pumice deposits mostly originating from the 2020 YBP eruption of the satellite cone of Montaña Blanca (Ablay *et al.* 1997). This has traditionally led to the assumption that TPV is essentially effusive and so its associated hazard is relatively minor. However, field revisions carried out in recent years (Martí *et al.* 2008; García *et al*. 2011, García *et al.* 2012) have revealed that the amount of explosive volcanism associated with TPV is much greater than was once thought. This has led Martí *et al.* (2011) to reconsider the threat that this active volcanic complex represents for the island of Tenerife and to analyze the potential explosive scenarios that could presumably develop in the near future.

We studied the most recent explosive episodes that have been preserved in the geological record of TPV in order to advance the analysis of the past eruptive activity in TPV and to characterize its explosive events with more accuracy, thereby improving the evaluation of its potential for future explosive episodes. The lack of continuous outcrops – due to the erosion of the deposits – and the apparent similarity of most of these deposits mean that stratigraphic correlation and the determination of the relative ages of these outcrops is not a straightforward task. Therefore, in addition to field and physical volcanology work, we also undertook a detailed petrological and geochemical study including mineral chemistry to identify possible fingerprints that would establish a precise correlation between these deposits and determine their relative stratigraphy. In this paper we 1) describe the relative stratigraphy of the deposits, 2) describe their petrological and geochemical characteristics, 3) establish the correlations between these deposits and their potential vents and, finally, 4) discuss the relevance of explosive volcanism in the Teide-Pico Viejo complex.

Geological Background

The TPV complex consists of two stratovolcanoes and several flank vents, which started to grow simultaneously within the caldera of Las Cañadas around 180–190 ka ago (Fig.1) (Hausen *et al.* 1956; Araña *et al.* 1971; Ablay 1997; Ablay *et al.* 1998; Ancochea *et al.* 1999; Ablay & Martí 2000; Carracedo *et al.* 2007). This volcanic depression originated as a result of several vertical collapses of the edifice of Las Cañadas, the former central volcanic edifice on Tenerife (Martí *et al.* 1997; Martí & Gudmundsson 2000). The TPV complex has a maximum elevation of 3718 m a.s.l (the summit of Teide) and steeply sloping flanks.

The volcanic stratigraphy of TPV was characterized by Ablay & Martí (2000) on the basis of a detailed field and petrological study. Subsequently, Carracedo *et al.* (2003, 2007) provided the first group of isotopic ages from TPV products. The eruptive history of the TPV complex consists of a main eruption period characterized by mafic-to-intermediate lavas that form the core of these stratovolcanoes and filled in most of the depression of Las Cañadas and the adjacent La Orotava and Icod valleys. Phonolitic eruptions predominated from 35 ka ago onwards and their products today cover the volcanoes' flanks and the infill sequence of the Icod Valley and part of La Orotava Valley (Ablay *et al.* 1998; Ablay & Martí 2000; Martí *et al.* 2008).

Phonolitic eruptions from TPV occurred both from the central vents and from a number of satellite vents distributed on the flanks. These flank vents have generated both effusive (i.e. lava flows and domes) and explosive eruptions, ranging in size from 0.01 to > 1 km^3 Dense Rock Equivalent (DRE). Effusive eruptions occurred during the whole period of phonolitic volcanism and generated thick lava flows and domes. Explosive eruptions were mostly concentrated in the Holocene (Table 1 and 2) and caused extensive pumice fall deposits and pyroclastic density currents (PDCs), some of which have been associated with

dome and lava-flow gravitational collapses during sub-Plinian to Plinian eruptions (Martí *et al.* 2008, 2011, García *et al.* 2011). Each of these eruptive centres is associated with a single eruption in which several phases can be distinguished (Ablay & Martí 2000).

Methodology

We conducted a detailed field study whose aim was to identify and characterize the different pyroclastic deposits present in TPV and to locate their possible vents and establish their relative stratigraphy. Fieldwork included the study of these outcrops (Fig.2) in an attempt to locate their potential vents on the basis of their stratigraphic positions, the macroscopic textural and mineralogical characteristics of their deposits, variations in grain-size and thickness, and macroscopic componentry analysis. Fieldwork also included sample collection for subsequent geochemical and mineralogical analysis whose aim was to identify fingerprints that would confirm stratigraphic correlations.

The mineralogical and geochemical analyses of the studied samples were only performed for correlative purposes given that a more detailed petrological and petrogenetic study was beyond the scope of this work. Our working hypothesis – based on previous petrological studies of TPV rocks (Ablay *et al.* 1997; Wiesmayer *et al.* 2011; Andújar *et al.* 2013) – was that products from the same eruption would have relatively homogenous mineralogical and geochemical compositions, while products from different eruptions would not. Whole rock analyses of 67 samples from different outcrops were performed by the GeoAnalytical Laboratory at Washington State University using its X-Ray Fluorescence (XRF) and Inductively Coupled Plasma Mass Spectrometry (ICP-MS) facilities (Table 3). The relative error of the measurement was less than 1% for the major and trace elements using the

114 XRF method, less than 5% for the REEs and less than 10% for the remaining trace elements
115 with ICP-MS.

116 Mineral compositions were determined using an electron microprobe (Camara SX-50,
117 Serveis Científic-Tècnics, University of Barcelona) with an acceleration voltage of 20 kV. The
118 sample current was 6 nA for glasses and 15 nA for minerals, while the beam size was 1 □m
119 for minerals and 10 □m for glasses. Although Na was analysed initially for only 20 s to
120 minimize loss, the peak counting times for the other elements were 10 s.

121 The charcoal that was found in association with three different pumice units was
122 analysed using accelerator mass spectroscopy (AMS) techniques by Beta Analytic Inc.
123 (Laboratory of Miami, USA) to study its carbon isotopic composition. These samples were
124 taken from different parts of the study area. Charcoal sample P1600 was located on the main
125 track that crosses the whole north face of the Teide-Pico Viejo Complex at the bottom of the
126 pumice deposit that overlies a paleosoil; 4 gr of the sample (laboratory number Beta-301363)
127 was taken and its age of 1790□30 yBP was determined using the IntCal04 calibration curve
128 (Reimer *et al.* 2004). Sample RB1 was from the Boquerón deposit yielded an age of 5630□60
129 yBP (García *et al*. 2012). The final ICS charcoal sample (laboratory number Beta-293009),
130 found at the top of the pumice deposit below an altered scoria unit in an outcrop in the south
131 of the study area, was aged at 3520□30 yBP.

132

133 **Stratigraphy**

134 Stratigraphic reconstruction, along with the variations in thickness and grain size established
135 during the fieldwork, enabled us to identify several pyroclastic deposits at different sites and
136 stratigraphic positions (Fig. 2 and 3; Table1) of these deposits, while some were clearly
137 associated with vents located on the flanks of TPV, the source vent of others remains

138 unknown. The flank vents on TPV represent an episode of felsic activity that produced about
139 1.7 ± 0.5 km^3 of phonolitic products from at least 10 satellite vents, located mostly on the NW,
140 N, E and SE flanks of TPV between 2200 and 2600 m a.s.l. and include (in clockwise order)
141 Roques Blancos, El Boquerón, Pico Cabras, Hoya del Abrunco, Montaña Las Lajas, Bocas de
142 Marie, Montaña Blanca, Los Roquillos, Montaña Majua and Montaña de la Cruz (Fig. 1). The
143 flank vents situated in the caldera of Las Cañadas that only emitted mafic magmas were not
144 considered to be part of the TPV complex (Ablay & Martí 2000) given that they are
145 associated with the activity of the rift systems.

146 For practical purposes, we separated the TPV pumice outcrops into two main groups
147 on the basis of their known or unknown potential vent sources: the pumice deposits that in the
148 field could be traced to known vents were Abejera, Abrunco, Pico Cabras, El Boquerón,
149 Montaña Majua, Montaña Blanca, Roques Blancos and Los Gemelos, while the samples with
150 unknown vents were named as 1600, ICS and Calderón.

151 The largest fallout deposit is associated with the products of a substantial explosive
152 eruption that occurred on Montaña Blanca on the eastern side of Teide (Fig.2). This deposit
153 corresponds to an intermediate phase of the Montaña Blanca eruption that occurred about 2 ka
154 ago and generated phonolitic domes and lava flows (Ablay *et al.* 1997). This fallout deposit
155 contains well-sorted, pale and angular pumice with a high concentration of lithic fragments of
156 obsidian and lavas. In proximal areas on Montaña Blanca the top of this deposit corresponds
157 to a welded facies consisting of flow-banded, poorly vesiculated obsidian with a relict clastic
158 texture, supporting poorly inflated angular pumice. This pumice fall deposit was interpreted as
159 deriving from a sub-Plinian phase from the main vent at Montaña Blanca that formed a 9-km
160 high eruption column (Ablay 1997; Folch & Felpeto 2005).

A second pumice fallout deposit is to be found inside the caldera of Las Cañadas at the bottom of the Teide volcano and is associated with Montaña Majua, a denuded pumice cone of ca. 700 m in diameter breached to the southeast by the emplacement of a thick lobate phonolite lava flow (~0.03±0.01 km^3). This pumice fallout deposit is a single, well-sorted, reversely graded deposit formed by non-welded angular pumice lapilli with a low content of juvenile obsidian and oxidised lithic fragments of lava. Proximal exposures reveal crude, centimetre-scale stratification and the development of crystal-rich layers in the basal portions. Distal localities are unstratified. This deposit was classified as Strombolian on the basis of dispersal criteria (Ablay 1997; Ablay & Martí 2000). Part of the Montaña Majua pumice deposits cover part of the slopes of El Teide, 0.6–1.2 km to the northwest.

An extensive pumice fallout field lies on the shoulder between the edifices of El Teide and Pico Viejo and has been associated with the phonolitic domes of Los Gemelos (Ablay *et al.* 1997). This field corresponds to well sorted, bedded, angular, pale-green pumice lapilli fallout deposits, grading upwards locally into densely welded spatter, with a high content of juvenile lithic clasts of obsidian and lavas.

The dome of Roques Blancos on the north-western flank of Pico Viejo (Fig.2) consists of two vents (Balcells & Hernández Pacheco 1989), both of phonolitic composition. Roques Blancos is the most voluminous (0.83±0.1 km^3) of all the compound phonolite lava flows that erupted from the parasitic fissure vents on TPV. It covers an area of 18±2 km^2, extending down the north flank of Pico Viejo and filling in the Icod Valley (Ablay & Martí 2000, Martí *et al*. 2011). There is a pyroclastic succession associated with Roques Blancos that consists of an up-to-65-cm thick lapilli-size pumice fall deposit characterized by poor exposure, with proximal outcrops with a stratified, inversely graded pumice deposit formed by non-welded, micro-vesiculated, angular-to-sub-angular lapilli pumice, with a low (>2 wt%) content of

lithic clasts (obsidian and lava fragments). This deposit is discontinuously distributed along the north-western flank of TPV (Fig. 2).

El Boquerón is a dome complex located on the north-western flank of the Pico Viejo stratovolcano close to the Roques Blancos dome complex (Fig. 2). The final eruption of El Boquerón occurred 5600 yBP (García *et al.* 2012) and generated a widely dispersed pumice fall deposit and 0.04 km^3 of lava flows, which flowed down into the Icod Valley. As in the case of the Montaña Blanca pumice, El Boquerón has been interpreted as being the result of a sub-Plinian eruption with a MER of 6.9–8.2 x 10^5 kg/s, DRE volume of 4–6 x 10^7 m^3 and a 9-km high eruption column (García *et al.* 2012). The pumice deposit is poorly preserved and has poor exposure. It corresponds to a well-sorted deposit composed of non-welded, micro-vesicular, angular-to-subangular, yellow-to-grey lapilli pumice with subordinate lithic clasts of obsidian and phonolitic lavas.

On the north flank of Teide between Abrunco and Pico Cabras (Fig. 2) there is a phonolitic pumice cone, approximately 900 m in diameter, that is breached by the emplacement of a phonolitic lava flow around 200 m to the west. This flow covers part of the pumice cone corresponding to Abrunco, the oldest of the vents on the north flank of TPV (García *et al*. 2011). Associated with this eruption there is a PDC deposit covered by fallout deposit originating from the same eruption (García *et al.* 2011). This pumice fall deposit is composed of well-sorted, yellow-to-grey angular lapilli pumice, with a few obsidian lithic fragments. The distal deposits have mostly been eroded out but in proximal areas may reach up to 2 m in thickness. The PDC deposit is fairly heterogeneous and poorly exposed and has different lithofacies throughout the outcrop (see García *et al*. 2011). This deposits overlies a clastogenic lava flow that was locally eroded by the pyroclastic current during its emplacement.

209 Other pumice deposits found on the north flank of El Teide are associated to the Pico
210 Cabras and Abejera domes (Fig. 2), two volumetrically significant vent complexes whose
211 lava-flow products extend into the Icod Valley and almost reach the northern cost of Tenerife.
212 Abejera is the youngest of these two domes and consists of two vents that produced three
213 blocky lava flows of evolved phonolite with a DRE volume of ~0.36 km^3 (Ablay & Martí
214 2000). Abejera also includes a partially reworked fallout deposit, a few centimetres thick in
215 proximal areas, formed of sub-rounded-to-rounded, poorly vesiculated lapilli pumice, and a
216 few obsidian lithic fragments (4% vol.). On the other hand, Pico Cabras emitted an important
217 lava flow (0.28 km^3 DRE volume) and a few well-preserved, locally reworked outcrops of
218 well-stratified, well-sorted, green-to-grey subangular lapilli pumice, with well-defined
219 stratification. Proximal deposits reach up to 2 m in thickness. However, we found no
220 stratigraphic indicators that could be used to correlate individual layers in the different
221 outcrops and so we describe the Pico Cabras pumice deposits as a single unit.
222 The ICS deposit is found within the calderas of Las Cañadas, inside the Ucanca
223 depression (Fig. 2). This deposit overlies an older lava flow and consists of a 1.7-m thick
224 yellow, angular, highly vesicular fine lapilli pumice, unconformably overlain by a 40-cm thick
225 red scoria deposit. Between the red scoria deposit and the pumice deposit we found charcoal
226 fragments that give a C^{14} age of 3450 +/- 30 yBP.
227 Another pumice deposit that is widely distributed on the northern flank of the TPV
228 complex – in particular along the road that runs E-W at an altitude of 1600 m a.s.l (Fig. 2) –
229 consists of a series of disperse outcrops of pumice fall deposits of unknown provenance. All
230 these outcrops have similar lithological, textural and compositional characteristics and so we
231 grouped them in the same deposit (P1600 deposit). Some of these outcrops situated on the
232 eastern side of TPV (Fig. 2) overlie the Pico Cabras lava flow, while towards the west they are

233 located between the Roques Blancos lava flows, as have been describe before. This
234 pyroclastic deposit consists of well-stratified, inversely graded, sub-angular, grey-to-yellow,
235 highly vesicular fine lapilli pumice, with a few lithic obsidian clasts (>2 wt%), reaching a
236 maximum thickness of 65 cm. Charcoal fragments found in a dark brown soil at the base of
237 this deposit give an age of 1770+/- 80 yBP, the same age as Carracedo *et al.* (2003, 2007)
238 attributed to the Roques Blancos dome. However, field stratigraphic relationships did not
239 provide any convincing evidence that could correlate this pumice deposit with the Roques
240 Blancos vent.

241 The final pumice deposit of unknown provenance identified in this field survey was
242 found inside El Calderón subsidence structure (Fig. 2) and consists of an asymmetric, circular
243 collapse structure of unknown origin, 30 m in diameter and with a depth of 4 m in its
244 shallowest part and around 15 m in the deepest part (e.g. Araña *et al*. 1989; Ablay & Martí
245 2000). On the walls of this depression a succession of three pyroclastic units is exposed with a
246 maximum thickness of 77 cm and a 3-m covering of clastogenic lava from Cuevas Negras
247 (Carracedo *et al.* 2007). From top to bottom we distinguished: Unit III, formed of 40 cm of
248 unsorted grey pumice clasts, with variable grain size from lapilli to bomb; Unit II, formed of a
249 20-cm thick, well-sorted dark grey mafic scoria clasts with lava fragments (6 % volume); and
250 Unit I, formed of a 17-cm thick layer of non-sorted lapilli-to-bomb pumice, yellow-to-grey in
251 colour with highly elongated vesicles, lithic clasts of lavas and obsidian (10 % volume) with
252 its upper 5–8 cm consisting of a red, welded pumice layer. The absence of stratigraphic
253 discontinuities suggests that these three units were deposited continuously, although their
254 origin is unknown. The differences between Unit II (mafic) and the other units (phonolitic)
255 and the absence of any evidence of mixing in the felsic units suggest that the intermediate
256 layer has a different provenance. It is possible that the two eruptions took place at the same

257 time, with Unit II originating from the rift zone and Units I and III from the TPV complex.
258 This is not unusual in either the TPV record or the pre-TPV Las Cañadas edifice (Ablay &
259 Martí 2000; Edgar *et al.* 2007).
260
261 **Petrology and geochemistry**
262 *Petrographic characteristics:*
263 Representative randomly collected pumice samples from all recognised pyroclastic
264 units from each deposit were examined. All the studied juvenile lapilli pumice samples were
265 microvesicular, glassy and phenocryst poor and in some cases had a total lack of phenocrysts
266 (i.e. Roques Blancos).
267 The overall phenocryst phases (Table 2) are represented by feldspar (Kfsp, Plg),
268 clinopyroxene (Cpx), biotite (Bt), titanomagnetite (Ttn-Mag), and ilmenite (Ilm); the
269 phenocryst content in the deposits varies between < 0.5 (vol. %) in Pico Cabras and P1600
270 and 3 (vol. %) in El Boquerón. Feldspar was the most common type of phenocryst found and
271 were euhedral-to-subhedral, with a maximum size of 2 mm and an average size of 0.5 mm. A
272 certain number of microlites (<100μm) were found in all deposits except in Pico Cabras, El
273 Calderón Unit III and Abrunco, where the microlite content was very low. Clinopyroxene was
274 less abundant, with an average size of 0.65 mm and a maximum size of 2 mm. Biotite was
275 present in the pumice samples (elongate and rectangular shapes) as phenocrysts of around 1
276 mm and as microlites in the groundmass (<100 μm). Fe-Ti oxides were the least abundant
277 minerals and were always relatively small (around 500–200 μm).
278 Pumice clasts were moderately-to-poorly vesicular and had heterogeneous textures
279 that varied in terms of their degree of vesicularity and crystallinity. Vesicles ranged in size
280 from a few millimetres to few micrometres and in shape from spherical to elongate or flat.

The thickness of the vesicle walls ranged from just a few to tens of micrometres, suggesting the occurrence of high nucleation rates and an expansion-dominated coalescence (Szramek *et al.* 2006). Vesicles were usually preserved, although a few amygdales replenished by secondary mineralization by calcite and, more rarely, by barite were also identified.

In deposits such as those at El Boquerón, El Abrunco and Los Gemelos groundmass crystallinity varies at specimen scale and is correlated with the degree of vesicularity: microlite-poor areas (5 % vol. of microlites) are also vesicle-poor, with only small round vesicles; microlite-rich areas (50 vol. % of microlites) have vesicularity up to 45 % vol. This relationship between vesicles and groundmass crystallinity is probably due to the effects of post-fragmentation expansion or even to clast recycling during less explosive phases (see Wright *et al*. 2006). Microlites consist of acicular sanidine with major axes ranging between 200 and 10 μm, as well as elongated biotite with major axis size of around 200 and 20 μm. Clinopyroxenes were less frequent than microlites and of different shapes (elongate and rectangular), and ranged in size from 200 to 10 μm. Occasionally, microlites were gathered in small groups in the crystal-rich glass, but more commonly were found as individual crystals. Clasts from incipiently welded facies had highly heterogeneous textures with abrupt variations in vesicle size and spherulitic aggregates.

Mineral Chemistry

Microprobe analysis (phenocrysts and vitric groundmass) was performed on pumice samples from all the different deposits. Clinopyroxene was present in all the pumice samples except in those from P1600, Roques Blancos, ICS and Pico Cabras. Following the classification of Morimoto (1988), most of the phenocrysts analysed correspond to diopside ($Wo_{51-46}En_{40-36}$ Fs_{15-10}), although El Calderón Units I and III correspond to augite (Wo_{45-31} En_{44-40} Fs_{25-15})

(Fig.4a). Most of the diopside crystals show slight normal and inverse zoning in Mg and Fe portions. In Fig.4b the variation diagrams of Mg vs. Fe^{2+} and Fe_2O_3 and SiO_2 vs. MgO for clinopyroxenes are shown and enable the different deposits to be differentiated.

Feldspar phenocrysts occur in all pumice deposits except those of El Calderón Unit III and Pico Cabras; their composition ranges from anorthoclase to sanidine and, exceptionally, oligoclase (El Calderón Unit I) (Fig. 5). Alkali feldspar of sanidine composition was found in the deposits from Montaña Blanca, P1600 and Abrunco but was not as common as anorthoclase, which were found in most of the studied deposits (Los Gemelos, Montaña Majua, Abrunco, ICS, Montaña Blanca and El Boquerón). Microprobe profile analyses performed on different feldspar phenocrysts showed zonation patterns in both the sanidine and the anorthoclase crystals. Analyses of feldspar crystal cores are shown in Fig. 5.

All the biotite crystals correspond to Mg and Ti-rich biotite and were present in the Los Gemelos, El Boquerón, Pico Cabras, ICS, Montaña Majua and El Calderón Unit I deposits (Fig.6a). The highest Mg and Ti content was found at ICS and Montaña Majua. (Fig.6b)

Fe-Ti oxides correspond to spinels (magnetite and ilmenite). Titano-magnetite compositions range from $Ups_{41.95}$ to $Ups_{56.71}$ and vary from one deposit to another: El Boquerón $Usp_{54.58}$; Majua $Ups_{47.39}$; Los Gemelos $Ups_{52.18}$; Pico Cabras $Ups_{46.75}$, Abrunco PDC $Ups_{42.98}$, Abrunco CMP $Ups_{41.95}$, El Calderón unit I $Ups_{56.71}$ and Montaña Blanca $Ups_{52.80,}$ (Fig.7). Ilmenite compositions range from $Ilm_{88.58}$ to $Ilm_{93.28}$: El Boquerón $Ilm_{93.21}$, Majua $Ilm_{91.63}$; Gemelos $Ilm_{93.28}$; Abrunco $Ilm_{89.07}$.

Whole rock geochemistry

328 Representative whole rock analyses of the studied pumice deposits are given in Table 3 and
329 Fig. 8. All the pumice samples studied from the TPV succession had a peraluminous (A/CNK
330 >1) phonolitic-to-trachy-phonolitic composition, with a SiO_2 content ranging from 51.21 to
331 60.56 wt %, and a total alkali content (Na_2O+K_2O) between 10.46 and 15.12 wt %.
332 These pumice deposits show the typical geochemical features of evolution by
333 fractional crystallisation, as indicated by the corresponding positive and negative correlations
334 between major and trace elements (Figs. 11 and 12) that occurs in the TPV phonolitic lavas
335 (Ridley 1970; Araña *et al*. 1989; Andújar *et al*. 2010; Wiesmaier *et al*. 2011).
336 Trace elements including REE show a similar pattern in all samples (Figs. 11 and 12)
337 albeit with some differences in the concentration of Ba, Sr, Ti and P, which are more evident
338 for the samples from El Calderón Unit I, ICS, Montaña Majua, and Abrunco PDC. There is
339 also a slight departure from the general REE pattern in these samples (Fig. 12), showing
340 subtle to absent Eu anomalies.
341
342 **Discussion**
343 Our detailed field study enabled us to identify a number of new phonolitic pyroclastic
344 deposits associated with the recent (Holocene) eruptive history of the TPV complex. The
345 presence of these deposits and the previously studied deposits generated by the Montaña
346 Blanca (Ablay *et al*. 1995) and El Boquerón (García *et al*. 2012) eruptions thus confirm the
347 significance of explosive volcanism in TPV. Although some of the pyroclastic deposits
348 identified in this study can be clearly correlated in the field with their corresponding vents
349 located on the flanks of the Teide and Pico Viejo stratovolcanoes, others are of unknown
350 origin.

351 The use of existing stratigraphic (Ablay & Marti 2000; Carracedo *et al*. 2007) and
352 geochronologic (Carracedo *et al*. 2007) data from the TPV complex and comparisons with the
353 new field data enabled us to establish the stratigraphy of these pyroclastic deposits, which all
354 date from the Holocene.

355 According to the stratigraphic relationships, the P1600 pumice deposit could be related
356 to either Pico Cabras or Roques Blancos. This deposit overlies the lavas from these two
357 eruptions but is closest to the pumices from Roques Blancos in terms of its geochemical and
358 petrological characteristics. Pico Cabras dates from more than 5911 yBP (see Fig. 3; Table 1)
359 and so cannot be related to Roques Blancos. In fact, this latter eruption dates from 1714 yBP
360 (Carracedo *et al.* 2007), which is similar to the age we obtained for the P1600 deposits
361 (1770+/- 80 yBP) (see Fig.3; Table 1). Therefore, we propose that the P1600 pumice deposit
362 is a distal facies of the Roques Blancos eruption.

363 The other two deposits of unknown origin, ICS and El Calderón, could not be
364 correlated to any known vent area using either field stratigraphic criteria or a mineralogical or
365 geochemical basis. In the case of the deposits in El Calderón, we mention above that the
366 interbedding of mafic and felsic units could indicate the occurrence of two simultaneous
367 eruptions, one from the north-western rift zone and the other from the central complex,
368 respectively. However, we failed to find any evidence that could correlate the units in El
369 Calderón with any specific eruption or vent site. Another possibility would be to associate the
370 sequence at El Calderón with a single eruption generating both mafic and felsic magmas. A
371 more recent example of this type of eruption is the Montaña Reventada, a young flank
372 eruption developed from a fissure vent system on the western flank of Pico Viejo. It generated
373 a composite lava flow consisting of lower basanite and upper trachy-phonolite units. Previous
374 studies have suggested that the Montaña Reventada erupted from the transition zone between

two separate plumbing systems, that is, the phonolitic system of the TPV complex and the basanite north-western rift zone, which would explain the evolution of the exposed lavas but not the associated explosive deposits (Araña *et al*. 1994; Wiesmaier *et al*. 2011).

The ICS deposits found in the interior of the Ucanca depression in the caldera of Las Cañadas cannot be clearly correlated to any known vent. The similar biotite composition in the ICS and Montaña Majua deposits (Fig. 7) suggest that these deposits have a common origin. This genetic relationship is also suggested by the similar patterns in the trace and REE elements present in both deposits (Figs. 13 and 14). However, the Montaña Majua deposits disperse southeast from the vent (Ablay *et al*. 1997; Ablay & Martí 2000), thus making any correlation with the ICS deposit located to the west unlikely (Fig. 2). Although the deposits at Montaña Blanca, Los Gemelos and Montaña Majua have been related by Ablay *et al.* (1997) to the same eruptive event (albeit to different vents), our data do not support this assumption. The mineralogical and geochemical composition of these deposits (Figs 5, 6, 8 and 9) is sufficiently different to attribute them to different eruptive events originating from different magma pockets. In addition, Carracedo *et al*. (2007) propose different ages for these three deposits and so they should be considered as corresponding to different eruptions.

Therefore, despite their apparent compositional homogeneity, whole rock geochemistry and mineral chemistry allow us to distinguish different deposits and to identify them as originating from different eruptions. Thermodynamic constraints show how sensitive the TPV phonolitic magmas are to changes in their constitutive parameters (Andújar *et al*. 2013). As well, stress studies on TPV systems have shown that each eruption is fed by a different batch of phonolitic magma that accumulated in a different position inside the edifice. This implies that different eruptions may produce deposits that are slightly different in composition. In a general sense the studied rocks can be divided roughly into two groups, a

399 relatively more evolved group (Pico Cabras, El Boquerón, Los Gemelos, Montaña Blanca,
400 P1600) and a less evolved group (El Calderón, Abrunco PDC and CMP, ICS, Abejera,
401 Montaña Majua), a classification that coincides with mineralogical compositions. Major and
402 trace element compositions suggest that all studied deposits derive from cogenetic magmas
403 and that the existing differences correspond to different evolutionary histories of the final pre-
404 eruptive stages, which may include differences in the position of each phonolitic reservoir, in
405 the oxygen fugacity or in the existence or otherwise of pre-eruptive mixing with deeper
406 magmas (see Ablay *et al*. 1997; Martí *et al.* 2008, Martí & Geyer 2009; Wiesmaier *et al.*
407 2012; Andújar *et al.* 2013). The REE contents do not define these groups quite so clearly but
408 do nevertheless indicate that the deposits at ICS, El Calderón Unit I and Abrunco depart
409 slightly from the general trend. (Figs. 11 and 12) Consequently, mineralogical and
410 geochemical correlations as well as field relationships can be useful tools for determining the
411 stratigraphic constraints of the studied deposits.

412 All the deposits that can be correlated with their respective vents (Montaña Blanca, El
413 Boquerón, Roques Blancos, Los Gemelos, Montaña Majua, Abrunco, Pico Cabras and
414 Abejera) are also associated with the extrusion of lavas and/or domes of, in some cases,
415 significant volume and extension. This indicates that in all these cases the explosive
416 volcanism corresponded to complex eruptions that also included effusive episodes. In some
417 cases the explosive phase occurred at the beginning of the eruption (Montaña Majua, El
418 Boquerón, Abrunco and Los Gemelos), while in others it took place at the end (Pico Cabras
419 and Abejera) or even during an intermediate stage (Montaña Blanca and Roques Blancos).
420 This implies that, despite the relatively similar composition of their magmas, these eruptions
421 had different dynamics, possibly as a consequence of local variations in the gas content of the
422 erupting magma in pre-eruptive and eruptive degassing conditions and/or in the pre-eruptive

423 conditions. It is also worth mentioning that none of the eruptions with identified vents
424 occurred from the central vents. This also suggests that different eruption behaviours may
425 have governed both flank and central eruptions. Despite using different approaches, both
426 Martí & Geyer (2009) and Andújar *et al.* (2013) were able to demonstrate that flank eruptions
427 are fed by reservoirs located at different depths and are subject to different stress conditions
428 from those feeding central eruptions.

429 The fact that all the studied deposits date from the Holocene raises the question as to
430 whether the TPV complex is entering a more explosive stage, as has been suggested by Martí
431 *et al.* (2008). Even though the erosion on the northern side of TPV is quite severe and has
432 affected the pyroclastic deposits in this sector, it seems unlikely that older deposits – if they
433 exist – would have been completed removed. It seems more plausible to suggest that no
434 pyroclastic deposits were produced in previous phonologic eruptions from TPV. Furthermore,
435 we were unable to find any TPV pyroclastic deposits older than those identified in this study
436 inside the calderas of Las Cañadas. Likewise, previous studies that used information from
437 water boreholes drilled inside the caldera reported no such type of deposits (Ablay & Martí
438 2000). All these findings tend to support the idea that the explosive character of TPV has
439 increased during the Holocene. This agrees with the petrological evolution from basanites to
440 phonolites shown by TPV magmas (Ablay *et al.* 1997; Wiesmaier *et al.* 2012) and the
441 tendency over time to move towards more evolved phonolitic terms that are richer in volatiles
442 (Ablay *et al.* 1997).

443

444 **Conclusion**

445 We have demonstrated the existence of at least eleven Holocene phonolitic explosive
446 episodes, ranging from Strombolian to sub-Plinian, associated with the TPV complex. Field

447 and petrological data have permitted us to establish the relative stratigraphy of these deposits
448 and to place them within the general stratigraphy of the TPV that has been proposed in
449 previous studies. The presence of these phonolitic pyroclastic deposits in the recent
450 stratigraphy of Teide demonstrates that phonolitic explosive activity is more significant than
451 previously thought and represents an important hazard for the island of Tenerife. Moreover,
452 the fact that all the studied deposits date from the Holocene and that no older deposits of
453 similar characteristics have been identified in this study suggest that the TPV complex is
454 entering into a more explosive stage, which coincides with the evolution shown by the
455 different phonolitic cycles identified in the pre-TPV Las Cañadas edifice.
456
457
458 **Acknowledgments**
459 This research was partially funded by MICINN grant CGL2008-04264, the IGN-CSIC
460 collaboration agreement for the study of Tenerife volcanism, and the European Commission.
461 The authors are grateful to the Teide National Park for permission to undertake this research
462 and the Cabildo of Tenerife for permission FYF 412/10. We would also like to thank all the
463 IGN staff working at the Geophysics Centre of Canarias for their support during the field
464 campaigns, as well as the staff of the Central Geophysics Observatory from Madrid. Thanks
465 are also due to Fidel Costa for his helpful comments.
466
467
468 **References**
469 ABLAY, G.J., ERNST, G.G.J., MARTÍ J., SPARKS, R.S.J. 1995. The 2ka subplinian eruption
470 of Montaña Blanca, Tenerife. *Bulletin of Volcanology*, **57**, 337-355.

471 ABLAY, G.J, CARROLL, M.R., PALMER, M.R., MARTÍ, J., SPARKS, R.S.J. 1998.
472 Basanite- phonolite lineages of the Teide-Pico Viejo volcanic complex, Tenerife, Canary
473 Islands. Journal of Petrology, **39**, 905-936.
474 ABLAY, G.J., 1997. Evolution of the Teide-Pico Viejo complex and magma system, Tenerife,
475 Canary Islands. *Dissertation*. University of Bristol
476 ABLAY, G.J., MARTÍ J. 2000. Stratigraphy, Structure, and Volcanic Evolution of the Pico
477 Teide-Pico Viejo formation, Tenerife, Canary Islands. *Journal of Volcanol Geothermal*
478 *Researcher,* **103**, 175-208, doi: 10.1016/s0377-0273(00)00224-9
479 ANCOCHEA, E., HUERTAS, M.J., FUSTER J.M., CANTAGREL J.M., COELLO J.,
480 IBARROLA, E., 1999. Evolution of the Cañadas edifice and its implications for the origin
481 of the Cañadas caldera (Tenerife, Canary Islands). *Journal of Volcanol Geothermal*
482 *Researcher*, **88**, 177-199.
483 ANDÚJAR, J., COSTA, F., MARTÍ, J., 2010. Magma storage conditions of the last eruption
484 of Teide volcano (Canary Islands, Spain). *Bulletin of Volcanology* **72**, 381-395.
485 ANDÚJAR, J., COSTA, F., SCAILLET, B. 2013. Storage conditions and eruptive dynamics
486 of central versus flank eruptions in volcanic islands: the case of Tenerife (Canary Islands,
487 Spain) *Journal of Volcanol Geothermal Researcher,* doi: 10.1016/j.jvolgeores.2013.05.004
488 ARAÑA, V, MARTÍ, J., APRICIO, A., GARCÍA-CACHO, L., GARCÍA-GARCÍA, R., 1994.
489 Magma mixing in alkaline magmas: An example from Tenerife (Canary Islands).
490 Lithos 32, 1-19

491

492 ARAÑA, V., BARBERI, F., FERRARA, G. 1989. El complejo volcanico del Teide-Pico
493 Viejo. In: Los volcanes y la caldera del Parque Nacional del Teide (Tenerife, Islas
494 Canarias). Editors V. Araña and J. Coello.

ARAÑA, V., 1971. Litología y estructura del edificio Cañadas, Tenerife (Islas Canarias). Estacion Geologica, **27**, 95-135.

BALCELLS, R., HERNANDEZ-PACHECO, A., 1989. El domo colada de Roques Blancos. In: Coello, J., Araña, V. (Eds.), *Los Volcanes y La Caldera del Parque Nacional del Teide (Tenerife, Islas Canarias). ICONA, Madrid*, 227-234.

CARMICHAEL, I.S E. 1967. The iron-titanium oxides of salic volcanic rocks and their associated ferromagnesian silicates. *Contributions to Mineralogy and Petrology*, **14,**36-64.

CARRACEDO, J.C., PATERNE, M., GUILLOU, H., PÉREZ TORRADO, F.J., PARIS, R., RODRÍGUEZ-BADIOLA. E., HANSEN, A. 2003 Dataciones radiométricas (14C y K/Ar) del Teide y el rift noroeste, Tenerife, Islas Canarias. *Estudios Geol*, **59**, 15-29

CARRACEDO, J.C., RODRÍGUEZ-BADIOLA. E., GUILLOU, H., PATERNE, M., SACAILLET, S., PÉREZ TORRADO, F.J., PARIS, R., HANSEN, A. 2007. Eruptive and structural history of Teide volcano and rift zones of Tenerife, Canary Islands. *Geological Society of American Bulletin*, **119**, 1027-1051. doi:10.1130/B26087.1

COSTA, F., CHAKRABORTY, S., DOHMEN, R., 2003. Diffusion coupling between trace and major elements and a model for calculation of magma residence times using plagioclase. *Geochimica et Cosmochim*ica Acta, **67**, 2189–2200.

DEER, W.A., HOWIE, R.A., ZUSSMAN, J., 1992. An Introduction to the Rock-Forming Minerals, 2nd ed. *AddisonWesley Longman China Limited, Hong Kong*.

EDGAR, C.J., WOLFF, J.A., OLIN, P.H., NICHOLS, H.J., PITTARI, A., CAS, R.A.F., REINERS, P.W., SPELL, T.L., MARTÍ, J., 2007. The late Quaternary Diego Hernandez Formation, Tenerife: a cycle of voluminous explosive phonolitic eruptions. *Journal of Volcanology and Geothermal Research* **160,** 59–85.

518 FOLCH, A., FELPETO, A. 2005. A coupled model for dispersal of tephra during sustained
519 explosive eruptions. *Journal of Volcanol Geothermal Researcher,* **145**, 337-349. doi:
520 10.1016/j.jvolgeores.2005.01.010
521 GARCÍA, O., MARTÍ, J., AGUIRRE-DÍAZ, G., GEYER, A., IRIBARREN, I. 2011.
522 Pyroclastic density currents from Teide-Pico Viejo (Tenerife, Canary Islands): implications
523 on hazard assessment. *TerraNova,* **23**, 220-224. doi: 10.1111/j.1365-3121.2011.01002.x
524 GARCIA, O., BONADONNA, C., MARTÍ, J., PIOLI, L. 2012. The 5,660 yBP Boquerón
525 explosive eruption, Teide-Pico Viejo complex, Tenerife. *Bulletin of Volcanology,* **74**, 2037-
526 2050. doi:10.1007/s00445-012-0646-5
527 GEYER, A., MARTÍ, J. 2009. Stress fields controlling the formation of nested and
528 overlapping calderas: Implications for the understanding of caldera unrest. *Journal of*
529 *Volcanology and Geothermal Research* , **181**, 185-195.
530 HAUSEN, H. 1956. Contributions to the geology of Tenerife. *Societas Science Fennica*
531 *Commentationes Physico Mathematicae*, **18**, 1–247
532 LE BAS, M.J., LE MAITRE, R.W., STRECKEISEN, A., ZANETTI, B., 1986. A chemical
533 classification of volcanic Rocks based on the total alkali – silica diagram. *Journal of*
534 *Petrology*, **27**, 745-754.
535 MARTÍ, J., MITJAVILA, J., ARAÑA, V. 1994. Stratigraphy, structure and geochronology of
536 the Las Cañadas caldera (Tenerife, Canary Islands). *Geology Magazine,* **131**, 715- 7.
537 MARTÍ, J., HURLIMANN, M., Ablay, G.J., GUDMUNDSSON, A. 1997. Vertical and lateral
538 collapses in Tenerife and other ocean volcanic islands. *Geology,* **25**, 879-882
539 MARTÍ, J., GUDMUNDSSON, A. 2000. The Las Cañadas caldera (Tenerife, Canary Islands):
540 an overlapping collapse caldera generated by magma-chamber migration. *Journal of*
541 *Volcanol Geothermal Researcher,* **103**, 161-173

542 MARTÍ, J., GEYER, A., ANDUJAR, J., TEIXÓ, F., COSTA, F. 2008. Assessing the potential
543 for future explosive activity from Teide-Pico Viejo stratovolcanoes (Tenerife, Canary
544 Islands). *Journal of Volcanol Geothermal Researcher,* **178**, 529–542.
545 doi:10.1016/j.jvolgeores.2008.07.011
546 MARTÍ, J., SOBRADELO, R., FELPETO, A., GARCÍA, O. 2011. Eruptive scenarios of
547 Phonolitic volcanism at Teide-Pico Viejo volcanic complex (Tenerife, Canary Islands).
548 *Bulletin of Volcanology*, **74**, 767-782. doi:10.1007/s00445-011-0569-6
549 PÉREZ TORRADO, F.J., CARRACEDO, J.C., PARIS, R., HANSEN, A. 2004.
550 Descubrimientos de depósitos freatomagmáticos en las calderas septentrionales de
551 estratovolcan Teide (Tenerife, Islas Canarias): relaciones estratigraficas e implicaciones
552 volcánicas. *Geotemas,* **6**, 163-166.
553 REIMER, P.J., BAILLIE, M.G.L., BARD, E., BAYLISS, A. 2004. Radiocarbon **46**, 1029–
554 1058
555 RIDLEY, W. 1970. The abundance of rock types on Tenerife, Canary Islands, and its
556 petrogenetic significance. *Bulletin of Volcanology*, **34,**196-204.
557 SZRAMEK. L, GARDNER, J., LARSEN, J. (2006). Degassing and microlite crystallization
558 of basaltic andesite magma erupting at Arenal Volcano, Costa Rica. *Journal of Volcanol*
559 *Geothermal Researcher,* **157**, 182–201. doi:10.1016/j.volgeores.2006.03.039
560 SUN, S., MCDONOUGH, W.F. 1989. Chemical and isotopic systematics of oceanic basalts:
561 implications fro mantle composition and processes. *Geological Society, London, Special*
562 *Publications,* **42**, 313-345. doi:10.1144/GSL.SP.1989.042.01.19
563 THOMPSON, R.N. 1982. Magmatism of the British Tertiary province Scottish. *Journal of*
564 *Geology,* **18**, 49-107.

565 TIERBOLD, S., KRONZ, A., GERHARD, W. 2006. Anorthite-calibrated backscattered
566 electron profiles, trace elements and growth textures in feldspars from Teide-Pico Viejo
567 volcanic complex (Tenerife). *Journal of Volcanol Geothermal Researcher,* **154**, 117-130.
568 doi:10.1016/j.jvolgeores.2005.09.023
569 TISCHENDORF, G., GOTTESMANN, B., FÖSTER, H.J., TRUMBULL, R.B. 1997. On Li-
570 bearing micas: estimating Li from electron microprobe analyses and improved diagram for
571 graphical representation. *Mineralogy Magazine*, **61**, 809–834.
572 ZELLMER, G.F., BLAKE, S., VANCE, D., HAWKESWORTH, C., TURNER, S., 1999.
573 Plagioclase residence times at two island arc volcanoes (Kameni Islands, Santorini, and
574 Soufriere, St. Vincent) determined by Sr diffusion systematics. *Contribution of Mineral*
575 *Petrology,* **136**, 345–357.
576 ZELLMER, G.F., SPARKS, R.S.J., HAWKESWORTH, C., WIEDENBECK, M., 2003.
577 Magma emplacement and remobilization timescales beneath Montserrat: insights from Sr
578 and Ba zonation in Plagioclase phenocrysts. *Journal of Petrology*, **44**, 1413-1431.
579 WIESMAIER, S., DEEGAN, F.M., TROLL, V.R., CARRACEDO, J.C., CHADWICK, J.P.,
580 CHEW, D.M. 2011. Magma mixing in the 1100 AD Montaña Reventada composite lava
581 flow, Tenerife, Canary Islands: interaction between rift zone and central volcano plumbing
582 systems. Contributions to Mineralogy and Petrology, **162**, 651-669
583 WRIGHT, H.M.N., CASHMAN, K.V., ROSI, M., CIONI, R. (2006) Breadcrust bombs as
584 indicators of vulcanian eruptions at Guagua Pichincha volcano, Ecuador. *Bulletin of*
585 *Volcanology*, **69**, 281–300. doi:10.1007/s00445-006-0073-6
586 WIESMAIER, S., TROLL, V.R., CARRACEDO, J.C., ELLAM, R.M, BINDEMAN, I.,
587 WOLF, J. 2012. Bimodality of Lavas in the Teide-Pico Viejo succession in Tenerife, the

role of crustal melting in the Origin of Recent Phonolites. *Journal of Petrology*, **53**, 2465-2495.

Figure captions

Figure 1. a) Location of the Canary Islands and Tenerife. b) Simplified geology and stratigraphy of Tenerife. Main vents are shown as black triangles, *T* Teide, *PV* Pico Viejo and *MB* Montaña Blanca.

Figure 2. Simplified geological map of the Teide-Pico Viejo complex (modified from Ablay & Martí 2000) showing the central and flank Holocene eruptions of felsic and hybrid compositions. Geochronological data from Carracedo *et al.* (2007). Main vents are shown as black triangles. The studied deposits and the corresponding samples are indicated by red circles (XRF+ICP analysed samples are indicated with blue circles). The pumice deposits associated with the main flanks of the volcanoes of TPV are shown with white dots. (projection: UTM 28N)

Figure 3: Age of the Holocene pumice fall out deposit of the Northwest (NW), North (N), East (E) and South (S) of the Teide - Pico Viejo volcanic complex. Geochronological data from García et al. (2011) and Carracedo et al. (2007). The legend colours fit with the map Fig. 2.

611 Figure 4. a) Classification diagram of clinopyroxenes (Morimoto 1988) from the TPV pumice
612 deposits. Clinopyroxene are classified using the total number of cations on a 6-oxygen basis;
613 the Fe_2O_3 was estimated according to the method used by Droop (1987). Red full circles,
614 Calderon Unit I; red empty circles, Calderon Unit III; black squares, Mtn. Blanca; yellow
615 triangles, Mtn. Majua; blue cross, El Boquerón; green squares, Los Gemelos; black stars,
616 Abrunco PDC; white starts, Abrunco (fall out). b) Selected correlation diagrams of core
617 analysis from the clinopyroxenes of the TPV pumice deposits SiO_2 vs. MgO, and Fe_2O_3 vs.
618 MgO.
619
620 Figure 5. Classification diagram of the feldspar (Ab-An-Or) TPV pumice deposit. The
621 formula composition was calculated on an 8-oxygen basis following the method described by
622 Deer *et al.* (1992). Major elements diagram of the feldspar core analysis: SiO_2 vs. K_2O, Na_2O,
623 CaO_2. Red circles, Calderon Unit I; black squares, Mtn. Blanca; blue circles, P1600 deposit;
624 blue cross, El Boquerón; green squares, Los Gemelos; black stars, Abrunco PDC; white starts,
625 Abrunco (fall out).
626
627 Figure 6. a) Plot of the studied samples in the classification diagram for micas (Tieschendorf
628 1995). The micas were calculated on a 24-oxygen basis and 4 OH group following the method
629 described in Deer *et al.* (1992). All the samples from TPV are classified as Mg- Biotite using
630 Tieschendorf's (1995) classification. The estimate for Li_2O is based on Yavurt *et al.* (2001)
631 and the equation Li_2O wt.%=155*$(MgO)^{-3.1,}$ for SiO_2>34 wt%; and MgO>6wt%. b) Haker
632 diagrams of biotite analysis, SiO_2 vs. Fe_2O_3 and SiO_2 vs. TiO_2. Yellow triangles, Montaña
633 Majua; red cross, ICS deposit; blue circles, El Boquerón; green squares, Los Gemelos; red
634 circles, Calderón Unit I.

635

636 Figure 7. Plots of Fe and Ti oxide compositions: a) FeO-TiO_2-Fe_2O_3 diagram. b) Usp% vs.
637 TiO_2 diagram. Magnetite and ilmenite formulas were calculated on a 4-oxygen basis; the total
638 FeO was recalculated following Carmichael's (1967) method. Red circles, Calderon Unit I;
639 yellow squares, Mtn. Majua; blue cross, El Boquerón; green squares, Los Gemelos; black
640 stars, Abrunco PDC; white starts, Abrunco (fall out).

641

642 Figure 8: Total alkalis-silica classification diagram (le Bas *et al.* 1986). Diagrams include
643 some data from Ablay *et al.* (1998) for comparison.

644

645 Figure 9: Variation of selected major oxides vs. MgO (wt%) for TPV pumice deposits. Three
646 analyses from Montaña Blanca and Montaña Majua by Ablay *et al.* (1998) have been
647 included.

648

649 Figure 10: Variation diagrams of selected trace elements vs. MgO and Zr (wt%) for TPV
650 pumice deposits. Red full circles, Calderon Unit I; red empty circles, Calderon Unit III; black
651 square, Montaña Blanca; blue circle, P1600 deposit; brown circle, Roques Blancos; yellow
652 triangles, Montaña Majua; green squares, Los Gemelos; red cross, ICS deposit; blue cross, El
653 Boquerón; red triangles, Abejera deposit; green cross, Pico Cabras; black stars, Abrunco PDC;
654 white starts, Abrunco (fall out).

655

656 Figure 11: Multi-element variation diagram for the pumice deposits in the TPV complex,
657 normalized to chondrite values as per Thompson *et al.* 1982. a) Analysis of all the pumice
658 deposits; b) Abrunco (black-and-white star), ICS (red cross), Majua (yellow triangles); c)

659 Montaña Blanca (black square), El Boquerón (blue cross), Pico Cabras (green cross), Los
660 Gemelos (green square), P1600 (blue sphere), Roques Blancos (brown sphere), Abejera (red
661 triangles) and Calderón Unit I (orange sphere).
662
663 Figure 12: Multi-element variation diagram for the pumice deposits of the TPV complex,
664 normalized to primitive mantle values as per McDonough and Sun (1969). a) Analysis of all
665 the pumice deposits; b) Abrunco (black-and-white star), ICS (red cross), Majua (yellow
666 triangles); c) Montaña Blanca (black square), El Boquerón (blue cross), Pico Cabras (green
667 cross), Los Gemelos (green square), P1600 (blue sphere), Roques Blancos (brown sphere),
668 Abejera (red triangles) and Calderón Unit I (red sphere).
669
670
671
672 **Table captions**
673 **Table 1.** Geochronological data from Carracedo *et al.* (2003, 2007) and García *et al.* (2012).
674 The deposits studied in this paper are shown in grey. [(a)] Dating from the outcrop inside the
675 caldera of unknown origin. [(b)] Dense Rock Equivalent.
676
677 **Table 2.** Summary of the phenocryst characteristics in all the pumice deposits studied. [(a)]
678 Abbreviations for vesicle shapes: (R) rounded, (E) elongated, (A) amoeboid.
679
680 **Table 3.** Whole rock analyses of pumice deposits in Teide - Pico Viejo volcanic complex.
681
682

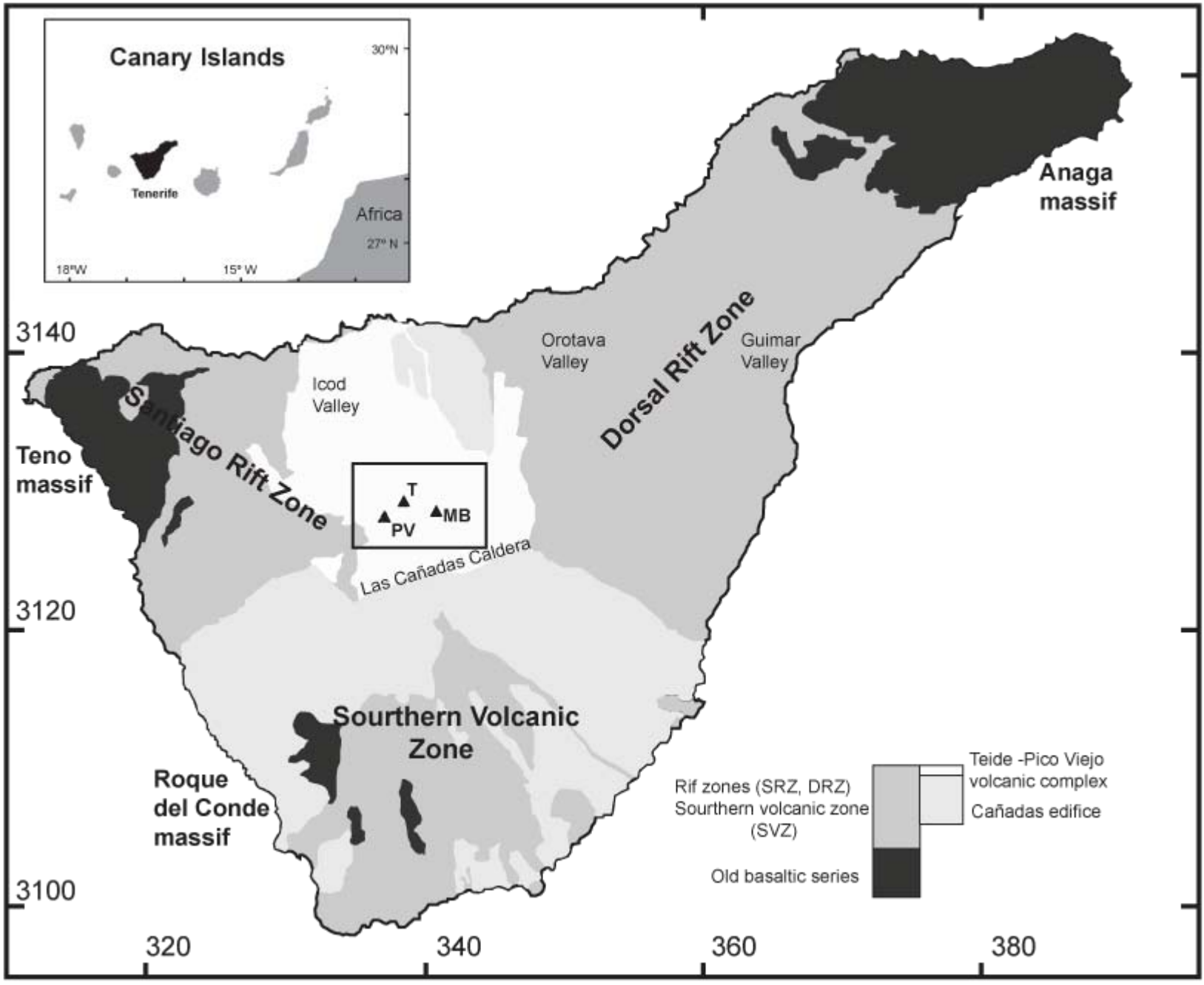
Canary Islands
30°N
Tenerife
Africa
27° N
18°W
15° W
3140
3120
3100
320
340
360
380
Anaga massif
Dorsal Rift Zone
Orotava Valley
Guimar Valley
Icod Valley
Santiago Rift Zone
Teno massif
T
PV
MB
Las Cañadas Caldera
Sourthern Volcanic Zone
Roque del Conde massif
Rif zones (SRZ, DRZ)
Sourthern volcanic zone (SVZ)
Old basaltic series
Teide -Pico Viejo volcanic complex
Cañadas edifice

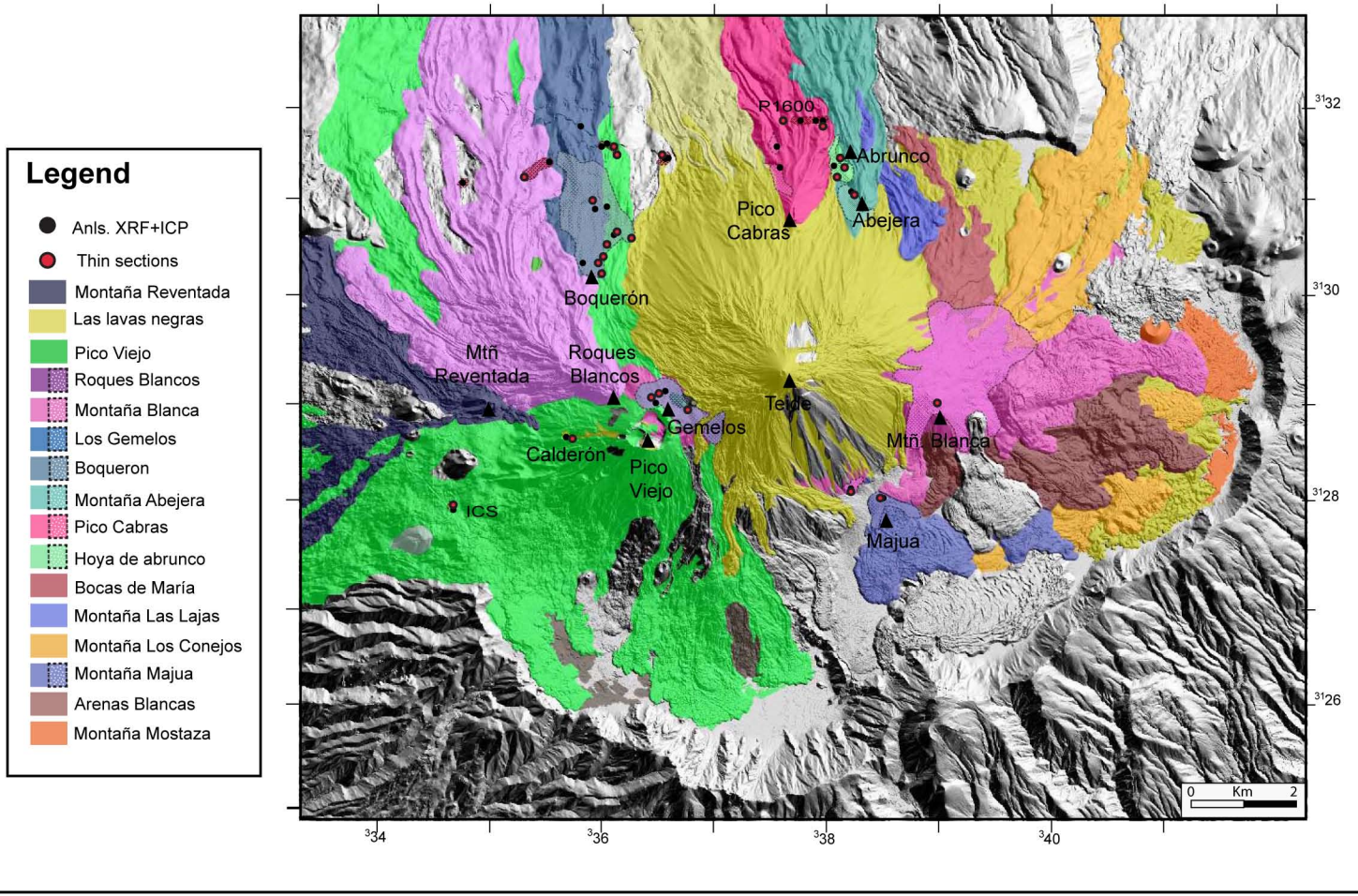
Legend
Anls. XRF+ICP
Thin sections
Montaña Reventada
Las lavas negras
Pico Viejo
Roques Blancos
Montaña Blanca
Los Gemelos
Boqueron
Montaña Abejera
Pico Cabras
Hoya de abrunco
Bocas de María
Montaña Las Lajas
Montaña Los Conejos
Montaña Majua
Arenas Blancas
Montaña Mostaza
P1600
Abrunco
Pico Cabras
Abejera
Boquerón
Mtñ Reventada
Roques Blancos
Teide
Gemelos
Calderón
Pico Viejo
ICS
Mtñ. Blanca
Majua
0 Km 2
3132
3130
3128
3126
334
336
338
340

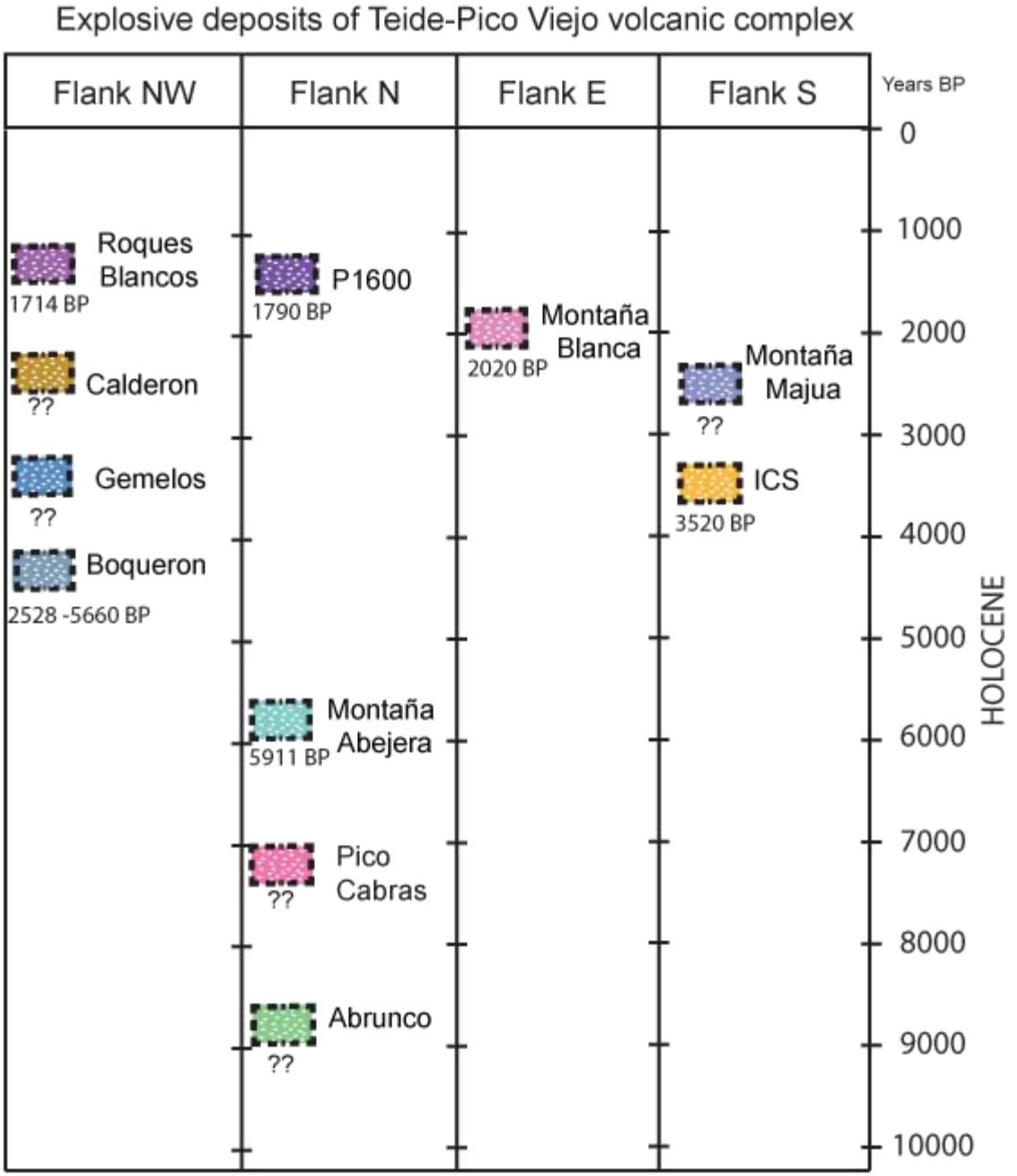
Explosive deposits of Teide-Pico Viejo volcanic complex
Flank NW
Flank N
Flank E
Flank S
Years BP
0
1000
2000
3000
4000
5000
6000
7000
8000
9000
10000
HOLOCENE
Roques Blancos
1714 BP
Calderon
??
Gemelos
??
Boqueron
2528 -5660 BP
P1600
1790 BP
Montaña Blanca
2020 BP
Montaña Majua
??
ICS
3520 BP
Montaña Abejera
5911 BP
Pico Cabras
??
Abrunco
??

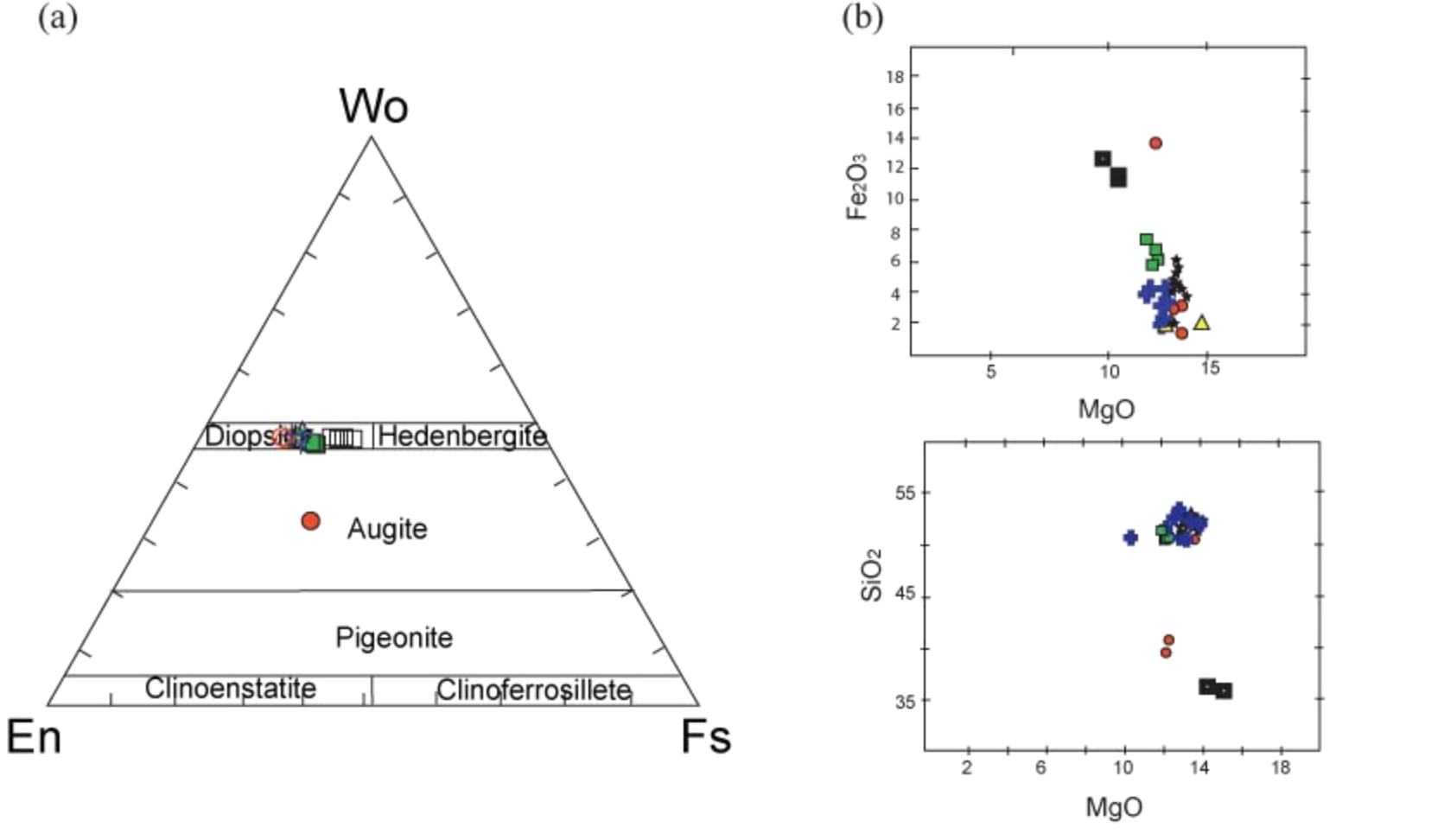
(a)
Wo
Diopside
Hedenbergite
Augite
Pigeonite
Clinoenstatite
Clinoferrosillete
En
Fs
(b)
Fe2O3
MgO
SiO2
MgO

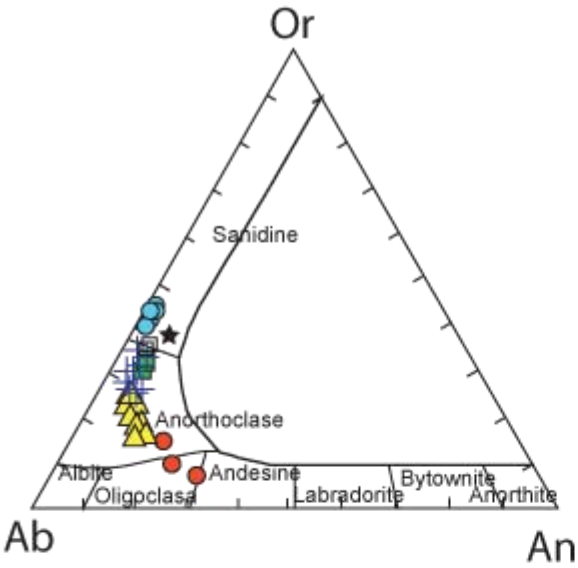
Or
Sanidine
Anorthoclase
Albite
Oligoclase
Andesine
Labradorite
Bytownite
Anorthite
Ab
An

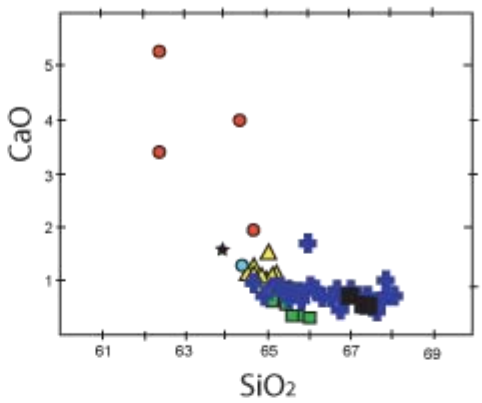
CaO
SiO2

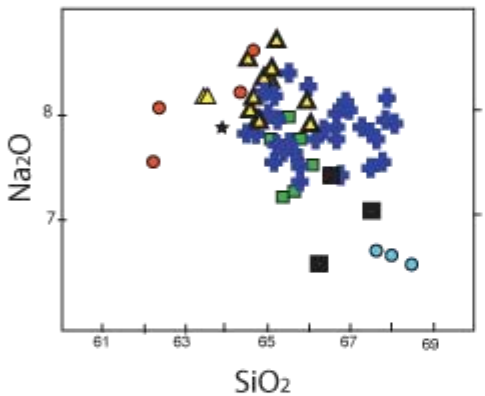
Na2O
SiO2

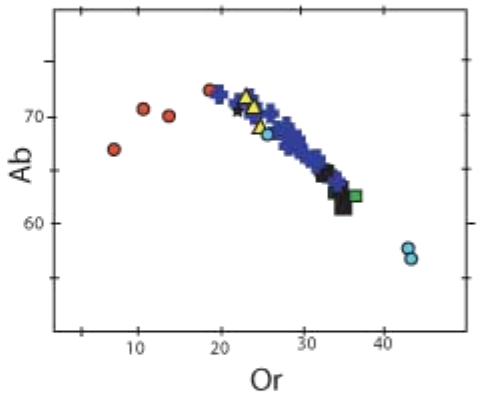
Ab
Or

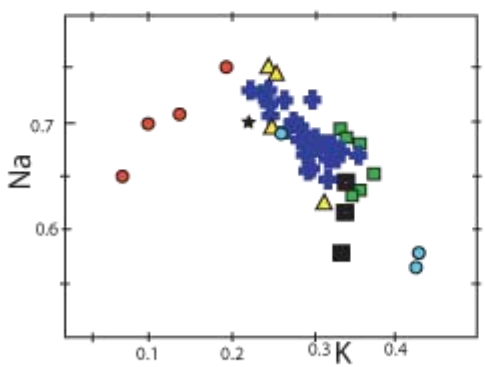
Na
K

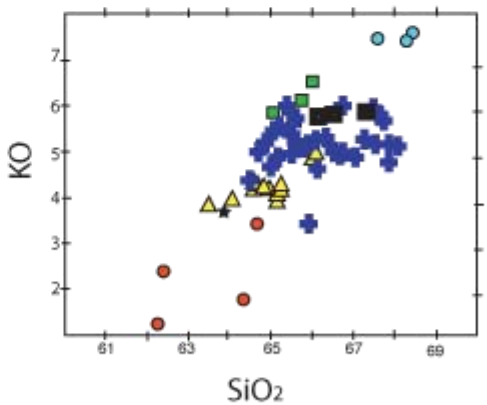
KO
SiO2

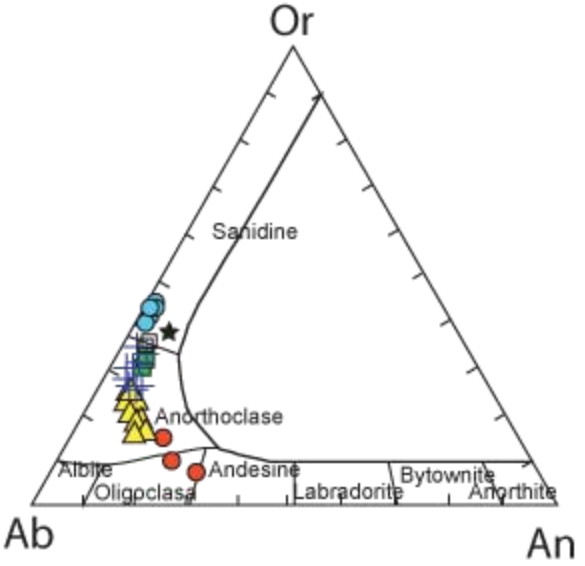
Or
Sanidine
Anorthoclase
Albite
Oligoclase
Andesine
Labradorite
Bytownite
Anorthite
Ab
An

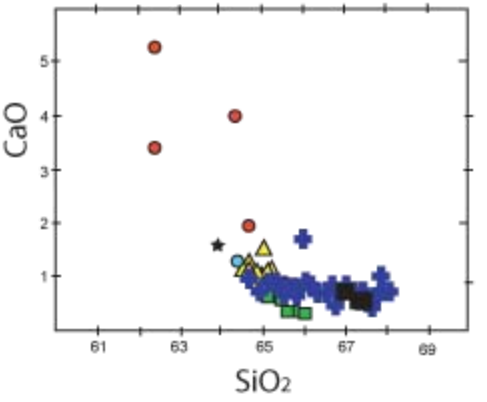
CaO
SiO2

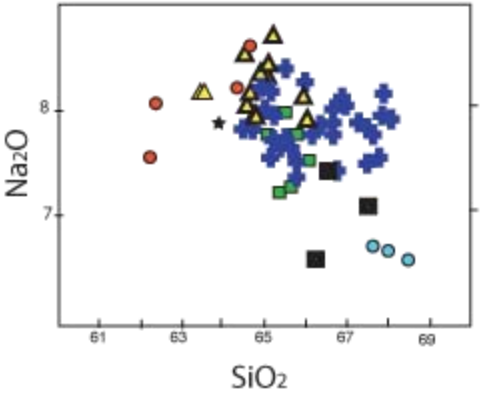
Na2O
SiO2

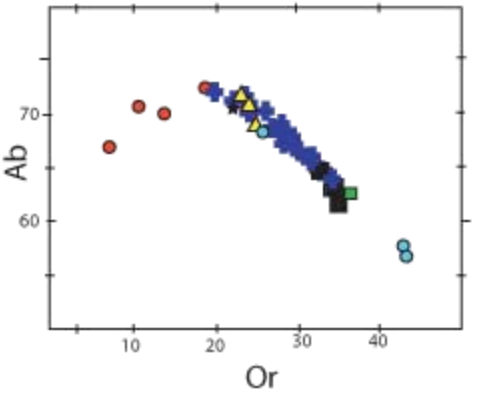
Ab
Or

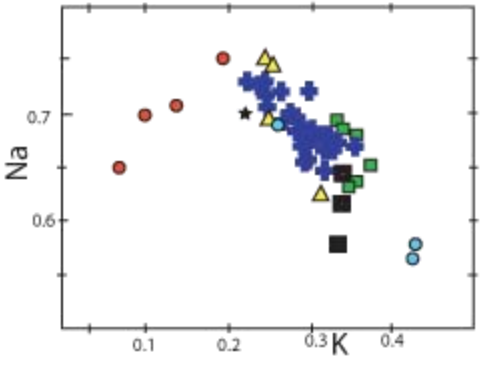
Na
K

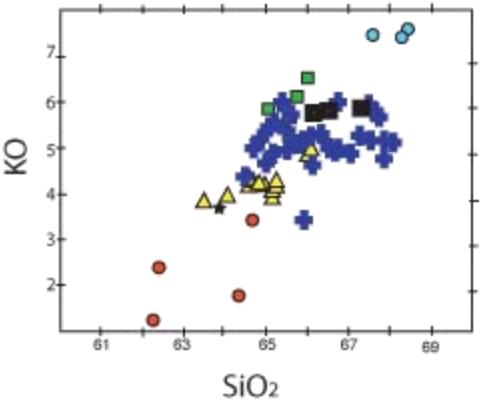
KO
SiO2

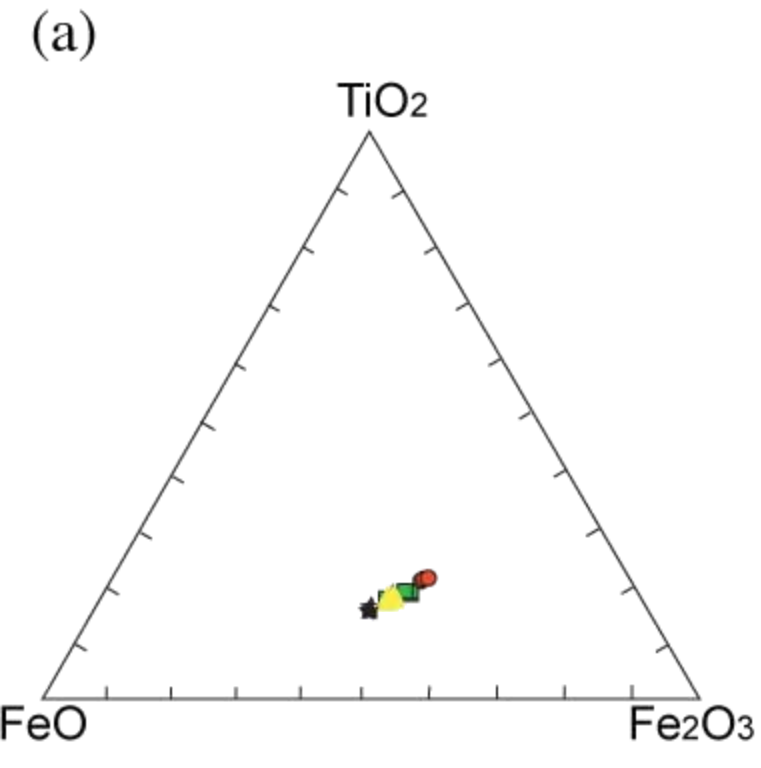
(a)
TiO2
FeO
Fe2O3

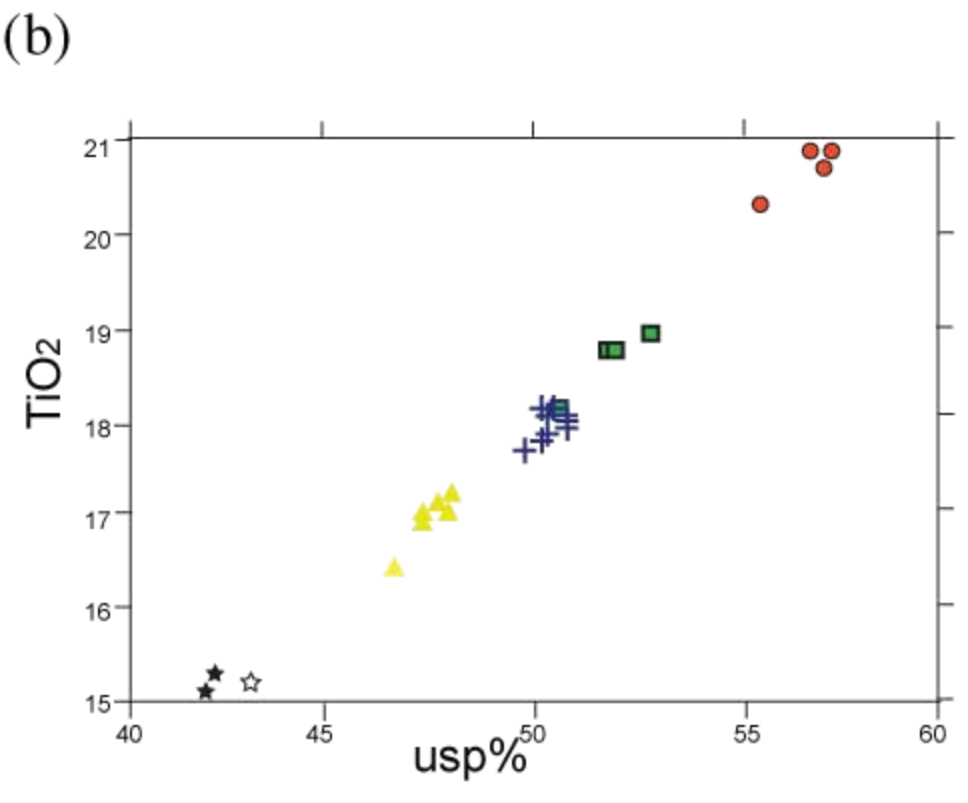
(b)
TiO2
21
20
19
18
17
16
15
40
45
50
55
60
usp%

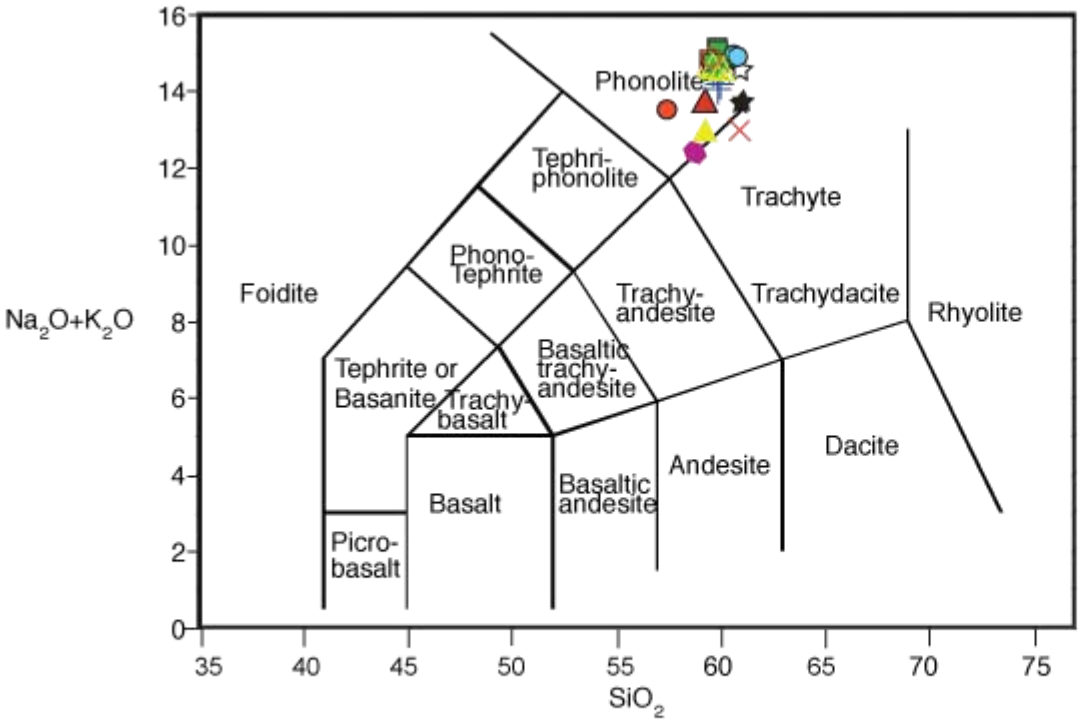

- Montaña Reventada (Wiesmaier et al. 2011)
- Calderon Unit I
- Calderon Unit III
- Mtn. Blanca
- Mtn.Blanca (Ablay et al. 1998)
- P1600
- Roques Blancos
- Mtn. Majua
- Mtn. Majua (Ablay et al. 1998)
- Gemelos
- ICS
- Boqueron
- Abejera
- Pico Cabras
- Abrunco PDC
- Abrunco (Fall out)

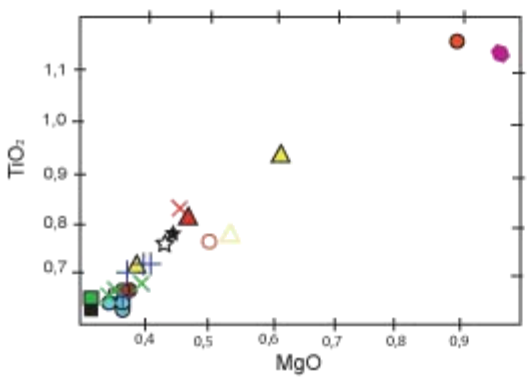
TiO2
1,1
1,0
0,9
0,8
0,7
0,4
0,5
0,6
0,7
0,8
0,9
MgO

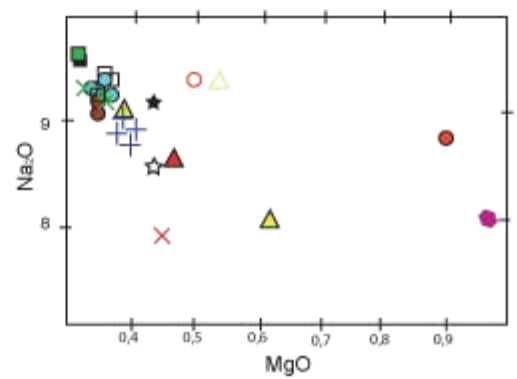
Na2O
9
8
0,4
0,5
0,6
0,7
0,8
0,9
MgO

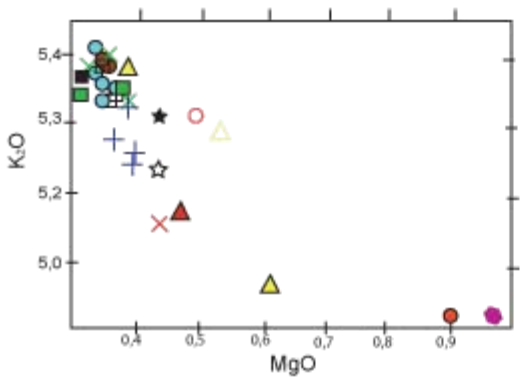
K2O
5,4
5,3
5,2
5,0
0,4
0,5
0,6
0,7
0,8
0,9
MgO

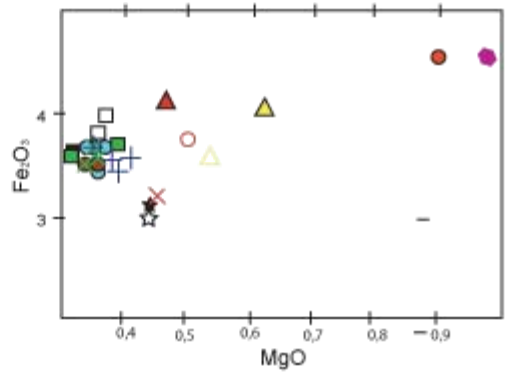
Fe2O3
4
3
0,4
0,5
0,6
0,7
0,8
0,9
MgO

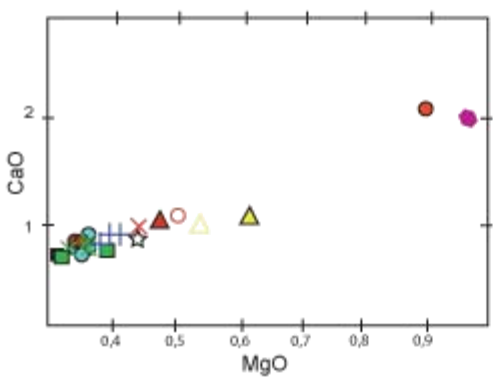
CaO
2
1
0,4
0,5
0,6
0,7
0,8
0,9
MgO

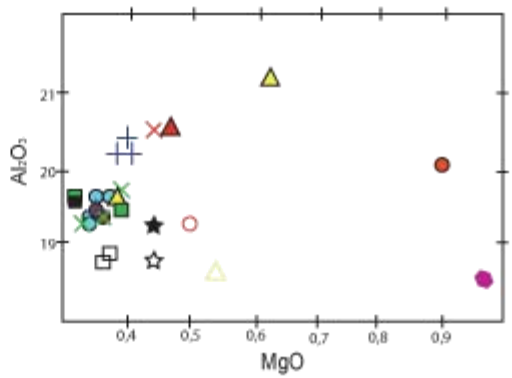
Al2O3
21
20
19
0,4
0,5
0,6
0,7
0,8
0,9
MgO

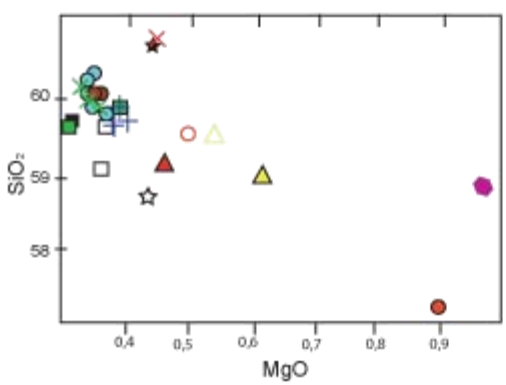
SiO2
60
59
58
0,4
0,5
0,6
0,7
0,8
0,9
MgO

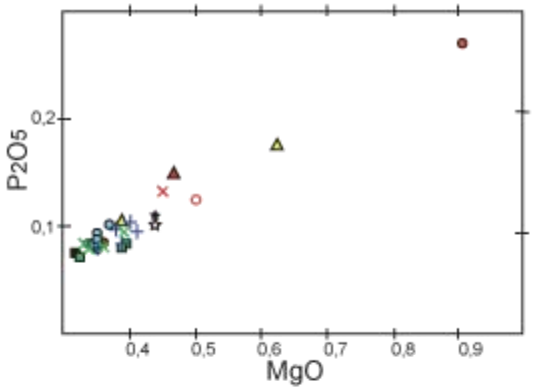
P2O5
0,2
0,1
0,4
0,5
0,6
0,7
0,8
0,9
MgO

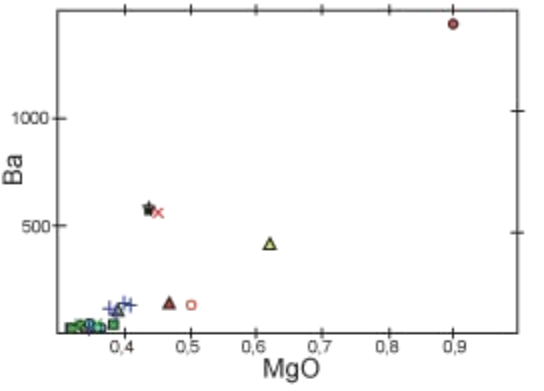
Ba
1000
500
0,4
0,5
0,6
0,7
0,8
0,9
MgO

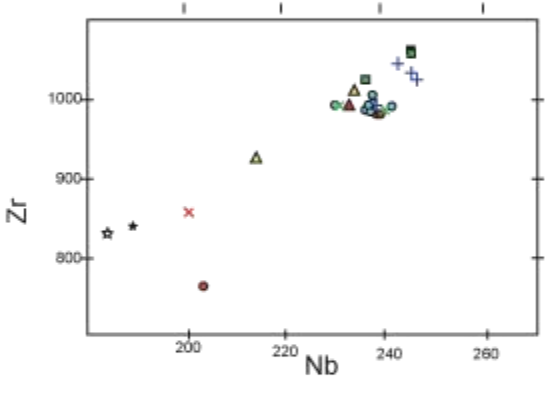
Zr
1000
900
800
200
220
240
260
Nb

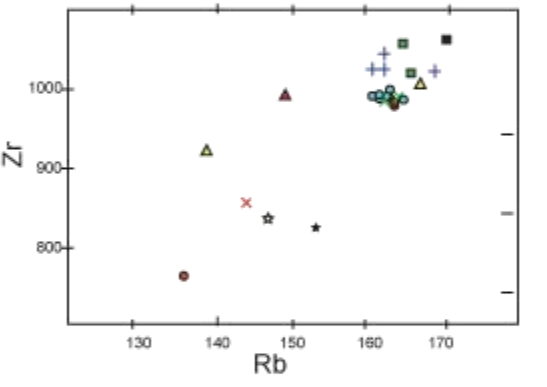
Zr
1000
900
800
130
140
150
160
170
Rb

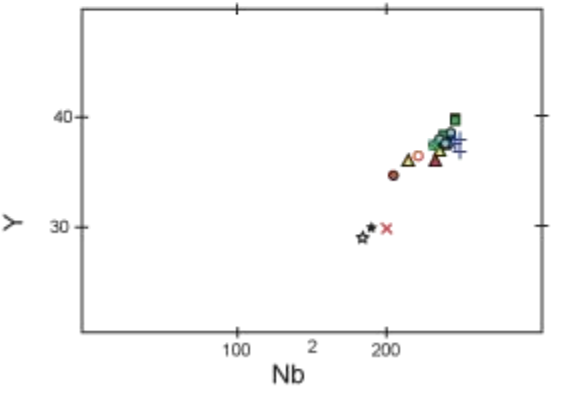
Y
40
30
100
2
200
Nb

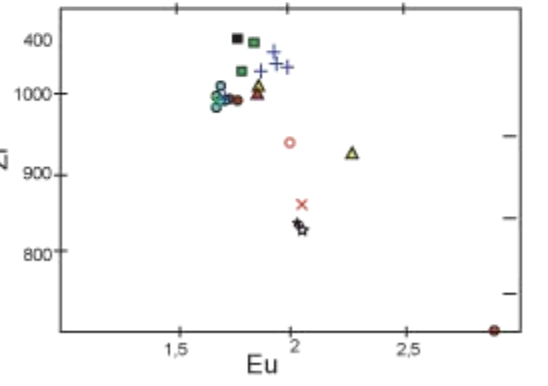
Zr
400
1000
900
800
1,5
2
2,5
Eu

(a)

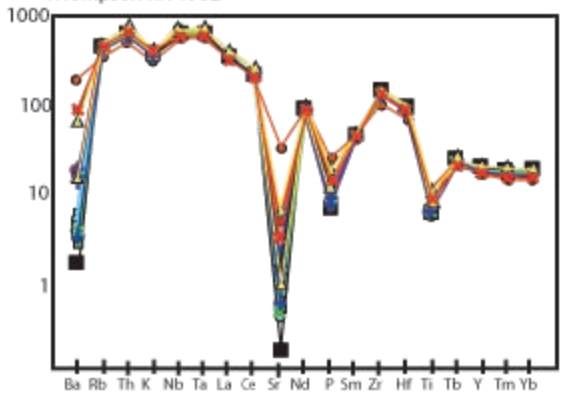
THompson RN 1982
1000
100
10
1
Ba Rb Th K Nb Ta La Ce Sr Nd P Sm Zr Hf Ti Tb Y Tm Yb

(b)

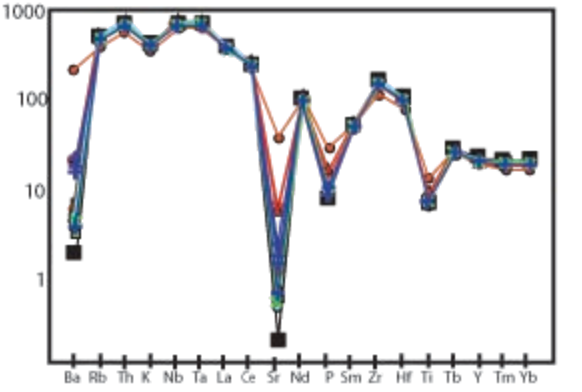
THompson RN 1982
1000
100
10
1
Ba Rb Th K Nb Ta La Ce Sr Nd P Sm Zr Hf Ti Tb Y Tm Yb

(c)

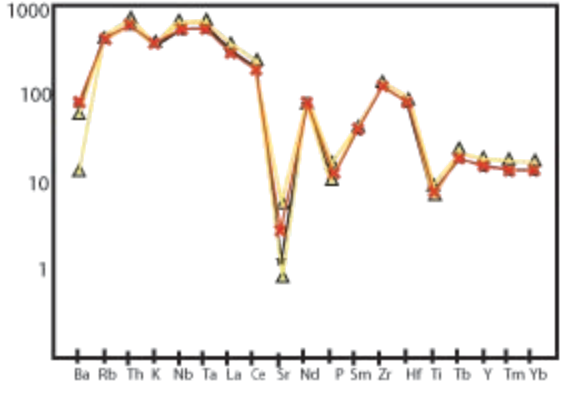
THompson RN 1982
1000
100
10
1
Ba Rb Th K Nb Ta La Ce Sr Nd P Sm Zr Hf Ti Tb Y Tm Yb

(a)

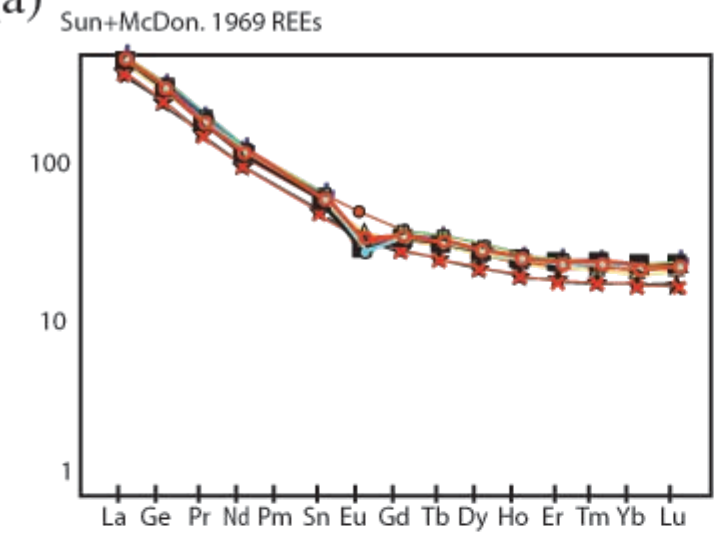
Sun+McDon. 1969 REEs
100
10
1
La Ge Pr Nd Pm Sn Eu Gd Tb Dy Ho Er Tm Yb Lu

(b)

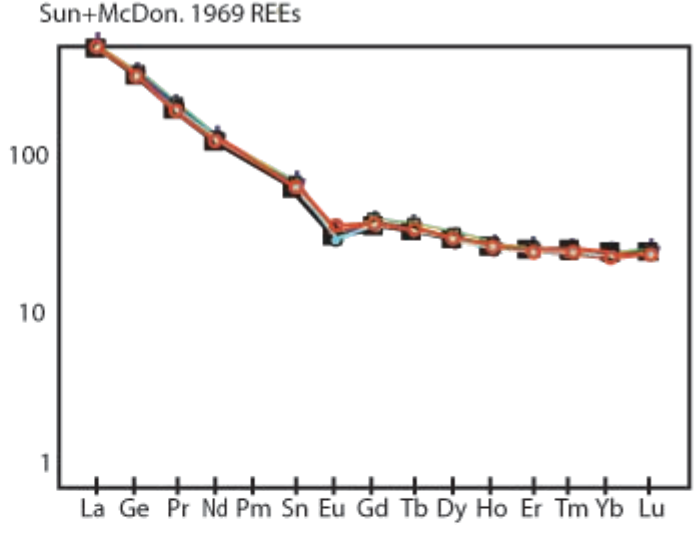
Sun+McDon. 1969 REEs
100
10
1
La Ge Pr Nd Pm Sn Eu Gd Tb Dy Ho Er Tm Yb Lu

(c)

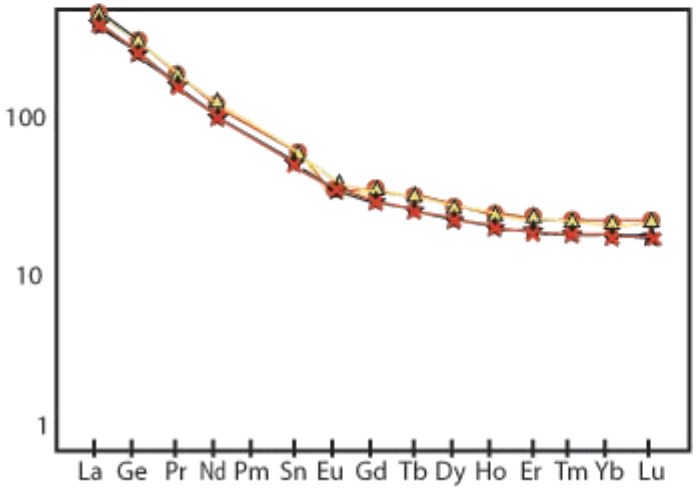
Sun+McDon. 1969 REEs
100
10
1
La Ge Pr Nd Pm Sn Eu Gd Tb Dy Ho Er Tm Yb Lu

Eruption Name	Years BP	Total Erupted volume (DRE)[(b)] in m^3	Total Erupted Mass, (kg)	Magnitude Scale
Montaña Reventada	895	138,194,471.1	3,45486E+11	4,54
Roques Blancos	1714-1790	833,890,093.4	2,08473E+12	5,32
Montaña Blanca	2020	107382578,7	2,68456E+11	4,43
ICS [(a)]	***3520***	Unknown	Unknown	Unknown
El Boqueron	2528-5660	44,283,790.64	1,10709E+11	4,04
Abejera Baja	5486	285,594,326	7,13986E+11	4,85
Abejera Alta	5911	361,123,567.2	9.02809E+11	4,96
Pico Cabras	5911-7900	285594326	7,13986E+11	4,85
Abrunco	<10000	2,086,022.525	5,215,056,313	2,72

UNITS		PHENOCRYSTAL %	FELDESPARS		BIOTITE		CLINOPYROXEN		Fe-Ti OXIDES		MICROLITES (<100µm)	VESICULARITY		
			%	Cm (max)	%	Cm (max)	%	Cm (max)	%	Cm (max)		Size (mm)	%	Shape[a]
ICS		0.5-0.1	12	500µm	80	300µm	-	-	8	200µm	**Bt, Kfsp**	**3**	**45**	**R, E**
Mtñ. Blanca		0.5-0.1	80	2mm	-	-	20	600µm	-	-	**Kfsp, cpx**	**5**	**48**	**R, E**
Mtñ. Majua		1.0-3.0	65	2mm	25	<1mm	7	200µm	3	500µm	**Kfsp, cpx**	**5**	**47**	**E**
Gemelos		1.0-3.0	85	2mm	5	200µm	5	600µm	5	500µm	**Kfsp, bt**	**500µm**	**35**	**R**
Boqueron		3.0	70	1mm	15	200µm	10	200µm	5	400µm	**Kfsp, bt**	**5**	**45**	**E,A,R**
Hoya Abrunco	**Fall Out**	0.5-0.1	-	-	50	2mm	40	1mm	10	200µm	**Kfsp, bt**	**6**	**52**	**E,A,R**
	PDC	0.5-0.1	5	200µm	10	200µm	80	500µm	5	200µm	**Kfsp, bt, cpx**	**3**	**54**	**E,A,R**
Pico Cabras		<0.5	-	-	-	-	-	-	-	-	**Kfsp, bt**	**<100/1**	**53**	**R, E**
P1600		<0.5	-	-	-	-	-	-	-	-	**-**	**>250/500**	**52**	**R, E**
Roques Blancos		<0.5	100	1mm	-	-	-	-	-	-	**-**	**>250/500**	**52**	**R, E**
Calderon	**Unit I**	1.0-3.0	50	<2mm	-	-	40	1mm	10		**Kfsp, cpx**	**5**	**48**	**R**
	Unit III	<0.5	-	-	-	-	80	1mm	20	<200µm		**200µm**	**42**	**R**

Table 3: Selected whole-rock analyses fro representantive pumice deposits.

Unit	Boqueron					Pico Cabras			Calderon	
Sample	P.U.L	B.H11	B.RT	B.RTJ1	B.RTJ2	PC.H4	P.CABRAS.C	PC-1	CALD.N.1	CALD.N.3
Locate (Lat/long)	335411E 3132795N	335636E 3131111N	335487E 3131660N	335290E 3131613N	335290E 3131613N	338793E 3132399N	339622E 3133287N	338715E 3132788N	334745E 3127300N	334745E 3127300N
SiO2	57.44	57.31	58.44	56.84	57.01	57.92	58.91	58.63	56.25	58.89
TiO2	0.687	0.679	0.628	0.696	0.694	0.662	0.633	0.628	1.129	0.760
Al2O3	19.43	19.44	18.90	19.43	19.28	19.10	18.89	18.90	19.63	19.06
FeO*	3.40	3.35	3.51	3.41	3.41	3.58	3.50	3.49	4.52	3.68
MnO	0.196	0.189	0.195	0.185	0.181	0.199	0.197	0.198	0.177	0.189
MgO	0.37	0.38	0.34	0.38	0.40	0.38	0.32	0.35	0.89	0.49
CaO	0.80	0.78	0.75	0.83	0.84	0.77	0.74	0.74	2.05	1.03
Na2O	8.53	8.76	9.07	8.34	8.53	8.83	9.18	9.26	8.66	9.34
K2O	5.14	5.23	5.42	5.02	5.08	5.30	5.45	5.46	4.76	5.36
P2O5	0.097	0.083	0.081	0.100	0.093	0.094	0.084	0.083	0.267	0.125
Sum	96.09	96.20	97.33	95.23	95.52	96.82	97.92	97.74	98.31	98.92
LOI (%)	3.79	2.92	2.35	4.11	3.64	2.21	1.94	1.63	0.99	1.24
Ni	3	2	3	3	2	3	3	3	5	3
Cr	1	2	2	3	3	4	2	4	0	1
Sc	1	0	1	1	2	1	2	2	1	2
V	15	14	8	14	17	13	7	9	18	16
Ba	113	94	24	135	129	47	26	29	1393	134
Rb	170	173	170	165	169	166	171	168	134	163
Sr	16	15	7	19	26	12	7	5	426	77
Zr	1047	1024	989	1031	1025	985	992	991	759	934
Y	37	37	38	37	37	37	38	38	35	36
Nb	236	231	225	234	232	225	226	226	199	217
Ga	28	30	29	28	29	29	29	28	27	28
Cu	2	1	1	2	1	1	2	2	3	3
Zn	118	121	125	114	114	127	126	126	114	123
Pb	21	21	20	20	20	20	20	20	20	18
La	112	106	112	108	108	110	108	110	105	108
Ce	191	193	186	192	191	188	187	189	181	186
Th	31	30	28	31	31	28	28	29	25	26
Nd	58	55	56	56	56	55	54	57	58	54
U	8	8	8	8	7	6	8	6	6	8

Table 3: continued

Unit	Abejera	P.1600								
Sample	M.A.P	P1600.ANL1	P.1600ANL2	P.1600ANL3	P.1600ANL4	P.1600ANL5	ROQ.BLAN.6	ROQ.BLAN.7	ROQ.BLAN.8	P1600.32
Locate (Lat/long)	340144E 3131919N	339467E 3133283N	339619E 3133302N	339181E 3133290N	336669E 3132612N	335519E 3132838N	334423E 3132503N	332773E 3132085N	335025E 3133164N	336600E 3132532N
SiO2	56.72	58.37	58.51	58.31	57.79	58.35	58.11	57.97	57.99	58.64
TiO2	0.776	0.635	0.634	0.635	0.647	0.625	0.632	0.627	0.638	0.628
Al2O3	19.67	18.86	18.84	18.95	19.01	18.73	19.00	18.72	19.02	18.81
FeO*	3.92	3.53	3.48	3.52	3.53	3.37	3.48	3.55	3.57	3.45
MnO	0.193	0.197	0.197	0.197	0.198	0.196	0.193	0.195	0.197	0.197
MgO	0.45	0.35	0.34	0.34	0.35	0.34	0.34	0.33	0.34	0.33
CaO	0.94	0.75	0.76	0.74	0.77	0.74	0.78	0.76	0.74	0.74
Na2O	8.23	9.12	9.15	9.12	8.90	8.97	8.94	8.97	8.80	9.09
K2O	4.93	5.42	5.44	5.42	5.31	5.40	5.30	5.35	5.33	5.47
P2O5	0.142	0.087	0.082	0.084	0.100	0.083	0.079	0.085	0.092	0.083
Sum	95.96	97.31	97.43	97.33	96.61	96.82	96.87	96.55	96.72	97.44
LOI (%)	3.97	1.94	1.88	1.88	2.63	2.45	2.40	2.29	2.93	2.14
Ni	3	3	3	3	3	3	2	4	3	3
Cr	4	3	2	2	2	1	2	1	2	2
Sc	2	1	1	1	1	1	0	1	1	1
V	18	11	9	9	9	12	9	10	11	9
Ba	134	24	24	24	37	28	26	24	40	26
Rb	155	169	171	169	165	168	167	169	169	171
Sr	61	6	8	6	13	7	7	7	8	4
Zr	991	990	986	989	991	979	991	984	1001	991
Y	35	38	37	37	38	37	38	37	36	37
Nb	226	226	225	225	225	223	226	225	226	226
Ga	28	28	29	30	29	29	30	29	30	30
Cu	3	2	1	1	2	1	5	1	2	2
Zn	122	125	124	122	125	124	123	123	124	129
Pb	20	20	19	20	21	20	19	21	20	20
La	105	110	105	110	111	105	111	105	106	111
Ce	184	191	190	187	191	191	190	188	186	190
Th	29	28	28	29	29	28	28	28	29	28
Nd	55	58	55	54	57	56	58	57	55	56
U	7	6	10	7	8	7	6	7	9	7

Table 3: continued

Unit	Montaña Blanca	ICS	Gemelos		Majua		Abrunco	
Sample	MTNBLANCA	ICS	Gemelos2	GEMELOS3	M.M.1	M.M.2	PDC	FALL OUT
Locate (Lat/long)	341702E 3128019N	332586E 3125928N	336413E 3127941N	336595E 3128168N	340736E 3126130N	340144E 3126170N	339798E 3132411N	334002E 3132228N
SiO2	58.35	57.36	58.95	58.82	55.69	58.45	59.68	58.80
TiO2	0.623	0.780	0.660	0.644	0.883	0.692	0.767	0.764
Al2O3	19.19	19.39	19.17	19.42	20.01	19.13	18.95	18.82
FeO*	3.53	3.07	3.63	3.58	3.84	3.28	3.06	2.98
MnO	0.200	0.166	0.190	0.201	0.191	0.191	0.167	0.167
MgO	0.31	0.43	0.38	0.32	0.58	0.38	0.44	0.44
CaO	0.71	0.91	0.76	0.72	0.96	0.79	0.86	0.86
Na2O	9.41	7.42	9.30	9.49	7.54	8.81	9.05	8.55
K2O	5.41	4.84	5.40	5.42	4.65	5.41	5.32	5.26
P2O5	0.072	0.128	0.081	0.076	0.168	0.105	0.108	0.104
Sum	97.79	94.48	98.54	98.67	94.52	97.22	98.39	96.74
LOI (%)	1.85	4.77	1.47	1.37	4.27	2.81	1.55	2.37
Ni	3	3	3	2	6	3	2	2
Cr	2	3	5	1	6	1	2	1
Sc	0	1	1	0	0	1	0	2
V	7	18	12	12	25	12	18	20
Ba	16	559	52	26	416	102	570	563
Rb	179	150	174	174	145	175	154	153
Sr	3	36	14	6	72	10	17	17
Zr	1065	858	1023	1059	922	1007	837	828
Y	39	30	39	40	36	37	30	29
Nb	242	190	234	242	207	228	185	184
Ga	31	26	29	30	27	29	27	26
Cu	1	0	3	2	5	2	1	0
Zn	131	99	127	130	119	122	107	106
Pb	22	17	21	23	19	20	16	17
La	112	97	110	118	106	107	94	94
Ce	198	162	193	199	189	188	163	163
Th	32	25	30	32	28	29	25	25
Nd	60	46	57	60	57	57	48	49
U	8	7	8	10	8	8	7	7

Appendix 2.1 Submit letter:

Proof of delivery of the paper: "*Stratigraphic correlation of Holocene phonolitic explosive episodes of the Teide-Pico Viejo Complex, Tenerife)"* in Journal of the Geological Society.

Home

Manuscript #	2013-086
Current Revision #	0
Submission Date	16th Jul 13
Current Stage	Initial QC Started
Title	Stratigraphic correlation of Holocene phonolitic explosive episodes of the Teide-Pico Viejo Complex, Tenerife.
Running Title	Explosive episodes of Teide-Pico Viejo.
Manuscript Type	Research Article
Special Section	N/A
Corresponding Author	Olaya García (Grupo de Volcanología de Barcelona)
Contributing Authors	Silvina Guzmán , Joan Martí
Abstract	Teide and Pico Viejo are twin stratovolcanoes (TPV) that form one of the largest alkaline volcanic complexes in the world. They began forming inside the caldera of Las Cañadas about 200 ka ago and are largely made up of an accumulation of mafic, intermediate and more recent felsic products that form lava flows. However, a number of significant pyroclastic deposits dating from the Holocene are also present. In order to quantify the explosive contribution to the construction of TPV we re-examined its stratigraphy and identified several Holocene phonolitic explosive episodes ranging from Strombolian to sub-Plinian that are represented by fallout and pyroclastic density current deposits. Although some of the pumice deposits have been related to known vent sites, a few are still of unknown origin. The use of field criteria as well as geochemical and mineralogical analysis help provide reliable criteria for robust correlations and for establishing the relative stratigraphy of the deposits. The presence of these pyroclastic deposits in the recent history of the TPV complex suggests that these stratovolcanoes are entering into a more explosive stage that represents a non-avoidable hazard for the island of Tenerife.
Open Access	Yes, I want to make my article fully Open Access

Manuscript Items

1. Author Cover Letter PDF (34KB) Source File (DOC) 69KB
2. Merged File containing manuscript text, 12 Figure files and 3 Table files. PDF (15449KB)
   a. Article File PDF (190KB) Source File (DOC) 102KB
   b. Figure 1 PDF (349KB) Source File (TIF) 347KB
      Figure
   c. Figure 2 PDF (11252KB) Source File (TIF) 7882KB
      Figure
   d. Figure 3 PDF (265KB) Source File (TIF) 301KB
      Figure
   e. Figure 4 PDF (191KB) Source File (TIF) 195KB
      Figure
   f. Figure 5 PDF (262KB) Source File (TIF) 268KB
      Figure
   g. Figure 6 PDF (258KB) Source File (TIF) 258KB
      Figure
   h. Figure 7 PDF (148KB) Source File (TIF) 164KB
      Figure
   i. Figure 8 PDF (278KB) Source File (TIF) 288KB
      Figure
   j. Figure 9 PDF (238KB) Source File (TIF) 259KB
      Figure
   k. Figure 10 PDF (177KB) Source File (TIF) 203KB
      Figure
   l. Figure 11 PDF (1190KB) Source File (TIF) 812KB
      Figure
   m. Figure 12 PDF (1171KB) Source File (TIF) 826KB
      Figure
   n. Table 1 PDF (27KB) Source File (DOC) 39KB
      Geochronological data from Carracedo et al. (2003, 2007) and García et al. (2012). The deposits studied in this paper are shown in grey. (a) Dating from the outcrop inside the caldera of unknown origin. (b) Dense Rock Equivalent.
   o. Table 2 PDF (90KB) Source File (DOC) 81KB
      Summary of the phenocryst characteristics in all the pumice deposits studied. (a) Abbreviations for vesicle shapes: (R) rounded, (E) elongated, (A) amoeboid.
   p. Table 3 PDF (91KB) Source File (XLS) 56KB
      Whole rock analyses of pumice deposits in Teide - Pico Viejo volcanic complex.

Manuscript Tasks

Send Manuscript Correspondence
Check Status

Appendix 3. Pyroclastic density currents from Teide-Pico Viejo (Tenerife, Canary Islands): implications on hazard assessment.

Terra Nova

doi: 10.1111/j.1365-3121.2011.01002.x

Pyroclastic density currents from Teide–Pico Viejo (Tenerife, Canary Islands): implications for hazard assessment

Olaya García,[1] Joan Martí,[2] Gerardo Aguirre,[3] Adelina Geyer[4] and Ilazkiñe Iribarren[1]

[1]*Centro Geofísico de Canarias del I.G.N. C/La Marina 20, 2º, 38001 S/C de Tenerife, Spain;* [2]*Instituto de Ciencias de la Tierra 'Jaume Almera', CSIC, LLuis Solé Sabaris s/n, 08028 Barcelona, Spain;* [3]*Centro de Geociencias, Campus UNAM-Juriquilla, Querétaro, Querétaro CP 76230, México;* [4]*CIMNE, International Center for Numerical Methods in Engineering, Edifice C1, Campus Nord UPC, Gran Capità, s/n, 08034 Barcelona, Spain*

ABSTRACT

The Teide–Pico Viejo stratovolcanoes constitute one of the major potentially active volcanic complexes in Europe but have traditionally been considered to be non-explosive and not to represent a significant threat to the island of Tenerife. However, the reconstruction of their eruptive record is still far from complete, and better knowledge of their volcano-stratigraphy and physical volcanology is required to undertake a comprehensive hazard assessment of these volcanoes. We conducted a detailed field investigation of the northern side of Teide–Pico Viejo, a poorly known area, and identified several deposits of explosive eruptions of phonolitic magmas. Herein we report for the first time the presence of density current deposits, including ignimbrites and block and ash deposits, in the Holocene eruptive history of the Teide–Pico Viejo stratovolcanoes. We discuss the characteristics of these deposits, their eruption mechanisms and their implications for hazard assessment at Teide–Pico Viejo.

Terra Nova, 23, 220–224, 2011

Introduction

Teide–Pico Viejo twin stratovolcanoes, Tenerife, form one of the largest active volcanic complexes in Europe. Their eruptive activity has traditionally been considered as effusive (Ablay and Martí, 2000; Carracedo *et al.,* 2007), with the only known exception being the 2-ka subplinian eruption of Montaña Blanca (Ablay *et al.,* 1995), and minor pyroclastic deposits of unknown origin. This has led workers to the assumption that volcanic hazard at Teide–Pico Viejo is mostly related to the emplacement of lava flows (Carracedo *et al.,* 2007), which according to their field and physical characteristics correspond to relatively slow-moving flows, with run-out distances up to 15 km. However, a recent revision of the past history of Teide–Pico Viejo (Martí *et al.,* 2008), reveals that explosive activity related to phonolitic magmas has been more significant than initially assumed, so that their potential for generating explosive eruptions in the future should not be neglected.

We have conducted a detailed field revision of the Teide–Pico Viejo products, focusing in particular on those derived from explosive eruptions of phonolitic magmas. We have concentrated our study mostly on the northern side of Teide–Pico Viejo, an inaccessible and relatively unexplored area which is poorly known compared to other sectors of these volcanoes.

We have been able to identify and document for the first time the presence of several pyroclastic density current (PDC) deposits associated with different explosive episodes of Teide–Pico Viejo. The PDC deposits include ignimbrites and block and ash deposits, which derived from markedly different eruption and emplacement mechanisms. We describe their field characteristics and discuss their origin and significance in the volcanological evolution of Teide–Pico Viejo. Finally, we evaluate the importance of the presence of these deposits in terms of hazard assessment at Teide–Pico Viejo.

Correspondence: Dr Joan Marti, Institute of Earth Sciences 'Jaume Almera', CSIC, LLuis Sole Sabaris s/n, Barcelona 08028, Spain. Tel.: +34 93 409 54 10; fax: +34 93 411 00 12; e-mail: joan.marti@ija.csic.es

Volcanic evolution of Teide–Pico Viejo

Teide–Pico Viejo stratovolcanoes started to grow *c.* 180–190 ka ago within the Las Cañadas caldera (Fig. 1) (Ablay and Martí, 2000). This central volcanic complex originated from the interaction of two different magmatic systems that evolved simultaneously, giving rise to a complete series from basalt to phonolite (Ablay *et al.,* 1998; Martí *et al.,* 2008). The structure and volcanic stratigraphy of the Teide–Pico Viejo stratovolcanoes were characterized by Ablay and Martí (2000), based on a detailed field and petrological study. More recently, Carracedo *et al.* (2007) have provided the first group of isotopic ages from Teide–Pico Viejo products.

The eruptive history of the Teide–Pico Viejo comprises a main stage of eruption of mafic to intermediate lavas that form the core of the volcanoes and also infill most of the Las Cañadas depression and the adjacent La Orotava and Icod valleys (Fig. 1). About 35 ka ago phonolites became predominant at Teide–Pico Viejo. These felsic eruptions occurred from central and flank vents, range in volume from 0.01 to 1 km^3 (DRE), and have mostly generated thick lava flows and domes. Most of the phonolitic eruptions from Teide–Pico Viejo show signs of magma mixing, suggesting that they were triggered by intrusion of basaltic magmas into shallow phonolitic reservoirs (Martí *et al.,* 2008). In addition, basaltic eruptions have also occurred from the flanks or the central vents of the Teide–Pico Viejo stratovolcanoes alternating with phonolitic volcanism.

Pyroclastic density current deposits

Phonolitic pyroclastic deposits are present along the Icod Valley (Fig. 1)

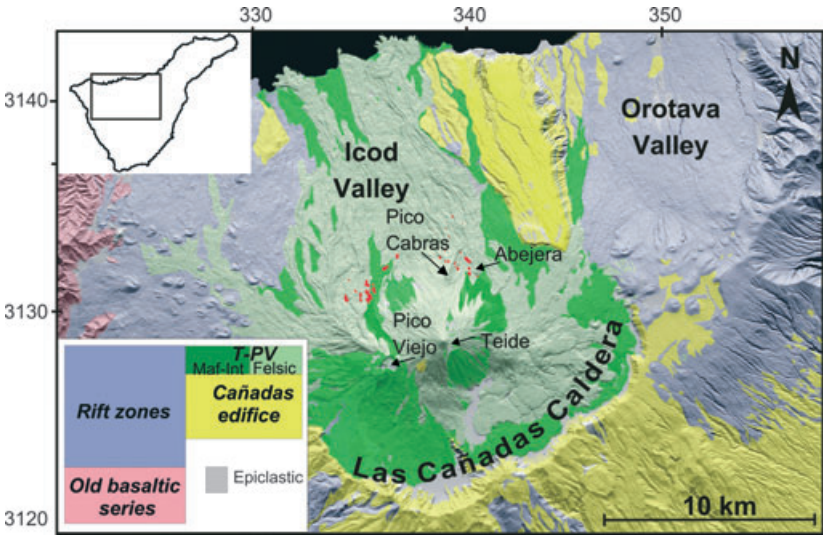

Fig. 1 Simplified geological map of Teide–Pico Viejo stratovolcanoes, based on IGME (2009) and Ablay and Martí (2000), and location of the main outcrops (in red) of phonolitic pyroclastic deposits identified in this study. Upper inset: Tenerife contour and studied area. Lower inset: general stratigraphy of Tenerife (see Martí *et al.* (2008) for more details).

from the highest slopes to the coast, while at the southern side of Teide these outcrops are less abundant. The stratigraphy of these eruptive products is not well established yet, and further work combining petrology, mineral chemistry, geochronology and stratigraphy is required to determine the exact position and distribution of each unit in the stratigraphic record and its significance in the evolution of these volcanoes. However, we have identified several different types of PDC deposits and of discontinuous coarse to fine grained, pumice fall deposits, which suggest the existence of explosive eruptions from Teide–Pico Viejo and different from the Montaña Blanca eruption. Phonolitic fallout deposits have been deeply eroded and show a variable degree of preservation depending on topography and burial by younger products. This makes it difficult to establish reliable stratigraphic correlations at present. In contrast, PDC deposits, despite having been deeply eroded too, have been partially preserved within gullies on the northern flank of Teide–Pico Viejo and show features that allow them to be identified and interpreted in terms of eruption dynamics and emplacement mechanisms. We have observed the presence of pumice-rich, ignimbrites and block and ash deposits which show very distinct lithological and sedimentological characteristics.

Pumice-rich ignimbrites

Comparisons between the relative stratigraphy and composition of the different deposits reveal that they represent the products of several explosive episodes that occurred during the recent (Holocene) history of Teide–Pico Viejo. The poor degree of preservation of most of these deposits, as well as the discontinuity of their outcrops makes it difficult to determine their exact stratigraphic position and extent. However, in some cases the preserved outcrops allow to identify the main characteristics of the deposits and to infer their eruption and emplacement mechanisms

This is the case, for instance, of the Abrunco ignimbrite, a non-welded, pumice-rich, pyroclastic flow deposit that outcrops, between the Pico Cabras and Abejera lava domes (Fig. 1), which is the best preserved example and representative of other pumice flow deposits observed. The Abrunco ignimbrite can be recognized in at least three separated outcrops where it overlies previous lava flows and reworked deposits and shows an irregular and discontinuous upper contact with clastogenic lava of the same mineralogical composition. The ignimbrite is not homogeneous and shows different lithofacies irregularly distributed along the deposit (Fig. 2). A *fine-grained laminated lithofacies* appears at the base of the ignimbrite irregularly distributed along the three

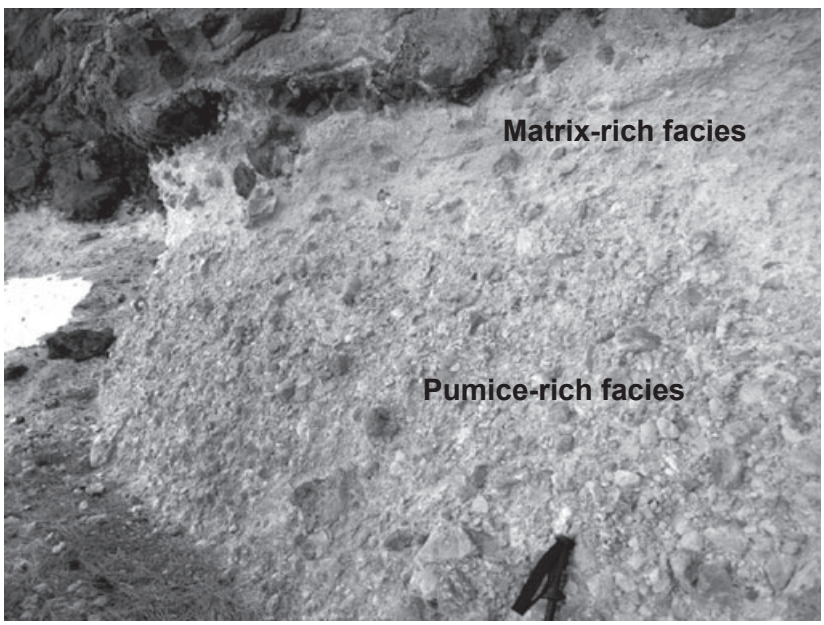

Fig. 2 Detail of the ignimbrite showing the matrix-rich and pumice-rich facies. Note the irregular contact of the ignimbrite with the clastogenic lava above and how fragments of the clastogenic lavas are engulfed by the ignimbrite while some pumice blocks have been eroded and incorporated into the lava.

outcrops. It is mostly composed of coarse to fine juvenile ash together with subordinate ash size lithic clasts. It does not contain pumice fragments of lapilli size or larger. This facies is thinly laminated and occasionally shows cross-bedding. The characteristics of this facies suggest that it could correspond to a pyroclastic surge deposit immediately preceding the emplacement of the ignimbrite. A *pumice-rich lithofacies*, forming a non-welded, poorly sorted, massive deposit, is normally found at the central part of the ignimbrite. It contains abundant angular pumice lapilli of both dense and vesicular (i.e. spherical and tube), which are supported by a fine ash matrix. Sometimes this facies forms lenses surrounded by the matrix-rich facies towards the lower part of the ignimbrite.

A *matrix rich lithofacies* is composed of scarce dense and expanded, including tube and spherical, pumice clasts surrounded by an abundant lapilli and ash matrix of the same composition. The size of pumice lapilli ranges from a few centimetres to 30 cm. Rare vent-derived, angular lithic clasts also appear in this lithofacies and are similar in size to the pumices. The matrix-rich lithofacies is commonly found in the upper parts of the ignimbrite and defines an irregular contact with the overlying clastogenic lavas. This finding, together with the fact that fragments of the clastogenic lavas are engulfed by the ignimbrite while some pumice blocks have been eroded and incorporated into the lava, suggest that the emplacement of the clastogenic lava occurred when the ignimbrite was still unconsolidated. This indicates that the emplacement of the ignimbrite and the clastogenic lava were not separated by a significant time break, probably corresponding to two consecutive phases of the same eruption.

The contacts between the different ignimbrite facies are always irregular, sometimes discontinuous and even gradual in some occasions, but we have not observed erosional contacts among them. The absence of fragments from the clastogenic lavas and the presence of vent-derived lithic clasts in the ignimbrites suggest that they formed from an explosive eruption rather than by gravitational collapse of lava domes or advancing lava flows. The variety of lithofacies observed in the Abrunco ignimbrite may have resulted either from changes at source or by flow changes during emplacement. The presence of the thinly laminated unit at the base of the deposits could be interpreted as a ground surge deposit generated by the turbulent ash cloud flow front, which could be caused by high flow front velocity and considerable topographical irregularity (ground roughness). The abrupt and irregular topography of the northern side of Teide, characterized by frequent slope breaks, may have also favoured changes in the flow regime during the emplacement of the main ignimbrite bodies. This may have created localized highly turbulent conditions which lead to the elutriation of fines and the deposition of isolated pumice lenses and the pumice-rich facies in a similar way to the lee side pumice lenses in the Taupo Ignimbrite described by (Wilson, 1985) or in other ignimbrites from Tenerife (Pittari *et al.,* 2005). The continuation of the flow on a topographically modified ground may have led to the deposition of the massive part of the ignimbrite body thus forming the matrix-rich facies. We have not been able to correlate these ignimbritic deposits with the pumice fallout deposits that crop out at the north of Teide, so we cannot confirm if these ignimbrites formed by collapse of sustained column during plinian or subplinian eruptions or from transient vulcanian explosions associated with lava domes and flows, such as those observed in Montserrat (Calder *et al.,* 1999; Loughlin *et al.,* 2002). Anyway, the intimate association of the studied ignimbrites with clastogenic lavas at the top suggests that ignimbrites and lavas derive from the same eruption, which would have initiated with an explosive event progressively decreasing in intensity till a fire fountaining episode which would have generated the clastogenic lavas. The presence of pumice fall deposits, ignimbrites and clastogenic lavas at several stratigraphic horizons suggests that repeated phonolitic explosive eruptions have occurred during the Holocene at Teide–Pico Viejo.

Another characteristic of these ignimbrite deposits is the presence of lenses of reworked material irregularly interbedded with the pyroclastic facies. This reworked material is composed of abundant sub-rounded to rounded lithic and pumice fragments supported by a scarce reworked matrix. Pumices and lithics of these epiclastic lenses are of the same nature as those from the associated ignimbrite. These characteristics suggest a syn-depositional reworking of the ignimbrite by aqueous flows probably generated by a heavy rainfall triggered by the eruption (see e.g. Woods, 1993), and/or latter by seasonal rain that usually causes torrential effects on such steep topography. This would also explain the lack of preservation of most of the ignimbrite deposit(s).

Block and ash deposits

The second type of PDC deposit that we have recognized around the north side of Teide–Pico Viejo are block and ash deposits. These deposits are always of relatively small volume compared to some lavas, and can be followed for several kilometres downslope. Thickness varies from less than one metre to several metres depending on the palaeotopography on which they were emplaced. In some cases they grade downslope into debris flow deposits, some of them arriving at the northern coast of Tenerife. The block and ash deposits are nearly monolithological and are mostly composed of fragments of clastogenic lavas, and minor non-welded dense and expanded pumices of the same composition as the clastogenic lava fragments (Fig. 3). All these fragments are surrounded by an ash to fine lapilli size matrix mostly composed of juvenile clasts and some lithic fragments derived from the fragmentation and attrition of the previous components. These lithological and sedimentological characteristics make a clear distinction between block and ash and debris flow deposits also present on the northern slopes of Teide, as these last incorporate clasts from other lithologies, reduce significantly the amount of pumice and ash matrix, and show a better rounding of clasts and internal organization of the deposits compared to the block and ash deposits.

Field relationships and comparison of chemical and mineral compositions and textures show that the observed block and ash deposits derive from

Fig. 3 Example of a block and ash deposit found at the northern side of Teide–Pico Viejo in the Icod Valley. Fragments of sub-rounded to rounded clastogenic lavas are supported by an ash-lapilli size matrix of the same composition.

clastogenic lavas flows or lava domes. Most of the recent phonolitic lava domes and lava flows from Teide and Pico Viejo have a clastogenic nature and formed by agglutination and stretching of large juvenile fragments parallel to the flow direction. In some places these clastogenic lavas and domes include abundant non-welded pumices, suggesting that they derive from explosive episodes rather than from purely effusive eruptions. We propose that some of these clastogenic lavas, which were still very rich in gases, became block and ash flows when they collapsed gravitationally at an abrupt slope change, a common morphological feature at the northern side of Teide–Pico Viejo.

Discussion and conclusions

A detailed field study has allowed us to identify for the first time the presence of ignimbrites and block and ash deposits associated with the recent (Holocene) eruptive history of Teide–Pico Viejo. The presence of these deposits, together with fall products means that we should reconsider notions that Teide–Pico Viejo are predominantly effusive volcanoes that do not represent a significant threat to their surroundings.

The fact that the volume of pyroclastic deposits visible today is small compared to that of lavas does not necessarily imply that explosive activity has been insignificant in the recent evolution of Teide–Pico Viejo. On the contrary, we claim that phonolitic explosive activity has been more significant than previously thought in Teide–Pico Viejo during the Holocene. The evidence we have presented for the syn-depositional erosion of ignimbrites suggests that heavy rainfalls may have occurred in the area during these eruptions, which could already explain the rapid disappearance of a significant part of these deposits. Moreover, we must take into account the existence of important seasonal rainfall that would have also contributed to the erosion of the unconsolidated pyroclastic material. In fact, the Icod valley is characterized by the presence of prominent S-N narrow gullies that deeply erode the Teide–Pico Viejo products, and of abundant lahar and debris flow deposits that infill their lower parts.

Other evidence of the relevance of explosive volcanism in Teide–Pico Viejo is the presence of several discontinuous outcrops of thick (occasionally up to 4 m), primary (non-reworked) pumice fall deposits in some sectors of the north of Teide (Fig. 1). At least three of these outcrops have different stratigraphic positions and are older than the 2000 bp Montaña Blanca pumice. However, some other pumice fall deposits from the northern side of Teide may correlate with the Montaña Blanca pumice. Radiometric ages of some of these pumice fall deposits (Carracedo *et al.,* 2007) are similar to the Montaña Blanca, which implies that the Montaña Blanca eruption was larger than previously thought (Ablay *et al.,* 1995; Folch and Felpeto, 2005) and may well have been Plinian in dimension. A first comparison of the mineralogy and geochemistry of all these pumice deposits does not provide definitive clues to discriminate them, so a more detailed petrological work will be required to interpret the sequence of explosive eruptions in the recent geological record of Teide–Pico Viejo.

Hazard assessment at Teide–Pico Viejo, one of the largest volcanic complexes in Europe, is necessary to reduce risk in Tenerife, an island extensively populated and one of the main tourist destinations in Europe. It is widely accepted that pyroclastic density currents are one of the main volcanic hazards. Therefore, the presence of pyroclastic deposits in the recent volcanic history of Teide–Pico Viejo has implications for future hazard and in particular for the Icod valley, an area with a permanent population of more than 30 000 inhabitants which has received the direct impact of explosive volcanism from Teide–Pico Viejo in the past. In contrast with considerations that Teide–Pico Viejo represents only a modest hazard level for Tenerife (Carracedo *et al.,* 2007), we suggest that phonolitic explosive volcanism during the Holocene at Teide–Pico Viejo volcanoes and the existence of unquestionable signs of activity in historical times (fumaroles, seismicity) and even a clear unrest episode in 2004 (Martí *et al.,* 2009), implies that hazard at Teide–Pico Viejo is not negligible. Although a detailed reconstruction of the original extent of the phonolitic pyroclastic deposits of Teide–Pico Viejo is not possible due to the lack of preservation, their characteristics and comparison with similar deposits from recent eruptions (e.g.: Calder *et al.,* 1999; Loughlin *et al.,* 2002),

suggest that they could have easily reached areas that are today densely populated. Therefore, hazard assessment based on a detailed reconstruction of the recent stratigraphy, geochronology, and eruptive styles and products is urgently needed at Teide–Pico Viejo as a necessary tool to reduce volcanic risk in Tenerife.

Acknowledgements

The study has been partially supported by grants MEC (CGL-2006-13830) and MICINN (CGL2008-04264) and the IGN-CSIC collaboration agreement for the study of Tenerife volcanism. A. Geyer is grateful for her post-doctoral Beatriu de Pinos Grant 2008 BP B 00318. JM and GA are grateful for the bilateral program UNAM-CSIC. We thank R. Cas and R. Brown for their helpful and constructive reviews

References

Ablay, G.J. and Martí, J., 2000. Stratigraphy, structure, and volcanic evolution of the Pico Teide-Pico Viejo formation, Tenerife, Canary Islands. *J. Volc. Geoth. Res.*, **103**, 175–208.

Ablay, G.J., Ernst, G.G.J., Marti, J. and Sparks, R.S.J., 1995. The 2ka subplinian eruption of Montaña Blanca, Tenerife. *Bull. Volcanol.*, **57**, 337–355.

Ablay, G.J., Carroll, M.R., Palmer, M.R., Martí, J. and Sparks, R.S.J., 1998. Basanite-phonolite lineages of the Teide-Pico Viejo volcanic complex, Tenerife, Canary Islands. *J. Petrol.*, **39**, 905–936.

Calder, E.S., Cole, P.D., Dade, W.B., Druitt, T.H., Hoblitt, R.P., Huppert, H.E., Ritchie, L., Sparks, R.S.J. and Young, S.R., 1999. Mobility of pyroclastic flows and surges at the Soufriere Hills Volcano, Montserrat. *Geophys. Res. Lett.*, **26**(5), 537–540.

Carracedo, J.C., Rodríguez-Badiola, E., Guillou, H., Paterne, M., Scaillet, S., Pérez-Torrado, F.J., Paris, R., Fra-Paleo, U. and Hansen, A., 2007. Eruptive and structural history of Teide volcano and rift zones of Tenerife, Canary Islands. *Geol. Soc. Am. Bull.*, **119**, 1027–1051.

Folch, A. and Felpeto, A., 2005. A coupled model for dispersal of tephra during sustained explosive eruptions. *J. Volc. Geoth. Res.*, **145**, 337–349.

IGME, 2009. *Digital Continuos Geological Map of Spain at 1:50000 (Plan MAGNA). Tenerife*. http://www.igme.es/internet/default.asp. Accessed 08 September 2009.

Loughlin, S.C., Calder, E.S., Clarke, A., Cole, P.D., Luckett, R., Mangan, M.T., Pyle, D.M., Sparks, R.S.J., Voight, B. and Watts, R.B., 2002. Pyroclastic flows and surges generated by the 25 June 1997 dome collapse, Soufriere Hills Volcano, Montserrat. In: *The Eruption of Soufriere Hills Volcano, Montserrat, from 1995 to 1999* (T.H. Druitt and B.P. Kokelaar, eds). *Geol. Soc. Lond. Mem.*, **21**, 191–209.

Martí, J., Geyer, A., Andujar, J., Teixidó, F. and Costa, F., 2008. Assessing the potential for future explosive activity from Teide-Pico Viejo stratovolcanoes (Tenerife, Canary Islands). *J. Volc. Geoth. Res.*, **178**, 529–542.

Martí, J., Ortiz, R., Gottsmann, J., Garcia, A. and De La Cruz-Reyna, S., 2009. Characterising unrest during the reawakening of the central volcanic complex on Tenerife, Canary Islands, 2004–2005, and implications for assessing hazards and risk mitigation. *J. Volc. Geoth. Res.*, **182**, 23–33.

Pittari, A., Cas, R.A.F., and Martí, J., 2005. The occurrence and origin of prominent massive, pumice-rich ignimbrite lobes within the Late Pleistocene Abrigo Ignimbrite, Tenerife, Canary Islands. *J. Volc. Geoth. Res.*, **139**, 271–293.

Wilson, C.J.N., 1985. The Taupo eruption, New Zealand: II. The Taupo ignimbrite. *Phil. Trans. Roy. Soc. London*, **A 314**, 229–310.

Woods, A.W., 1993. Moist convection and the injection of volcanic ash into the atmosphere. *J. Geophys. Res.*, **98**, 17627–17636.

Received 9 May 2010; revised version accepted 7 April 2011

Appendix 4. The 5,660 yBP Boquerón explosive eruption, Teide–Pico Viejo complex, Tenerife.

Bull Volcanol
DOI 10.1007/s00445-012-0646-5

RESEARCH ARTICLE

The 5,660 yBP Boquerón explosive eruption, Teide–Pico Viejo complex, Tenerife

Olaya García · Costanza Bonadonna · Joan Martí · Laura Pioli

Received: 5 March 2012 / Accepted: 28 July 2012

Abstract Quantitative hazard assessments of active volcanoes require an accurate knowledge of the past eruptive activity in terms of eruption dynamics and the stratified products of eruption. Teide–Pico Viejo (TPV) is one of the largest volcanic complexes in Europe, but the associated eruptive history has only been constrained based on very general stratigraphic and geochronological data. In particular, recent studies have shown that explosive activity has been significantly more frequently common than previously thought. Our study contributes to characterization of explosive activity of TPV by describing for the first time the subplinian eruption of El Boquerón (5,660 yBP), a satellite dome located on the northern slope of the Pico Viejo stratovolcano. Stratigraphic data suggest complex shifting from effusive phases with lava flows to highly explosive phase that generated a relatively thick and widespread pumice fallout deposit. This explosive phase is classified as a subplinian eruption of VEI 3 that lasted for about 9–15 h and produced a plume with a height of up to 9 km above sea level (i.e. 7 km above the vent; MER of $6.9–8.2\times10^5$ kg/s). The tephra deposit (minimum bulk volume of $4–6\times10^7$ m^3) was dispersed to the NE by up to 10 m/s winds. A similar eruption today would significantly impact the economy of Tenerife (e.g. tourism and aviation), with major consequences mainly for the communities around the Icod Valley, and to a minor extent, the Orotava Valley. This vulnerability shows that a better knowledge of the past explosive history of TPV and an accurate estimate of future potentials to generate violent eruptions is required in order to quantify and mitigate the associated volcanic risk.

Keywords Teide · Explosive volcanism · Tephra deposits · Hazard assessment

Editorial responsibility: S. De la Cruz-Reyna

O. García (✉)
Centro Geofísico de Canarias del I.G.N.,
C/La Marina 20, 2°,
38001 Santa Cruz de Tenerife, Spain
e-mail: ogperez@fomento.es

C. Bonadonna · L. Pioli
Département de Minéralogie, Section des sciences de la Terre et de l'environnement, Université de Genève,
Rues des Maraichers 13,
1205 Geneva, Switzerland

J. Martí
Instituto de Ciencias de la Tierra Jaume Almera, CSIC,
Lluis Solé Sabarís s/n,
08028 Barcelona, Spain

Introduction

The Holocene explosive volcanic activity in Tenerife Island is concentrated mainly in the central volcanic complex (Ablay et al. 1998; Ablay and Martí 2000; Martí et al. 2008).

This central complex started to grow at about 4.5 Ma, or earlier, and remains active. Its evolution included several constructive and destructive episodes that gradually formed Las Cañadas caldera at the centre of the island (Martí et al. 1994; Ancochea et al. 1999). The last episode in the construction of the Tenerife central volcanic complex formed the Teide and Pico Viejo stratovolcanoes (TPV complex) within Las Cañadas caldera (Ablay and Martí 2000; Carracedo et al. 2007). Traditionally considered as mainly effusive volcanoes, current knowledge of TPV remains poor given that they form one of the main active volcanic complexes in Europe and are a significant threat to Tenerife (Martí et al. 2011; Marrero et al. 2012). Recent studies have revealed that explosive activity has been underestimated in the reconstructed TPV eruptive history (Martí et al. 2008, 2011; García

Published online: 11 September 2012

et al. 2011; Boulesteix et al. 2012). This implies that hazards at Tenerife might be underestimated if explosive volcanism from TPV is not considered. No precise data on the products of TPV explosive volcanism exist, however, and one of the most urgent needs is to characterise and quantify these eruptions.

The knowledge we have of explosive volcanism at TPV is restricted to a detailed study of the 2,000 BP Montaña Blanca subplinian eruption (Ablay et al. 1995; Folch and Felpeto 2005) and the identification of new fallout and PDC deposits on the northern flank of TPV (Perez-Torrado et al. 2004; Martí et al. 2008; García et al. 2011). Even this limited information suggests that an explosive eruption from TPV would today have a serious impact on critical infrastructures and the economy of the island as it would affect the air traffic, and some of the main energy and water lifelines (Martí et al 2011; Marrero et al. 2012). In this paper, we present a detailed study of the pumice fall deposits associated with El Boquerón dome complex, one of the Holocene flank vents located on the north of the Pico Viejo stratovolcano (Fig. 1). These deposits form the main unit produced by the El Boquerón explosive eruption and have not been described before. We infer the eruption characteristics (i.e. plume height, erupted volume, mass eruption rate and duration) based on a stratigraphic and textural analysis and discuss implications for associated hazards.

Geological background

The TPV complex consists of two stratovolcanoes which started to grow simultaneously within Las Cañadas caldera at around 180–190 ka (Hausen 1956; Araña 1971; Ablay 1997; Ablay et al. 1998; Ablay and Martí 2000; Carracedo et al. 2007) (Fig. 2). This volcanic depression originated as a result of several vertical collapses of the former Tenerife central volcanic edifice, Las Cañadas edifice (Martí et al. 1997; Martí and Gudmundsson 2000). The TPV complex has a maximum elevation of 3,718 m above sea level at the top of Teide and shows a very sharp morphology characterised by steep flanks. The eruptive activity of TPV produced about 150 km^3 of mafic, intermediate and felsic material (Ablay et al. 1998; Ablay and Martí 2000; Martí et al. 2008).

TPV stratovolcanoes have been very active during the Holocene, with more than 16 known eruptions (Carracedo et al. 2007; Martí et al. 2011), the last (Lavas Negras) having occurred at 1,150 yBP (Fig. 2).

The volcano stratigraphy of the TPV was characterized by Ablay and Marti (2000) based on a detailed field and

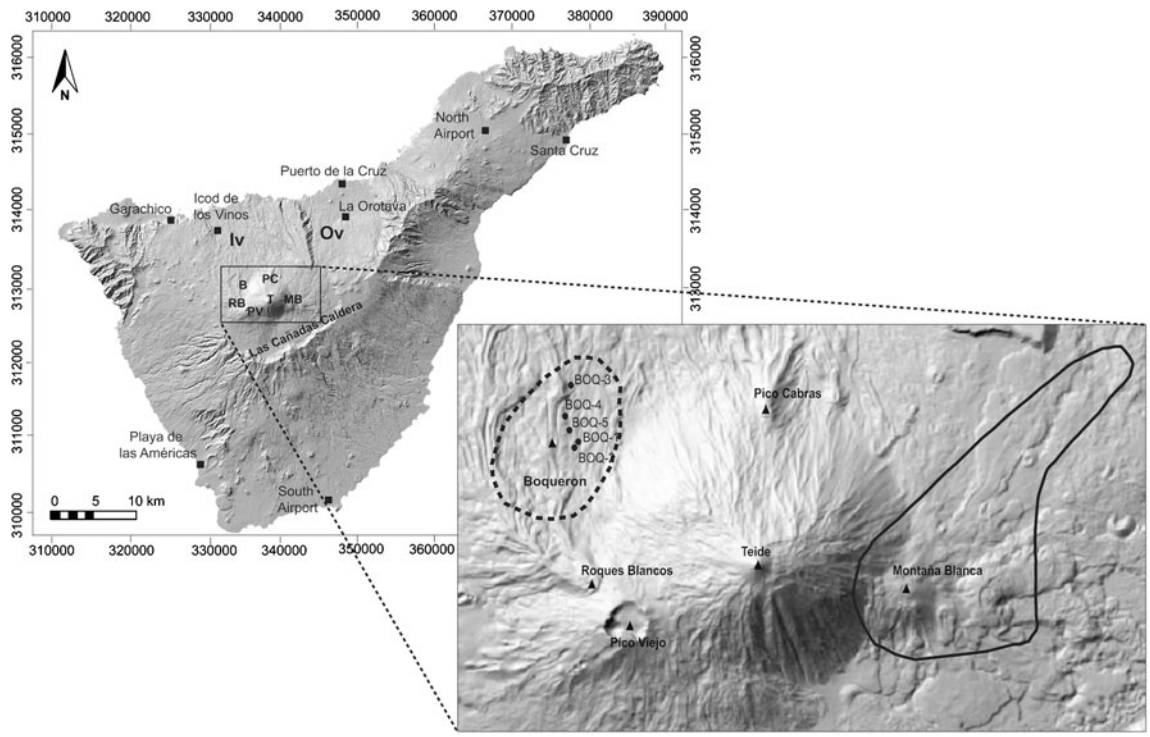

Fig. 1 Location map of study area and topographic map of Tenerife. Main vents and main drainage cuts of Boquerón lava flow are shown as *black triangles* and *black solid lines*, respectively. *Black circles* indicate our main outcrops (Fig. 2), the *dashed line* represents the 50-cm isopach contour of isopach A (Fig. 3) and the *thick line* represents the 30-cm isopach contour. *B* Boquerón, *MB* Montaña Blanca, *RB* Roques Blancos, *T* Teide, *PC* Pico Cabras, *PV* Pico Viejo, *Iv* Icod Valley, *Ov* Orotava Valley (projection: UTM 28 N)

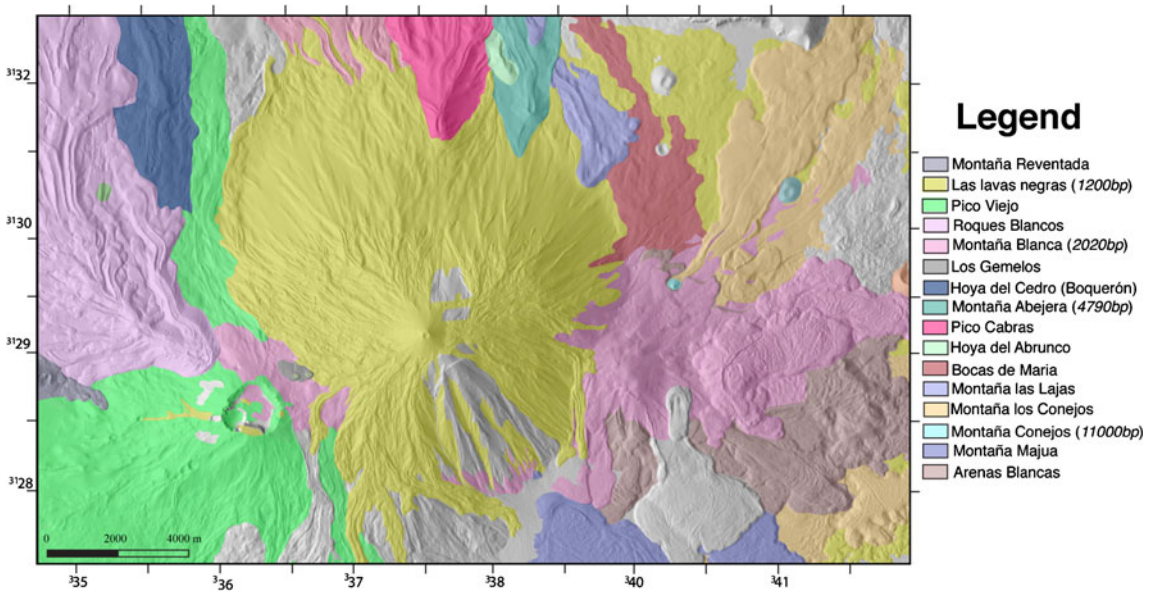

Fig. 2 Geological map of the Teide–Pico Viejo complex; adapted from Ablay and Martí (2000). The figure does not include all the volcanic events related to Pico Viejo–Teide stratovolcanoes, only those central and flank Holocene eruptions with felsic and hybrid composition. Geochronological data from Carracedo et al. (2003, 2007)

petrological study (Fig. 2). In addition, Carracedo et al. (2003, 2007) provided the first group of isotopic ages from TPV products. The eruptive history of TPV consists of a main stage of eruption of mafic to intermediate lavas that form the core of the stratovolcanoes and filled most of the Las Cañadas depression and the adjacent La Orotava and Icod valleys. Phonolitic eruptions have become predominant since 35 ka, and their products cover the volcanoes' flanks and the infill sequence of the Icod Valley and part of La Orotava valley (Fig. 1).

Phonolitic eruptions from TPV were generated both from the central vents and from a multitude of vents distributed around their flanks. The flank vents define several radial eruptive fissures on the slopes of the twin volcanoes, and have generated both effusive (i.e. lava flows and domes) and explosive eruptions, ranging in size from 0.01 to >1 km^3 Dense Rock Equivalent (DRE). Effusive eruptions have produced thick lava flows and domes. Explosive eruptions have generated extensive pumice fall deposits and pyroclastic density currents (PDCs) associated with both subplinian and plinian eruptions and also with dome and lava flow gravitational collapses in the cases of PDCs (Martí et al. 2008, 2011; García et al. 2011). All these eruptive centres are associated with a single eruption in which several phases may be distinguished (Ablay and Martí 2000).

The Boquerón is a dome complex located on the northwestern flank of TPV volcano. The last Boquerón eruption is of Holocene age (Carracedo et al. 2003) and produced both a large pumice fall deposit and 0.04 km^3 of lava flows, which reached the coastline along the Icod valley (i.e. 7.2 km run out; Fig. 1; Martí et al. 2011). In this paper, we present a detailed study of the fall deposit.

Methods

Given the poor exposure of the Boquerón deposit, the relevant outcrops were first identified based on aerial photographs and then thoroughly analysed and correlated through field investigations. Most of the studied outcrops are located on the northwest flank of TPV, at the base of Roques Blancos dome complex, and are concentrated in a 15-km^2 area around Boquerón (Fig. 1). The stratigraphy of the whole sequence of deposits was characterised based on detailed fieldwork. Correlations among the different units from different outcrops were made mainly based on textural features and crystal content and composition. Deposit thickness and maximum lithic sizes were determined at most outcrops. Forty samples were also collected in order to investigate grain size, chemistry, density and vesicularity of the juvenile pumices. The fraction coarser than −3 ϕ (i.e. >8 mm) was sieved manually in the field, whereas finer fractions >3 ϕ (<8 mm) were dried and sieved in the laboratory. Componentry analysis was made for particles coarser than 0 ϕ.

Density was measured on 100 juvenile clasts from the entire unit, collected at the outcrop BOQ-4 and with diameters ranging between 16 and 32 mm (Fig. 3). Pumice clasts were dried at 60 °C for 24 h and then cleaned with a brush, numbered and weighed. Finally, all clasts were coated with

Fig. 3 Pumice fall deposit from the Boquerón eruption. **a** Distal area: outcrop BOQ-3A. **b** Proximal area of pumice deposit with a large lithics: outcrop BOQ-2.TOP

cellulose acetate, dried and weighed again. Relative density was obtained comparing water and the dry weights. The results were converted into absolute density and bulk vesicularity using the Dense Rock Equivalent (DRE) density measured on finely crushed pumice specimens using a water pycnometer at the University of Geneva. The deposit density in the field was obtained by weighing a known in situ volume of pumice clasts, plus intergranular porosity and matrix from BOQ-3 outcrop. To investigate variations in morphology and vesicularity of juvenile clasts of the main unit, we used the scanning electron microscope (SEM) JEOLJSM 6400 at the University of Geneva.

Whole rock analyses were performed by the GeoAnalytical Laboratory at the Washington State University using X-ray fluorescence (XRF) and inductively coupled plasma mass spectrometry (ICP-MS) facilities. The relative error of the measurement is lower than 1 % for the major and trace elements for XRF method, less than 5 % for the REEs and less than 10 % for the remaining trace elements. Charcoal was also found in the soil below the bottom unit of Boquerón deposit, which overlies the paleosol, and 2.2 g of sample was analyzed by Beta Analytic Inc. Laboratory of Miami (USA) for carbon isotopic composition with accelerator mass spectroscopy (AMS) techniques. The specimen (i.e. laboratory number Beta-298872) age was determined after the IntCal04 calibration curve (Reimer et al. 2004).

Physical parameters of the main unit were also derived. The erupted volume was calculated applying the methods of exponential, power-law and Weibull integration (Pyle 1989; Bonadonna and Houghton 2005; Bonadonna and Costa 2012). Given the poor exposure of the deposits, two potential isopach maps were compiled based on the same dataset in order to investigate the uncertainty in the volume calculation. The thickness dataset was constructed based on 61 trenches excavated down to the underlying lava flow (in medial areas) or down to a maximum of 2 m when the lava flow was not present (in proximal areas).

The plume height was determined applying the method of Carey and Sparks (1986) to the isopleth map of lithic clasts. The maximum lithic sizes were measured based on the geometric mean average of the three axes of the five largest clasts sampled based on a horizontal sampling area of 0.5 m^2. We also compiled an isopleth map using the 50th percentile of the 20 largest clasts following the recommendations of the IAVCEI Commission on Tephra Hazard Modelling (Bonadonna et al. 2011, 2012).

Composition, stratigraphy and characteristics of deposits

The Boquerón eruption is associated with an old dome in the northwest flank of Pico Viejo stratovolcano. Charcoal fragments found in the dark red soil at the base of Boquerón deposit had a 13C/12C ratio of −22.9‰, corresponding to a conventional age of 5,630±60 yBP, corresponding to a calibrated radiocarbon age of 5,660±60 BP. The composition (shown in Table 1) of both the Boquerón juvenile fragments and lava flow is phonolitic, similar to other Holocene products of TPV (see Ablay et al. 1995).

The pyroclastic succession of the Boquerón deposit consists of a main pumice fall deposit characterised by a poor exposure, with proximal outcrops showing some evident stratification and some welding phenomena (Fig. 3). Individual layers are difficult to correlate and tend to merge in distal areas. As a result, we have characterised the Boquerón deposit as a single unit. Five representative outcrops were selected for detailed stratigraphic, grain size, componentry and textural studies and are shown in Fig. 4.

The Boquerón tephra deposit is dispersed over an area of about 15 km^2 NW of Teide. In distal areas (Fig. 2; BOQ-3), it consists of several centimetre-thick, well-sorted, non-

Table 1 Whole rock analyses of representative Boquerón samples

Unit sample	Boquerón Boq.r23	Boquerón Boq.r1	Boquerón Boq.pr
Major and minor elements (oxides, wt.%)			
SiO_2	59.46	58.44	59.14
TiO_2	0.727	0.63	0.70
Al_2O_3	19.34	18.9	19.44
FeO^*	3.45	3.51	3.41
MnO	0.19	0.19	0.19
MgO	0.43	0.34	0.38
CaO	0.87	0.75	0.76
Na_2O	8.92	9.07	9.08
K_2O	5.50	5.42	5.59
P_2O_5	0.114	0.081	0.070
Total	99.0	97.33	98.77
LOI (%)	0.89	2.35	0.87
Trace elements (ppm)			
Ni	4	3	4
Cr	2	2	2
Sc	0	1	1
V	14	8	13
Ba	192	24	87
Rb	169	170	186
Sr	13	7	10
Zr	964	989	1,041
Y	36	38	38
Nb	219	225	235
Ga	28	29	29
Cu	1	1	2
Zn	119	125	125
Pb	19	20	20
La	110	112	112
Ce	186	186	192
Th	28	28	30
Nd	55	56	57
U	7	8	7

Boq.r23 is a lava from a Boquerón lava flow; it was taken from one point close to point 6 (Table 2), and Boq.r1 and Boq.pr are juvenile lapilli clasts and were taken from no-welded bed at point 4 (Table 2)

welded, massive bed of pumice lapilli. Grain size distribution of the studied samples is characterised by Md phi and sorting varying between −1.4 and −3.2 phi and 1.4 and 1.0, respectively. Lithic content is mostly constant for all deposits, increasing slightly from the bottom (7 vol.%) to the top (10 vol.%; Fig. 4); lithic clasts predominantly consist of obsidian and phonolitic lava fragments. Juvenile clasts consist of microvesicular, crystal-poor, angular to subangular yellow to grey pumice lapilli. At medial locations (Fig. 4; BOQ-2), the unit has a thickness of a few decimetres and displays internal stratification with symmetric, coarse–fine–coarse graded bedding. The contact between beds is gradational. At proximal locations (Fig. 4; BOQ-5 and BOQ-2), the deposit consists of an alternation of moderately to incipiently welded lapilli and bomb beds and non-welded lapilli beds with exposed thickness up to 6.37 m (outcrop BOQ-5). These layers are moderately to poorly sorted, with average size from lapilli to bombs. In the welded beds, the degree of welding increases from bottom to top with gradual transition to the lower non-welded beds. The welded beds are typically lithic-poor. At some locations, the welded beds display rheomorphic features suggesting remobilization on steep slopes. The welding of the proximal deposits suggests higher deposition rates and high depositional temperatures associated with low magma viscosity, favouring clast agglutination and deformation (Carey et al. 2008). This appears to be a common process in the phonolitic eruptions of the TPV complex, and also affected the older plinian fall deposits cropping out in the Las Cañadas walls (Ablay et al. 1995; Soriano et al. 2002).

In contrast, the contact between non-welded layers is sharp (Fig. 4; BOQ-4). The bottom of the whole unit lies over a paleosol or, in distal areas, directly above lava flows. Carracedo et al. (2003) located the vent of this eruption at the S margin of the lava flow. This hypothesis is confirmed by the distribution of thickness and grain size of the tephra layer (Fig. 5 and Table 2).

Results

Volume

In order to estimate the error associated with the volume calculation of a poorly exposed tephra deposit, we decided to hand draw two possible isopach maps based on the same dataset (isopach maps A and B in Fig. 5 with associated thickness shown in Table 2). Map A is compiled based on a conservative interpretation of field data, while Map B can be considered as just an example of possible contouring that can be drawn to consider a larger dispersal than Map A but still compatible with the same dataset. In fact, Map B is compiled based on the assumption of a more gradual thinning where the deposit is not accessible (i.e. mainly to the SW and NE of the vent) and can be then considered as an upward boundary for the volume calculation (with a relative difference of 30 % in the square root of area value of the 50-cm contour). The thinning trends resulting from each map can be described by one exponential segment and both a Weibull and a power-law curve on a semi-log plot of thickness versus square root of isopach area.

Volume calculations were then made from the two different maps applying the methods of exponential, power-law and Weibull integrations (Pyle 1989; Bonadonna and

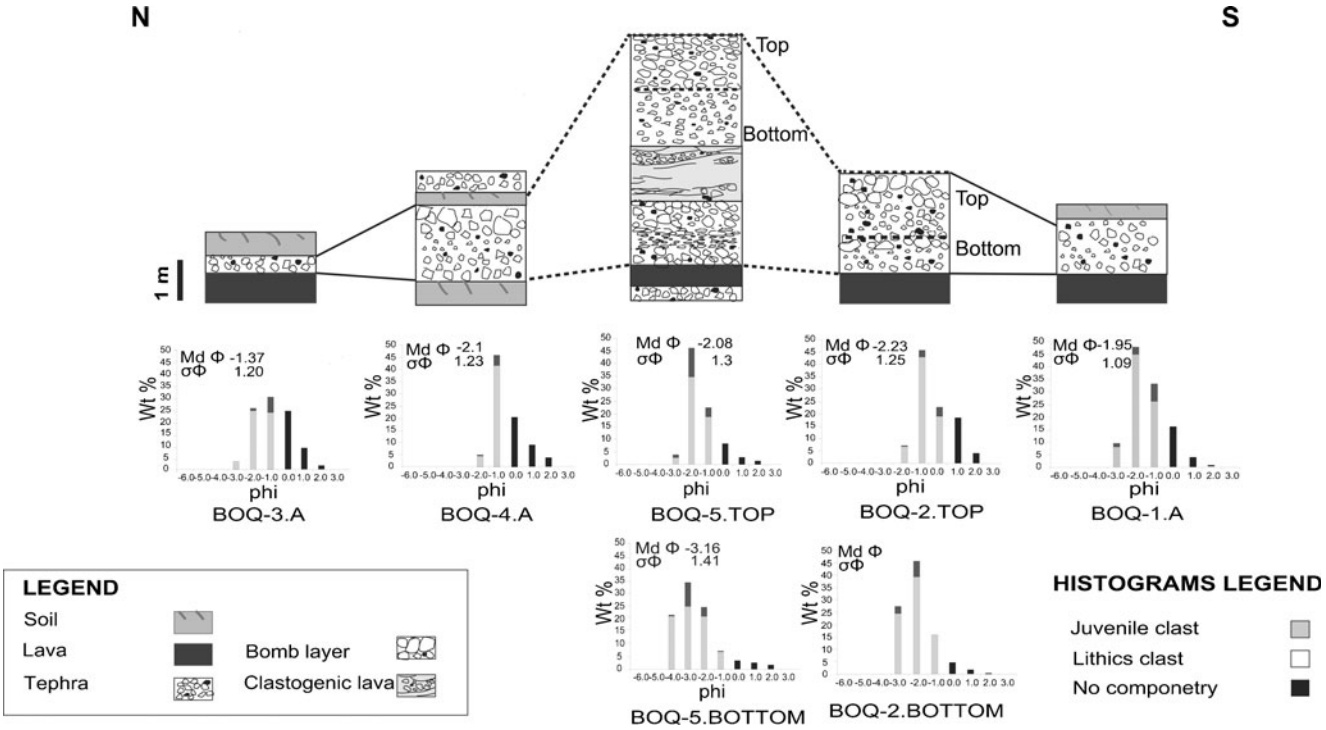

Fig. 4 Stratigraphic columns of five representative sections from Boquerón deposits with the associated grain size and componentry. Location of the outcrops is shown in Fig. 1 and thickness in Table 2

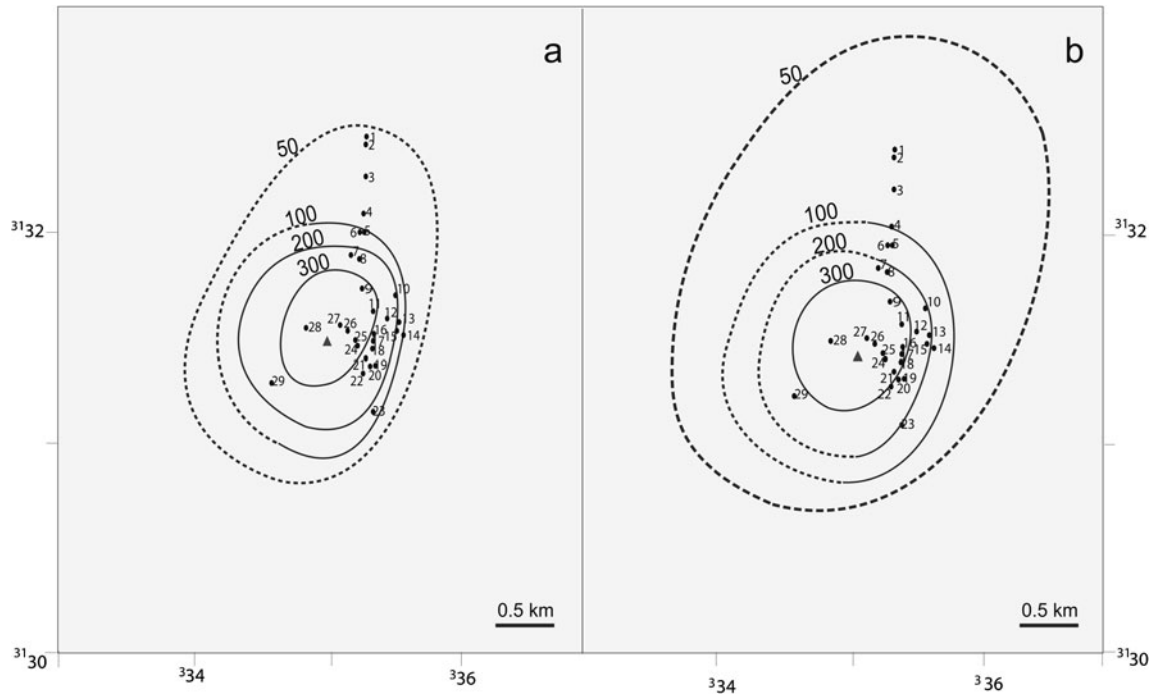

Fig. 5 Isopach maps of the Boquerón deposit with thickness expressed in centimetre: (**a**) isopach map A; (**b**) isopach map B. Sample numbers are indicated on the map, and thickness values are reported in Table 1. *Dashed lines* are extrapolated contours. Given the poor exposure of the deposit, two isopach maps have been compiled that are compatible with our dataset in order to estimate the error in the volume calculation

Table 2 Thickness values of samples points in isopach maps A and B of Fig. 3

Point	Thickness (cm)	UTM X	UTM Y
1	60	335356	3132377
2	62	335356	3132337
3	**40**	**335328**	**3132052**
4	37	335314	3131765
5	58	335312	3131620
6	50	335285	3131609
7	**164**	**335288**	**3130977**
8	>120	335225	3131436
9	**637**	**335311**	**3131145**
10	>79	335636	3131111
11	>120	335416	3130977
12	>165	335546	3130946
13	>79	335655	3130878
14	110	335698	3130773
15	>140	335636	3130811
16	**271**	**335437**	**3130789**
17	>180	335416	3130722
18	>188	335402	3130645
19	>112	335426	3130531
20	>197	335390	3130520
21	>140	335340	3130583
22	>99	335315	3130456
23	>180	335412	3130163
24	>160	335266	3130698
25	>185	335254	3130733
26	>180	335172	3130816
27	**>160**	**335092**	**3130857**
28	>165	334801	3130818
29	>200	334463	3130400

Numbers in bold show the thickness of the main outcrops; *Point 3* is BOQ-3

Houghton 2005; Bonadonna and Costa 2012; Table 3). The calculated volumes are 1.0 and 1.7×10^7 m^3 for the two exponential integrations, $3.7\pm0.4\times10^7$ and $7.3\pm1.2\times10^7$ m^3 for the two power-law integrations and 4.2×10^7 and 6.3×10^7 m^3 for the two Weibull integrations (for isopach A and B respectively; Fig. 5). The erupted mass varies between 0.6 and 4.4×10^{10} kg based on a deposit density of 600 kg m^{-3}. The distal limits of integration for the power-law calculation (50 to 100 km square root of area values; Table 3) were chosen based on both the thinning trend of Boquerón and Montaña Blanca (Ablay et al. 1995). In fact, these two deposits show very similar features with a thickness of about 10–50 cm around 3–5 km from the vent (square root of area values). We assume that the most distal sedimentation would then occur around 50 to 100 km from the vent (square root of area values). The error of the power-law integration was calculated based on the variation of these distal integration limits. The uncertainty associated with the compilation of the isopach map is 40 % for exponential method, 50 % for the power-law method and 32 % for the Weibull method. As a result, we base our discussion below on the most stable values given by the Weibull integration. The associated DRE volume, based on a deposit density of 600 kg/m^3 and a magma density of 2,570 kg/m^3, ranges from 9.9×10^6 to 1.5×10^7 m^3.

Plume height, wind speed, mass eruption rate and eruption duration

As mentioned above, two isopleth maps were compiled based on the five largest lithics (Fig. 6a) and on the 50th percentile of a population of 20 lithics (Fig. 6b). Plume height and wind velocity at the time of the eruption were derived by applying the method of Carey and Sparks (1986) to both isopleth maps. Only the 0.8-cm isopleth contour gave consistent estimates for both maps, and resulted in a plume height of about 7 km above the vent (i.e. about 9 km above sea level) for both the five largest clasts and the 50th percentile method and wind velocities up to 10 m/s. The Boquerón tephra deposit was mainly dispersed northeastward, in agreement with the dominant wind direction in the area. In fact, the average wind direction in TPV complex, as calculated based on NOAA local wind data collected in the last 10 years, shows a dominant eastward wind direction from 5 to 20 km above sea level with uniform seasonal distribution and standard deviation decreasing from ±90° to ±45° with altitude (Fig. 7).

The mass eruption rate (MER) was calculated applying both the method of Wilson and Walker (1987) and Sparks (1986) (Table 4). The method of Wilson and Walker (1987) resulted in a MER of 6.9×10^5 kg/s, while the method of Sparks (1986) resulted in a MER of 8.2×10^5 kg/s (for a tropical atmosphere and a plume temperature of 600 °C appropriate for phonolitic magmas). The eruption duration was estimated between about 9–10 h for isopach A and about 13–15 h for isopach B based on the ratio between erupted mass (Weibull integration) and the two MER values described above (Table 4).

Classification

Based on the volume range described above, the Boquerón explosive phase classifies as having a volcanic explosivity index (VEI) of 3. The associated magnitude is between 2.8 and 3.6, and the intensity is 9 on the scales of Pyle (2000) (Table 3). The bt vs. bc/bt plot of Pyle (1989) suggests an eruptive style between strombolian and subplinian, with the subplinian field being characterised by minimum plume heights of 14 km (Fig. 8). The thinning trend, however,

Table 3 Summary of volume calculations associated with the exponential (Pyle 1989), power-law (Bonadonna and Houghton 2005) and Weibull (Bonadonna and Costa 2012) integrations

		Volume ($\times 10^7$ m^3)	Mass ($\times 10^{10}$ kg)	Magnitude		
					bt (km)	bc/bt
Exponential	Isopach A	1.0	0.6	2.8	2.0	0.3
	Isopach B	1.7	1.0	3.0	1.3	0.4
					m	
Power law	Isopach A	3.7±0.4	2.2±0.3	3.3	1.8	–
	Isopach B	7.3±1.2	4.4±0.7	3.6	1.6	–
					θ	λ
Weibull	Isopach A	4.2	2.5	3.4	4.7	13.8
	Isopach B	6.3	3.8	3.6	5.5	18.1

Mass is calculated based on a deposit density of 600 kg/m^3 ; magnitude is calculated according to Pyle (2000); bt and bc are the thickness half-distance and the half-distance ratio, respectively, calculated according to Pyle (1989); m is the absolute value of the coefficient of the power-law best fit; θ and λ are two characteristic scales of the Weibull best fit. The error of the power-law integration is calculated based on variable distal limits of integrations (i.e. 50, 75 and 100 km)

follows the typical pattern of subplinian eruptions and, in particular, shows similar characteristics to that of the Montaña Blanca deposit (Fig. 9). Values of thickness half distance (bt) for Boquerón maps A and B are between 0.3 and 0.5 km in agreement with bt values of Montaña Blanca deposit (i.e. 0.4–0.8 km), of the 26 September 1997 vulcanian explosion of Montserrat (i.e. 0.7 km), of Chaiten layer α (i.e. 0.7 km) and with the proximal bt values of Ruapehu (i.e. 0.2 km) and Chaiten layer β (i.e. 0.8 km). These values are lower than values of Plinian eruptions that typically range from 1 to 60 km (Pyle 1989).

Clast vesicularity and textural characterization

The phenocryst content of the Boquerón pumices account for 3 to 7 vol.%. Phenocrysts consist of millimetre-sized, euhedral biotite, alkaline feldspar, clinopyroxene and minor apatite, magnetite and ilmenite.

Juvenile lapilli are usually microvesicular, glassy and phenocryst poor. The differences between juvenile clasts can be substantial, both in density and texture (Figs. 10 and 11). Their density ranges from 360 to 1,150 kg/m^3 with average of 744 kg/m^3 and standard deviation of 190 kg/m^3

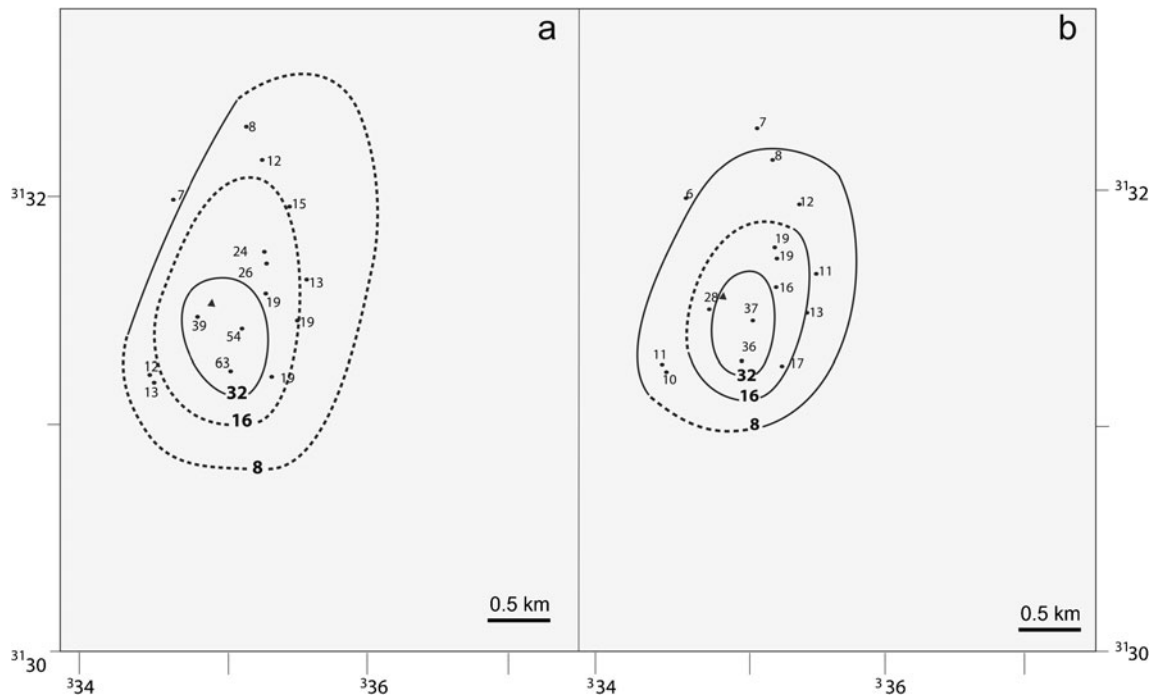

Fig. 6 Isopleth maps of Boquerón deposit for the largest lithics using two different methods: (**a**) the average of the three axes of the five largest clasts; (**b**) 50th percentile of a 20-clast population. *Dashed lines* are extrapolated contours

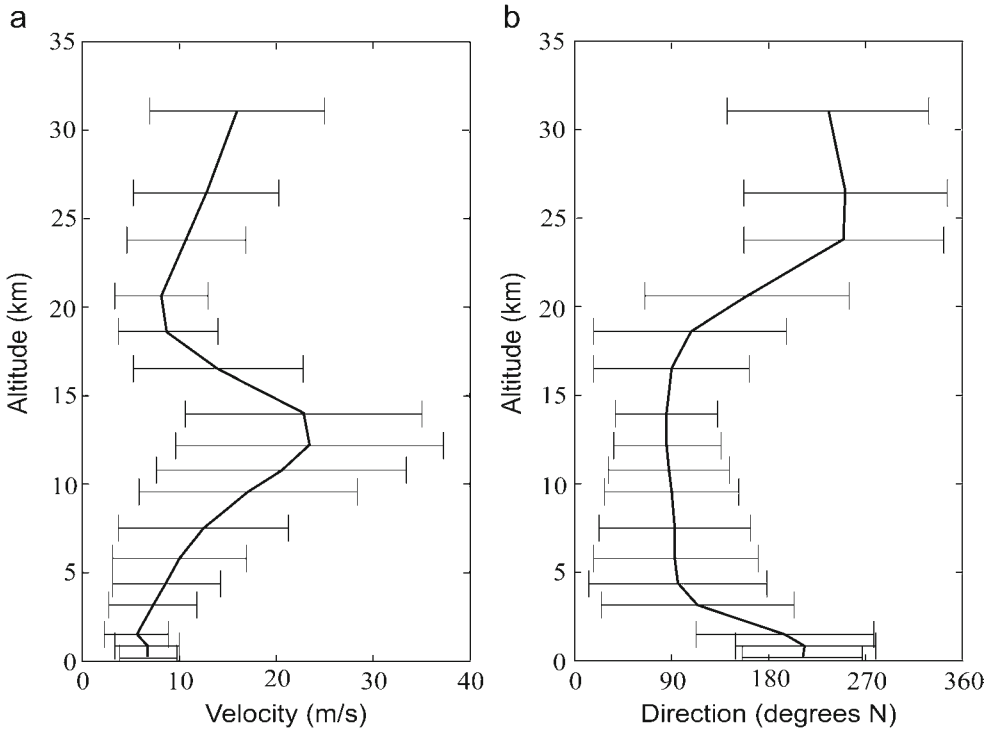

Fig. 7 Wind profiles calculated for Teide–Pico Viejo Volcano for the last 10 years (2000–2010; wind data from NOAA, US National Oceanic and Atmospheric Administration, www.cdc.noaa.gov). **a** Variation of wind velocity profile with altitude. **b** Variation of wind direction, which is expressed as degrees from north where the wind blows. Data are presented as a median value with associated *error bars*

(Fig. 10). The density distribution is unimodal with a dense tail. Considering a measured DRE density of 2,540±133 kg/m^3, the vesicularity ranges from 86 to 33 vol.%, and the clasts could be classified as from poorly to highly vesicular (Houghton and Wilson 1989).

Vesicles range from a few millimetres to few micrometres in size and display different shapes, from spherical to elongate or flat (Fig. 10a). The largest vesicles have complex and irregular shapes (Fig. 10a). The majority of clasts display homogenous textures with high vesicularity, small vesicles with complex shapes and glassy groundmass (Fig. 10b), and vesicle walls thickness ranges from few micrometres to a few tens of micrometres, suggesting high nucleation rates, and an expansion dominated coalescence (Szramek et al. 2006).

Moderately to poorly vesicular clasts have heterogeneous textures, with vesicularity and crystallinity varying at the millimetre scale. Vesicles are separated by thicker (a few tens to few hundreds of micrometres) walls (Fig. 11d) and cluster in groups. Larger vesicles are usually confined to the central portion of the clasts. In addition, groundmass crystallinity varies at the specimen scale and is correlated with the vesicularity: microlite-poor areas (5 vol.% of microlites) are also vesicle-poor, with only small round vesicles; microlite-rich areas (50 vol.% of microlites) have vesicularity up to 45 vol.%. This relationship between vesicles and groundmass crystallinity is possibly due to the effects of post-fragmentation expansion or even by clast recycling during lower explosivity phases (Wright et al. 2006). The boundaries between microlite-poor areas and microlite-rich areas are generally sharp (Fig. 11b).

Microlites consist of acicular sanidine with major axes ranging between 200 and 10 μm. Occasionally, microlites are gathered in small groups in the crystal-rich glass, but it is more common to see individual crystals. Clasts from incipiently welded facies show highly heterogeneous textures with abrupt variations in vesicles size and spherulitic aggregates.

Table 4 Summary of the MER and eruption duration calculation based on a plume height of 6.8 km (calculated with the method of Carey and Sparks 1986) and for the methods of Wilson and Walker (1987) and Sparks (1986)

	MER (×10^5 kg/s)	Duration (isopach A) (h)	Duration (isopach B) (h)
Wilson and Walker (1987)	6.9	10.2	15.1
Sparks (1986)	8.2	8.6	12.7

The eruptions duration is calculated based on the ratio between the erupted mass (calculated based on the Weibull integration applied to isopach A and B of Fig. 3) and the two values of MER

Discussion

The Boquerón subplinian eruption produced a vigorous plume reaching up to 9 km above sea level. The wind dispersion was to the Northeast in agreement with the main wind pattern of the area and with the dispersion of the Montaña Blanca eruption (Ablay et al. 1995; Folch and Felpeto 2005). Despite the low column height, the

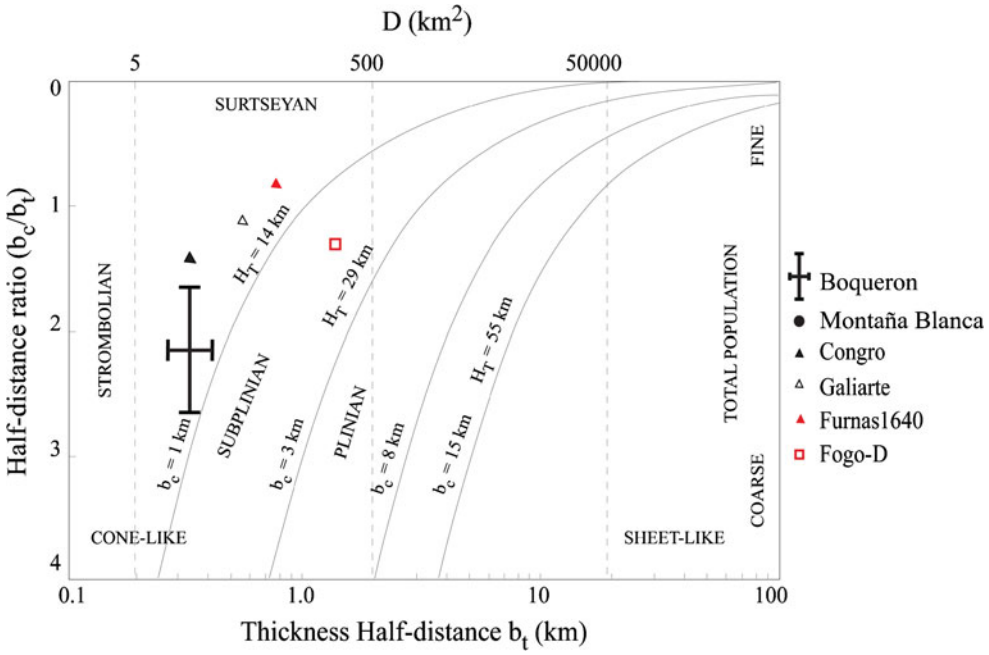

Fig. 8 Classification plot of Pyle (1989). Boquerón data are indicated as median value with associated *error bar*. *Error bar* is calculated based on the two isopach maps of Fig. 3. Data of Congro, 3,800 yBP, Sao Miguel, Azores (Booth et al. 1978); Furnas 1640, Sao Miguel, Azores (Thorinsson and Sigvaldson 1972a, b); Fogo D, Cape Verde (Rose et al. 1983) and Montaña Blanca, 2 Ka Tenerife (Ablay et al. 1995) eruptions are also shown for comparison

Boquerón eruption is also comparable to other subplinian events in terms of deposit dispersal, erupted volume and thinning trend (Fig. 9). As an example, the Boquerón volume and thinning trends are very similar to those for the eruptions of Montaña Blanca (i.e. 1.4×10^8 m^3 based on isopach map from Ablay et al. 1995) and Fuego 1974 (Rose et al. 2008). The complex stratigraphy, which is evident at proximal locations, could be indicative of complex eruption dynamics, coupling a main climactic phase to minor explosive phases that formed the welded horizons in the deposit, or to fluctuations in the eruptive intensity. Finally, we note that our new radiometric data suggest a maximum age for the Boquerón eruption of 5,660 yBP. This age is much older, but compatible with the value (2,528±185 yBP) obtained by

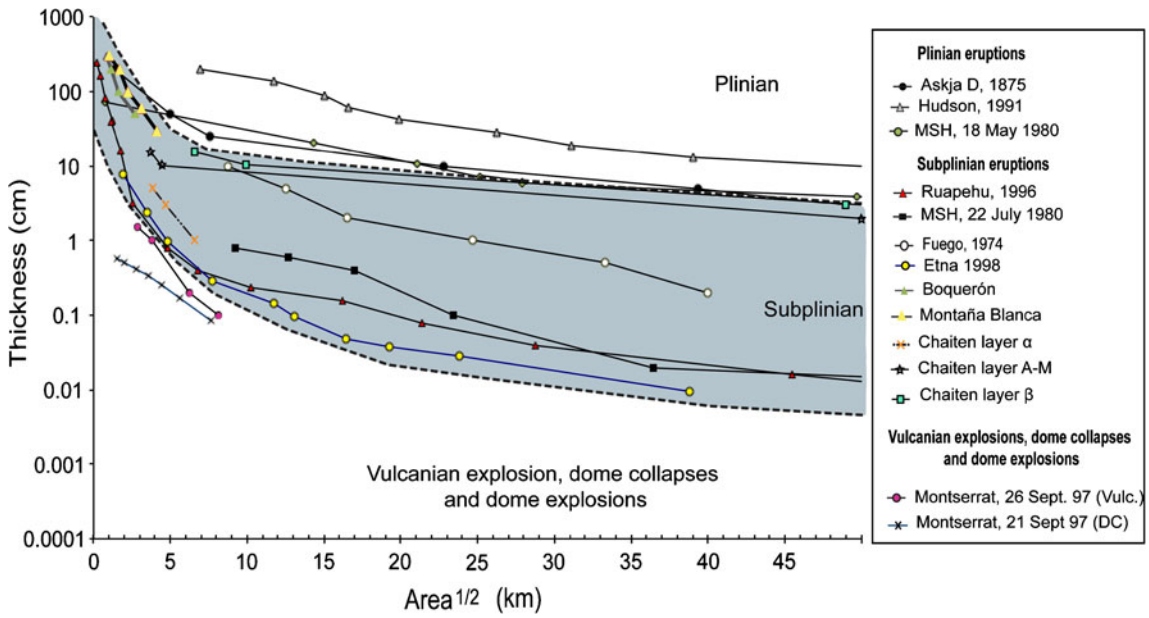

Fig. 9 Semi-log plot of thickness versus the square root of the area of the Boquerón deposit compared with the thinning trend of other deposits produced by explosive eruptions. Data are from Askja D, 1875 (Sparks et al. 1981); Hudson, 1991 (Scasso et al. 1994); Mount St. Helens, 18 May 1980 (Sarna-Wojciki et al. 1981); Ruapehu, 17 June 1996 (Bonadonna and Houghton 2005); Montserrat, 26 September 1997 (Bonadonna et al. 2002); Montserrat, 21 September 1997 (Bonadonna et al. 2002); Fuego, 1974 (Rose et al. 2008); Etna, 1998 (Bonadonna and Costa 2012); Montaña Blanca, 2 Ka (Ablay et al. 1995); and Chaiten, May 2008 (Alfano et al. 2010)

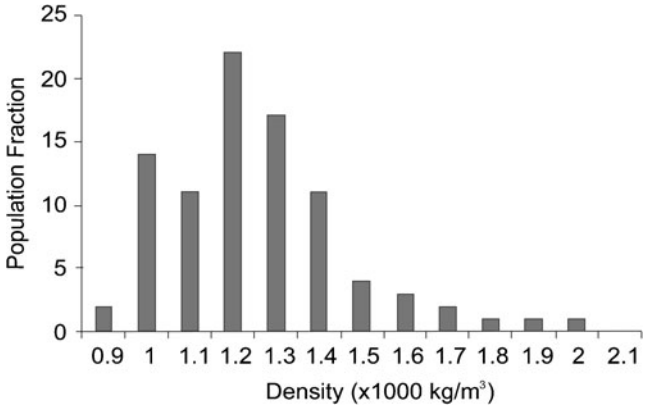

Fig. 10 Density distribution histogram of juvenile clasts from Boquerón unit

Carracedo et al. (2007) from a charcoal in the paleosol. Both ages are consistent with the regional stratigraphy (Ablay and Martí 2000).

Deposit dispersal, eruption column and duration

In order to estimate the uncertainty involved in calculating the volumes of deposits characterised by poor exposure, we constructed two possible isopach maps based on the same set of data. The error associated with the two compilations of the isopach map is about 30 %, 40 % and 50 % for Weibull, the exponential and the power-law method, respectively. These values are of the same order of magnitude of other estimations of volume-calculation uncertainties made on better-exposed deposits (e.g. 30 % estimated uncertainty for the exponential method by Cioni et al. (2011) on the 512 AD Vesuvius eruptions). In addition, Bonadonna and Costa (2012) have already shown how the stability of the Weibull method is better than that of the other two empirical methods because it depended on only three free parameters (i.e. λ, θ, and n). As a result, the volume can be constrained more easily (when ≥3 points are available) and without the need of arbitrary and subjective choices, such as the number of exponential segments and the integration limits.

The plume height was derived using the method of Carey and Sparks (1986). In particular, the height derived based on the average of geometric mean of the five largest clasts was compared to the height derived based on the 50th percentile of a 20-clast population suggested by the IAVCEI Commission on Tephra Hazard Modelling (Bonadonna et al. 2011; Bonadonna et al. 2012). In fact, the method of the 50th percentile is considered more stable even though it still needs to be calibrated with the original plots of Carey and Sparks (1986). As a result, we confidently conclude that the plume reached a maximum height of 7 km above the vent (i.e. 9 km above sea level). The uncertainty in the calculation of the MER based on two different methods is around 16 % (Wilson and Walker 1987; Sparks 1986), which results

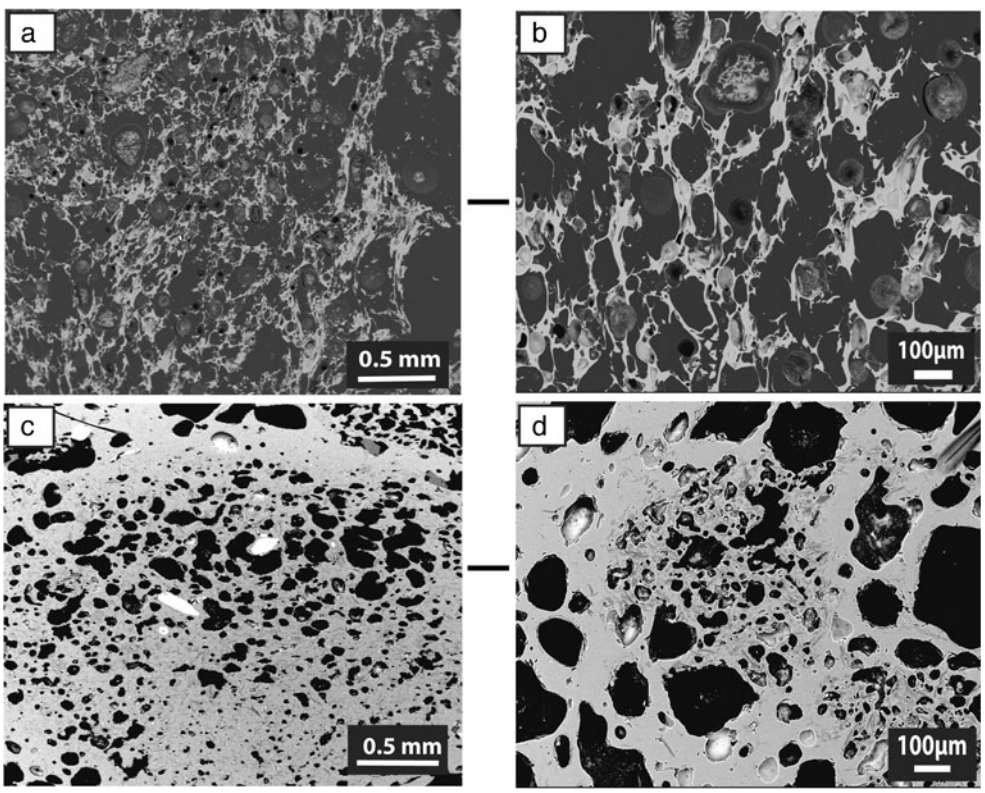

Fig. 11 Selected backscattered SEM images (×25 and ×200 magnification) of juvenile clasts of different vesicularity. Vesicles are in *black*, while the glass and microlites groundmass are in *grey*. **a** Sample with high vesiculation. **b** Detail of vesicles in the sample with high vesiculation. **c** Sample with low vesiculation. **d** Detail with vesicles in the sample of low vesiculation

in an uncertainty in the inferred eruption duration of up to 43 % based on the two MER values and the Weibull-derived volume associated with isopach maps A and B (Table 4).

Textures

Boquerón juvenile pumice fragments have been characterised on the basis of vesicularity and groundmass texture. The differences between juvenile clasts can be substantial, both in density and texture (Figs. 10 and 11). The majority of clasts display homogenous textures with high vesicularity, small vesicles with complex shapes and glassy groundmass, suggesting high nucleation rates, and an expansion-dominated coalescence (Szramek et al. 2006). In contrast, the lower vesicularity clasts display heterogeneous textures with smaller, rounded vesicles and higher groundmass crystallinity, possibly due to the effects of post-fragmentation expansion and clasts recycling during lower explosivity phases (Wright et al. 2006). In addition, the welding of the proximal deposits suggests higher deposition rates and high depositional temperatures associated with low viscosity, favouring clast agglutination and deformation (Carey et al. 2008). This appears to be a common process for phonolitic eruptions of the TPV complex, and for older plinian fall deposits cropping out in the Las Cañadas walls (Ablay et al. 1995; Soriano et al. 2002).

Volcanic hazard and risk

TPV is one of the largest volcanic complexes in Europe and is located at the top of a densely populated island that is also a very popular destination for tourism. The main known volcanic hazard is associated with basaltic fissural eruptions, which mainly take place along the two active rift zones. However, there is also clear evidence of effusive and explosive phonolitic volcanism during the Holocene, with significant hazard implications, not only for the Las Cañadas area but also for the Icod valley, which connects the TPV complex to the N coast of the island. In fact, among the known lateral eruptions of the TPV complex, at least 16 have produced phonolitic magmas, which can also be associated with highly mobile, low-viscosity lava flows (Dingwell et al. 1998; Giordano et al. 2000; Gottsmann and Dingwell 2001). Like the Boquerón, most of these eruptions were also dome forming with vents located at the flanks of the TPV (2,300 m above sea level), and they also had associated PDCs (Martí et al. 2008, 2011). Among them, the Montaña Blanca (2,020 BP) is the best known and most recent eruption (Ablay et al. 1995). It produced a 10-km high eruption column and a tephra deposit with a volume of 1.4×10^8 m^3 dispersed over an area of 30 km^2 (based on maps of Ablay et al. 1995). The last eruption in Tenerife was the basaltic strombolian eruption of Chinyero, 1909, on the NW rift, which did not cause major disruption to population (Solana and Aparicio 1998). The only known eruption that has caused fatalities and major disruption in Tenerife occurred in 1706, when a basaltic lava flow, originated from a vent on the Santiago rift (outside the TPV), almost destroyed Garachico, the former capital of the island, inducing a massive spontaneous evacuation (Solana and Aparicio 1998). Since then, Tenerife has experienced population growth significantly higher than the national average, and it is now the most populated island of Spain with more than 900,000 inhabitants. In addition, Tenerife is one of the main tourist destinations in Europe with more than five million visitors per year, and the main populated municipalities in Tenerife (Santa Cruz, San Cristobal de la Laguna and Puerto de la Cruz) are less than 30 km away from the TPV. Aviation could also be significantly affected by a new explosive eruption of the TPV. In fact, all Canarias airports fall in a circle of 300 km radius centred on the TPV complex, with the Canary Islands lying along one of the main civil aviation corridors for flights from Europe to Central and South America and vice versa. Martí et al. (2011) have already shown that a subplinian eruption from the Boquerón vent (i.e. calculations based on a plume height of 9 km above sea level and volume of 0.05 km^3) would significantly affect the Northern coast of Tenerife, including the towns of Icod de los Vinos, Santa Cruz, La Orotava, Puerto de la Cruz and the North airport. All the roads in the northern part of the island and the main road that connects the North to the South would be covered by 1 mm to 5 cm of ash. Given that our detailed study of the Boquerón eruption results in a similar plume height and volume as modelled by Martí et al. (2011) (i.e. 7 km and 0.04–0.06 km^3 respectively), we would expect that another eruption of this type would be associated to disruption equivalent to that described by Martí et al. (2011).

Conclusions

Despite poor levels of exposure, we have provided an accurate study of the deposits associated with the last Boquerón eruption based on a detailed description of stratigraphy and sedimentological features, including the morphology, textural features and composition of the juvenile fraction. This has allowed for a reconstruction of the eruption dynamics and the main physical parameters. As a result, we can conclude that

1. Empirical calculations resulted in a tephra volume between 1 and 8×10^7 m^3 with the best estimate between 4 and 6×10^7 m^3 (based on the Weibull integration of two possible maps). The uncertainty associated with the volume calculation of tephra deposits is about 30 %,

40 % and 50 % for the Weibull, exponential and the power-law integrations, respectively.

2. The plume reached a maximum height of 9 km above sea level (i.e. 7 km above the vent) with a corresponding MER and duration of 6.9–8.2×10^5 kg/s and 9–15 h, respectively.
3. The explosive phase could be classified as a VEI=3 subplinian eruption based on dispersal and thinning characteristics. Magnitude and intensity are 3.4–3.6 and 9, respectively.
4. The proximal welding and stratification of the deposit, together with the typical pumiceous textures of the majority of the lapilli, suggest complex dynamics, shifts from highly explosive phases to minor phases, and dispersal high temperature bombs in proximal locations.
5. If a Boquerón-style eruption were to happen again, it would have a large impact on the now densely populated island of Tenerife, particularly towards the north, and on various economic sectors, such as the aviation business.

Acknowledgments This research has been partially funded with MICINN grant CGL2008-04264 and the IGN-CSIC collaboration agreement for the study of Tenerife volcanism. The authors are grateful to the National Park of Teide for giving us permission to undertake this research and Cabildo of Tenerife for giving us FYF 412/10 permission. They are also grateful to David Moure, Dario Pedrazzi, Ilazkiñe Iriberren, Natividad Luengo, Stavros Meletlidis, Pedro Torres, Stephanie Barde-Cabusson, Victor Cabrera and all the staff working at the Geophysics Centre of Canarias for their support during the field campaigns, including the staff working in the Central Geophysics Observatory (IGN). They also thank Agathe Martignier of the Department of Mineralogy of University of Geneva (Switzerland) for assistance with the SEM analyses, and Sebastien Biass helped in processing the NOAA wind data. This paper greatly benefited from editorial handling by S. De la Cruz and careful reviews of two anonymous reviewers.

References

Ablay GJ, Martí J (2000) Stratigraphy, structure, and volcanic evolution of the Pico Teide-Pico Viejo formation, Tenerife, Canary Islands. J Volcanol Geotherm Res 103:175–208. doi:10.1016/s0377-0273(00)00224-9

Ablay GJ, Carroll MR, Palmer MR, Martí J, Sparks RSJ (1998) Basanite- phonolite lineages of the Teide-Pico Viejo volcanic complex, Tenerife, Canary Islands. J Petrol 39:905–936

Ablay GJ (1997) Evolution of the Teide-Pico Viejo complex and magma system, Tenerife, Canary Islands. Dissertation. University of Bristol, Bristol

Ablay GJ, Ernst GGJ, Martí J, Sparks RSJ (1995) The 2 ka subplinian eruption of Montaña Blanca, Tenerife. Bull Volcanol 57:337–355

Alfano F, Bonadonna C, Volentik ACM, Connor CB, Watt SFL, Pyle DM, Connor LJ (2010) Tephra stratigraphy and eruptive volume of the May, 2008, Chaitén eruption, Chile. Bull Volcanol 73:613–630. doi:10.1007/s00445-010-0428-x

Ancochea E, Huertas MJ, Fuster JM, Cantagrel JM, Coello J, Ibarrola E (1999) Evolution of the Cañadas edifice and its implications for the origin of the Cañadas caldera (Tenerife, Canary Islands). J Volcanol Geotherm Res 88:177–199

Araña V (1971) Litología y estructura del edificio Cañadas, Tenerife (Islas Canarias). Est Geol 27:95–135

Bonadonna C, Cioni R, Pistolesi M, Connor CB, Scollo S, Pioli L (2012) Determination of the largest clasts of tephra deposits for the characterization of explosive eruptions: report of the IAVCEI Commission on Tephra Hazard Modelling. Bull Volcanol (submitted). https://vhub.org/resources/870

Bonadonna C, Costa A (2012) Estimating the volume of tephra deposits: a new simple strategy. Geology 40:415–418. doi:10.1130/G32769.1

Bonadonna C, Scollo S, Cioni R, Pioli L, Pistolesi M (2011) Determination of the largest clasts of tephra deposits for the characterization of explosive volcanic eruptions. Report of the IAVCEI Commission on Tephra Hazard Modelling

Bonadonna C, Houghton BF (2005) Total grain size distribution and volume of tephra-fall deposits. Bull Volcanol 67:441–456. doi:10.1007/s00445-004-0386-2

Bonadonna C, Macedonio G, Sparks RSJ (2002) Numerical modelling of tephra fallout associated with dome collapses and vulcanian explosions: application to hazard assessment on Montserrat. In: Druitt TH, Kokelaar BP (eds) The eruption of Soufrière Hills Volcano, Montserrat, from 1995 to 1999. Geological Society of London, London, pp 517–537

Booth B, Croasdale R, Walker GPL (1978) A quantitative study of five thousand years of volcanism on Sao Miguel, Azores. Phil Trans R Soc London A288:271–319

Boulesteix T, Hildenbrand A, Soler V, Gillot PY (2012) Eruptive response of oceanic islands to giant landslides: new insights from the geomorphologic evolution of the Teide-Pico Viejo volcanic complex (Tenerife, Canary). Geomorphology 138:61–73. doi:10.1016/j.geomorph.2011.08.025

Carey R, Houghton B, Thordarson T (2008) Contrasting styles of welding observed in the proximal Askja 1875 eruption deposits I: Regional welding. J Volcanol Geotherm Res 171:1–19. doi:10.1016/j.jvolgeores.2007.11.020

Carey S, Sparks RSJ (1986) Quantitative models of the fallout and dispersal of tephra from volcanic eruption columns. Bull Volcanol 48:109–125

Carracedo JC, Rodríguez-Badiola E, Guillou H et al (2007) Eruptive and structural history of Teide volcano and rift zones of Tenerife, Canary Islands. Geol Soc Am Bull 119:1027–1051. doi:10.1130/B26087.1

Carracedo JC, Paterne M, Guillou H et al (2003) Dataciones radiométricas (14C y K/Ar) del Teide y el rift noroeste, Tenerife, Islas Canarias. Est Geol 59:15–29

Cioni R, Bertagnini A, Andronico D, Cole PD, Mundula F (2011) The 512 AD eruption of Vesuvius: complex dynamics of a small scale subplinian event. Bull Volcanol 73:789–810. doi:10.1007/s00445-011-0454-3

Dingwell DB, Hess KU, Romano C (1998) Extremely fluid behavior of hydrous peralkaline rhyolites. Earth Planet Sci Lett 158:31–38

Folch A, Felpeto A (2005) A coupled model for dispersal of tephra during sustained explosive eruptions. J Volcanol Geotherm Res 145:337–349. doi:10.1016/j.jvolgeores.2005.01.010

García O, Martí J, Aguirre-Díaz G, Geyer A, Iribarren I (2011) Pyroclastic density currents from Teide-Pico Viejo (Tenerife, Canary Islands): implications on hazard assessment. TerraNova 23:220–224. doi:10.1111/j.1365-3121.2011.01002.x

Giordano D, Dingwelll DB, Romano C (2000) Viscosity of a Teide phonolite in the welding interval. J Volcanol Geotherm Res 103:239–245

Gottsmann J, Dingwell DB (2001) Cooling dynamics of spatter-fed phonolite obsidian flows on Tenerife, Canary Islands. J Volcanol Geotherm Res 105:323–342

Hausen H (1956) Contributions to the geology of Tenerife (Canary Islands). Soc Sci Fennicae Comm Phys-Mat 18:254

Houghton B, Wilson CJN (1989) A vesicularity index for pyroclastic deposits. Bull Volcanol 51:451–462

Marrero JM, García A, Llinares A et al (2012) A direct approach to estimating the number of potencial fatalities from an eruption: application to the central volcanic complex of Tenerife Island. J Volcanol Geotherm Res 219–220:33–40. doi:10.1016/j.jvolgeores.2012.01.008

Martí J, Sobradelo R, Felpeto A, García O (2011) Eruptive scenarios of phonolitic volcanism at Teide-Pico Viejo volcanic complex (Tenerife, Canary Islands). Bull Volcanol 74:767–782. doi:10.1007/s00445-011-0569-6

Martí J, Geyer A, Andujar J, Teixó F, Costa F (2008) Assessing the potential for future explosive activity from Teide-Pico Viejo stratovolcanoes (Tenerife, Canary Islands). J Volcanol Geotherm Res 178:529–542. doi:10.1016/j.jvolgeores.2008.07.011

Martí J, Gudmundsson A (2000) The Las Cañadas caldera (Tenerife, Canary Islands): an overlapping collapse caldera generated by magma-chamber migration. J Volcanol Geotherm Res 103:161–173

Martí J, Hurlimann M, Ablay GJ, Gudmundson A (1997) Vertical and lateral collapses in Tenerife and other ocean volcanic islands. Geology 25:879–882

Martí J, Mitjavila J, Araña V (1994) Stratigraphy, structure and geochronology of the Las Cañadas caldera (Tenerife, Canary Islands). Geol Mag 131:715–717

Perez-Torrado FJ, Carracedo JC, Paris R, Hansen A (2004) Descubrimientos de depósitos freatomagmáticos en las calderas septentrionales de estratovolcan Teide (Tenerife, Islas Canarias): relaciones estratigraficas e implicaciones volcánicas. Geotemas 6:163–166

Pyle DM (1989) The thickness, volume and grain size of tephra fall deposits. Bull Volcanol 51:1–15

Pyle DM (2000) Size of volcanic eruptions. In: Sigurdsson H (ed) Encyclopedia of volcanoes. Academic, London, pp 263–269

Reimer PJ, Baillie MGL, Bard E, Bayliss A et al (2004) Radiocarbon 46:1029–1058

Thorinsson S, Sigvaldson GE (1972a) The Hekla eruption of 1970. Bull Volcanol 36:269–288

Rose WI, Self S, Murrow PJ, Bonadonna C, Durant AJ, Ernst GGJ (2008) Nature and significance of small volume fall deposits at composite volcanoes: insights from the October 14, 1974 Fuego eruption, Guatemala. Bull Volcanol 70:1043–1067

Rose WI, Wunderman RL, Hoffman MF, Gale L (1983) A volcanologist's review of atmospheric hazards of volcanic activity: Fuego and Mt St Helens. J Volcanol Geotherm Res 17:133–157

Sarna-Wojcicki AM, Shipley S, Waitt JR, Dzurisin D, Wood SH (1981) Areal distribution thickness, mass, volume, and grain- size of airfall ash from the six major eruptions of 1980. US Geol Surv Prof Pap 1250:577–600

Scasso R, Corbella H, Tiberi P (1994) Sedimentological analysis of the tephra from 12–15 August 1991 eruption of Hudson Volcano. Bull Volcanol 56:121–132

Solana MC, Aparicio A (1998) Reconstruction of the 1706 Montaña Negra eruption. Emergency procedures for Garachico and El Tanque, Tenerife, Canary Islands. In: Firth CR, McGuire WJ (eds) Geol Soc London Spec Pub 161, pp 209–216

Soriano C, Zafrilla S, Martí J, Bryan S, Cas R, Ablay G (2002) Welding and rheomorphism of phonolitic fallout deposits from the Las Canadas caldera, Tenerife, Canary Islands. Geol Soc Am Bull 114:883–895

Sparks RSJ (1986) The dimensions and dynamics of volcanic eruption columns. Bull Volcanol 48:3–15

Sparks RSJ, Wilson L, Sigurdsson H (1981) The pyroclastic deposits of the 1875 eruption of Askja, Iceland. Philos Trans R Soc Lond 299:241–273

Szramek L, Gardner J, Larsen J (2006) Degassing and microlite crystallization of basaltic andesite magma erupting at Arenal Volcano, Costa Rica. J Volcanol Geother Res 157:182–201. doi:10.1016/j.volgeores.2006.03.039

Thorinsson S, Sigvaldson GE (1972b) The Hekla eruption of 1970. Bull Volcanol 36:269–288

Wilson L, Walker GPL (1987) Explosive volcanic eruptions—VI. Ejecta dispersal in plinian eruptions: the control of eruption conditions and atmospheric properties. Geophys J R Astr Soc 89:657–679

Wright HMN, Cashman KV, Rosi M, Cioni R (2006) Breadcrust bombs as indicators of vulcanian eruptions at Guagua Pichincha volcano, Ecuador. Bull Volcanol 69:281–300. doi:10.1007/s00445-006-0073-6

Appendix 5. Eruptive scenarios of phonolitic volcanism at Teide-Pico Viejo volcanic complex (Tenerife, Canary Islands)

Bull Volcanol (2012) 74:767–782
DOI 10.1007/s00445-011-0569-6

RESEARCH ARTICLE

Eruptive scenarios of phonolitic volcanism at Teide–Pico Viejo volcanic complex (Tenerife, Canary Islands)

J. Martí · R. Sobradelo · A. Felpeto · O. García

Received: 18 April 2011 / Accepted: 17 October 2011 / Published online: 30 November 2011

Abstract Recent studies on Teide–Pico Viejo (TPV) complex have revealed that explosive activity of phonolitic and basaltic magmas, including plinian and subplinian eruptions, and the generation of a wide range of pyroclastic density currents (PDCs) have also been significant. We perform a statistical analysis of the time series of past eruptions and the spatial extent of their erupted products, including lava flows, fallout and PDCs. We use an extreme value theory statistical method to calculate eruption recurrence. The analysis of past activity and extent of some well-identified deposits is used to calculate the eruption recurrence probabilities of various sizes and for different time periods. With this information, we compute several significant scenarios using the GIS-based VORIS 2 software (Felpeto et al., J Volcanol Geotherm Res 166:106–116, 2007) in order to evaluate the potential extent of the main eruption hazards that could be expected from TPV. The simulated hazard scenarios show that the southern flank of Tenerife is protected by Las Cañadas caldera wall against lava flows and pyroclastic density currents, but not against ash fallout. The Icod Valley, and to a minor extent also the La Orotava valley, is directly exposed to most of TPV hazards, in particular to the gravity driven flows. This study represents a step forward in the evaluation of volcanic hazard at TPV with regard to previous studies, and the results obtained should be useful for intermediate and long-term land-use and emergency planning.

Keywords Teide–Pico Viejo · Tenerife · Phonolitic volcanism · Eruption recurrence · Eruptive scenarios · Hazard assessment

Editorial responsibility: S. Nakada

J. Martí (✉) · R. Sobradelo
Institute of Earth Sciences "Jaume Almera", CSIC,
Lluis Solé Sabarís s/n,
08028 Barcelona, Spain
e-mail: joan.marti@ija.csic.es

A. Felpeto
Observatorio Geofísico Central,
Instituto Geográfico Nacional (IGN),
c/Alfonso XII, 3,
28014 Madrid, Spain

O. García
Centro Geofísico de Canarias,
Instituto Geográfico Nacional (IGN),
c/La Marina 20, 2°,
38001 Santa Cruz de Tenerife, Spain

Introduction

Tenerife is the largest (~2,050 km^2) and most populated (>900,000 inhabitants) of the Canary Islands. As for the rest of this volcanic archipelago, its mild climate and impressive volcanic landscapes, including the dormant Teide and Pico Viejo complex (TPV), have contributed to make it one of the main tourist destinations in Europe with more than five million visitors per year. The presence of recurrent historical volcanism on this island is a convincing reason to undertake volcanic hazard assessment for risk-based decision-making in land-use planning and emergency management and, consequently, to improve the security of its inhabitants and its numerous visitors.

The main concern about potential future volcanic activity on Tenerife has traditionally been addressed towards basaltic eruptions taking place along the two active rift zones, as they have occurred in historical times (Carracedo et al. 2007, 2010). However, despite the occurrence of numerous eruptions during the Holocene

(Carracedo et al. 2007) and of unequivocal signs of activity in historical times (fumaroles, seismicity) (IGN seismic catalogue) and even an unrest episode in 2004 (García et al. 2006; Pérez et al. 2005; Gottsmann et al. 2006; Martí et al. 2009; Domínguez Cerdeña et al. 2011), TPV has not been considered as a major threat.

Although the highest probability of having a new eruption on Tenerife corresponds to a basaltic eruption along the rift zones, which today would also represent a significant trouble for the island, the probability of having a new eruption from the TPV central complex is not negligible. This is indicated by the number of eruptions that it has produced during the Holocene (see Carracedo et al. 2007), most of them of phonolitic composition and triggered by intrusion of deep basaltic magma into shallow felsic magma chambers (Martí et al. 2008a).

The complexity of any volcanic system and its associated eruptive processes, together with the lack of data that characterises many active volcanoes, particularly those with long periods between eruptions, makes volcanic hazard quantification very challenging, as there is often not enough observational data to build a robust statistical model. This is the case for TPV, about which information on their past eruptive history and its present state of activity is still incomplete. This restricts the existing techniques for forecasting its future behaviour to within a minimum margin of confidence. However, different efforts have been made to assess volcanic hazard at TPV in the form of event tree structures representing possible eruptive scenarios and using the available geological and geophysical information (Martí et al. 2008b; Sobradelo and Martí 2010). Bayesian inference and expert judgement elicitation techniques have been applied to these event trees to estimate the long-term probability for each scenario within a given time window. This has allowed us to rationalise our current knowledge of TPV and provides a tool for understanding and anticipating the future behaviour of these volcanoes. These previous studies have not yet, however, been able to quantify the recurrence and extent for each possible scenario.

In order to move one step forward in the hazard assessment at TPV, it is important to estimate the temporal and spatial probability of an eruption for various time windows in the near future and study in detail-specific eruptive scenarios for each of the main associated hazards. This study focusses on phonolitic volcanism, as it has been clearly dominant at TPV through the Holocene and also because it would produce the most hazardous scenarios. In this paper, we first do a threat analysis of the TPV complex using the Ewert et al. (2005) template in order to compare them with other volcanoes of similar characteristics. Then we calculate the temporal and spatial probability of a phonolitic eruption from TPV using available data. After that, we computed several significant scenarios using the GIS-based VORIS 2 software (Felpeto et al. 2007) in order to evaluate the potential extent of the main eruption hazards expected from TPV. Finally, we discuss the results obtained and compare them with the Bayesian technique previously applied to estimate the long-term hazard. The elaboration of a quantitative hazard map for the whole island of Tenerife, including a probabilistic estimate for each point of the map of being impacted by the different hazards considered, is beyond the purpose of this study and will constitute the specific goal of a new paper.

Geological background

TPV complex is composed by the twin Teide and Pico Viejo stratovolcanoes that started to grow simultaneously at about 180–190 ka within the Las Cañadas caldera (Fig. 1), which is a volcanic depression formed by several vertical collapses of the former Tenerife central volcanic edifice (Las Cañadas edifice) following explosive emptying of a high-level magma chamber. Occasional lateral collapses of the volcano flanks also occurred and modified the resulting caldera depression (Martí et al. 1994, 1997; Martí and Gudmundsson 2000). The construction of the present central volcanic complex on Tenerife encompasses the formation of these twin stratovolcanoes, which derive from the interaction of two different shallow magma systems that evolved simultaneously, giving rise to a complete series from basalt to phonolite (Ablay et al. 1998; Martí et al. 2008a).

The structure and volcanic stratigraphy of the TPV was characterised by Ablay and Martí (2000), based on a detailed field and petrological study. Later, Carracedo et al. (2003, 2007) provided the first group of isotopic ages from TPV products, and Martí et al. (2008a) analysed the potential for future TPV activity. More recently, García et al. (2011) identified the products of several explosive eruptions of phonolitic composition from these volcanoes. The reader will find in these works more complete descriptions of the stratigraphic and volcanological evolution of TPV.

TPV mostly consists of mafic to intermediate products, with felsic materials volumetrically subordinate overall (see Martí et al. 2008a). Felsic products, however, dominate the recent output of the TPV system. Eruptions at TPV have occurred from their central vents but also from a multitude of vents distributed on their flanks (Fig. 1). Mafic and phonolitic magmas have been erupted from these vents. The Santiago del Teide and Dorsal rift axes (Fig. 1), the two main tectonic lineations currently active on Tenerife, probably join beneath TPV complex (Carracedo 1994; Ablay and Martí 2000). Some flank vents at the western side of Pico Viejo are located on eruption fissures that are sub-parallel to fissures further down the Santiago del Teide

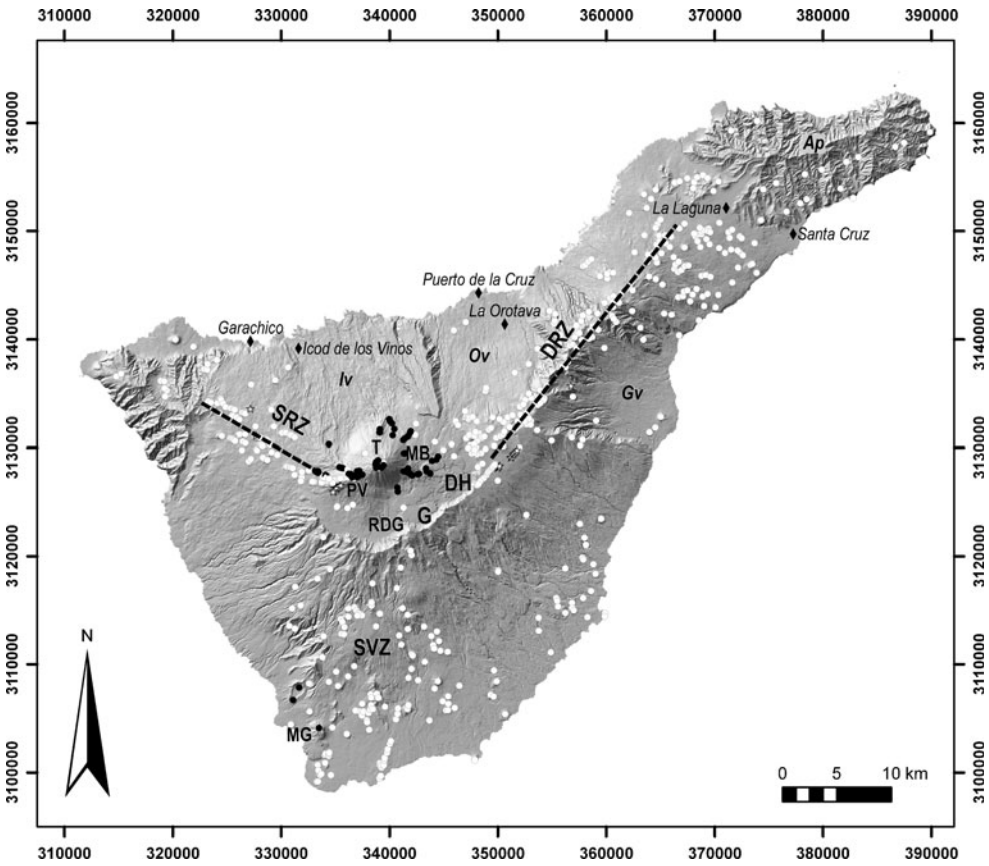

Fig. 1 Simplified geological and topographic map of Tenerife illustrating the general distribution of visible vents. *Black symbols* mafic and intermediate vents; *white symbols* felsic vents; *stars* historic and sub-historic vents; *circles* other vents. *Grey squares* some main population centres. *DH* Diego Hernández, *DRZ* Dorsal rift zone, *G* Guajara, *MB* Montaña Blanca, *MG* Montaña Guaza, *RDG* Roques de García, *T* Teide volcano, *PV* Pico Viejo volcano, *SRZ* Santiago rift zone, *SVZ* Southern volcanic zone, *Iv* Icod valley, *Ov* Orotava valley, *Gv* Güimar valley, *Ap* Anaga peninsula (projection: UTM 28N)

rift and define the main rift axis. On the eastern side of Teide, some flank vents define eruption fissures orientated parallel to the Dorsal rift.

The eruptive history of the TPV comprises a main stage of eruption of mafic to intermediate lavas that form the core of the volcanoes and also infill most of the Las Cañadas depression and the adjacent La Orotava and Icod valleys. At about 35 ka, the first phonolites appeared, and since then, they have become the predominant composition in the TPV eruptions. Basaltic eruptions have also continued mostly associated with the two main rift zones. The available petrological data suggest that the interaction of a deep basaltic magmatic system with a shallow phonolitic magmatic one beneath central Tenerife controls the eruption dynamics of TPV (Martí et al. 2008a). Most of the phonolitic eruptions from TPV show signs of magma mixing, suggesting that eruptions were triggered by intrusion of deep basaltic magmas into shallow phonolitic reservoirs.

Phonolitic activity from TPV shows repose intervals around 250–1,000 years, according to the isotopic ages published by Carracedo et al. (2003, 2007). Phonolitic eruptions from TPV range in volume from 0.01 to >1 km^3 and mostly produce thick clastogenic lava flows and domes, occasionally associated with explosive episodes ranging from subplinian to plinian, which have generated extensive pumice fall deposits and PDCs (Ablay et al. 1995; Martí et al. 2008a; García et al. 2011). The emplacement of clastogenic lava flows and domes have also generated explosive episodes when block and ash flows were generated by gravitational collapses (García et al. 2011).

Some significant basaltic eruptions have occurred as well from the flanks or the central vents of TPV. All basaltic eruptions have developed explosive strombolian to violent strombolian phases leading to the construction of scoria cones and occasionally producing intense lava fountaining and violent explosions with the formation of ash-rich eruption columns. Violent basaltic phreatomagmatic eruptions have also occurred from the central craters of the TPV, generating high-energy, pyroclastic density currents. Table 1 summarises 16 phonolitic eruptions documented geologically for TPV during Holocene.

Threat analysis

Quantification of the threat posed by volcanoes is an important issue when trying to define the monitoring level required by each volcano, especially in comparison with others. Ewert et al. (2005) developed the National Volcano

Table 1 TPV Holocene phonolitic eruptions

Event ID	Eruption Name	Years BP	Total erupted DRE (m^3)	Total erupted mass (kg)	Magnitude scale
1	Montaña Reventada	895	138,194,471.1	3.45486E+11	4.5384
2	Lavas Negras	1,150	474,452,978	1.18613E+12	5.0741
3	Roques Blancos	1,714–1,790	833,890,093.4	2.08473E+12	5.3190
4	Montaña Blanca	2,020	107,382,578.7	2.68456E+11	4.4289
5	Montaña Majua	3,520?	69,744,811.59	1.74362E+11	4.2415
6	El Boqueron	2,528–5,660	44,283,790.64	1.10709E+11	4.0442
7	Cañada Blanca	2,528–5,911	70,115,211.27	1.75288E+11	4.2438
8	Abejera Baja	5,486	285,594,326	7.13986E+11	4.8537
9	Abejera Alta	5,911	361,123,567.2	9.02809E+11	4.96
10	Pico Cabras	5,911–7,900	285,594,326	7.13986E+11	4.8537
11	Abrunco	<10,000	2,086,022.525	5,215,056,313	2.7173
12	Montaña de la Cruz	<10,000	131,444,541.8	3.28611E+11	4.5167
13	Arenas Blancas	<10,000	101,381,078.6	2.53453E+11	4.4039
14	Montaña de los Conejos	≥10,000	70,723,423.92	1.76809E+11	4.2475
15	Bocas de Maria	≥10,000	23,265,710.9	58,164,277,258	3.7647
16	Montaña Las Lajas	≥10,000	10,769,291.55	26,923,228,872	3.4301

Ages from Carracedo et al. (2007) and Olaya García (unpublished data)

Early Warning System (NVEWS) intending to assess the threat posed by US volcanoes, proposing an analysis scheme based on several factors. These factors can be divided into two main groups: those associated with hazard and those associated with exposure of human, social and economical elements potentially affected by the hazard, i.e. with risk. The product of the sums of all the factors of each type gives a threat score that allows the classification of the US volcano in four categories, grouped by the required monitoring level.

Other authors have applied NVEWS analysis to other volcanoes, such as Kinvig et al. (2010), who recently applied this analysis to Nysiros volcano (Greece). In this paper, we applied the NVEWS scheme in order to quantify the threat posed by TPV and to facilitate the comparison with other volcanoes. Scores given to each factor (labelled from (a) to (y)) and the total result are shown in Table 2. Brief explanations of the factors we took into account are given in the next sections, while Table 2 caption indicates how the corresponding scores were assigned and lists the bibliographic/web sources used.

Hazard factors

TPV includes two stratovolcanoes (a), with major explosive activity during the last 10,000 years (see Table 1) with calculated magnitudes up to 5. In a few cases where associated pyroclastic fall deposits have been preserved, it has been also possible to estimate a Volcanic Explosivity Index (VEI) value, which combines magnitude, intensity (eruption rate) and explosivity (eruption column high) of the eruption (Newhall and Self 1982), for these particular cases, which ranges from 3 to 4 (b) (d) (see below). The historical period of Tenerife is relatively short as it starts with the conquering of the island by the Spanish crown in 1496. Since then, four eruptions (all of them basaltic) have occurred on the island, only one on TPV (1798, Chahorra eruption). During the Holocene, at least 16 phonolitic eruptions occurred in TPV as shown in Table 1 (e), including most of the volcanic hazards: pyroclastic flows, lava flows, lahars… (f)(g)(h), although there is no evidence for a volcanic tsunami (j). TPV hydrothermal systems are large enough to justify its potential for hydrothermal explosions (i). This fact plus the steep slopes of their flanks and their history of sector collapses (Ablay and Martí 2000) show its potential for new sector collapses (k). In 2004–2005, an episode of volcanic unrest took place in the island of Tenerife, characterised by a great increase on the seismic activity around the TPV system and changes in the fumarolic system (m)(o).

Exposure factors

The first exposure factor measures the population in a circle of 30 km centred on the volcano. This circle centred on TPV comprises most of Tenerife Island, leaving out only the Anaga peninsula, which includes the two most populated municipalities of the island (Santa Cruz and San Cristóbal de la Laguna), so almost the same population lives inside and outside the circle. Based on public data published by the National Institute of Statistics (http:\\www.ine.es) for 2009, the population included in the circle is

Table 2 TPV NVEWS scoring factors

		Scoring ranges
Teide–Pico Viejo hazard factors		
(a)	Volcano type	1
(b)	Maximum Volcanic Explosivity Index	1
(c)	Explosive activity in past 500 years?	0
(d)	Major explosive activity in past 5,000 years?	1
(e)	Eruption recurrence	1
(f)	Holocene pyroclastic flows?	1
(g)	Holocene lahars?	1
(h)	Holocene lava flow?	1
(i)	Hydrothermal explosion potential?	1
(j)	Holocene tsunami?	0
(k)	Sector collapse potential?	1
(l)	Primary lahar source?	0
(m)	Observed seismic unrest?	1
(n)	Observed ground deformation?	0
(o)	Observed fumarolic or magmatic degassing?	1
	Total of hazard factors	11
Teide–Pico Viejo exposure factors		
(p)	Log_{10} of Volcano Population Index at 30 km	4
(q)	Log_{10} of approximate population downstream or downslope	0
(r)	Historical fatalities?	0
(s)	Historical evacuations?	0
(t)	Local aviation exposure	2
(u)	Regional aviation exposure	5
(v)	Power infrastructure	1
(w)	Transportation infrastructure	1
(x)	Major development or sensitive areas	1
(y)	Volcano is a significant part of a populated island	1
	Total of exposure factors	15
	Sum of all hazard factors × Sum of all exposure factors = Relative threat ranking	165

We tried to use conservative values for the scores of each factor in order to minimise the uncertainty caused by the lack of data in some cases, so that the threat score obtained is a minimum. (a) Volcano type tries to quantify how dangerous a volcano is and has two categories: type 0 volcanoes, including cinder cones, basaltic volcanic fields, shields, tuff rings and fissure vents, and type 1 volcanoes which are generally more explosive, including stratovolcanoes, lava domes, complex volcanoes, maars and calderas. (b) The VEI is an indicator of the explosive character and size of an eruption (Newhall and Self 1982). In the NVEWS scheme, the scores are 1 for VEI of 3–4, 2 for a VEI of 5–6 and 3 for a VEI of 7–8. (c) Explosive activity and (d) major explosive activity refer to the presence of repeated explosive episodes in the past eruptions record, as scores as 1 for VEI≥3 within the last 500 years and VEI≥4 within the last 5,000 years, respectively. (e) Eruption recurrence: It scores 4 if the eruption interval is 1–99 years, 3 if it is 100–1,000, 2 if it 1,000 to several thousands, 1 if eruption interval is 5,000–10,000 years and 0 if there are not Holocene eruptions. For factors (f) to (o), possible scores are 1 or 0 if the answer is yes or not, respectively (see Ewert et al. 2005 for more details). For exposure factors and their possible scores, see text and Ewert et al. (2005, p. 47). Information sources: (a) Ablay and Martí (2000); (b) García et al. (2011); (c)–(e) Carracedo et al. (2007); (f)–(h) Martí et al. (2008b) and García et al. (2011); (i) Del Potro and Hurlimann (2008) and Rodriguez Losada et al. (2009); (k) Ablay and Martí (2000) and Ablay and Hürlimann (2000); (m) Spanish Geographical Institute (http://www.ign.es), García et al. (2006) and Martí et al. (2009); (o) Hernández et al. (1998), Pérez et al. (2005) and Martí et al. (2009); (p) Spanish National Institute of Statistics (http:\\www.ine.es); (t)–(u) Association of Spanish Airports (http://www.aena.es)

about 442,000. However, Tenerife is one of the main tourist destinations of Europe, so the touristic population should also be taken into account. During 2009, the mean daily hotel occupancy in the island was about 52,000 tourists, so the value of (p) factor can reach 5 (see Table 2). There is almost no difference in the population downstream of the volcano that lies beyond, versus within, the above-mentioned circle.

No fatalities have been recorded during eruptions at Tenerife. A massive evacuation occurred during 1706,

when basaltic lava flows almost destroyed Garachico, the former capital of the island, but that basaltic eruption had its vent on the Santiago rift, not on TPV (s).

TPV poses a significant threat to aviation, as all the eight Canarian airports fall in a circle of 300 km radius centred between the two stratovolcanoes. The mean number of daily passengers in this circle was around 82,200 during 2009 (t)(u). The Canary Islands constitute one of the main civil aviation corridors for flights from Europe to Central and South America and vice versa.

Evaluation of temporal and spatial probability of a phonolitic eruption in TPV

Temporal probability

Mid-/long-term assessment of the temporal probability of occurrence of a volcanic eruption of certain (or exceeding a) magnitude or size is usually computed by analysing the sequence of past eruptions in a volcano and characterising them by a measure of their size or magnitude (Pyle 2000). This may be indicated as magnitude, understanding it as a measure of the total volume of magma erupted, or as VEI. Unfortunately, only a small proportion of eruptions have been witnessed, so for most cases the data required to estimate the size of an eruption have to be collected in the field from physical volcanology studies of the eruption products. An additional complexity comes from the fact that it is very common that the record of volcanic eruptions is incomplete, especially for the pre-historical section of the record and the low-magnitude eruptions, and this may significantly affect the accuracy and completeness of the reconstruction of the volcano's eruption record.

In the case of TPV, at least 16 phonolitic eruptions can be identified on stratigraphic and geochronological bases in the Holocene (Carracedo et al. 2007; Martí et al. 2008a; Olaya Garcia, unpublished data, 2011). At least 15 of these eruptions were of magnitude M greater than 3, based on minimum volumes exposed (Table 1) and applying the equation proposed by Pyle (2000) to calculate the magnitude scale as follows:

$$\text{Magnitude}(M) = \log_{10}(\text{total erupted mass, kg}) - 7 \qquad (1)$$

For example, the magnitude for the first eruption in Table 1 "Montaña Reventada" is $M = \log_{10}(3.45486\text{E}+11) - 7 = 4.5384$. Some of these eruptions also included explosive phases that generated fall deposits of different extents and thicknesses. Despite the poor preservation of these deposits, their characterisation in terms of grain size and thickness variations has allowed us to assign a minimum VEI value to each of them. It was not possible to determine with precision the total volume corresponding to the fall deposits, so the total volume of erupted magma (magnitude) for the eruptions including effusive and explosive phases was probably underestimated compared to those volumes for eruptions without associated fall deposits. The absence of pyroclastic deposits does not necessarily mean that these other eruptions were not explosive at all, as it is also possible that the corresponding pyroclastic deposits could have been completely eroded. For this reason, we used M, principally based on the volume of lavas exposed, instead of VEI, as it offers a better estimate of the minimum size of the TPV eruptions and allows comparisons among them.

In this paper, we used a non-homogeneous Poisson process with a generalized Pareto distribution (GPD) as an intensity function (NHGPPP) to model the TPV time series and compute the temporal probabilities of at least one eruption in a given time interval (Coles 2001; Mendoza-Rosas and De la Cruz-Reyna 2008; Sobradelo et al. 2011). NHGPPP is an extreme value theory statistical method, very robust for modelling small time series of incomplete geological records and useful for obtaining estimates of the probability of intermediate- to high-magnitude eruption events (Coles 2001). We used this method because the incomplete geological record of the eruption products from TPV requires an estimation technique that is not very sensitive to the fact that we have a small dataset. This method is also appropriate when we have a time series of extreme values like this which is a dataset containing very few, probably incomplete, data. The GPD is a robust tool which allows modelling extreme values, such as the "rare" high-magnitude eruptions.

The fact that there is one eruption documented with $M<3$ and that the number of eruptions with $M=3$ is significantly lower than those of $M=4$ makes us believe that the catalogue may be incomplete. To account for the possible missing data or inaccuracies in the catalogue, the occurrence rates for Ms 4 and 5 were used to extrapolate unobserved records using the best fit to the class VEI values of eruptions. In order to estimate these values, we used the power law described by Newhall and Self (1982), which was originally defined for VEIs but that in our case is applied to magnitudes, as higher magnitudes also imply potentially higher VEI. We therefore redefine this power law by saying that the eruption occurrence rate λ_M (number of eruptions per unit time) of each class M is related to the eruption size as:

$$\log \lambda_M = a - b \times M \qquad (2)$$

where a and b are constants that describe the power law decay of occurrences with increasing size M over a given time interval.

In order to apply the NHGPPP, we used the exceedance over a threshold (EOT) to sample the original data; this is $X_i>u$ for some value of i. The reader will find a complete explanation of this methodology in Coles (2001) and Mendoza-Rosas and De la Cruz-Reyna (2008). Sobradelo et al. (2011) have applied the same method to the Canary Islands historical records.

The EOT method includes all the values of the variable that exceed an a priori established threshold, u, fixed according to the model needs, providing a physically based definition of what must be considered an extreme event. The choice of the threshold value has a strong subjective component. This random variable is defined by the transformed random variable $Y=u$, for all $X_i>u$ where Y is the excess over the threshold u, the M value in our case. The parameter that was used as random variable to estimate the probability of occurrence of a future eruption and thus the volcanic hazard was the time interval T between eruptions, also called repose period, together with the M size.

Figure 2 shows a scatterplot of the repose periods, where the duration of the interval T_i+1 between two successive eruptions is plotted against the duration of the previous repose interval T_i. The diagram in Fig. 2 shows a large dispersion of points. The correlation coefficient between consecutive repose times is 0.5457, indicating a low serial correlation. We do not have enough evidence to say that consecutive repose intervals are time-dependent based on these data, so we assume independence of repose times for the purpose of this study.

For the particular case of volcanic eruptions, the size of the eruptions and the time of their occurrence are viewed as points in a two-dimensional space, which formally is the realisation of a point process. The intensity measure 321 $\Lambda_B>u$ of this two-dimensional Poisson process on the space $B=[t_1,t_2]\times(u,\infty)$ with $[t_1,t_2]\subset[0,1]$ is given by

$$\Lambda_B=(t_2-t_1)\left(1-\frac{\beta(1-u)}{\theta}\right)^{1/\beta} \tag{3}$$

where β and θ are the parameters of the GPD, computed using a diagnostic method introduced by Davison and Smith (1990) which also serves to decide how well the model fits the data. This method is based on the property that the mean excess over a threshold u, for any $u>0$, is a linear function of u. The mean excess is defined as

$$E(X-u|X>u)=\frac{\theta-\beta u}{1+\beta} \tag{4}$$

for $\beta>1$, $u>0$ and $(\theta-\beta u)>0$. The expected value was estimated using the sample mean excess computed from the data. In Fig. 3, we plot the sample mean of the excesses versus their thresholds. The x-axis is the threshold and the y-axis is the sample mean of all excesses over that threshold. As we can see, the mean excess follows a nearly straight line, with an R^2 of 0.9996, suggesting a good fit. A regression line for the mean of exceedances over the threshold has been added to confirm the series follows the GPD.

Hence, according to Davison and Smith (1990), the preceding results indicate that the NHGPPP was satisfactory and appropriate to model our data. The Pareto generalized parameters for the process, derived from the regression parameters in Fig. 3 and Eq. 4, are 0.768 for shape and 5.689 for the scale. Using Eq. 2, we estimated the intensity $\widehat{\lambda}$ of the NHGPPP and obtained the probability estimations of at least one eruption of a certain M size in a given time interval. Table 3 shows the probability of having at least one eruption $\Pr(X\geq1)$ computed as 1 minus the probability of having no eruption $1-\Pr(X=0)$ of a certain M size in a given time window, estimated using the NHGPPP with intensity rate $\widehat{\lambda}$. To measure the volatility of the estimated

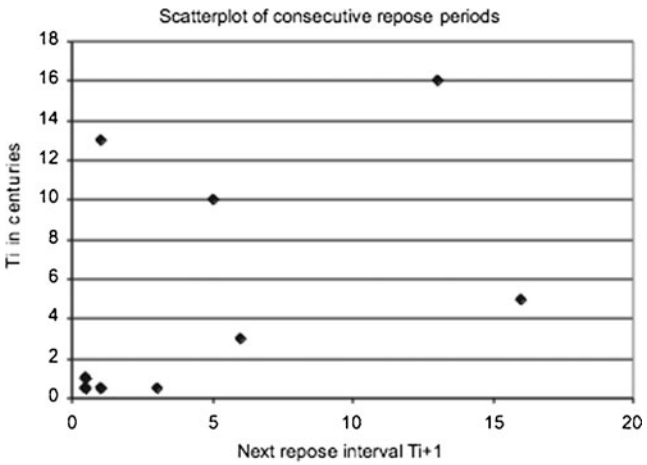

Fig. 2 Scatterplot of consecutive repose intervals for TPV time series

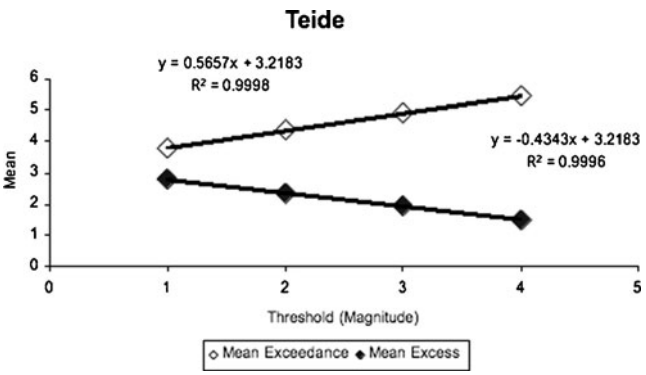

Fig. 3 Plot of exceedance and excess mean vs. threshold for TPV

Table 3 Probability of at least one event of size $M>x$ in the next t years in the TPV complex estimated with a NHGPPP

Years	Pr(X=0) (%)	$\widehat{\lambda}$	Pr(X=>1) (%)	$\widehat{\sigma}$
M>2				
1	99.8	0.002	0.2	0.0002
20	95.4	0.047	4.6	0.003
50	88.9	0.118	11.1	0.007
100	79.0	0.236	21.0	0.011
500	30.7	1.180	69.3	0.009
	1,000	09.4	2.360	90.6
	0.002			
M>3				
1	99.8	0.002	0.2	0.0001
20	96.3	0.038	3.7	0.003
50	90.9	0.095	9.1	0.006
100	82.7	0.190	17.3	0.010
500	38.6	0.951	61.4	0.011
	1,000	14.9	1.901	85.1
	0.003			
M>4				
1	99.9	0.001	0.1	0.0001
20	97.1	0.029	2.9	0.002
50	92.9	0.073	7.1	0.005
100	86.4	0.146	13.6	0.008
500	48.1	0.732	51.9	0.013
	1,000	23.1	1.464	76.9
	0.006			
M>5				
1	99.9	0.001	0.1	0.0001
20	97.9	0.021	2.1	0.002
50	94.9	0.052	5.1	0.004
100	90.0	0.105	10.0	0.007
500	59.2	0.525	40.8	0.014
	1,000	35.0	1.050	65.0
	0.010			
M>6				
1	99.9	0.001	0.1	0.0001
20	98.7	0.013	1.3	0.001
50	96.7	0.033	3.3	0.002
100	93.6	0.066	6.4	0.004
500	71.8	0.332	28.2	0.013
1,000	51.5	0.663	48.5	0.014

(Pr(X=0) and Pr($X\geq1$) are the probability of having no eruption and the probability of having at least one eruption, respectively, of a certain size in a particular time interval; is the estimated parameter rate for the NHGPPP, and is the estimated standard deviation for the Pr($X\geq1$) computed with the NHGPPP, based on the delta method)

probabilities, we computed the standard deviation $\widehat{\sigma}$ of the estimator using the delta method to determine its asymptotic distribution.

Spatial probability

Felpeto et al. (2007) and Martí and Felpeto (2010) have proposed the term volcanic susceptibility for the spatial probability of vent opening. Martí and Felpeto (2010) compute this probability for long-term analysis based on a multicriteria analysis. Similarly, Marzocchi et al. (2010) in their system BET-VH compute the spatial probability based on a Bayesian approach.

The evaluation of susceptibility of phonolitic eruptions in the island of Tenerife made by Martí and Felpeto (2010) assumed that the main stress field in the island has remained constant for the last 35 ky. The input data used were the location of felsic centres and felsic alignments younger than 35 ka, all of them belonging to TPV complex. Intensity functions for each dataset were computed separately applying the kernel technique (Connor and Hill 1995; Martin et al. 2004), and finally, the susceptibility map (Fig. 4) was computed assuming a non-homogeneous Poisson process whose intensity function is a combination of the previously calculated functions (see Martí and Felpeto 2010 for details).

Spatiotemporal probability

Once both the temporal and the spatial probability of occurrence of a phonolitic eruption in TPV were calculated, the next step consisted in the computation of a map that, for a specific time interval t and a specific magnitude M, showed the probability for each cell of hosting a future vent. We assumed to have N possible cells that could host a future vent and that we had computed the spatial probability of each cell using the spatial probability method explained above. Let s_i be the spatial probability of a vent opening in cell i, for i ranging from 1 to N. Let $P_{t,M}$ be the temporal probability of having an eruption (and consequently a vent opening) of magnitude M within the next t years, computed using the NHGPPP explained earlier. The group of N cells used to compute the spatial probability are mutually exclusive and exhaustive; that is, the same vent cannot be in more than one cell at the same time, and the sum of all s_i is 1.

As this paper is a first step to assess the spatiotemporal probability for TPV, for simplicity in the methodology, we assumed the two probabilities were independent. This means that the probability of having an eruption of size M in $t$years does not depend on the location. In other words, both the temporal and spatial probabilities were calculated separately using methods previously developed independently of one another. In this respect, we may be underestimating the total probabilities. Further work is needed to develop a more complete model which takes into account the three variables together: time, size and location.

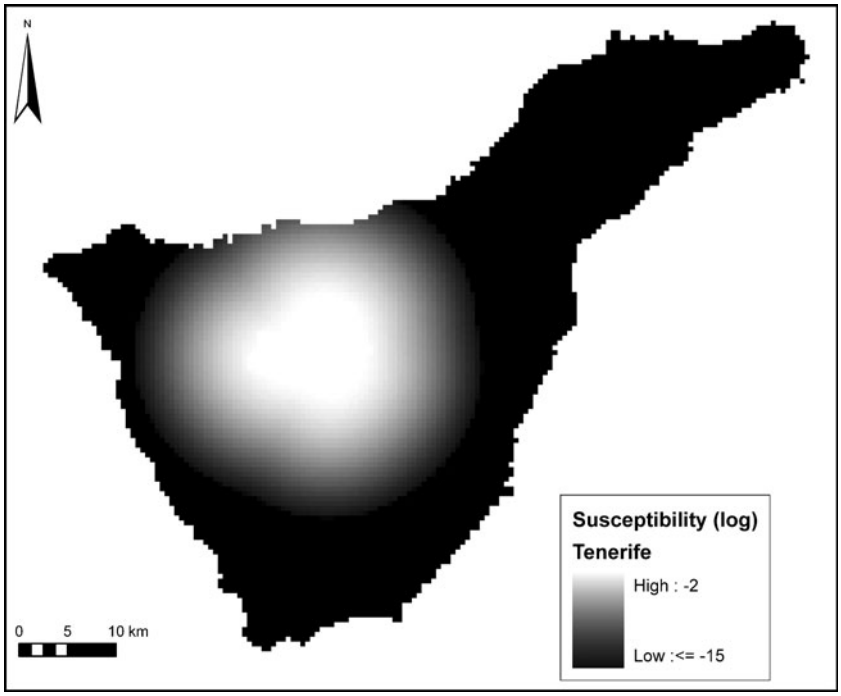

Fig. 4 Susceptibility map of phonolitic eruptions in Tenerife with cell size of 500×500 m (from Martí and Felpeto 2010)

The spatiotemporal probability of having an eruption of magnitude M within the next t years in cell i is:

$$qi_{t,M} = s_i \times p_{t,M} \tag{5}$$

For i=1, …, N; M=2, 3, 4, 5, 6; t=1, 20, 50, 100, 500, 1,000where

$$\sum_{i=1}^{N} s_i = 1 \tag{6}$$

the cells are exhaustive and

$$\sum_{i=1}^{N} s_i \times p_{t,M} = p_{t,M} \tag{7}$$

With the aim of obtaining the group of N cells that are mutually exclusive and exhaustive that represent TPV system, we selected from Fig. 4 the area of susceptibility values higher than 3×10^{-5} that encloses the 98.7% of the total probability of the susceptibility map. The values of this area were normalized by dividing by the integral across the whole area, obtaining an exhaustive group of cells. Figure 5 shows an example of how the spatiotemporal probability is computed using Eq. 5, for the probability of having an eruption of magnitude >2 in the next 20 years.

Eruptive scenarios

In order to illustrate potential future phonolitic eruptions on TPV, we have computed several representative scenarios. We chose lava flows, ash fall and pyroclastic density currents (PDC) as the three main hazards that can be expected in a phonolitic eruption from TPV, based on what can be seen in the geological record (Martí et al. 2008b; García et al. 2011)

Simulations were performed considering different vents, including central vents located at both craters of Teide and Pico Viejo and flank vents located around TPV edifice at approximately 2,300 m a.s.l. Both kinds of eruptions can be expected in TPV, as shown in the Holocene eruptive record and in numerical studies simulating magma emplacement inside TPV (Martí and Geyer 2009). All the scenarios have been computed with the GIS-based system VORIS (Felpeto et al. 2007, www.gvb-csic.es).

Lava flows

The numerical simulation of phonolitic lava flows were computed with a maximum slope model (Felpeto et al. 2001). Parameters required by the model are maximum flow length and height correction, whose values were chosen based on recent phonolitic lava flows (lmax= 30 km, hc=10 m). Simulations were performed over a digital elevation model (DEM) with 50 m of cell size. Due to the morphology of both central peaks and the characteristics of the model selected, Teide central vent was considered to be an area of 0.17 km^2 centred in the peak, and Pico Viejo central vent was considered to be an area of 0.17 km^2 around the crater rim. The result of each simulation is a probability map showing the probability of

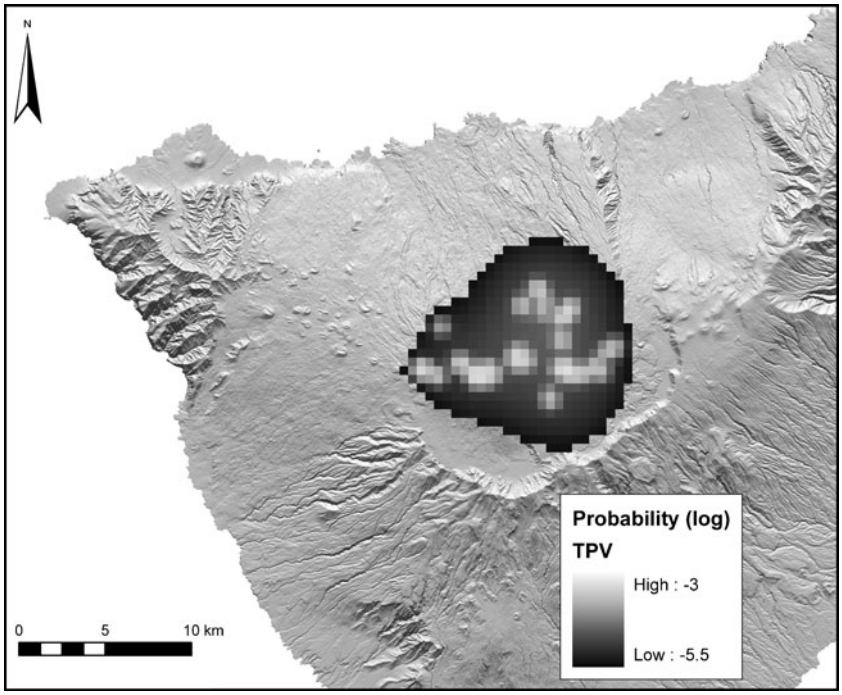

Fig. 5 Probability map of a phonolitic eruption $M \geq 3$ in the next 20 years (cell size 500× 500 m). The area outside the central *black-grey* zone is assumed to have a zero probability for hosting phonolitic eruptions with $M \geq 3$ in the next 20 years

each cell to be invaded by phonolitic lava flows. Examples of the simulations for the central vents are shown in Fig. 6.

PDCs

Numerical simulations of PDCs were computed with the energy cone model (Malin and Sheridan 1982; Sheridan and Malin 1983), over a DEM with a 50-m cell size. The values chosen for the input parameters are 200 m for equivalent collapse height and 0.21 for Heim coefficient. The result of each simulation is the area potentially reachable by the PDC and the expected flow velocity value in each cell, computed following Toyos et al. (2007). Figure 7 shows the simulations for both central eruptions, where the potentially reachable area is very wide, and a simulation for a flank vent at the north, whose reachable area is considerably smaller.

Ash fall

Ash fall from phonolitic eruptions in TPV could be expected from different eruptive styles. Those considered

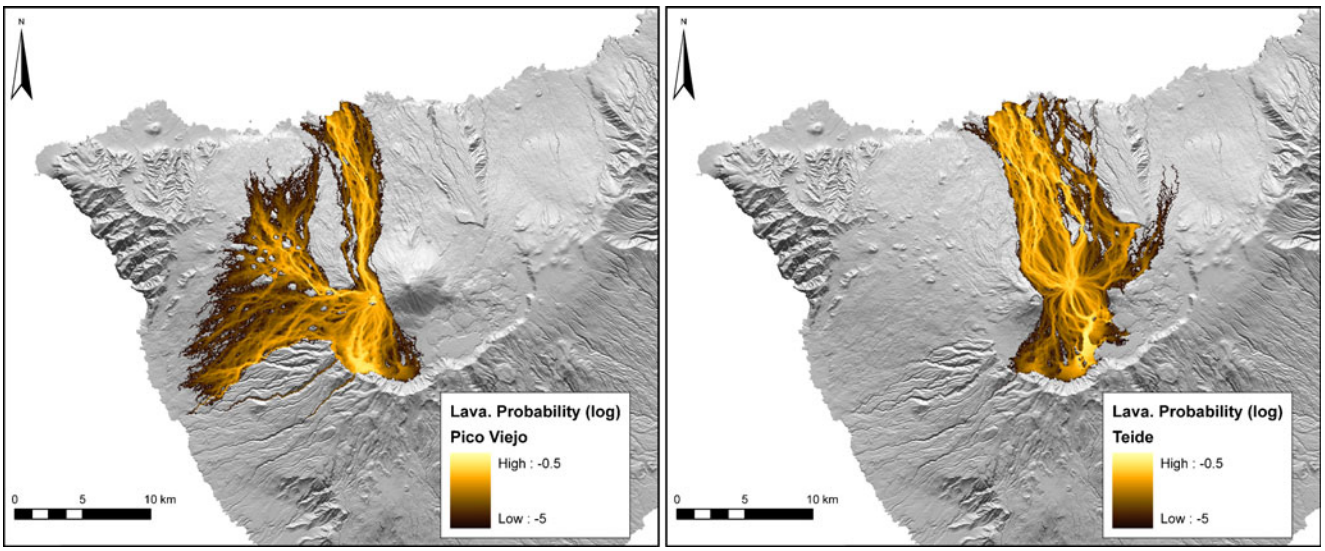

Fig. 6 Phonolitic lava flow scenarios for Pico Viejo (*left*) and Teide (*right*) central vents (see text for details)

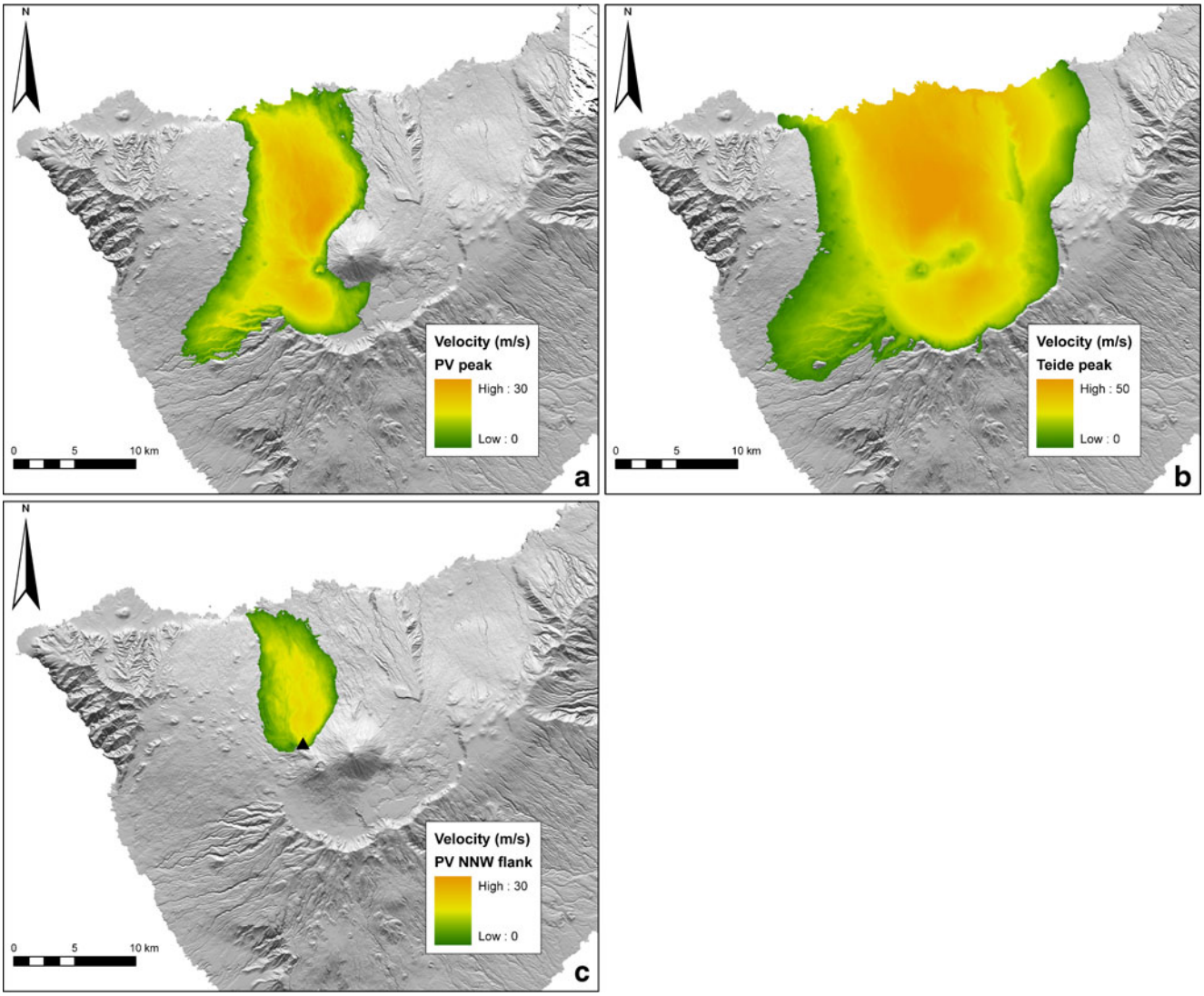

Fig. 7 PDC scenarios. **a** Pico Viejo central vent, **b** Teide central vent and **c** vent located on black triangle (see text for details)

in this paper are violent strombolian, subplinian and plinian, which are the most significant ones in terms of probability of occurrence according to the long-term event trees published for TPV (Martí et al. 2008a; Sobradelo and Martí 2010). All the simulations were done considering a vent located in the northern flank of TPV at the same distance from the two craters. The wind data used were obtained from a deep atmospheric sounding of an arbitrarily selected day (1 April 2010).

Plinian and subplinian events were simulated with the advection–diffusion model described in Folch and Felpeto (2005) considering the source term described by

Table 4 Summary of the input parameters used in the simulations of ash fallout scenarios

Model	Violent strombolian FALL3D	Subplinian Folch and Felpeto (2005)	Plinian Folch and Felpeto (2005)
Column height	1.4 km	8 km	25 km
Volume emitted		0.05 km^3	0.8 km^3
Mass flow rate	5×10^4 kg/s		
Duration	3 h		
Mean φ/φ standard deviation	1/1	−2/1.5	0/1.5

the Suzuki (1983) expression. Simulation of violent strombolian eruption was computed with FALL3D 6.1 model (Costa et al. 2006). The input parameters for the subplinian eruption reproduce the best known explosive event of TPV, the Montaña Blanca eruption (Ablay et al. 1995; Folch and Felpeto 2005). Due to the lack of detailed data of deposits from the other two eruption types, the input parameters were chosen based on bibliographic data from other volcanoes. A summary of the input parameters is shown in Table 4. Figure 8 shows the results of the simulations.

Validation of results

Based on existing geological data, we assessed the volcanic hazard for Teide–Pico Viejo as probabilities of occurrence of at least one eruption exceeding a certain magnitude over different time periods. Like this, for example, given the data and assuming a future behaviour of the volcano similar to the past 10,000 years, we can say that in the next 50 years, there will be at least one eruption on TPV of magnitude $M>2$ with a probability of 11.1%. This probability jumps to 21.0% for the next 100 years, and a probability of 90.6% is obtained for the next 1,000 years (Table 3). The escalation rate is more significant in the first 500 years (Fig. 9).

To validate the model, we compared the probability results in Table 3 with the probability obtained from the Bayesian event tree model of Sobradelo and Martí (2010). The event tree was built to outline all possible eruptive scenarios at TPV and to assign a long-term probability of occurrence to each scenario. The Bayesian probabilities were computed only for the time window of 100 years. Therefore, when comparing with the results from the

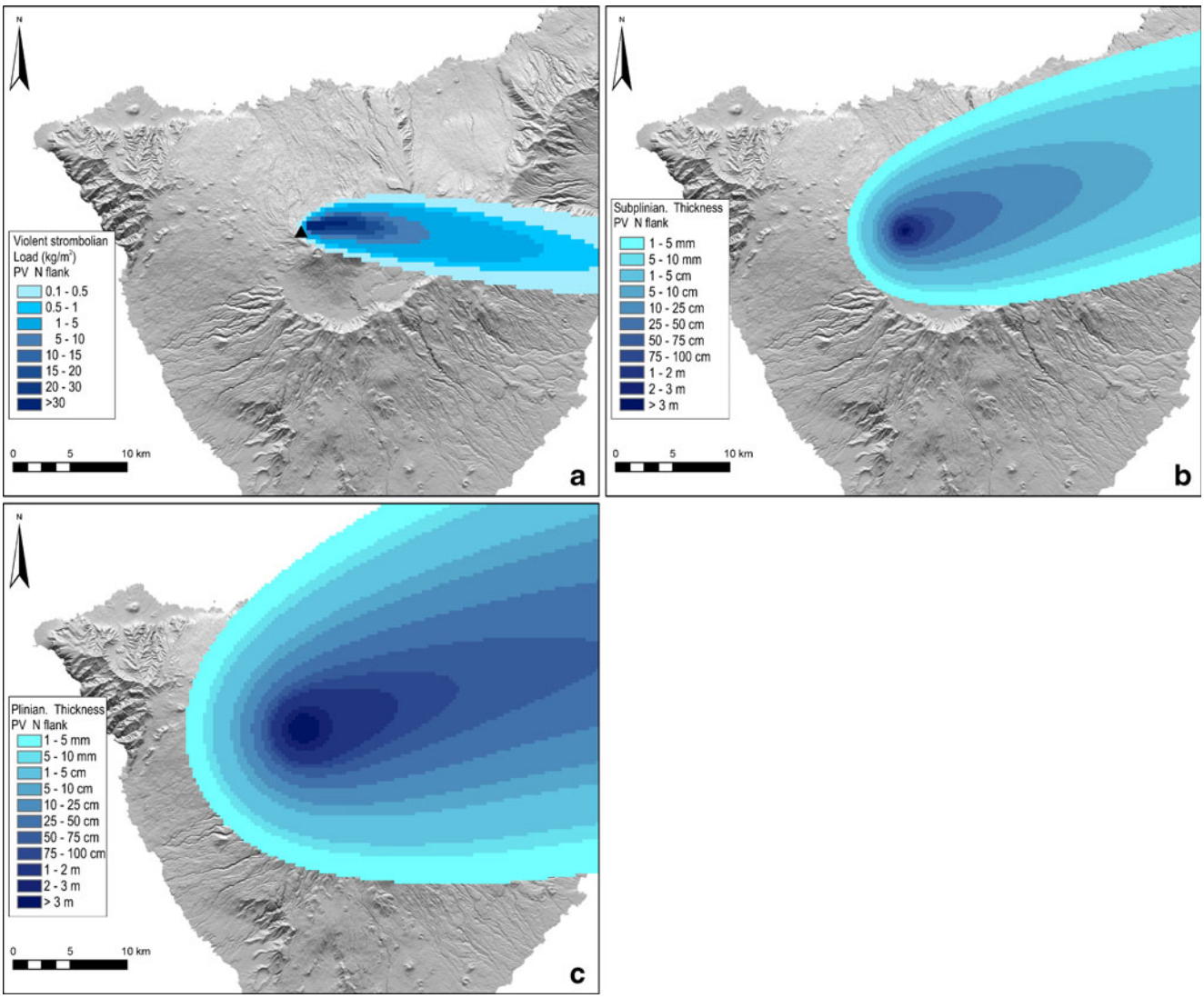

Fig. 8 Ash fall scenarios. **a** Violent strombolian, **b** subplinian and **c** plinian (see text for details)

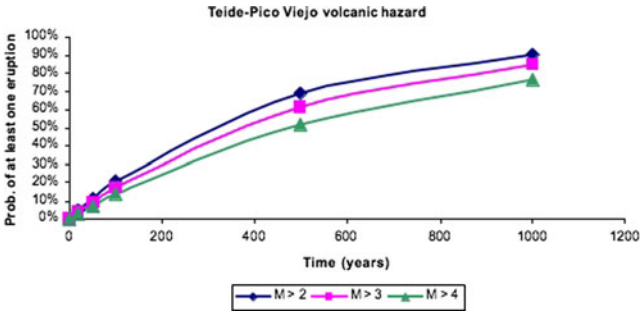

Fig. 9 Probabilities calculated with NHGPPP of at least one eruption, with a size *M* greater than a given size threshold for the TPV eruptive series

extreme value theory method in Table 3, we can only compare the probabilities of an eruption of different sizes within one time window of 100 years. Table 5 shows on the second row the probabilities of having a magmatic unrest episode with magmatic eruption of phonolitic composition anywhere in the TPV during the next 100 years, computed using the Bayesian event tree model. The extreme value method was built using the number of eruptions occurring over time intervals, expressed in terms of the eruption occurrence rate for each class magnitude *M*, and extrapolated using the more complete records in the catalogue (Mendoza-Rosas and De la Cruz-Reyna 2008). The extreme value method takes into account the possible incompleteness of the data by extrapolating from the most reliable data points. The Bayesian model, on the other hand, is a subjective approach which starts with the state of total uncertainty and computes the final probabilities based on an incomplete data catalogue, without further adjustment. This explains why the Bayesian probability in Table 5 second row for magnitude >4 (3.0%) falls abruptly relative to that for magnitude >3 (11.2%). The NHGPPP gives more weight to the more extreme events, such as events of magnitude >4 (13.6% versus 3.0%). For events of magnitude >2, the Bayesian probability (14.2%) is lower than the NHGPPP probability (21.1%) since the latter uses a larger number of extrapolated occurrences for events of magnitude 3, while the Bayesian method computes the results based on the single event registered in the catalogue. This comparison allows us to validate the consistency of the probability results obtained here, but also reassures us in the choice of using the extreme value method to overcome the limitations in the data.

Table 5 Comparison of probability results from Bayesian event tree (Sobradelo and Martí 2010) and NHGPPP presented in this paper

Time (years)	*M*>2 (%)	*M*>3 (%)	*M*>4 (%)	
100	21.1	17.3	13.6	Extreme value theory
100	14.2	11.2	3.0	Bayesian event tree

See text for explanation

Discussion

The TPV constitutes one of the main potentially active volcanic complexes in Europe but traditionally has not been considered to be explosive and to represent a significant threat to the island of Tenerife. However, the results obtained in this work suggest that hazard associated with TPV is not negligible and should be carefully considered in order to quantify volcanic risk in Tenerife.

Although NVEWS (Ewert et al. 2005) was specially designed to identify the level of monitoring required by US volcanoes in order to define an effective early warning system, it offers a simple approach for classifying active volcanoes according to their level of threat. In this sense, we consider NVEWS perfectly applicable to TPV, and the resulting value representative of the real level of threat TPV represents for Tenerife. The NVEWS analysis of volcanic threat, even assuming very conservative values for some of the evaluated factors, gives a value of 165, which classifies TPV as a very high threat volcano, comparable to Redoubt, Crater Lake or Augustine in the USA. It is worth mentioning that the level of volcano monitoring in Tenerife has improved significantly since 2004, when the Spanish Geographic Institute (IGN) implemented its multiparametric surveillance network (see www.ign.es), so that it can be said that TPV now has the required monitoring level that is appropriate to a very high threat volcano according to the NVEWS (Ewert et al. 2005).

Eruptions of volcanoes considered “dormant” or “inactive” have produced major disasters in the past. The volcanic hazard from volcanoes with a long recurrence interval tends to be ignored, especially when little or no historical data exist. This is the case for TPV. The probability results obtained here using extreme value theory, consistent with the results obtained in previous work using Bayesian inference, confirm once again the existence of significant volcanic hazard from TPV. This together with others signs of activity mentioned earlier should constitute sufficiently convincing reasons to accept that TPV is an active volcanic complex that may erupt again in the near future. Unfortunately, we have increasing evidence of the sudden awakening of long dormant volcanoes (e.g. Chichón 1982, Unzen 1991, Pinatubo 1991, Montserrat 1995–, Chaitén 2008). Conducting hazard assessment of volcanoes where knowledge of the past volcanological history is poor, geochronological data are scarce and there is not historical eruptive activity and is not an easy task. In these cases, the lack of knowledge of

previous unrest episodes and of the precursors to previous eruptive events precludes using repetitive patterns of precursors to anticipate new eruptions (see Sandri et al. 2004). This is the case at TPV, meaning that we do not know how a future reawakening would manifest and which could be the precursory patterns for new eruptions. Comparison with better known volcanoes, in particular with those that have erupted in recent times and from which we have good monitoring records, could help in predicting the future behaviour of TPV. However, experience demonstrates that each volcano has its own behaviour and that the definition and application of common patterns to interpret eruption precursors, particularly if we are dealing with composite volcanoes, should be done with care.

In the case of TPV, Martí et al. (2008a) indicated that its eruptive behaviour is controlled by the close relationship between deep basaltic and shallow phonolitic magma systems, to the extent that most of the TPV phonolitic products show evidence of magma mingling and/or mixing. From the existing radiometric ages and the stratigraphic relationships between the erupted products, it is clear that most of phonolitic eruptions are preceded by several basaltic eruptions and in some cases both occur simultaneously (e.g. Montaña Reventada, Araña et al. 1994; Wiesmaier et al. 2011). A similar pattern has also been observed in the pre-TPV central complex (Las Cañadas Edifice) (Martí et al. 2008a). Therefore, it is logical to infer that similar mechanisms have controlled the accumulation, evolution and eruption of magma at shallow levels during the past history of the Tenerife central complex, despite a progressive decrease in the magma available with time. In other words, the eruption of phonolitic magma at TPV is directly dependent on the amount of basaltic magma delivered at shallow depths into the central system. We then suggest that the eruption frequency at TPV is related to the eruption frequency of basaltic volcanism on Tenerife, which in historical times has produced eruptions in 1492, 1705, 1706, 1798 and 1909, with the last eruption from Teide dated at 1,150 years B.P. (Carracedo et al. 2007).

The main phonolitic erupted products of TPV correspond to lava flows that were emplaced towards the south into Las Cañadas depression and to the north in the Icod and La Orotava valleys. Most of the phonolitic lavas from TPV are clastogenic lavas formed by agglutination of large pyroclastic fragments generated in fire fountaining episodes. The rheological properties and flow behaviour of these lavas (Dingwell et al. 1998; Giordano et al. 2000; Gottsmann and Dingwell 2001) are characterised by a low viscosity at relatively low temperatures, which allow them to flow for long distances preserving an average thickness of tens of metres. In some cases, these lavas have flowed down into the Icod valley for more than 16 km reaching the coast, an area that today is highly populated. These lavas typically preserve a considerable amount of magmatic gas. This is consistent with the relative large amount of volatiles found in the TPV phonolites (Ablay et al. 1995). An effect of this high content of gas in the TPV lavas is that they may transform into block and ash flows when they collapse gravitationally in slope breaks. Deposits of such pyroclastic density currents have been found in stratigraphic continuity with some lavas inside the gullies of the Icod valley, sometimes reaching the coast or being transformed into debris flow deposits at distal facies (García et al. 2011).

In addition to the fragmental origin of most of the TPV lavas and their occasional explosive transformation into pyroclastic density currents, there is evidence of larger explosive eruptions at TPV (García et al. 2011). This evidence is provided by the presence of discontinuous outcrops of pumice fall deposits, but their precise stratigraphic location in the TPV eruptive record is still not known. However, we can confirm that at least three phonolitic explosive eruptions of subplinian dimension, or perhaps even plinian, different from that of the already known Montaña Blanca eruption (Ablay et al. 1995; Folch and Felpeto 2005), have occurred from TPV during the Holocene. Moreover, the presence of ignimbrites is also confirmed in the eruption record of TPV, some of them with minimum run-out distances of several kilometres as it is indicated by the remnants of these deposits found in the Icod Valley, but which could have reached the coasts and entered the sea if we compare them with other ignimbrites of similar characteristics and volume (e.g. Calder et al. 1999; Loughlin et al. 2002). The ignimbrites may have derived either from collapse of eruption columns or from gravitational collapse of domes and clastogenic lava flows. This second option is certainly at least the origin for the block and ash deposits found in the Icod Valley, where the steep topography has facilitated such processes (García et al. 2011).

Therefore, we have considered in our analysis fall deposition and PDC hazards, in addition to lava flows, as representative of the potential hazards that might occur in a future eruption of TPV. The scenarios we have generated allow us to assess their potential extent. All these primary hazards would today easily reach the main populated areas to the north of TPV but could even reach other important locations on the other flanks in the case of plinian and subplinian fallout depending on wind direction.

In addition to the direct hazards that we have assumed in this paper, it is also important to take into account those hazards that could indirectly derive from a renewal of the eruptive activity at TPV. These mainly include debris flows and sector collapses, for which there is also evidence in the recent geological record. Some of the ignimbrites from TPV show evidence of syn-depositional erosion which suggest that heavy rainfalls may have occurred in the area

during these eruptions (García et al. 2011). It is also significant that at the north of Tenerife, important seasonal rainfalls contribute to the erosion and remobilisation of the unconsolidated volcanic material, forming important debris flows. The existence of small-scale sector collapses at the north flank of TPV has also been pointed out by previous authors (Ablay and Martí 2000; Ablay and Hürlimann 2000)

In this study, we have only considered the phonolitic eruptions, as they have the potential to generate the most important hazards at TPV, but it is worth noting that basaltic eruptions have also occurred at this volcanic complex. Most of these eruptions have been strombolian to violent strombolian and have generated lava flows with a variable extent and restricted scoria lapilli deposits. Some significant phreatomagmatic episodes have also occurred related at the former craters of Teide and the present one in the case of Pico Viejo (Ablay and Martí 2000; Perez-Torrado et al. 2004). These phreatomagmatic eruptions produced high-energy pyroclastic surges that flowed to the north for several kilometres into the Icod valley. The extent of these deposits is similar to some of the phonolitic PDCs from TPV, so the hazard scenarios we have developed for phonolitic PDCs also apply to potential basaltic surges emplaced towards the north of TPV.

Conclusions

In this study, we have presented the temporal and spatial probabilities for a phonolitic eruption at TPV and have discussed their implications in terms of hazard assessment. The computation of both temporal and spatial probabilities of a phonolitic eruption at TPV and the characterization of the main expected scenarios constitute the fundamental basis for building up the phonolitic hazard maps for TPV. An important conclusion we can draw from these results is that TPV has to be identified as a volcanic complex that may pose serious hazard on the island of Tenerife and in particular to its northern side. The hazard scenarios we have simulated show that the southern flank of Tenerife is protected by the Cañadas caldera wall against lava flows and pyroclastic density currents, but not against ash fallout. The Icod Valley, and in a minor extent also the La Orotava valley, is directly exposed to most of TPV hazards, in particular to the gravity driven flows, due to the steep topography of that side of the island and the lack of topographic barriers. According to these results and to the fact that Tenerife is a densely populated island, it is strongly recommended that preparedness plans, emergency and disaster management procedures be put into place to quickly react and minimise loss during a volcanic crisis.

Acknowledgements This research has been in part funded by MICINN grant CGL2008-04264 and by a IGN-CSIC collaboration agreement. We thank the National Park of Teide for giving us permission to undertake this research. Many thanks to Laura Sandri and Olivier Jacquet for their constructive reviews

References

Ablay GJ, Hürlimann M (2000) Evolution of the north flank of Tenerife by recurrent giant landslides. J Volcanol Geotherm Res 103:135–159

Ablay GJ, Martí J (2000) Stratigraphy, structure, and volcanic evolution of the Pico Teide–Pico Viejo formation, Tenerife, Canary Islands. J Volcanol Geotherm Res 103:175–208

Ablay GJ, Ernst GGJ, Martí J, Sparks RJ (1995) The 2 ka subplinian eruption of Montaña Blanca, Tenerife. Bull Volcanol 57:337–355

Ablay GJ, Carroll MR, Palmer MR, Martí J, Sparks RSJ (1998) Basanite–phonolite lineages of the Teide–Pico Viejo volcanic complex, Tenerife, Canary Islands. J Petrol 39:905–936

Araña V, Martí J, Aparicio A, García-Cacho L, García-García R (1994) Magma mixing in alkaline magmas: an example from Tenerife (Canary Islands). Lithos 32:1–19

Calder ES, Cole PD, Dade WB, Druitt TH, Hoblitt RP, Huppert HE, Ritchie L, Sparks RSJ, Young SR (1999) Mobility of pyroclastic flows and surges at the Soufriere Hills Volcano, Montserrat. Geophys Res Lett 26:537–540

Carracedo JC (1994) The Canary Islands: an example of structural control on the growth of large oceanic-island volcanoes. J Volcanol Geotherm Res 60:225–241

Carracedo JC, Paterne M, Guillou H, Pérez-Torrado FJ, Paris R, Rodríguez-Badiola E, Hansen A (2003) Dataciones radiométricas (14C y K/Ar) del Teide y el rift noroeste, Tenerife, Islas Canarias. Est Geol 59:15–29

Carracedo JC, Rodríguez-Badiola E, Guillou H, Paterne M, Scaillet S, Pérez-Torrado FJ, Paris R, FraPaleo U, Hansen A (2007) Eruptive and structural history of Teide volcano and rift zones of Tenerife, Canary Islands. Geol Soc Am Bull 119:1027–1051

Carracedo JC, Guillou H, Nomade S, Rodríguez-Badiola E, Pérez-Torrado FJ, Rodríguez-González A, Paris R, Troll VR, Wiesmaier S, Delcamp A, Fernández-Turiel JL (2010) Evolution of ocean-island rifts: The northeast rift zone of Tenerife, Canary Islands. Geol Soc Am Bull. doi:10.1130/B30119.1

Coles S (ed) (2001) An introduction to statistical modeling of extreme values. Springer, London, p 228

Connor CB, Hill BE (1995) Three nonhomogeneous Poisson models for the probability of basaltic volcanism: application to the Yucca Mountain region. J Geophys Res 100:10,107–10,125

Costa A, Macedonio G, Folch A (2006) A three-dimensional Eulerian model for transport and deposition of volcanic ashes. Earth Planet Sci Lett 241:634–664

Davison A, Smith R (1990) Models for exceedances over high thresholds. J Roy Statis Soc 52:393–442

Del Potro R, Hurlimann M (2008) Geotechnical classification and characterisation of materials for stability analyses of large volcanic slope. Engi Geol 98:1–17

Dingwell DB, Hess KU, Romano C (1998) Extremely fluid behavior of hydrous peralkaline rhyolites. Earth Planet Sci Lett 158:31–38

Domínguez Cerdeña I, Del Fresno C, Rivera L (2011) New insight on the increasing seismicity during Tenerife's 2004 volcanic reactivation. J Volcanol Geotherm Res 206:15–29

Ewert J, Guffanti M, Murray T (2005) An assessment of volcanic threat and monitoring capabilities in the United States—framework for a National Volcanic Early Warning System, NVEWS. US Geoll Sur Open-File Rep 1164:1–62

Felpeto A, Araña V, Ortiz R, Astiz M, García A (2001) Assessment and modelling of lava flow hazard on Lanzarote (Canary Islands). Nat Haz 23:247–257. doi:10.1023/A:1011112330766

Felpeto A, Martí J, Ortiz R (2007) Automatic GIS-based system for volcanic hazard assessment. J Volcanol Geotherm Res 166:106–116

Folch A, Felpeto A (2005) A coupled model for dispersal of tephra during sustained explosive eruptions. J Volcanol Geotherm Res 145:337–349

García A, Vila J, Ortiz R, Macià R, Sleeman R, Marrero JM, Sánchez N, Tárraga M, Correig AM (2006) Monitoring the reawakening of Canary Island's Teide volcano. EOS Trans 87(61):65

García O, Martí J, Aguirre-Díaz G, Geyer A, Iribarren I (2011) Pyroclastic density currents from Teide–Pico Viejo (Tenerife, Canary Islands): implications on hazard assessment. TerraNova 23:220–224. doi:10.1111/j.1365-3121.2011.01002.x

Giordano D, Dingwelll DB, Romano C (2000) Viscosity of a Teide phonolite in the welding interval. J Volcanol Geotherm Res 103:239–245

Gottsmann J, Dingwell DB (2001) Cooling dynamics of spatter-fed phonolite obsidian flows on Tenerife, Canary Islands. J Volcanol Geotherm Res 105:323–342

Gottsmann J, Wooller L, Marti, Fernandez J, Camacho A, González P, García A, Rymer H (2006) New evidence for the reawakening of Teide volcano. Geophys Res Lett 33(L20311). doi:10.1029/2006GL027523

Hernández PA, Pérez N, Salazar JML, Nakai S, Notsu K, Wakita H (1998) Diffuse emission of carbon dioxide, methane and helium-3 from Teide volcano, Tenerife, Canary Islands. Geophys Res Lett 25:3311–3314

Kinvig HS, Winson A, Gottsmann J (2010) Analysis of volcanic threat from Nisyros Island, Greece, with implications for aviation and population exposure. Nat Haz Earth Syst Sci 10:1101–1113

Loughlin SC, Calder ES, Clarke A, Cole PD, Luckett R, Mangan MT, Pyle DM, Sparks RSJ, Voight B, Watts RB (2002) Pyroclastic flows and surges generated by the 25 June 1997 dome collapse, Soufriere Hills Volcano, Montserrat. In: Druitt TH, Kokelaar BP (eds) The eruption of Soufriere Hills Volcano, Montserrat, from 1995 to 1999. Mem Geol Soc London 21. Geological Society of London, London, pp 191–209

Malin MC, Sheridan MF (1982) Computer-assisted mapping of pyroclastic surges. Science 217:637–639

Martí J, Felpeto A (2010) Methodology for the computation of volcanic susceptibility. An example for mafic and felsic eruptions on Tenerife (Canary Islands). J Volcanol Geotherm Res 195:69–77

Martí J, Geyer A (2009) Central vs flank eruptions at Teide–Pico Viejo twin stratovolcanoes (Tenerife, Canary Islands). J Volcanol Geotherm Res 181:47–60

Martí J, Gudmundsson A (2000) The Las Cañadas caldera (Tenerife, Canary Islands): an overlapping collapse caldera generated by magma-chamber migration. J Volcanol Geotherm Res 103:161–173

Martí J, Mitjavila J, Araña V (1994) Stratigraphy, structure and geochronology of the Las Cañadas caldera (Tenerife, Canary Islands). Geol Mag 131:715–727

Martí J, Hurlimann M, Ablay GJ, Gudmundson A (1997) Vertical and lateral collapses in Tenerife and other ocean volcanic islands. Geology 25:879–882

Martí J, Aspinall WP, Sobradelo R, Felpeto A, Geyer A, Ortiz R, Baxter P, Cole P, Pacheco JM, Blanco MJ, Lopez C (2008a) A long-term volcanic hazard event tree for Teide-Pico Viejo stratovolcanoes (Tenerife, Canary Islands). J Volcanol Geotherm Res 178:543–552

Martí J, Geyer A, Andujar Teixó F, Costa F (2008b) Assessing the potential for future explosive activity from Teide–Pico Viejo stratovolcanoes (Tenerife, Canary Islands). J Volcanol Geotherm Res 178:529–542

Martí J, Ortiz R, Gottsmann J, Garcia A, De La Cruz-Reyna S (2009) Characterising unrest during the reawakening of the central volcanic complex on Tenerife, Canary Islands, 2004–2005, and implications for assessing hazards and risk mitigation. J Volcanol Geotherm Res 182:23–33

Martin AJ, Umeda K, Connor CB, Weller JN, Zhao D, Takahashi M (2004) Modeling long-term volcanic hazards through Bayesian inference: an example from the Tohoku volcanic arc, Japan. J Geophys Res 109:B10208

Marzocchi W, Sandri L, Selva J (2010) BET_VH: a probabilistic tool for long-term volcanic hazard assessment. Bull Volcanol 72:705–716. doi:10.1007/s00445-010-0357-8

Mendoza-Rosas AT, De la Cruz-Reyna S (2008) A statistical method linking geological and historical eruption time series for volcanic hazard estimations: applications to active polygenetic volcanoes. J Volcanol Geotherm Res 176:277–290

Newhall CG, Self S (1982) The volcanic explosivity index (VEI): an estimate of the explosive magnitude for historical eruptions. J Geophys Res 87:1231–1238

Pérez NM, Coello C, Marrero R, González Y, Brrancos PJ (2005) Premonitory geochemical and geophysical signatures of volcanic unrest at Tenerife, Canary Islands. Geophys Res Abst 7:09993, SRef-ID: 1607-7962/gra/EGU05-A-09993

Perez-Torrado FJ, Carracedo JC, Paris R, Hansen A (2004) Descubrimiento de depósitos freatomagmáticos en la laderas septentrionales del estratovolcán Teide (Tenerife, Islas Canarias): relaciones estratigráficas e implicaciones volcánicas. Geotemas 6:163–166

Pyle DM (2000) Sizes of volcanic eruptions. In: Sigurdsson H (ed) Encyclopedia of volcanoes. Academic, San Diego, pp 263–269

Rodríguez-Losada J, Hernández-Gutiérrez LE, Olalla C, Perucho A, Serrano A, Eff-Darwich A (2009) Geomechanical parameters of intact rocks and rock masses from the Canary Islands: implications on their flank stability. J Volcanol Geotherm Res 182:67–75

Sandri L, Marzocchi W, Zaccarelli L (2004) A new perspective in identifying the precursory patterns of eruptions. Bull Volcanol 66:263–275

Sheridan MF, Malin MC (1983) Application of computer-assisted mapping to volcanic hazard evaluation of surge eruption: Vulcano, Lipari, Vesuvius. Explosive volcanism. J Volcanol Geotherm Res 17:187–202

Sobradelo R, Martí J (2010) Bayesian event tree for long-term volcanic hazard assessment: application to Teide-Pico Viejo stratovolcanoes, Tenerife, Canary Islands. J Geophys Res 115: B05206. doi:10.1029/2009JB006566

Sobradelo R, Martí J, Mendoza-Rosas AT, Gómez G (2011) Volcanic hazard assessment for the Canary Islands (Spain) using extreme-event statistics. Nat Hazards Earth Syst Sci 11:2741–2753. doi:10.5194/nhess-11-2741-2011

Suzuki T (1983) A theoretical model for dispersion of tephra. In: Shimozuru D, Yokoyama I (eds) Arc volcanism: physics and tectonics. Terra Scientific, Tokyo, pp 95–113

Toyos G, Cole P, Felpeto A, Martí J (2007) A GIS-based methodology for hazard mapping of small volume pyroclastic density currents. Nat Haz 41:99–112

Wiesmaier S, Deegan FM, Troll VR, Carracedo JC, Chadwick JP, Chew DM (2011) Magma mixing in the 1100 AD Montaña Reventada composite lava flow, Tenerife, Canary Islands: interaction between rift zone and central volcano plumbing system. Contrib Mineral Petrol. doi:10.1007/s00410-010-0596-x